FUNCTIONALIZED POLYOXOMETALATES FOR ADVANCED APPLICATIONS

by

JEFFERY D. KARCHER

B.S., Oklahoma State University, 2001

AN ABSTRACT OF A DISSERTATION

submitted in partial fulfillment of the requirements for the degree

DOCTOR OF PHILOSOPHY

Department of Chemistry
College of Arts and Sciences

KANSAS STATE UNIVERSITY
Manhattan, Kansas

2007

Abstract

Polyoxometalates have attracted much attention over the last few decades and have been studied in a wide variety of fields such as catalysis, medicine, imaging, photochromism, and magnetic materials. While many of these systems are easy to prepare, the ability to functionalize polyoxometalates is an ongoing challenge.

Two approaches used to functionalize polyoxometalates involve insertion of metal fragments into a lacunary polyoxometalate or the direct replacement of terminal oxo ligands with the isoelectronic organoimido ligand. This process has been proven successful in many cases and with a wide variety of organoimido compounds. One of our group's goals has been to synthesize a functionalized hexamolybdate species that is capable of metal coordination. However, previous results have been hindered because the electron withdrawing effect of the cluster is transmitted to the metal binding sites.

In order to combat the electron withdrawing effect of the cluster, 4-amino piperidine dithiocarbamate ligands, which have no conjugation in the ring and are capable of metal binding, have been synthesized and characterized. A series of transition metal complexes have been made and a single crystal has been grown of a nickel(II) complex. Attempts to attach these species to clusters are described.

Imido hexamolybdate clusters have been functionalized with styryl and iodophenyl groups. The styrene functionalized hexamolybdate was copolymerized with 4-chloromethylstyrene in moderate yields. This copolymer has the capabilities for further substitution at the chloromethyl group. The iodophenyl functionalized hexamolybdate was fully characterized including a single-crystal X-ray structural determination. This functionalized hexamolybdate can be used in carbon-carbon bond formation through coupling reactions.

A chromium(V) nitrido polyoxometalate has been synthesized from a lacunary Keggin precursor and characterized. This nitrido species shows promise as a nitrogen transfer agent. Likewise, this nitrido species could be an entry point to other derivatives through reactions with various nucleophiles and electrophiles.

FUNCTIONALIZED POLYOXOMETALATES FOR ADVANCED APPLICATIONS

by

JEFFERY D. KARCHER

B.S., Oklahoma State University, 2001

A DISSERTATION

submitted in partial fulfillment of the requirements for the degree

DOCTOR OF PHILOSOPHY

Department of Chemistry
College of Arts and Sciences

KANSAS STATE UNIVERSITY
Manhattan, Kansas

2007

Approved by:

Major Professor
Eric A. Maatta

Copyright

Abstract

Polyoxometalates have attracted much attention over the last few decades and have been studied in a wide variety of fields such as catalysis, medicine, imaging, photochromism, and magnetic materials. While many of these systems are easy to prepare, the ability to functionalize polyoxometalates is an ongoing challenge.

Two approaches used to functionalize polyoxometalates involve insertion of metal fragments into a lacunary polyoxometalate or the direct replacement of terminal oxo ligands with the isoelectronic organoimido ligand. This process has been proven successful in many cases and with a wide variety of organoimido compounds. One of our group's goals has been to synthesize a functionalized hexamolybdate species that is capable of metal coordination. However, previous results have been hindered because the electron withdrawing effect of the cluster is transmitted to the metal binding sites.

In order to combat the electron withdrawing effect of the cluster, 4-amino piperidine dithiocarbamate ligands, which have no conjugation in the ring and are capable of metal binding, have been synthesized and characterized. A series of transition metal complexes have been made and a single crystal has been grown of a nickel(II) complex. Attempts to attach these species to clusters are described.

Imido hexamolybdate clusters have been functionalized with styryl and iodophenyl groups. The styrene functionalized hexamolybdate was copolymerized with 4-chloromethylstyrene in moderate yields. This copolymer has the capabilities for further substitution at the chloromethyl group. The iodophenyl functionalized hexamolybdate was fully characterized including a single-crystal X-ray structural determination. This functionalized hexamolybdate can be used in carbon-carbon bond formation through coupling reactions.

A chromium(V) nitrido polyoxometalate has been synthesized from a lacunary Keggin precursor and characterized. This nitrido species shows promise as a nitrogen transfer agent. Likewise, this nitrido species could be an entry point to other derivatives through reactions with various nucleophiles and electrophiles.

Table of Contents

List of Figures

List of Tables

Acknowledgements

I would first and foremost like to acknowledge my major professor, Dr. Eric A. Maatta. Without his guidance and support, my experience at Kansas State University would not have been as enjoyable as it has turned out to be. I am grateful for your patience, guidance and understanding throughout my time here. You have truly influenced my life in a positive way and I am a better person because of it. I could not have asked to work for a better person and you have always treated me with the utmost respect even when times were difficult. I cannot say thanks enough for the experiences that you have brought to me, especially the time spent in France.

I would like to thank my committee members for their professionalism and much needed help and encouragement throughout this entire process.

I would like to thank everyone that helped me along the way, especially, Dr. John Desper for his amazing work on single crystal analysis and Jeff Lange for his HPLC work. Also, Dr. Lou Wojcinski and Kris Mijares for their endless help in lab and office conversations. Richard Bachamp, Tobe Eggers, and Jim Hodgson for their tireless work on making my life easier. Dr. Anna Proust and Dr. Rene Thouvenot for allowing me to study with them in Paris, something I will never forget. Thanks to my close friends Nate, Kurt, Scott, Greg, Gavin, Brock, and Al for always being there and willing to help me when I needed it. Finally, I would like to thank the US Department of Energy for funding during my time here which made many of these events possible.

Dedication

First, I would like to give thanks to God for without him none of this would be possible. To my parents Jerry and Carol, I cannot thank you enough for the love you have given to me and the values you have instilled in me. I am truly blessed to have you in my life. To my brother Arron, I am extremely grateful for your constant guidance and support. I truly lookup to you and admire everything you have accomplished and have in life. I can only hope that I will attain the happiness that you possess.

To my friends who are too numerous to list, the softball team, golf buddies, and good ole drinking buddies, I thank everyone of you. Without you my time spent here would have been short. You made my experience here enjoyable and one of the best of my life. I will take with me memories that are unforgettable, “goody-goody”, and friendships that will last a lifetime.

CHAPTER 1 - General Introduction

1.1 Brief History

Polyoxometalates (POMs) are self-assembled nano-sized anionic metal oxide clusters.[1,2] They are typically synthesized under acidic aqueous conditions and have counter ions that can be alkali metal cations, ammonium, or alkylammonium cations, etc. (Figure 1-1).

$$8\ H^+ + 7\ MoO_4^{2-} \longrightarrow [Mo_7O_{24}]^{6-} + 4\ H_2O$$

$$23\ H^+ + 12\ WO_4^{2-} + HPO_4^{2-} \longrightarrow [PW_{12}O_{40}]^{3-} + 12\ H_2O$$

Figure 1-1 Reaction Equations for the Formation of POMs in Acidic Conditions.[1]

There are two broad classes of POMs, isopoly and heteropoly (Figure 1-2).[1] In the heteropoly case, X is the hetero atom and is located in the center of the cluster. The element (M) that composes the framework is usually molybdenum or tungsten. The hetero atom is often P^{+5} or Si^{+4}, but there are numerous examples for over 70 different elements.

$[M_mO_y]^{p-}$ Isopoly anions

$[X_xM_mO_y]^{q-}$ Heteropoly anions

Figure 1-2 Typical Molecular Formula for Isopoly and Heteropoly Anions.[1]

The first POM discovered was by Berzelius in 1826 which was the ammonium salt of $[PMo_{12}O_{40}]^{3-}$.[3] This POM was later (1848) used by Svanberg and Struve[4] as a useful determination of phosphorous. Although many POMS had been reported, their structures were not fully understood until 1933 when Keggin[5] determined the structure of $H_3PW_{12}O_{40}$ (Figure 1-3)

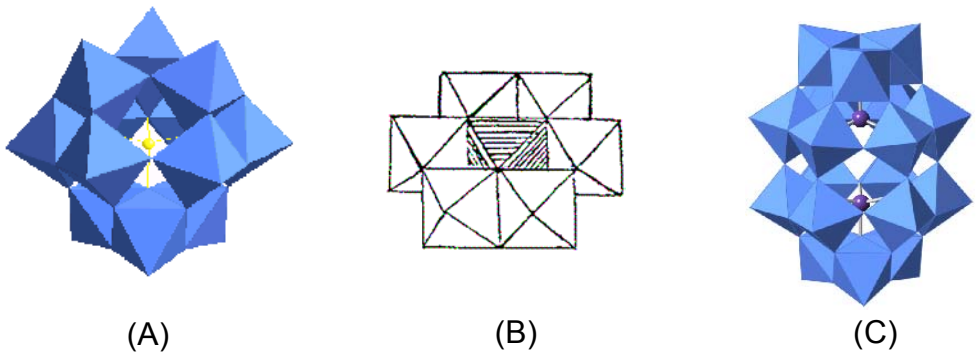

Figure 1-3 Polyhedron Representation of A) Keggin type B) Anderson-Evens type[6], C) Wells Dawson type.

by powder diffraction. Any POM that has the general ratio of 12:1 is given the name Keggin. In 1948, Evans[7] determined another POM structure, $[Te^{VI}Mo_6O_{24}]^{-6}$ (6:1), through single-crystal X-ray studies; this is now commonly called the Anderson-Evans structure (Figure 3). Dawson[8] was responsible for the next major discovery in 1953. He solved the structure of $[P_2W_{18}O_{62}]^{-6}$ (18:2) which is referred to as the Wells-Dawson structure (Figure 1-3). Many more have since been established, but these are the main structures in heteropoly anions.

Beside the wide range of elements involved in the well defined structures of POMs, POMs have very pronounced and interesting properties. The metal atoms that compose the framework are generally fully oxidized when prepared. This leads to perhaps POMs' greatest feature which is their ability as strong oxidizers and to undergo multiple, reversible electron reductions. This typically leads to a drastic color change resulting in a characteristic blue color. These POMs are called heteropoly blues. Some POMs have been reported to accept as many as 32 electrons before decomposition of the cluster. Oxidized POMs tend to be air and water stable. They can be made to be soluble in aqueous and organic media. A typical size range is roughly 6-25 Å with ionic weights that can reach upwards to 10,000 amu. POMs tend to be stable to acidic conditions. However, cluster decomposition can occur under basic conditions (Figure 1-4).[1] These conditions vary for POMs as some occur at different pH levels with varying reaction times.

$$[CrMo_6O_{24}H_6]^{3-} + 9\ OH^- \longrightarrow 6\ H_2O + Cr(OH)_3 + 6\ MoO_4^{2-}$$

$$[PW_{12}O_{40}]^{3-} + 23\ OH^- \longrightarrow 11\ H_2O + 12\ WO_4^{2-} + HPO_4^{2-}$$

Figure 1-4 The Effect of Basic Conditions on POMs.

1.2 Hexamolybdate Structure

In 1952, Lindqvist[9] discovered a new type of POM that had the general formula $[M_6O_{19}]^{n-}$, (M = Mo, W, Nb, Ta, and V) (Figure 1-5). These 6:1 POMs came to be known as the Lindqvist structure. Lindqvist POMs have an overall octahedral geometry. The cluster is

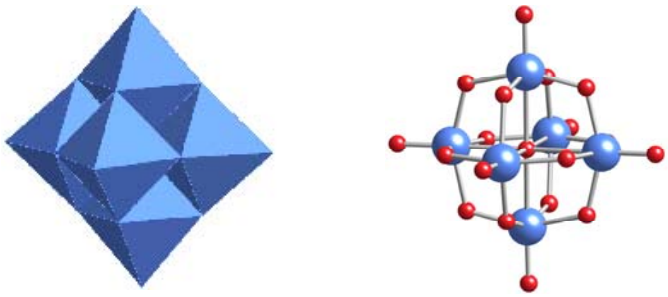

(A) (B)

Figure 1-5 Representation of the Lindqvist Structure A) Polyhedron B) Ball and Stick (Red Balls = Oxygen atoms, Blue Balls = Metal atoms).

composed of one central oxygen that is octahedrally bound to all the metal atoms. Also, each metal atom has one terminal oxygen atom and is bridged by four different oxygen atoms. The lengths of the metal-oxygen bonds help identify each oxygen's bond character (Table 1). From these bond lengths, the terminal oxygens (O_A) express some triple bond character.

Table 1 Bond Lengths (Å) for Selected $[M_6O_{19}]^{n-}$ anions.

Anion	M-O_A	M-O_B	M-O_C	Refs.
$[Mo_6O_{19}]^{2-}$	1.68	1.93	2.32	10
$[W_6O_{19}]^{2-}$	1.69	1.92	2.33	11
$[Ta_6O_{19}]^{8-}$	1.80	1.99	2.38	1
O_A(terminal oxygens)	O_B(bridging oxygens)	O_C(central oxygen)		

One particular Lindqvist POM is of importance, hexamolybdate ($[Mo_6O_{19}]^{2-}$). This POM is particularly special in the fact that it can be directly functionalized to incorporate organoimido ligand (organic "pieces"). This unique feature has made $[Mo_6O_{19}]^{2-}$ a very popular POM to study in recent years.

Over the last few decades, the functionalization of $[Mo_6O_{19}]^{2-}$ has been investigated by Maatta[12,13] and more recently Peng.[14] There are currently three procedures that allow $[Mo_6O_{19}]^{2-}$ to become functionalized. The first procedure was developed by Maatta in 1992. It involved the direct reaction of tetrabutyl ammonium salt ,$TBA_2[Mo_6O_{19}]$ and a phosphineimine with mild heat (Figure 1-6). The formation of the functionalized $TBA_2[Mo_6O_{19}]$ is believed to occur through the formation of a four membered intermediate between a terminal molybdenum-oxygen

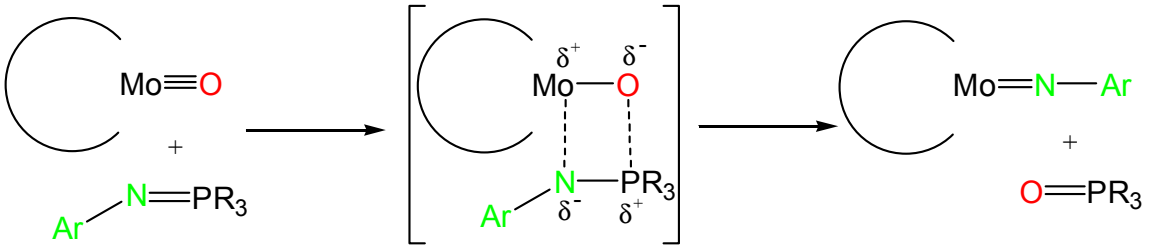

Figure 1-6 Reaction Mechanism for the Substitution of $TBA_2[Mo_6O_{19}]$ with a Phosphineimine.

unit and the phosphorous-nitrogen unit of the phosphineimine. This procedure produces good yields, but there is some minor work up to remove the triphenylphosphine oxide by-product and long reaction times may be required. The second procedure developed by Maatta was in 1994. Just as in the previous case, $TBA_2[Mo_6O_{19}]$ is directly reacted with an isocyanate (Figure 1-7).

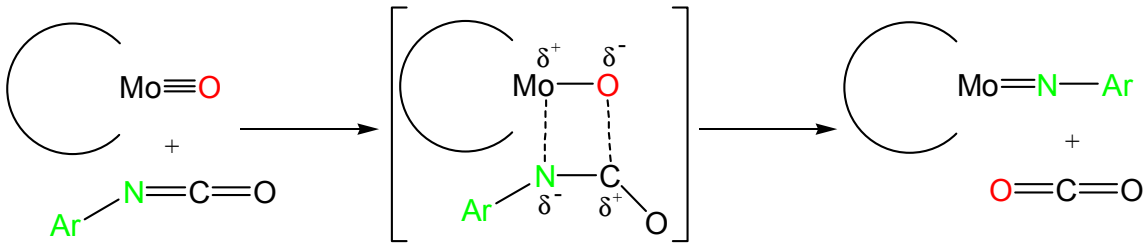

Figure 1-7 Reaction Mechanism for the Substitution of $TBA_2[Mo_6O_{19}]$ with an isocyanate.

Functionalization is believed to occur through a four membered intermediate which involves the carbon-nitrogen unit of the isocyanate and a terminal molybdenum-oxygen bond from the cluster. This procedure is very good is producing quality yields, but perhaps its most attractive feature is the by-product is carbon dioxide. The carbon dioxide is simply allowed to dissipate into the atmosphere and only the product remains. However, long reaction times are common

for this procedure. Finally, the third procedure was developed by Peng in 2001. Here, $TBA_2[Mo_6O_{19}]$ is combined with an initiator, N,N'-Dicyclohexylcarbodiimide (DCC), and an aromatic amine (Figure 1-8) under refluxing conditions. The precise mechanism is not known, but it is believed that the DCC forms an intermediate with a terminal molybdenum-oxygen bond which then is activated. This activated species then interacts with the amine. This procedure has been reported to have very good yields and fast reaction times, but as with the first procedure, there is a urea by-product that needs to be removed.

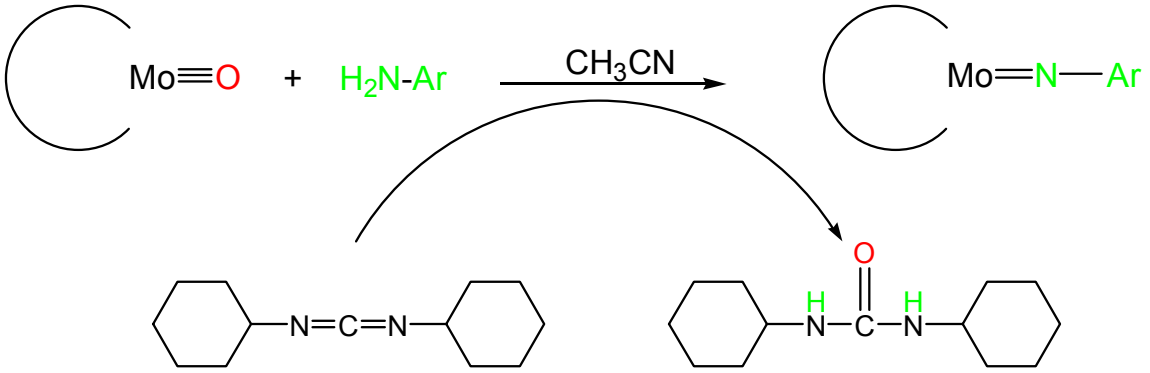

Figure 1-8 Reaction Mechanism for the Substitution of $TBA_2[Mo_6O_{19}]$ with DCC and an Aromatic Amine.

With the ability to functionalize hexamolybdate with organic "pieces", in theory the only limiting factor is imagination; in practice not all isocyanates nor phosphineimines afford organoimido hexamolybdates. Intrinsic effects can play a huge role in the determination of which derivative of $TBA_2[Mo_6O_{19}]$ to produce. There are many published examples of functionalized $TBA_2[Mo_6O_{19}]$.[2]

1.3 Keggin Structure

The Keggin POMs ($[XM_{12}O_{40}]^{n-}$) fall under the heteropoly anion type. As mentioned, the first discovered was an ammonium salt, $(NH_4)_3[PMo_{12}O_{40}]$ (Figure 1-9), by Berzelius.[3] However, the structure was not fully known until Keggin solved the structure in 1933. The structure found had an overall tetrahedral symmetry (T_d). It consisted of a central PO_4 tetrahedron surrounded by 12 MoO_6 octahedra arranged in four groups of three edge sharing octahedra (Mo_3O_{13}).

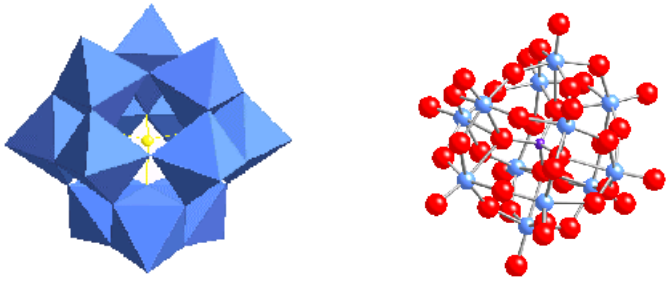

Figure 1-9 Structure Representation of the Keggin POM A) Polyhedron B) Ball and Stick (Red Balls = Oxygen atoms, Blue Balls = Metal atoms).

These Mo_3O_{13} groups are linked together by shared corners to each other and the central PO_4 tetrahedron. Since then, isomers have been discovered of the Keggin structure (Figure 1-10). The isomers result from one (β), two (γ), three (δ), or four (ε) M_3O_{13}

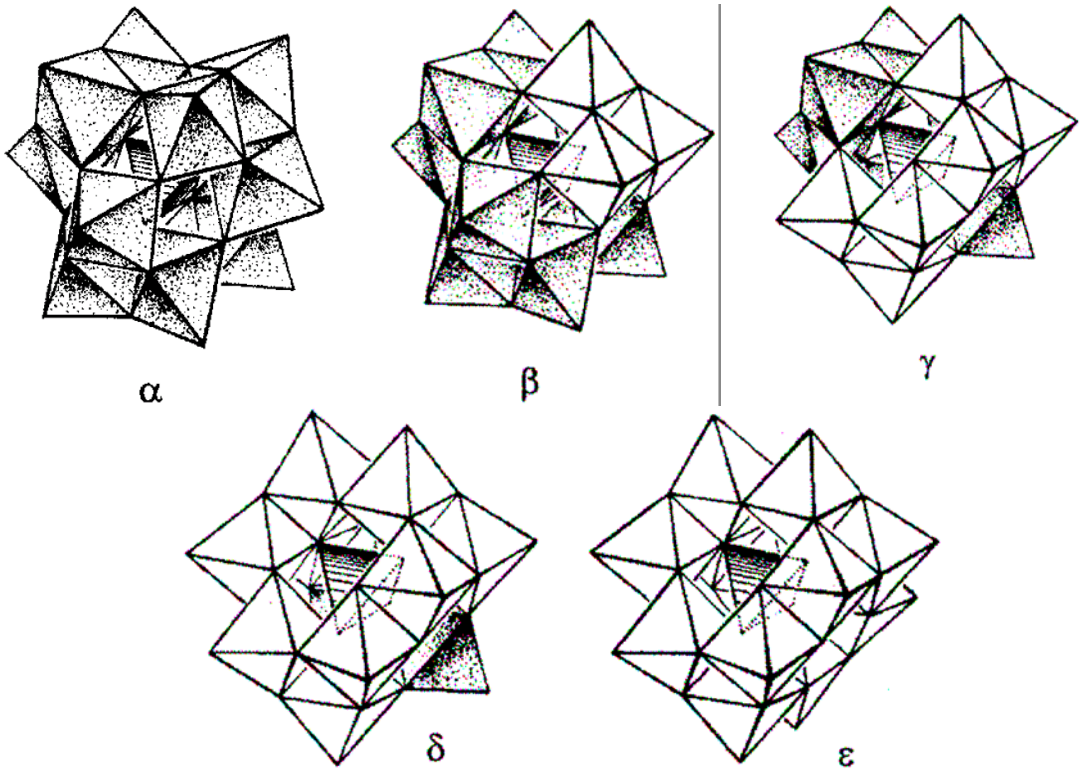

Figure 1-10 Polyhedron Representation of the five Keggin isomers.[15]

groups, indicated by the clear polyhedron, being rotated by $\pi/3$.[15] Perhaps more intriguing, the Keggin POM can be chemically modified by having one of its terminal oxygen-metal units removed. The process by which the metal-oxygen unit is removed is generally the treatment of the parent Keggin with a mild base such as bicarbonate. It is generally referred to as a lacunary Keggin, $[XM_{11}O_{39}Z]^{n-}$ (Figure 1-11).[15] However, the lacunary Keggin is not limited to just the removal of one terminal metal-oxygen, but the removal of up to three terminal metal-oxygens has been accomplished. With this discovery, the Keggin POM has become one of the most intensely studied POMs to date.

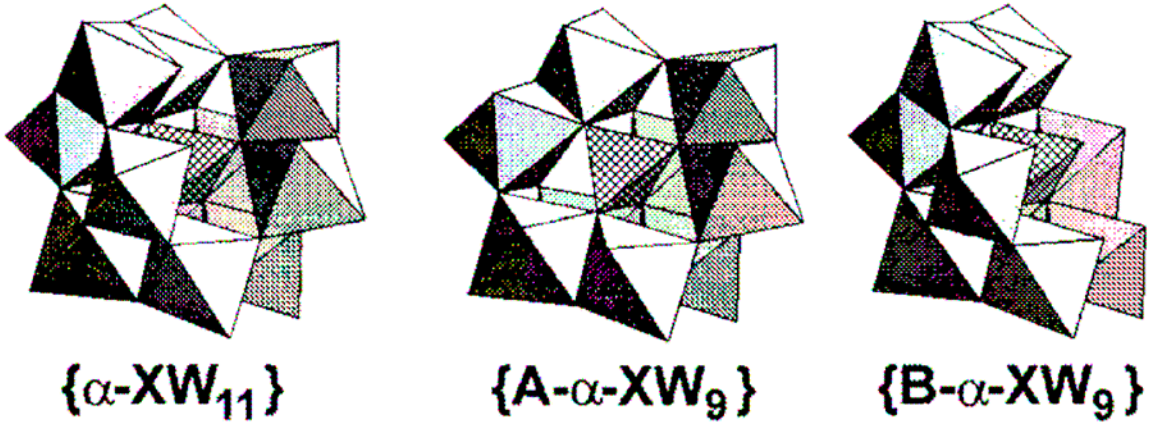

Figure 1-11 Polyhedron Representation of Lacunary Keggin Structures.[15]

The lacunary Keggin has had a variety of metal atoms re-incorporated into its vacancies. These metal atoms are typically octahedrally-coordinated with the lacunary Keggin acting as a pentadentate ligand. There have been many ligands observed in the sixth coordination site of the metal atom. The incorporation of the metal atom is straightforward and usually consists of combining aqueous solutions of the lacunary Keggin and the desired metal atom. However, some care is needed in the synthesis of the lacunary Keggins because not all are hydrolytically stable and can convert back to the parent Keggin.

1.4 Functionalization of POMs

1.4.1 Transition Metals

An attractive feature regarding POMs, heteropoly or isopoly, and an aspect that promises to extend their utility, is the ability to functionalize them. The simplest way to achieve a functionalized POM is to incorporate a transition metal into the cluster. If group 5 and 6 elements are considered to be the foundation for cluster composition, then there are examples of all of the first row transition metal cations substituted into the Keggin and/or Dawson clusters. The transition metal is not limited to one atom in the cluster as there are reports in which multiple metal atoms have been incorporated (Figure 1-12). Not only can transition metal atoms be incorporated into POMs, but also organometallic species involving transition metals. For molybdate clusters, examples are known that bear ruthenium cymene (Figure 1-12), titanium Cp, and rhodium Cp^* units among others.[2] Also, these transition metals can bring new properties to POMs if they have unpaired d- electrons which can lead to magnetic material. Some of the magnetic material will be discussed later. Catalysts can arise from transition metal substituted POMs which again will be discussed later. Dawson clusters that can incorporate f-block transition metal cations are being investigated as sequestering agents for nuclear waste.[2]

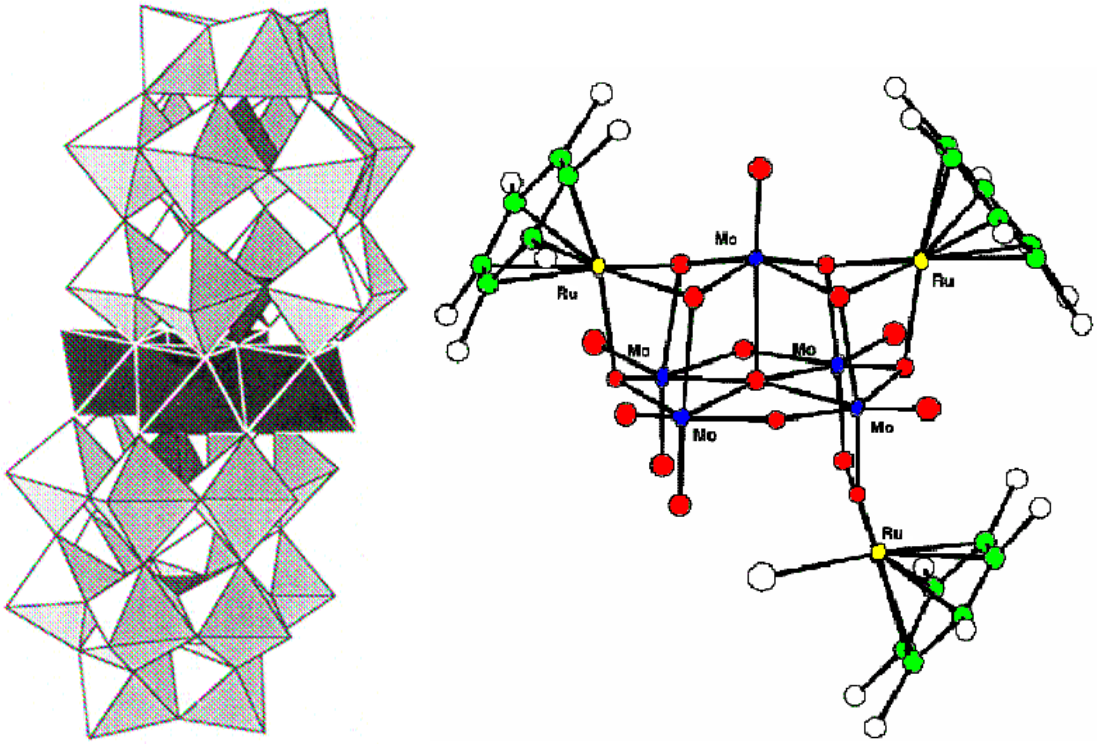

Figure 1-12 POM structures incorporating multiple addenda atoms $[Mn_4(H_2O)_2(P_2W_{15}O_{56})_2]$ (left)[16] and of $[Ru(C_6Me_6)_3Mo_5O_{18})]$ (right)[17].

1.4.2 Main Group Elements

A very useful POM would be one that is substituted with a halogen. Perhaps, if a halogenated POM is obtained, further chemical modification could proceed through the halogen bond. However, there are very few reported structures. The halogens tend to replace oxygens of the cluster that are not terminal. This leads to the halogen being "protected" by the cluster and inaccessible to further chemical modification. However, there have been some terminal halogen substituted POMs reported such as $[Mo_4O_{10}(OMe)_4Cl_2]^{2-}$ [18] (Figure 1-13), $[W_6O_{14}Cl_{10}]^{2-}$ [19], and $[PW_9O_{28}Br_6]^{3-}$.[20]

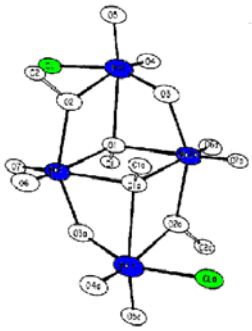

Figure 1-13 Ball and Stick Representation of $[Mo_4O_{10}(OMe)_4Cl_2]^{2-}$.[18]

Few examples of group 16 elements incorporated into POMs have been reported. The first was by Klemperer in 1985.[21] This particular case took advantage of the reactivity of the [NbO] unit in $[W_5O_{18}NbO]^{3-}$ with hexamethyldisilathiane and produced $[W_5O_{18}NbS]^{3-}$. Later, Keggin clusters were synthesized that incorporated both thio[22] and seleno[23] species.

Alkoxo substituted POMs are perhaps the most abundant of the main group substituted POMs. However, there is but only one POM, Lindqvist type, which has terminal alkoxo ligands. These, $[(MeO)MW_5O_{19}]^{n-}$ M = Ti, Zr, Nb, Ta, Mo, or W (Figure 1-14), were discovered by Errington in 1996.[24] All other alkoxo ligands are incorporated through doubly or triply bridging sites. Alkoxo ligands have been used to stabilize some POMs, specifically $[V_6O_{19}]^{8-}$, that were previously unknown.[25]

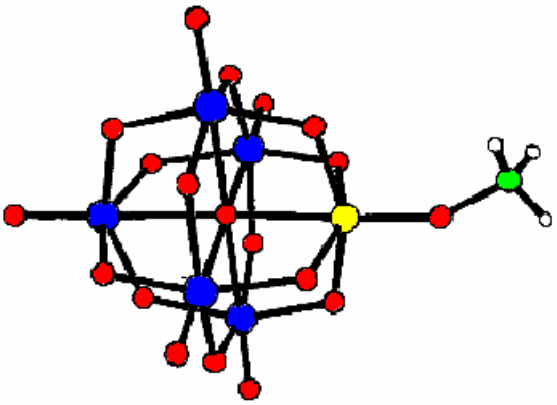

Figure 1-14 Ball and Stick Representation of Alkoxo Lindqvist $[W_5O_{18}TiOCH_3]^{3-}$.[24]

In this particular case, the alkoxo ligands stabilize the V_6O_{13} core by capping three vanadium centers. Gouzerh[26] has found similar results with Anderson POMs (Figure 1-15). Depending on the metal incorporated in the POM, the alkoxo ligands cap the POM in different

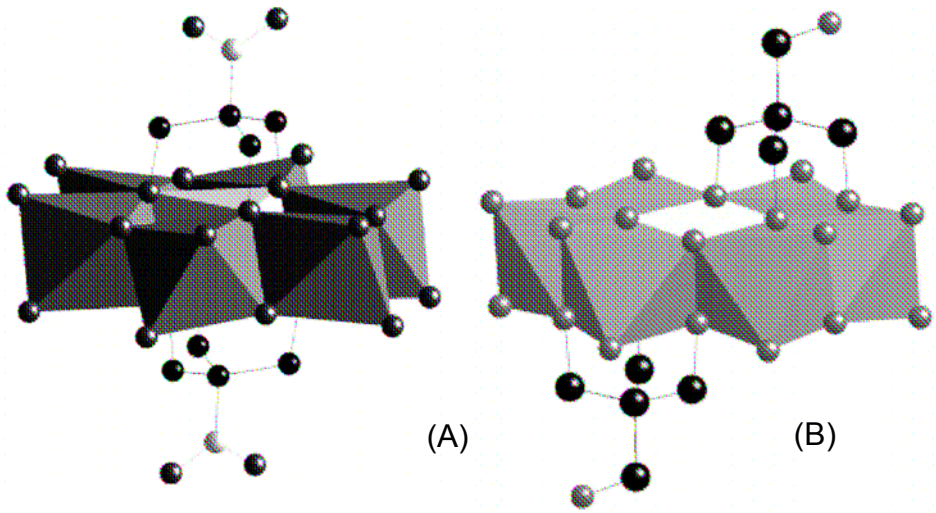

Figure 1-15 Polyhedron & Ball and Stick Representation for $[MnMo_6O_{18}\{MeC(CH_2O)_3\}_2]^{3-}$ (A)[26] and $[H_2ZnMo_6O_{18}\{MeC(CH_2O)_3\}_2]^{2-}$ (B)[26].

places. Even with these developments, there is still need for further elaboration of these alkoxo POMs by way of the R-group. Perhaps further chemical reactivity can be obtained and more intriguing POMs obtained.

Group 14 derivatives have been made with Keggin, Dawson, and Lindqvist POMs. The Keggin clusters of organosilyl and organogermyl fragments were found in the late 1970s by

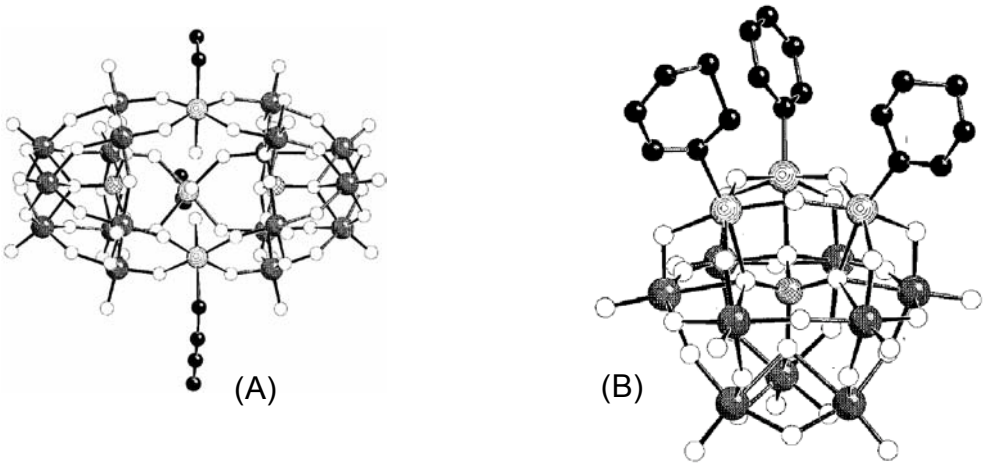

Figure 1-16 Ball and Stick Representation of α-$[(SiW_9O_{34})_2(n\text{-}BuSnOH)_3]^{14-}$ (A)[27] and β-$[SiW_9O_{37}(SnPh)_3]^{7-}$ (B)[27].

Knoth[27] and Pope[28] respectively. Later in 1990s, the Keggin[27] (Figure 1-16), Dawson[28], and Lindqvist[29] organotin POMs were characterized. An attractive feature of group 14 substituted POMs is the organic substituents. Clearly, more intriguing and versatile organic groups are being substituted onto POMs. This now leads into the discussion of POMs more relevant to this thesis: those that are substituted by group 15 elements, in particular nitrogen.

Nitrogen has been substituted into POMs in a variety of ways, including as a metal nitride. This is usually achieved by reaction of a lacunary POM and with a metal nitride source. However, there are but only a few of these nitrido POMs known. The first nitride POM was reported by Zubieta which was a Lindqvist type ($[Mo_6O_{18}N]^{3-}$)[30]; Zubieta later reported the synthesis of a Keggin Tc nitride,[31] but neither was thoroughly characterized. Maatta and collaborators have synthesized and characterized Keggin Os and Re nitrides (Figure 1-17) as well as a Dawson Os nitride (Figure 1-17).[32]

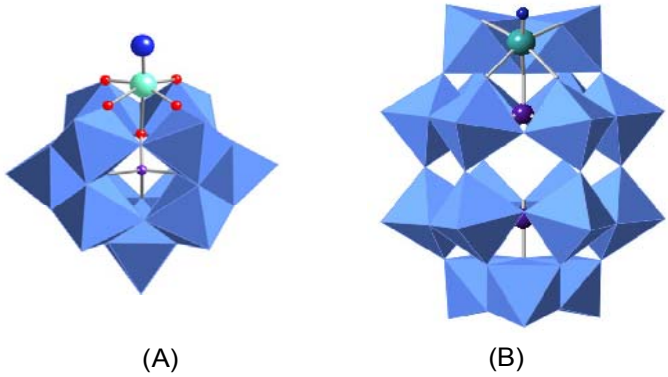

Figure 1-17 Polyhedron Representation of the Keggin Metal Nitride (A)[32] and the Dawson Metal Nitride (B)[32].

The more successful approach in substituting nitrogen containing species into POMs is via direct substitution. This approach has seen the most success with the Lindqvist type. Organoimido, RN^{2-}, and organohydrazido, $RR'N_2^{2-}$, ligands are isoelectronic with the oxo ligand which is a key feature enabling substitution of POMs. The synthetic routes used to obtain the substituted POMs was already discussed. A wide range of organoimido ligands have been used in the substitution of POMs. The ligands can be very simple in nature, or quite elaborate. The Maatta group has focused on obtaining these types of substituted POMs. They have obtained a n-butylimido, cyclohexylimido, and a diisopropylphenylimido hexamolybdate (Figure 1-18).[33] These new POMs have laid the ground work for understanding how the substituted

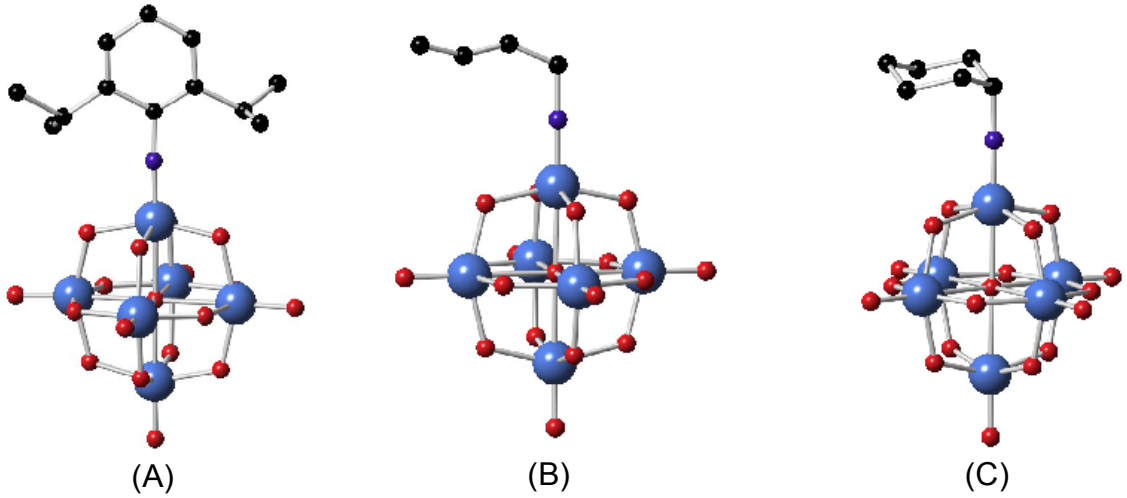

Figure 1-18 Ball and Stick Representation of Diisopropylphenylimido- (A)[33], n-Butylimido- (B)[33], and Cyclohexylimido- (C)[33] Hexamolybdate Structures.

hexamolybdate is affected by the imido ligands. It has been observed that the imido ligands add electron density to the POM. These effects have been observed through ^{95}Mo NMR studies where the imido molybdenum is significantly shifted upfield. Likewise, the bridging oxygens of the imido molybdenum have longer bond distances than those of the oxo molybdenum. Also, the ^{17}O NMR studies have supported this idea with the terminal oxygens been shifted upfield which is consistent with added electron density. These observations support the idea that the imido ligand is donating electron density to the POM. More elaborate hexamolybdate species were obtained with multiple terminal oxygens being replaced (Figure 1-19).[32,34] This series revealed through cyclic voltametry studies that cluster electron density is increased linearly as each imido ligand is substituted onto the POM.

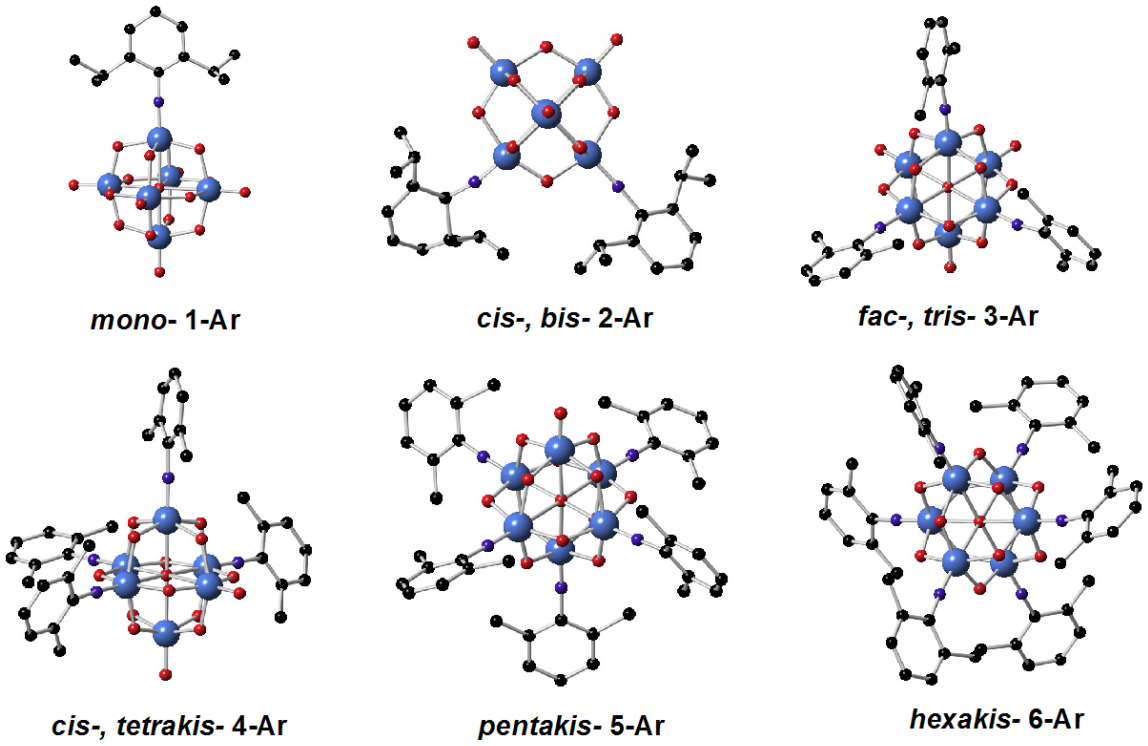

Figure 1-19 Ball and Stick Representation of Multiple imido Substituted Hexamolybdates.[34]

With this knowledge, more interesting imido ligands were desired. The Maatta group has since tried to obtain a substituted hexamolybdate that could interact with other metal atoms. Pyridylimido, carboxyphenylimido, and methoxypyridylimido-hexamolybdates (Figure 1-20) have been synthesized and characterized.[35] All of these substituted POMs in principle have the

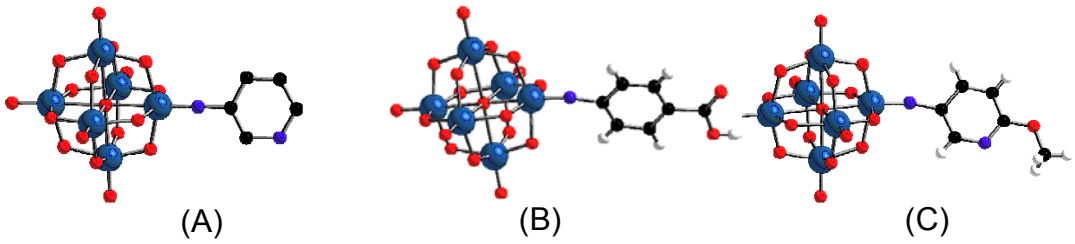

Figure 1-20 Ball and Stick Representation of Pyridylimido- (A)[35], Carboxyphenylimido- (B)[35], and Methoxypyridylimido- (C)[35] Hexamolybdate.

ability to coordinate to a metal atom using the imido substituent's functional group. However, this desired result has yet to be observed. Peng has been able to obtain a hexamolybdate species with a terpy functionality through a Sonogashira coupling reaction and in fact observed metal coordination (Figure 1-21).[36]

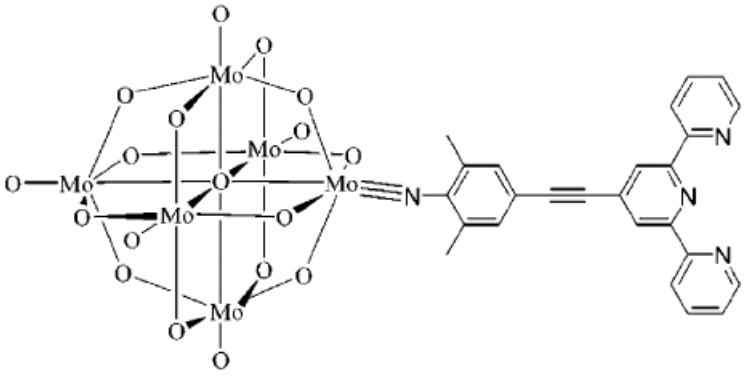

Figure 1-21 Structure of the Terpyimido Hexamolybdate.[36]

A very promising substituted hexamolybdate, a ferrocenylimido (Figure 1-22)[37], was synthesized by the Maatta group. This deep blue crystalline material was first assumed to be a reduced POM because of the color. However, upon further investigation, it was proved to be otherwise. In fact, this new POM displayed very unique characteristics. The material was photoactive. Upon exposing the material to light, electron transfer was observed. This functionalized hexamolybdate produced 6 unpaired electrons creating a very exciting material. This find has spurred on the research of synthesizing other functionalized hexamolybdates that can interact directly or through coordination of another metal atom.

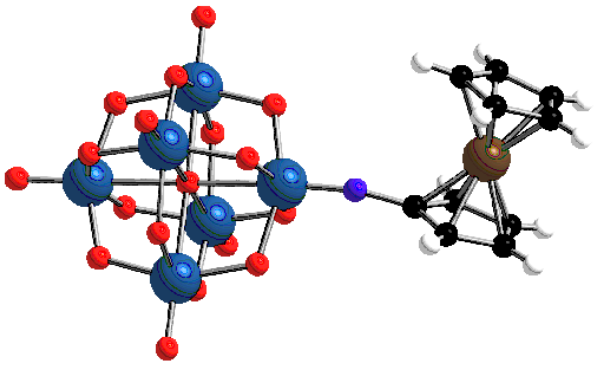

Figure 1-22 Ball and Stick Representation of Ferrocenylimido Hexamolybdate.[37]

With the success of the ferrocenylimido, the idea of connecting two hexamolybdate clusters together using a di-imido linker was sought. Errington and Maatta both were able to accomplish this feat. Errington[38] was able to link them with a phenylene bis-imido ligand while

Maatta[39] was able to link the hexamolybdates together with not only the phenylene bis imido, but also with a cyclohexyl bis-imido (Figure 1-23).

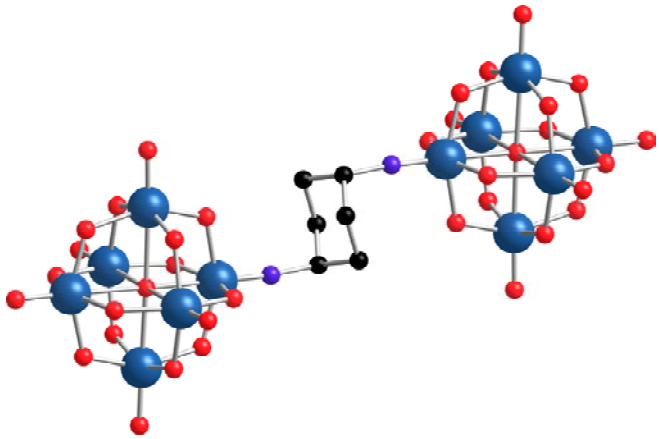

Figure 1-23 Ball and Stick Representation of Cyclohexyl bis-imido Hexamolybdate.[39]

Finally, one last approach has been made to functionalize POMs onto a polymer backbone. There is a report involving a Keggin POM $[\{\gamma\text{–}SiW_{10}O_{36}\}\{H_2C{=}C(Me)C(O)OPrSiO)_4\}]^{4-}$ [40], with polymerizable units, but only the hexamolybdate cases will be discussed. Maatta was the first to produce a functionalized hexamolybdate with polymerizable group. A styrylphosphineimine was reacted with hexamolybdate to yield the styrylimido hexamolybdate (Figure 1-24).[41] This was then

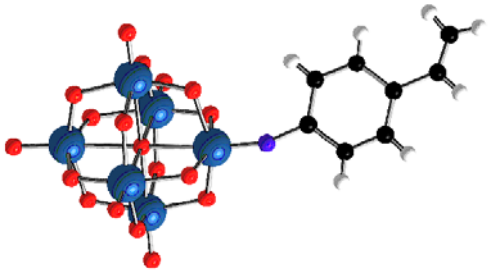

Figure 1-24 Ball and Stick Representation of Styrylimido Hexamolybdate.[41]

copolymerized with 4-methylstyrene to yield a copolymer in a 2.7:1 ratio (4-methylstyrene : styrylimido hexamolybdate). This styrylimido hexamolybdate could also be cross linked using 4-methylstyrene and divinylbenzene. Another hexamolybdate imido polymer has been reported by Peng. In Peng's polymers, the polymers are formed through coupling reactions with various acetylene and halogenated monomers (Figure 1-25).[42]

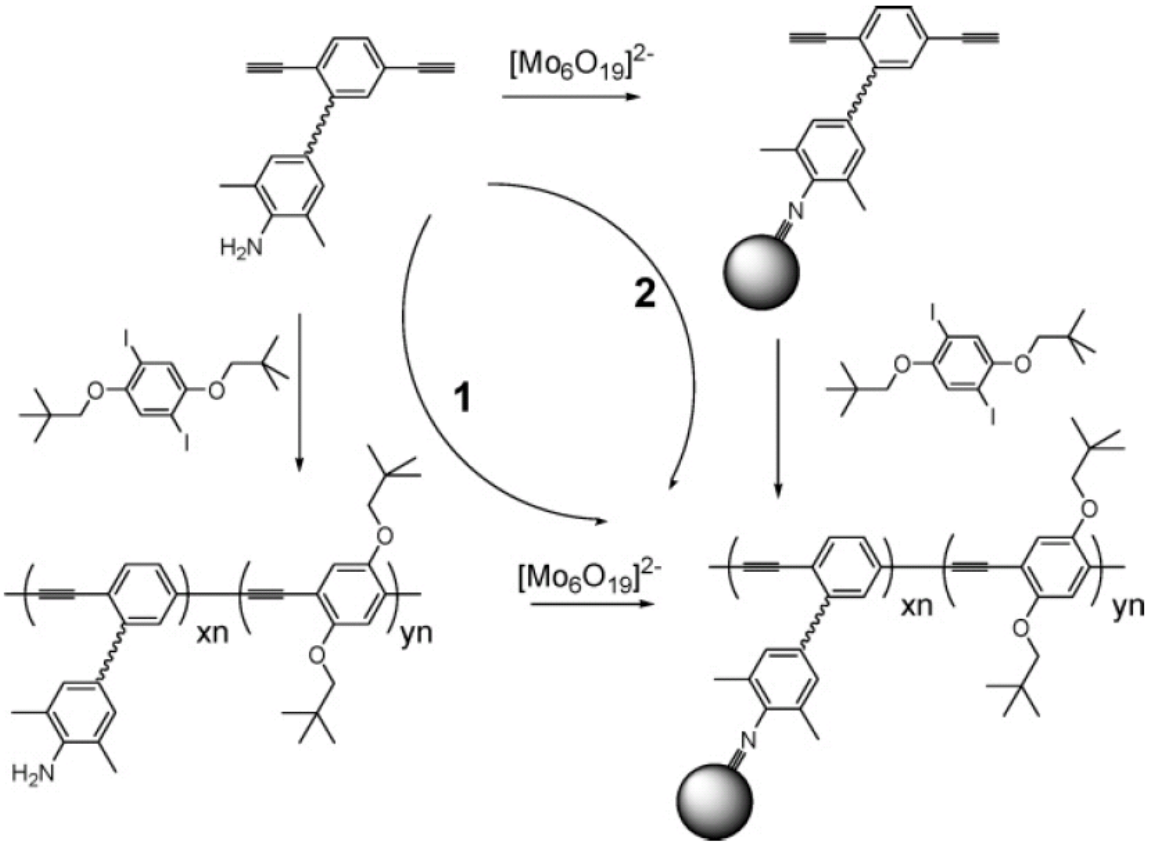

Figure 1-25 Reaction Scheme of the Polymerization by Peng.[42]

1.5 Scope

This thesis will describe the synthesis and characterization of new functionalized polyoxometalates that involve organoimido ligands and a chromium nitride. Chapter 2 will illustrate the synthesis and characterization of a Keggin Cr nitride ($TBA_5PW_{11}O_{39}Cr(N)$) along with studies of its reactivity in nitrogen transfer to an olefin. Chapter 3 will discuss the synthesis and characterization of new metal coordination compounds involving a dithiocarbamate functionality and their potential for becoming new imido ligands for the functionalization of hexamolybdate. Chapter 4 will discuss the synthesis and characterization of a new copolymer involving the styrylimido hexamolybdate and 4-chloromethyl styrene and its future capabilities. Chapter 5 will detail the synthesis and characterization of an iodophenylimido hexamolybdate

([$TBA_2Mo_6O_{18}N$-C_6H_4I]) and its future applications along with the synthesis of 4-amino- and 4-nitro-2,2'-bipyridine.

[1] M.T. Pope, Heteropoly and Isopoly Oxometalates: Springer: Berlin, 1983.
[2] J.J. Borras-Almenar, E. Coronado, A. Muller, and M. Pope, Polyoxometalate Molecular Science: Kluwer, Dordrecht, 2001.
[3] Berzelius, J.J., *Pogg. Ann.*, **1826**, *6*, 369, 380.
[4] Svanberg, L., Struve, H., *J. Prakt. Chem.*, **1848**, *44*, 257, 291.
[5] Keggin, J., *Nature*, **1933**, *131*, 908.
[6] Baker, L., Glick, D., C*hem. Rev.*, **1998**, *98*, 3.
[7] Evans, H.T., *J. Am. Chem. Soc.*, **1948**, *70*, 1291.
[8] Dawson, B., *Acta. Cryst.*, **1953**, *6*, 113.
[9] Pope, M., Muller, A., *Angew. Chem. Int. Ed. Engl.*, **1991**, *30*, 34.
[10] Nagano, O., *Acta. Cryst.* **1979**, *B35*, 465.
[11] Fuchs, J., Freiwald, W., Hartl, H., *Acta. Cryst.*, **1978**, *B34*, 1764.
[12] Du, Y., Rheingold, A., Maatta, E.A., *J. Am. Chem. Soc.*, **1992**, *114*, 345.
[13] Strong, J., Ostrander, R., Rheingold, A., Maatta, E.A., *J. Am. Chem. Soc.*, **1994**, *116*, 3601.
[14] Wei, Y., Xu, B., Barnes, C., Peng, Z., *J. Am. Chem. Soc.*, **2001**, *123*, 4083.
[15] Muller, A., Peters, F., C*hem. Rev.*, **1998**, *98*, 239.
[16] Gomez-Garcia, C., Borras-Almenar, J., Coronado, E., Ouahab, L., *Inorg. Chem.*, **1994**, *33*, 4016.
[17] Artero, V., Proust, A., Herson, P., Gouzerh, P., *Chem. Eur. J.*, **2001**, *7*, 3901.
[18] Kang, H., Lui, S., Shaikh, S., Nicholson, T., Zubieta, J., *Inorg. Chem.*, **1989**, *28*, 920.
[19] Clegg, W., Errington, R., Hockless, D., Radshaw, C., *Polyhedron*, **1989**, *8*, 1788.
[20] Errington, R., Wingad, R., Clegg, W., Elsegood, M., *Angew. Chem. Int. Ed. Engl.*, **2000**, *39*, 3889.
[21] Klemperer, W., Schwartz, C., *Inorg. Chem.*, **1985**, *24*, 4459.
[22] Cadot, E., Bereau, V., Secheresse, F., *Inorg. Chim. Acta*, **1995**, *239*, 39.
[23] Radkov, E., Lu, Y., Beer, R., *Inorg. Chem.*, **1996**, *35*, 551.
[24] Clegg, W., Elsegood, M., Errington, R., Havelock, J., *J. Chem. Soc., Dalton Trans.*, **1996**, 681.
[25] Chen, Q., Zubieta, J., *Inorg. Chem.*, **1990**, *29*, 1456.
[26] Hasenknopf, B., Delmont, R., Herson, P., Gouzerh, P., *Eur. J. Inorg. Chem.*, **2002**, 1081.
[27] Knoth, W., *J. Am. Chem. Soc.*, **1979**, *101*, 2211.
[28] Zonnevijlle, F., Pope, M., *J. Am. Chem. Soc.*, **1979**, *101*, 2731.
[29] Krebs, B., in M.T. Pope and A. Muller, Polyoxometalates: from Solids to Anti-Retroviral Activity, Kluwer, Dordrecht, 1994.
[30] Kang, H., Zubieta, J., *Chem. Comm.*, **1988**, 1192.
[31] Abrams, M., Costello, C., Shaikh, S., Zubieta, J., *Inorga. Chim. Acta.*, **1991**, *180*, 9.
[32] Dablemont, C., Hamaker, C., Thouvenot R., Sojka, Z., Che, M., Maatta, E.A., Proust, A., *Chem. Eur. J.*, **2006**, *12*, 9150.
[33] Strong, J., Yap, G., Ostrander, R., Liable-Sands, L., Rheingold, A., Thouvenot, R., Gouzerh, P., Maatta, E.A., *J. Am. Chem. Soc.*, **2000**, *122*, 639.
[34] Strong, J., Haggerty, B., Rheingold, A., Maatta, E.A., *Chem. Comm.*, **1997**, 1137.
[35] Moore, A., PhD Thesis, Kansas State University, **1998**.
[36] Xu, B., Peng, Z., Wei, Y., Powell, D., *Chem. Comm.*, **2003**, 2562.
[37] Stark, J., Young, V., Maatta, E.A., *Angew. Chem. Int. Ed. Engl.*, **1995**, *34*, 2547.

[38] Clegg, W., Errington, R., Fraser, K., Holmes, S., Schafer, A., *Chem. Comm.*, **1995**, 455.
[39] Stark, J., Rheingold, A., Maatta, E.A., *Chem. Comm.*, **1995**, 1165.
[40] Mayer, C., Labuil, V., Lalot, T., Thouvenot, R., *Angew. Chem. Int. Ed. Engl.*, **1999**, *38*, 3672.
[41] Moore, A., Kwen, H., Beatty, A., Maatta, E.A., *Chem. Comm.*, **2000**, 1793.
[42] Xu, B., Lu, M., Kang, J., Wang, D., Brown, J., Peng, Z., *Chem. Mater.*, **2005**, *17*, 2841.

CHAPTER 2 - A Chromium Nitride Keggin Polyoxometalate

2.1 Introduction

2.1.1 Synthesis of Nitrido Complexes

Nitrido complexes have been studied for many years. During this time, six bonding modes have been identified (Figure 2-1).[1] The majority of the complexes contain either terminal or linearly bridging nitrides. However, in an extreme bridged case, the angle between the metal centers can be as low as 91.3º.[1]

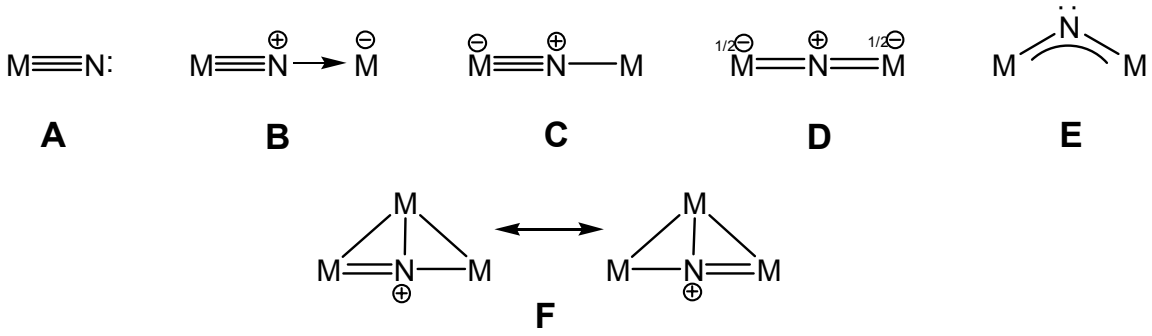

Figure 2-1 Bonding modes of the nitrido ligand: A = terminal, B = asymmetric, linear bridge of the donor-acceptor type, C = asymmetric, linear bridge with covalent bond, D = symmetric, linear bridge, E = bent bridge, F = T-shaped.[1]

Nitrido complexes can be synthesized in a variety of ways. One useful reagent is the bromide of Millon's base ($[Hg_2N]Br$). For example, when $[Hg_2N]Br$ is adding to tungsten hexachloride in boiling carbon tetrachloride, a binuclear nitrido complex is formed and upon further heating yields the tungsten nitride $[WCl_3N]_x$ (Figure 2-2).[1,2]

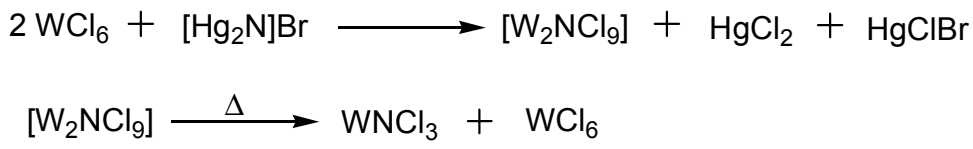

Figure 2-2 Reaction of the Bromide of Millon's Base to produce tungsten nitrido complexes.[1,2]

Nitrogen transfer can yield metal nitride complexes. Reactions of silyated or stannylated amines with metal halides can produce either a dinuclear or mononuclear nitrido complexes.[1] Product formation is controlled by temperature, with higher temperatures (T>20ºC) yielding the mononuclear system (Figure 2-3).[3]

$$2\ WCl_6 + N(SiMe_3)_3 \xrightarrow{T < 20^oC} [W_2NCl_9] + 3\ ClSiMe_3$$

$$WCl_6 + N(SiMe_3)_3 \xrightarrow{T \approx 20^oC} WNCl_3 + 3\ ClSiMe_3$$

Figure 2-3 Reaction of a Silylated Amine to produce a Nitrido Complex.[3]

Reaction of ammonia with metal halides have produced nitrido complexes. However, mononuclear nitrido complexes have not been reported using this route.[1] Dinuclear nitrido complexes have been synthesized using ammonium halide salts (Figure 2-4).[4] Also, a unique

$$2\ NbBr_5 + 4\ NH_4Br \longrightarrow (NH_4)_3[Nb_2NCl_{10}] + 4\ HBr$$

$$2\ WBr_6 + 14\ NBrH \longrightarrow 3\ (NH_4)_3[W_2NBr_{10}] + 20\ HBr + N_2$$

Figure 2-4 Reaction of Ammonia to produce a Nitrido Complex.[4]

tantalum nitrido complex has been reported by the reaction of ammonia with a Ta precursor, $[(tBuCH_2)_3Ta{=}CHtBu]$.[5] This produces a complex where an interesting T-shaped μ_2-nitrido

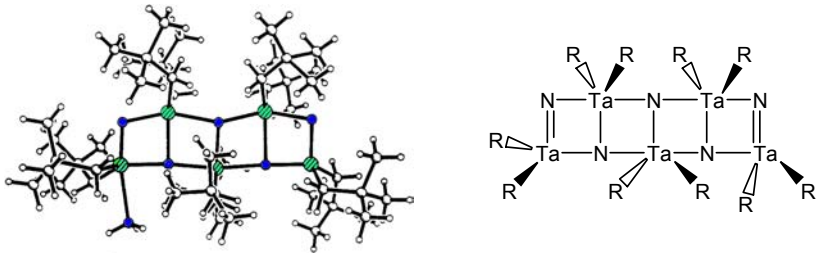

A B

Figure 2-5 Structure of $[\{(t\text{-Butyl-}CH_2)_2TaN\}_5{\cdot}NH_3]$ (A)[5] and Schematic representation of the Ta_5N_5 framework (B).

bridges have an angle of 98º (Figure 2-5) in the structure.[5] Amminal complexes, typically of Os or Cr, can lead to metal nitrides as well. When strong oxidizing agents are used with Os and Cr

ammine complexes, deprotonation occurs forming mononuclear nitrido complexes (Figure 2-6).[6,7]

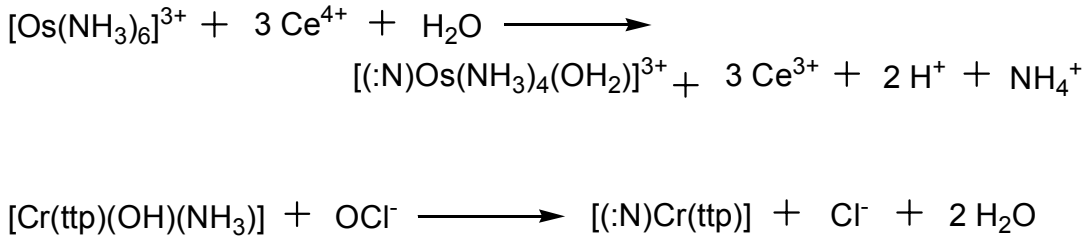

Figure 2-6 Reaction of Ammonia-Metal Complex to produce a mononuclear Nitrido Complex.[6,7]

Azide (N_3) ligands are very common sources for nitrido formation. The N_3 ligand is usually thermally decomposed or photolytically cleaved to produce N_2 and the metal nitride.[1] Many examples exist for synthesizing chromium nitrides from the corresponding azido complexes (Figure 2-7).[8]

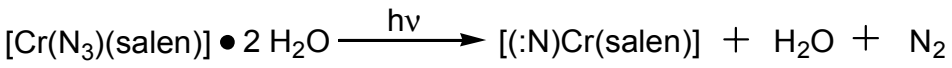

Figure 2-7 Photolysis of an Azide to produce a Nitrido Complex.[8]

2.1.2 Chemical Reactions with Nitrido Complexes

Addition of Lewis acids to nitrido ligands have been known since the '70s. Here, a Re nitride was reacted with boron trihalides to produce a complex with a general formula, where X $[X_2Re{\equiv}N{-}BY_3(PR_3)_3]$ = Cl, Br and Y = F, Cl, Br.[9] The nitride can also undergo electrophilic attack by carbonium ions. In particular, a Mn porphyrin nitride can be activated by trifluoractetic anhydride. This active species has then been reported to transfer the imido to an olefin (Figure 2-8).[10]

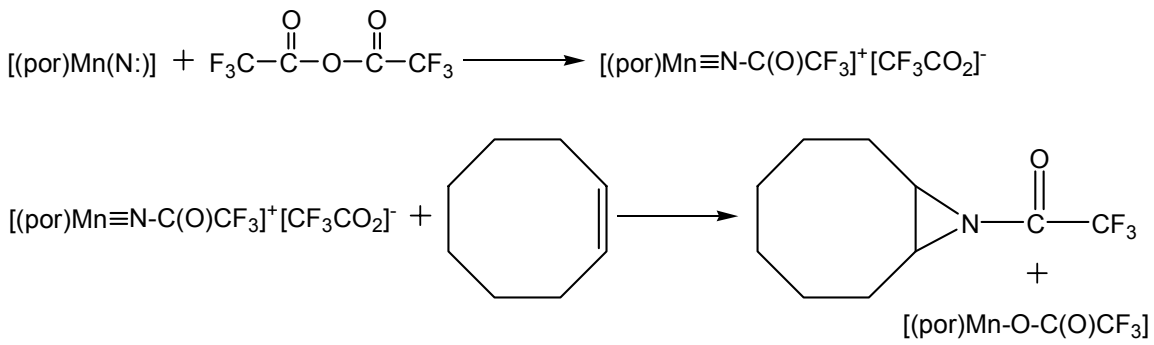

Figure 2-8 Reaction of a Mn Nitrido Porphyrin and sequential imido transfer to an olefin.[10]

The reaction of nitrides with phosphines have been reviewed.[1,11] The resulting phosphoraniminato ($[NPR_3]^-$) lignads are isoelectronic with OPR_3 lignads (Figure 2-9).[1]

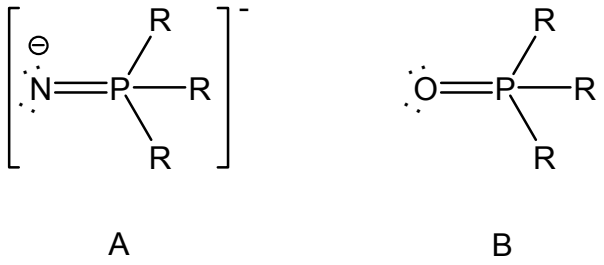

Figure 2-9 Structural representation of the isoelectronic character of phosphoraniminato(A) and phosphine oxide(B).

Nitrides have also been reported to react with element sulfur and undergo substitution reactions.[1] Such substitution reactions generally involve chloronitrido complexes because the chlorine ligand can be displaced easily.

2.1.3 Polyoxometalate Nitride Complexes

The lacunary Keggin ($[XM_{11}O_{39}]^{(n+4)-}$) derives from the parent Keggin structure ($[XM_{12}O_{40}]^{n-}$) from which one $[M^{VI}O]^{4+}$ unit has been removed (Figure 2-10). The lacunary Keggin can now be utilized as a pentadentate ligand presenting five exposed oxygens (red balls in Figure 2-10). Tungsten is usually the preferred cluster framework in such reactions because it

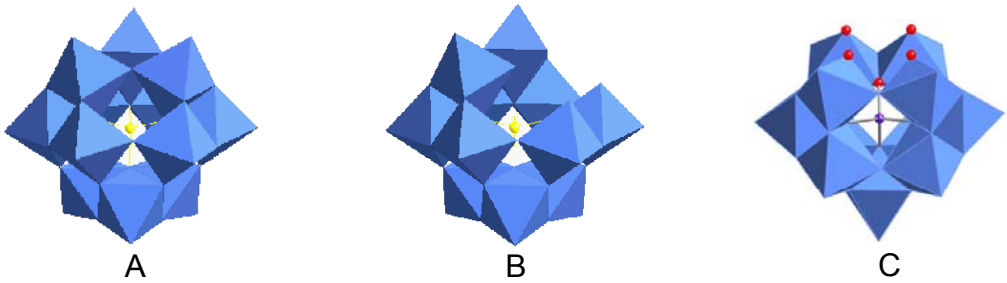

Figure 2-10 Polyhedron representation of $[XM_{12}O_{40}]^{n-}$ (A) and lacunary $[XM_{11}O_{39}]^{(n+4)-}$ (B). The lacunary view in C highlights the five oxygens capable of pentadentate coordination.

is less likely to undergo structural transformation and is more difficult to reduce than the molybdenum analog.[12] The first examples of metal fragments incorporated into lacunary Keggin structures were reported in 1966.[13] The first POM nitrido complex reported was $[Mo_6O_{18}(N)]^{3-}$ by Zubieta in 1988.[14] It, however, was not formed using a lacunary POM, but by self assembly (Figure 2-11).

$$2\,[MoCl_4(N)] + 5\,[Mo_2O_7]^{2-} \xrightarrow{H_2O} 2\,[Mo_6O_{18}(N)]^{3-} + 6\,Cl^- + 2\,HCl$$

Figure 2-11 Cluster assembly of dimolybdate and a nitrido metal complex to produce the first ever nitrido POM.[14]

The next reported nitrido POM was obtained through reaction of the lacunary Keggin, $[PW_{11}O_{39}]^{7-}$, and the nitrido metal complex, $TBA[Tc(N)Cl_4]$.[15] Maatta and Proust have synthesized an Os nitrido Keggin, $[TBA]_4[PW_{11}O_{39}OsN]$, a Re nitrido Keggin, $[TBA]_4[PW_{11}O_{39}ReN]$, via the lacunary Keggin POM (Figure 2-12).[16] They both have recently reported the synthesis of an Os nitrido Dawson, $[TBA]_7[P_2W_{17}O_{61}OsN]$.[17]

$$[TBA][Os(N)Cl_4] + [TBA]_4[H_3PW_{11}O_{39}] \xrightarrow{Et_3N} [TBA]_4[PW_{11}O_{39}Os(N)]$$

$$[TBA][Os(N)Cl_4] + K_{10}[P_2W_{17}O_{61}] \xrightarrow{[TBA]Br} [TBA]_7[P_2W_{17}O_{61}Os(N)]$$

Figure 2-12 Reaction of a nitrido osmium complex with lacunary Keggin and Dawson POMs.[16,17]

The latter three nitrido POMs have been fully characterized by ^{183}W NMR and mass spectrometry. The Os nitrido Keggin has been further studied by 2D COSY and cyclic

voltametry.[17] Herein, I will describe the synthesis, characterization, and reactivity of a new Cr^{V} nitrido Keggin complex.

2.2 Results and Discussion

2.2.1 Results

The Cr nitrido Keggin complex, $[TBA_5][PW_{11}O_{39}CrN]$ was synthesized in a similar procedure as described above, but the difference appears in the unique delivery of the Cr nitride to the POM. The Cr nitride precursor, $[NCr^{V}(THF)_x]^{2+}$, was obtained through a nitrogen atom transfer reaction as described by Bendix.[18] The first inter-metal nitrogen atom transfer was reported by Takahashi[10] and later by Woo[19] and Neely[20].

In order to obtain the Cr nitride precursor, first a Mn^{V} nitrido salen complex, $[NMn^{V}C_{16}H_{14}N_2O_2]$, was obtained by a reported literature method.[20] Secondly, the Cr^{III} chloride tetrahydrofuran complex, $[Cr^{III}Cl_3(THF)_x]$ was synthesized according to literature.[21] The Mn nitrido salen complex was then reacted with the Cr^{III} chloride-tetrahydrafuran complex in acetonitrile to yield a "naked" Cr^{V} nitrido species, $[NCr^{V}(THF)_x]^{2+}$ in solution and a precipitate that consisted of the Mn^{III} chloride salen complex (Figure 2-13). The Mn chloride salen was removed from the solution by filtration to yield a solution of $[NCr^{V}(THF)_x]^{2+}$.

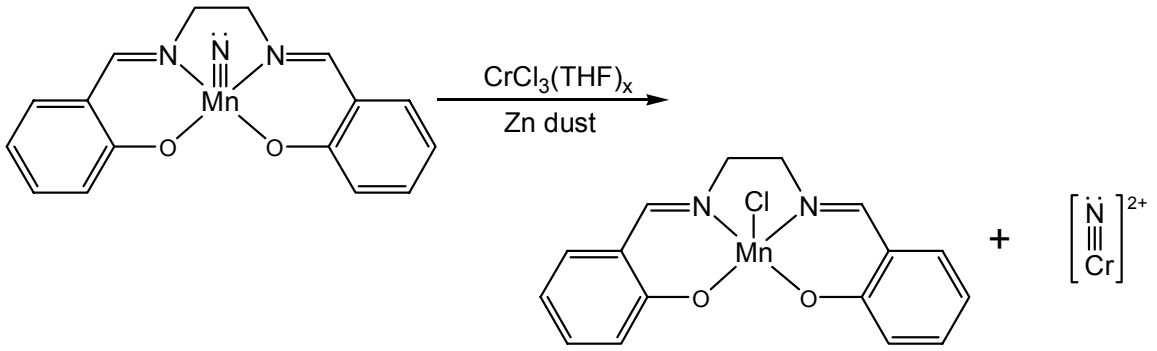

Figure 2-13 Reaction scheme for the formation of the "naked" Cr nitride.

The lacunary Keggin complex, $[TBA]_4[H_3PW_{11}O_{39}]$, was dissolved in acetonitrile and introduced into the solution along with 1 equivalent of [TBA]Br and 4 equivalent of Et_3N. The amine was added to the solution to absorb HBr produced during the exchange of the hydrogen counterion for the TBA counterion in an attempt to prevent any side products resulting from the reaction of HBr and the POM. The [TBA]Br was added to provide the needed counter ion for the product. The resulting pumpkin-colored precipitate was then collected on a frit, washed with

ether, and dried to yield the desired Cr nitrido Keggin complex, $[TBA]_5[PW_{11}O_{39}Cr^VN]$. Purification was completed by slow diffusion of ether into an acetonitrile solution of $[TBA]_5[PW_{11}O_{39}Cr^VN]$ to yield pumpkin colored crystals in moderate yields (59%).

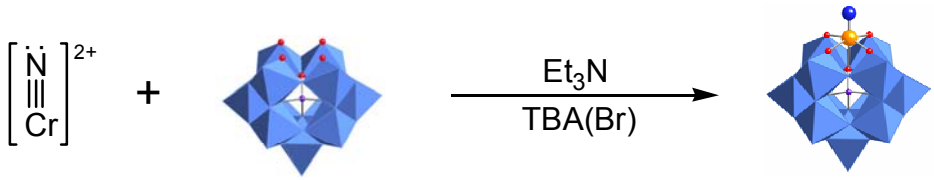

Figure 2-14 Reaction scheme for the insertion of the "naked" Cr nitride, $[NCr^V(THF)_x]^{2+}$, with the lacunary Keggin, $[TBA]_4[H_3PW_{11}O_{39}]$, to form the complex $[TBA]_5[PW_{11}O_{39}Cr^VN]$.

Characterization of the Cr^V nitrido Keggin was limited to the fact that in this case Cr is d^1 and paramagnetic. This, unfortunately, resulted in no NMR data being recorded. However, IR spectroscopy and mass spectroscopy was preformed on the POM. The best evidence supporting the formation of the Cr nitrido Keggin was obtained through mass spectrometric analysis (Figure 2-15). The major peak in the spectrum was observed at 3955 m/z as expected for $[TBA]_5[PW_{11}O_{39}Cr^VN]$. However, there is one interesting feature in which another peak, albeit minor in intensity, appears at 3941 m/z. This correlates to the loss of 14 m/z which we attribute to the loss of the nitrido functionality, $[TBA]_5[PW_{11}O_{39}Cr]$. This observation was considered very encouraging because it may indicate the desired N-atom transfer reactivity of the $[TBA]_5[PW_{11}O_{39}Cr^VN]$. This analysis also shed some light on the purity of the Cr nitrido Keggin from the initial stages of the synthesis. The mass spectrum was found to be nearly identical whether a crude sample from the initial precipitate or crystals was analyzed. In fact, multiple recrystalizations resulted in mass spectrums that had smaller intensities of the 3955 peak and larger intensities of the 3941 peak. Also, a color change was observed after multiple recrystalizations from a pumpkin color to a bright red color.

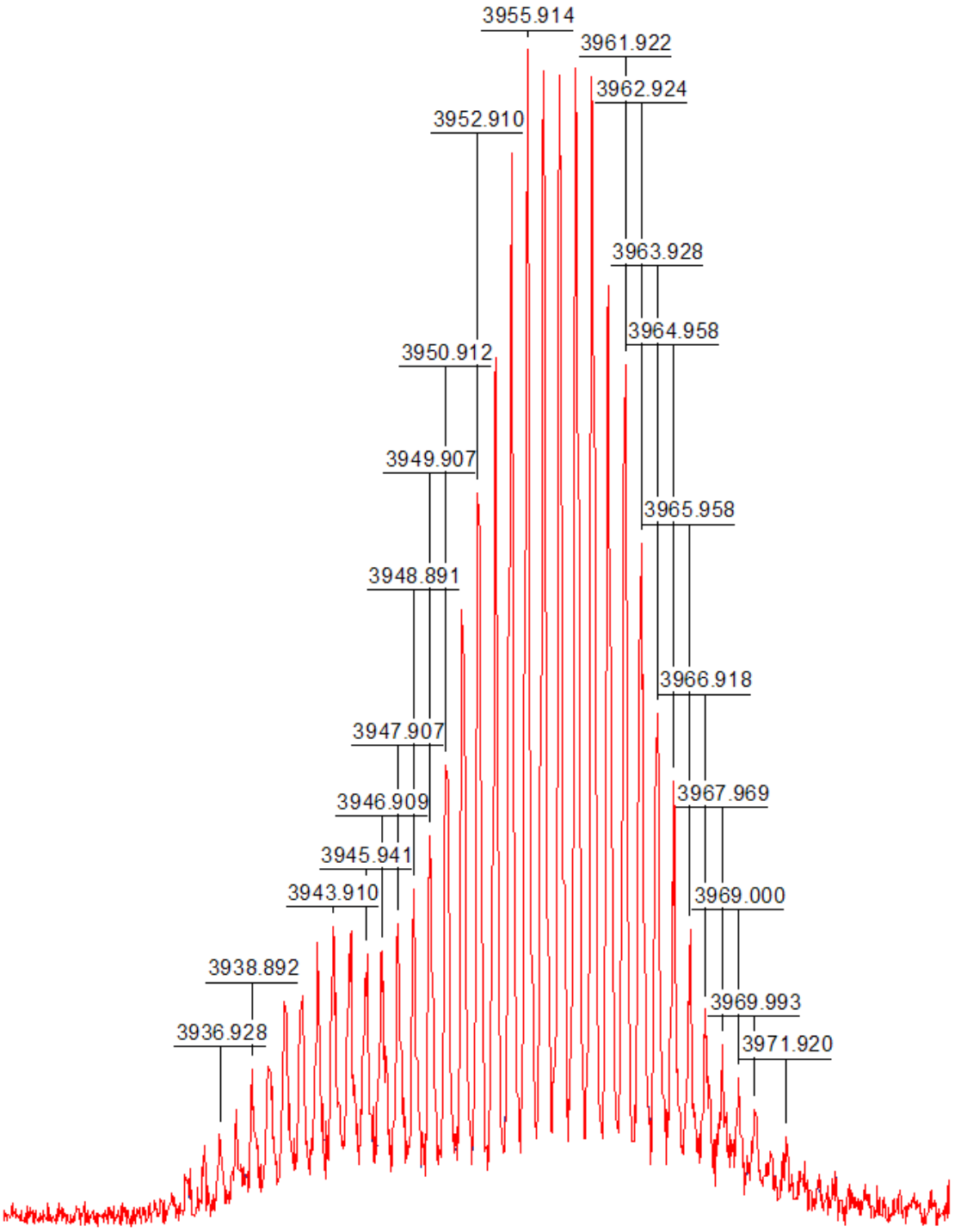

Figure 2-15 Observed mass spectrum of $[TBA]_5[PW_{11}Cr^{V}N]$.

IR studies conducted on the Cr nitrido Keggin produced similar results as the previously reported Os nitrido and Re nitrido Keggin structures.[17] These similarities should be expected as the basic structure of the POM has not been changed. The W-O stretches are all similar in

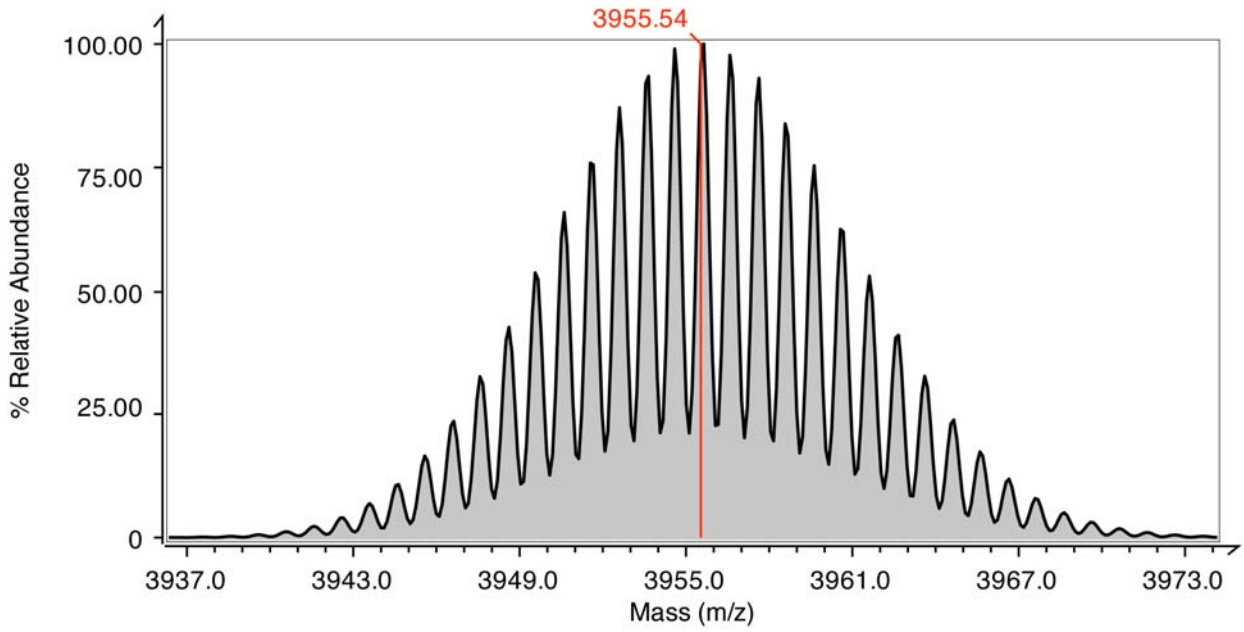

Figure 2-16 Simulated mass spectrum of $[TBA]_5[PW_{11}Cr^{V}N]$.

frequency. The intense peak around 1070 cm^{-1} is assigned to the antisymmetric stretch of the PO_4 tetrahedron which implies relatively strong interaction with the substituted metal. The metal nitride stretch is observed in the chromium nitrido case, but was not reported for the other Keggin compounds (Table 2).

Table 2 Selected IR stretches for the Keggin, lacunary Keggin, and Nitrido Keggin POMs.

	Frequency (cm^{-1})				
Compound	ν (P-O)	ν (W-O_t)	ν (W-O_c-W)	ν (W-O_e-W)	ν (M-N)
$[\alpha\text{-}PW_{12}O_{40}]^{3-}$	1080	973	893	810	-----
$[\alpha\text{-}H_3PW_{11}O_{39}]^{4-}$	1100	950	878	790	-----
$[\alpha\text{-}PW_{11}O_{39}Os(N)]^{4-}$	1072	963	884	811	-----
$[\alpha\text{-}PW_{11}O_{39}Re(N)]^{4-}$	1072	961	881	802	-----
$[\alpha\text{-}PW_{11}O_{39}Cr(N)]^{5-}$	1063	960	891	814	1002
O_t = terminal oxygen, O_c = corner bridging oxygen, O_e = edge bridging oxygen					

The reactivity of the Cr nitrido Keggin was investigated by one particular process. It was to see if the nitrido POM could be an effective donor for nitrogen transfer reactions. The process

followed was very similar to that of Groves.[10] The Cr nitrido POM was dissolved in dry acetonitrile. A slight excess of triflouroacetic anhydride (TFAA) was added slowly by a syringe and followed by the addition of cyclooctene (Figure 2-16).

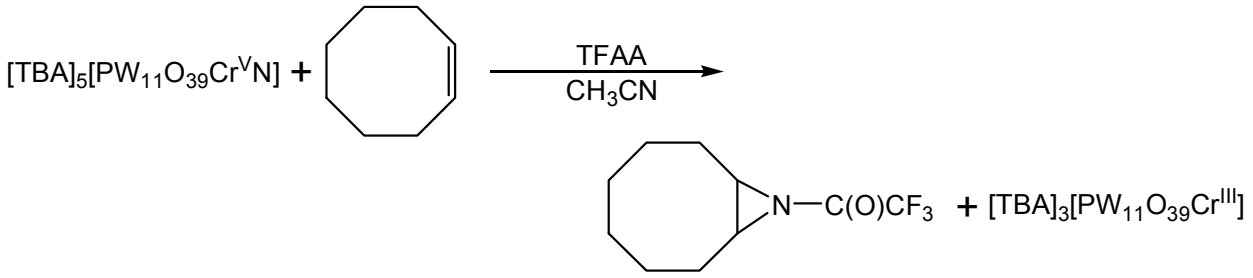

Figure 2-17 Reaction scheme for the imido transfer to cyclooctene.

Within 30 seconds, the reaction had turned from a pumpkin color to a light green. This change in color is a very good indication that Cr has been reduced from Cr^{V} to Cr^{III} (which is typically green in color). The resulting precipitate was removed and the green solution was analyzed. Unfortunately, ^{1}H NMR was ineffective because of the lingering effects of the paramagnetic Cr. Attempts to remove the paramagnetic Cr species from the solution were unsuccessful. Column chromatography was attempted to remove the paramagnetic Cr and either the aziridne product was destroyed or was never removed from the column. Mass spectrometry was performed on every sample obtained and produced a spectrum that corresponded to the expected mass of the aziridine product plus one sodium atom (244 amu). This observation has yet to be explained, but was observed in every sample. The sodium source has yet to be identified, but the mostly likely source is from the matrix used in the instrument. HPLC was also used to investigate the reaction products. This was performed on two separate HPLC setups and in both cases produced a spectrum that consisted of one new unassigned peak. This unassigned peak, we believe, was the result of the formation of the aziridine. The peak due to cyclooctene is ~8.5 min. and the new peak was observed at a retention time of ~12.3 min.. This could be consistent with the formation of the aziridine product. Unfortunately, reproducibility is a problem. The reaction conditions have been varied and/or repeated exactly to the initial process and have failed in producing a color change and/or azidirine formation. New samples of the Cr nitrido POM have been synthesized, but again have yielded no results. Likewise, new TFAA

and cyclooctene samples have been purchased and again yielded no results. Further investigation on the transfer of the nitrido to an olefin is still currently underway.

The Cr nitrido POM was also reacted with a dimethylphenylphosphine, $(Ph)PMe_2$. Initial observations were encouraging due to a color change (pumpkin to green). However, no analytical data supporting the formation of the phosphineimine was obtained. IR data did not reveal any strong stretches in the expected region for the P-N bond. Mass spectrometry was inconclusive due to the number of complicated peaks observed. Matching the mass number observed in the spectra to a possible product was unsuccessful. Further attempts to produce a phosphineimine Cr POM are currently underway.

For future studies (Figure 2-17), the Cr nitrido POM needs to be investigated with alkyating agents. There is good evidence that this will be successful in the fact that the transfer of the nitrido to an olefin has been observed. Future studies could include the reaction with methyl iodide or perhaps the isolation of the active species in the nitrogen transfer reaction resulting from the addition of the trifluoroacyl fragment.

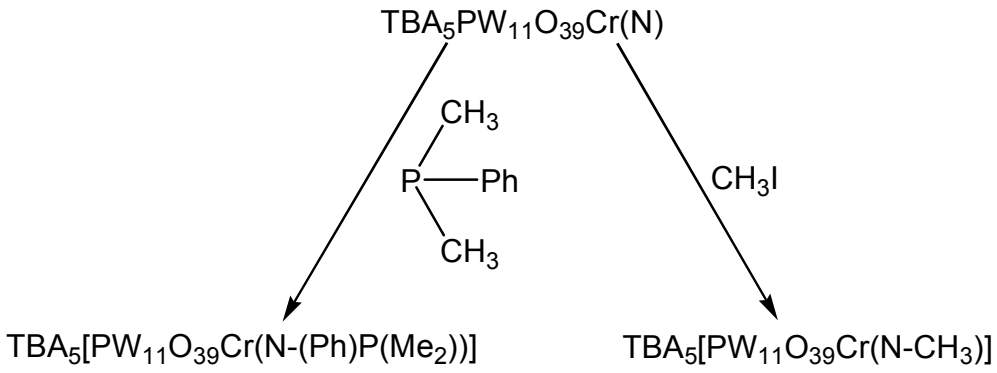

Figure 2-18 Future Reaction Schemes for Cr Nitrido Keggin

2.2.2 Conclusions

A new and exciting chromium nitride Keggin has been synthesized and characterized by IR and mass spectrometry. The chromium nitride has been tested for its ability to transfer its nitrogen to an olefin. Evidence for formation of an aziridine has been observed by mass spectrometry, and likewise, a new peak consistent with the formation of an aziridine was observed in HPLC experiments. Unfortunately, these nitrogen transfer reactions are not yet

reproducible. Further experiments need to be conducted in order to fully understand the reactivity of the nitride. As described above, reactions with phosphines and alkylating agents will also be investigated.

2.3 Experimental

2.3.1 Instrumentation

Starting materials were purchased from Aldrich and used without further purification. THF was dried over sodium and CH_3CN was dried over CaH_2. ^1H NMR spectra were recorded on a Varian Unity plus 400 MHz or 200 MHz spectrometer in CD_3CN or CD_3Cl. Compounds were prepared for infrared (IR) analysis on a Nicolet Protégé 460 as KBr pellets. Mass spectra, MALDI-TOF/ TOF-MS, were collected on a Bruker Daltonics Ultraflex TOF/TOF.

$[TBA]_4[H_3PW_{11}O_{39}]$[22], Mn(N) salen[20], $CrCl_3(THF)_x$[21], $NCr(THF)_x$[18], were prepared according to literature methods.

The chromatographic system consisted of a HP1090 high-performance liquid chromatography with a HP3396 Series III integrator. There was a 10-mL injection loop employed. The column consisted of a Zorbax ODS (DuPont Intruments) 4.6mm X 25cm C_{18} stationary phase with 5 micron particle size column. The column separations were evaluated at a solvent flow rate of 1 mL/min. The detection was done at 254 nm. The mobile phase was acetonitrile/water. The gradient for the first 10 min was 70/30. The gradient was increased to 90% acetonitrile over the next 10 minutes at a rate of 2%/min. This gradient was held for another 10 minutes.

2.3.2 Synthesis

2.3.2.1 Preparation of Lacunary $TBA_4H_3PW_{11}O_{39}$ Keggin (1)[22]

$$Na_2WO_4\bullet 2H_2O + Na_2HPO_4\bullet 7H_2O \xrightarrow[TBABr]{\text{Conc. HCl}} [TBA]_4[H_3PW_{11}O_{39}] \quad (\mathbf{1})$$

$Na_2HPO_4 \cdot 7H_2O$ (1.48 g, 5.5 mmol) and $Na_2WO_4 \cdot 2H_2O$ (20.0 g, 60.6 mmol) were added to an Erlenmeyer flask and dissolved in 40 mL of water. To this solution, 4 mL of concentrated HCl was added very slowly with a pipette over 15 minutes. If a white precipitate formed, it was allowed to dissolve before any further HCl was added. Upon complete addition, the solution was stirred at room temperature for one hour and a white precipitate formed. Next, concentrated HCl was added dropwise with a pipette until the pH reached a value between 5.5 and 5.0 during which the white precipitate dissolved again. For the next 30 minutes, dilute HCl was added to keep the pH in this range. A solution of TBABr (8.0 g, 25 mmol) in 60 mL of water was added to induce precipitation of the product. The product was collected onto a frit and washed several times with water and ether. To the remaining solution, the pH is lowered to a range of 1.1 to 1.2 with dilute HCl. The solution is stirred for another 10 minutes to complete the precipitation. The white precipitate is collected on a frit and washed with water and ether. The combined precipitate was dried under vacuum to remove any volatiles. Yield (19.8 g, 98%).
^{31}P NMR (CD_3CN): δ = -11.91 (s). IR (KBr pellet, cm^{-1}): 957 (s) and 886 (s).

2.3.2.2 Preparation of Manganese Nitride Salen (2)[20]

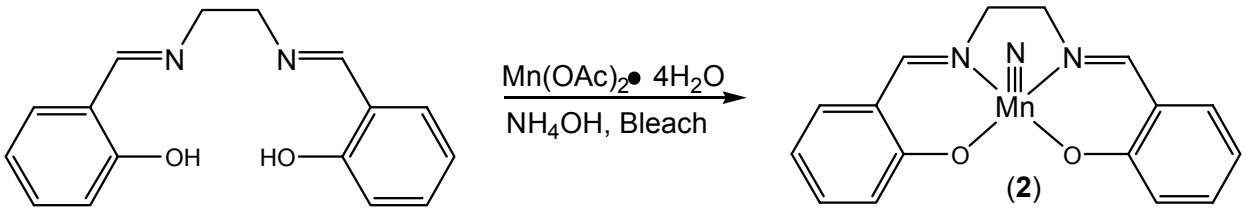

(**2**)

Salen (8.26 g, 30.8 mmol) was suspended in 400 mL of methanol and heated to 55°C. $Mn(OAc)_2$ (7.9 g, 32.4 mmol) was added in small portions to produce a brown solution. This

brown solution was refluxed for 1 hour. The solution was then cooled to room temperature and stirred for another 30 minutes. Next, 31 mL of concentrated NH_4OH was added with a pipette over 5 minutes. 0.7M NaOCl (280 mL) was added with a pipette over 40 minutes. After complete addition, the solution was placed in an ice bath and 400 mL of dichloromethane was added very slowly. The mixture was warmed to room temperature and stirred for 15 minutes. 200 mL of water was added and the organic layer was separated with a separatory funnel. The aqueous layer was further extracted with additional dichloromethane. All dichloromethane fractions were combined and washed with an additional 200 mL of water. The solvent was removed and a green precipitate was obtained. Pure product was obtained by column chromatography (elutent dichloromethane). Yield (5.15 g, 70%).

^{1}H NMR ($CDCl_3$): δ = 3.77 (m, 2H), 3.89 (m, 2H), 6.69 (M, 2H), 7.17 (m, 4H), 7.39 (m, 2H), and 8.06 (s, 2H).

2.3.2.3 Preparation of Chromium Trichloride Tetrahydrofuranate (3)[21]

Anhydrous $CrCl_3$ (12.21 g, 77.1 mmol) was mixed with a small amount (0.15 g) of zinc dust in a Soxhlet thimble inside the glovebox. 140 mL of dry THF was transferred to a flask and connected to the Soxhlet extractor. The setup was refluxed overnight to yield a dark purple solution in the receiving flask. The solvent was removed on the vac-line and the purple precipitate was stored in the glovebox. Yield (9.30 g, 76%).

IR (Nujol, cm^{-1}): 1010 (s) and 880 (s).

2.3.2.4 Preparation of "Naked" Chromium Nitride (4)[18]

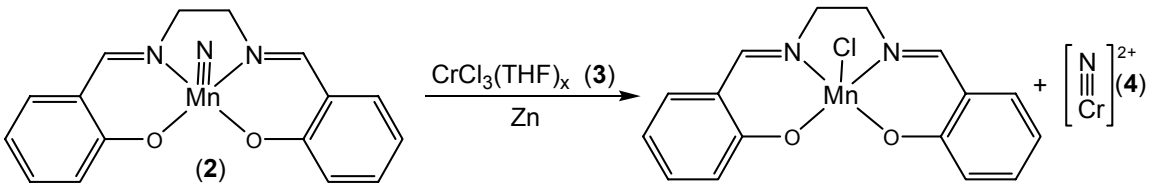

(**3**) (0.906 g, 2.42 mmol) was added to a flask in the glovebox. To this flask, (**2**) (.810 g, 2.42 mmol) was added along with 25 mL of dry acetonitrile. Immediate color change occurred and this mixture was stirred for 30 minutes at room temperature. An insoluble brown precipitate was filtered off and the resulting yellow-brown solution was used as is in the following step. Yield (assumed to be quantitative).

2.3.2.5 Preparation of Chromium Nitride Keggin (5)

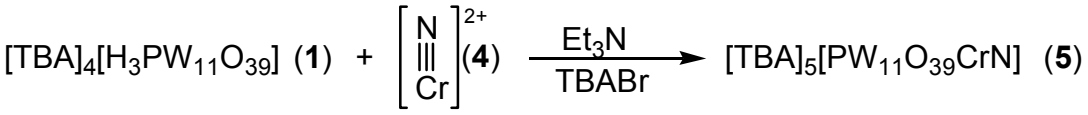

To the solution of (**4**), (**1**) (8.83 g, 2.42 mmol) was added along with 4 equivalents (0.55 mL) of Et_3N by syringe. Also, 1 equivalent (0.322 g) of [TBA]Br was added. This mixture was stirred at room temperature overnight to produce a pumpkin colored precipitate. The precipitate was collected on a frit and dried under vacuum. Yield (5.69 g, 59%).

IR (KBr pellet, cm^{-1}): 1100 (s), 1063 (s), 1002 (w), 960 (s), 891 (s), and 814 (s). MS (MALDI, *m/z*): 3955 calculated for ($C_{80}H_{180}N_6PW_{11}O_{39}Cr$)= 3955.51.

2.3.2.6 Nitrogen Atom Transfer Procedure

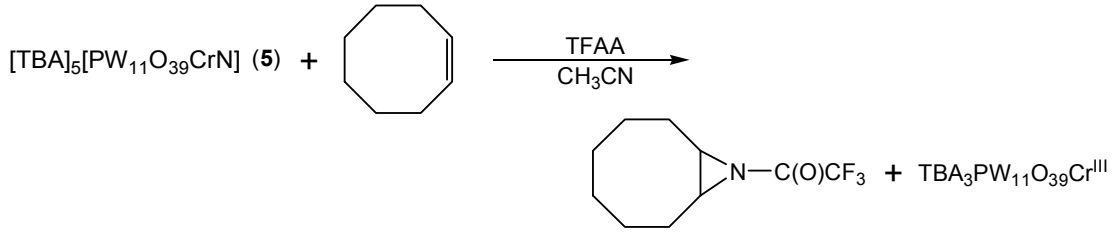

(**5**) (0.259 g, 0.0806 mmol) was dissolved in 10 mL of dry acetonitrile under a flow of argon. To the pumpkin colored solution, TFAA (0.014 mL, 0.0967 mmol) was added by syringe followed by the addition of cyclooctene (0.114 mL, 0.0806 mmol) and stirred for 8 hours at room temperature. The solution turned green within 30 seconds. The solution was filtered to remove any precipitates and analyzed.

MS (MALDI, *m/z*): 244 calculated for ($C_{10}H_{14}NOF_3Na$)= 244.21. HPLC: ~12.3 min.

[1] Dehicke, K., Strahle, J., *Angew. Chem.*, **1981**, *93*, 451; *Angew. Chem. Int. Ed. Engl.*, **1981**, *20*, 413; *Angew. Chem. Int. Ed. Engl.*, **1992**, *31*, 955.
[2] Godmeyer, T., Dehnicke, K., Fluck, E., *Z. Anorg. Allg. Chem.*, **1988**, *565*, 41.
[3] Godmeyer, T., Berg, A., Gress, H., Mueller, U., Dehnicke, K., *Z. Naturforsch B.*, **1988**, *40*, 999.
[4] Horner, M., Frank, K., Strahle, J., *Z. Haturforsch B.*, **1986**, *41*, 423.
[5] Holl, M., Wolczanski, P., Van Duyne, G., *J. Am. Chem. Soc.*, **1990**, *112*, 7989.
[6] Buchler, J., Dreher, C., Lay, K., *Z. Naturforsch B.*, **1982**, *37*, 1155.
[7] Buchler, J., Dreher, C., Lay, K., Lee, Y., Scheidt, W., *Inorg. Chem.*, **1983**, *22*, 888.
[8] Arshankow, S., Poznjok, A., *Z. Anorg. Allg. Chem.*, **1981**, *481*, 201.
[9] Chatt, J., Heaton, B., *J. Chem. Soc. A.*, **1971**, 705.
[10] Groves, J., Takahashi, T., *J. Am. Chem. Soc.*, **1983**, *105*, 2073.
[11] Dehnicke, K., Strahle, J., *Polyhedron*, **1989**, *8*, 707.
[12] M. T. Pope, "Heteropoly and Isopoly Oxometalates", Springer-Verlag: New York, 1983.
[13] Baker, L., Baker, V., Eriks, K., Pope, M., Shibata, M., Rollins, O., Fang, J., Koh, L., *J. Am. Chem. Soc.*, **1966**, *88*, 2329.
[14] Kang, H., Zubieta, J., *Chem. Comm.*, **1988**, 1192.
[15] Abrams, M., Costello, C., Shaikla, S., Zubieta, J., *Inorg. Chim. Acta.*, **1991**, *180*, 9.
[16] Kwen, H., Tomlinson, S., Maatta, E.A., Dablemont, C., Thouvenot, R., Proust, A., Gouzerh, P., *Chem. Comm.*, **2002**, 2970.
[17] Dablemont, C., Hamaker, C., Thouvenot, R., Sojka, Z., Che, M., Maatta, E.A., Proust, A., *Chem. Eur, J.*, **2006**, *12*, 9150.
[18] Birk, J., Bendix, J., *Inorg. Chem.*, **2003**, *42*, 7608.
[19] Woo, L., Goll, J., Czapla, D., Hays, J., *J. Am. Chem. Soc.*, **1991**, *113*, 8478.
[20] Bottomley, L., Neely, F., *Inorg. Chem.*, **1997**, *36*, 5435.
[21] Herwig, W., Zeiss, H., *J. Org. Chem.*, **1958**, *23*, 1404.
[22] Ho, R., Ph.D. Thesis, Columbia University, **1979**.

CHAPTER 3 - Synthesis of a Series of Metal Dithiocarbamate Complexes

3.1 Introduction

3.1.1 Dithiocarbamates

Dithiocarbamates ($R_2CNS_2^-$ or DTCs) are monoanionic 1,1-dithio ligands (Figure 3-1) and have been reviewed many times.[1,2,3] It is not entirely clear when the first was discovered,

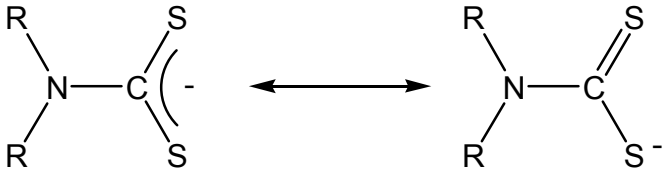

Figure 3-1 The dithiocarbamate functionality.

but Debus reported the synthesis of dithiocarbamic acids in 1850.[4] The first transition metal complex is thought to be reported by Delepine in 1907.[5] His observations included water soluble salts with alkali and alkali earth metals, but transition metals and lanthanides precipitated from water. From these observations, DTCs complexes have gained popularity in HPLC, GC, fungicides, and pesticides as well as spawning other DTC related ligands (Figure 3-2).[3]

DTCs have typically been synthesized with secondary amines (R_2NH), carbon disulfide (CS_2), and a base (usually NaOH or KOH) as depicted in Figure 3. The sodium and potassium salts are usually very soluble in water, but have limited solubility in common organic solvents. Solubility in organic solvents can be improved by preparation of ammonium salts of these ligands. Transition metal DTC complexes are usually synthesized by direct ligand addition (Figure 3-3). DTC complexes are known for all transition metals and in some case multiple oxidation states (Table 3).[3]

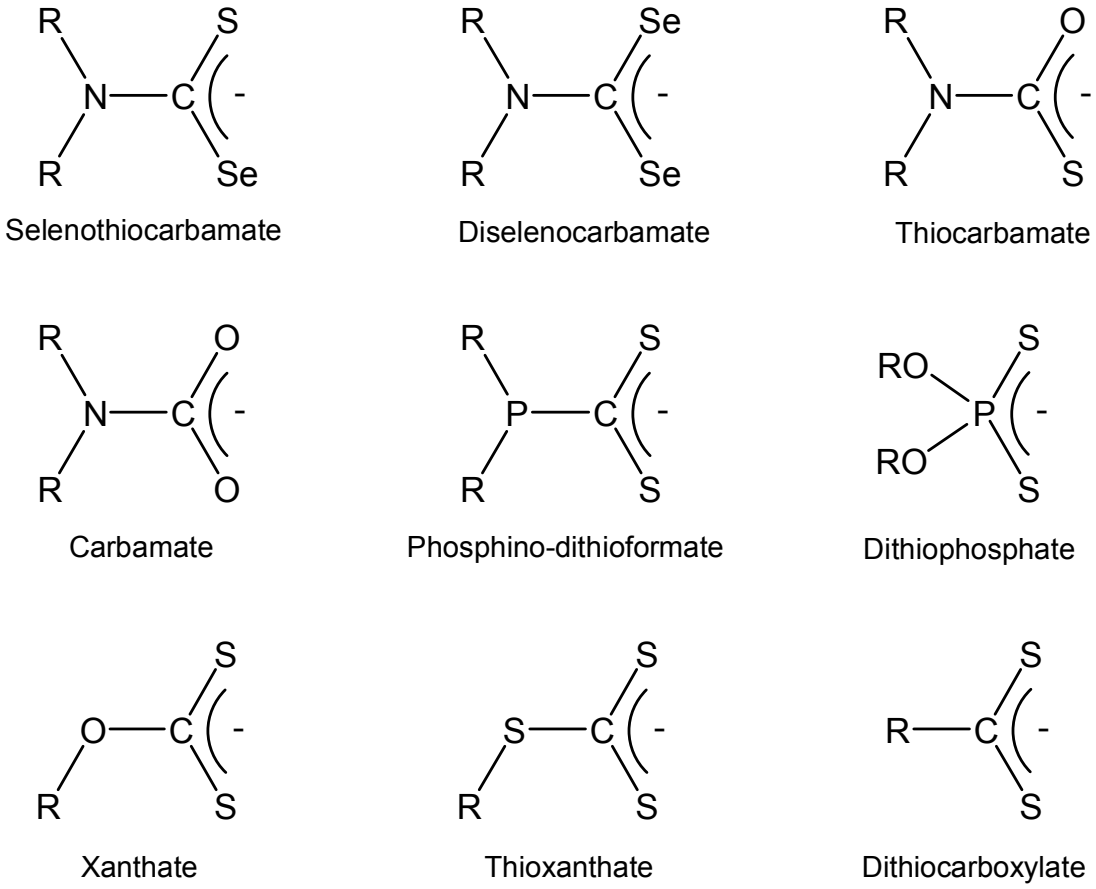

Figure 3-2 Functional groups that are related to dithiocarbamates.[3]

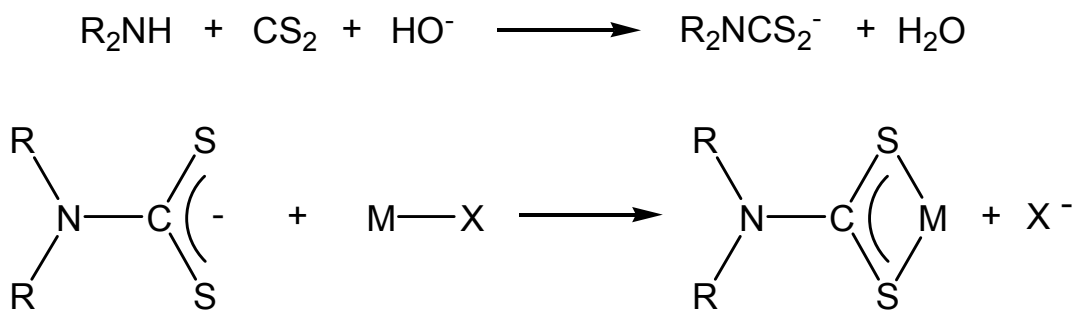

Figure 3-3 Reaction scheme for the formation of dithiocarbamates and dithiocarbamate metal complexes.

Table 3 Oxidation states of transition metal complexes involving dithiocarbamates.[3]

Ti	+4	V	+3	Cr	0	Mn	+1	Fe	+2	Co	+1	Ni	+1	Cu	+1	Zn	+2
	+3		+4		+2		+2		+3		+2		+2		+2		
			+5		+3		+3		+4		+3		+3		+3		
					+4		+4				+4		+4				
Zr	+4	Nb	+3	Mo	0	Tc	+1	Ru	+2	Rh	+1	Pd	+2	Ag	+1	Cd	+2
			+4		+1		+2		+3		+2		+3		+2		
			+5		+2		+3		+4		+3						
					+3		+4										
					+4		+5										
					+5												
					+6												
Hf	+4	Ta	+3	W	0	Re	+1	Os	+2	Ir	+1	Pt	+2	Au	+1	Hg	+2
			+4		+2		+2		+3		+3		+3		+2		
			+5		+3		+3		+4				+4		+3		
					+4		+4		+6								
					+5		+5										
					+6												

DTCs can bind from one to four transition metals in a variety of coordination modes (Figure 3-4).[3] By far the most common coordination mode is the chelating mode (A). The two sulfur atoms coordinate to the metal in equal strength displaying the characteristic that the electrons are equally distributed between the sulfur atoms.

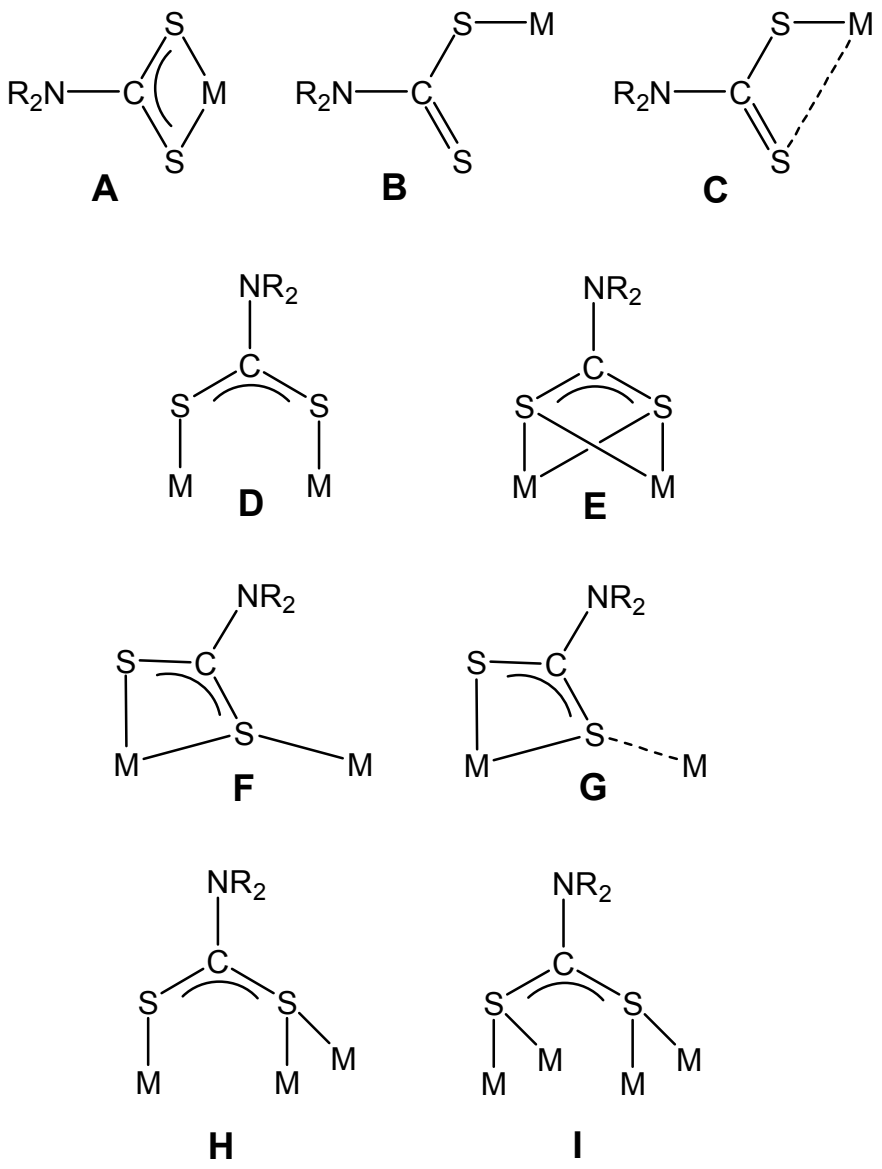

Figure 3-4 Possible coordination modes for dithiocarbamates.[3]

As monoanionic species, DTCs can be thought of as four electron donor ligands. However, when counting electrons, neutral DTCs are considered to be three electron donors. The chelating mode is known for all transition metal atoms. The other coordination modes are somewhat less observed.

The monodentate coordination mode (B) is usually observed when steric effects do not allow bidentate ligands. Figure 3-5 is a prime example where the triazacyclononane ligand is

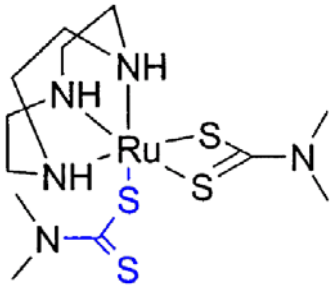

Figure 3-5 Terminally bound dithiocarbamate (Mode B).[6]

tightly bound to the ruthenium and cannot be displaced by the second sulfur atom of the DTC.[6] In the asymmetric coordination mode (C), mercury and gold are usually involved. This coordination mode is observed when the metal prefers a linear two-coordinate geometry (Figure 3-6).[7]

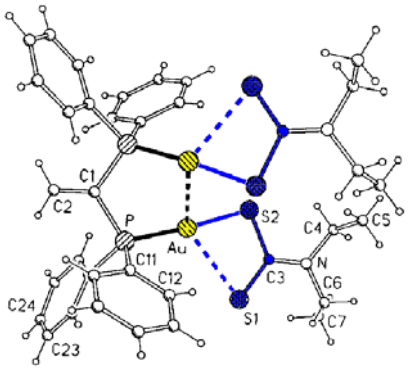

Figure 3-6 Asymetric binding dithiocarbamate (Mode C).[7]

The η^1,η^1-coordination mode (D) is not a common coordination mode for DTCs, but has been observed in tungsten, platinum, and gold complexes. Here, each sulfur atom is coordinated to one metal center (Figure 3-7).[8] In coordination mode (E), each sulfur atom is bound to each metal center. This has only been observed in dirhodium cases (Figure 3-7).[9]

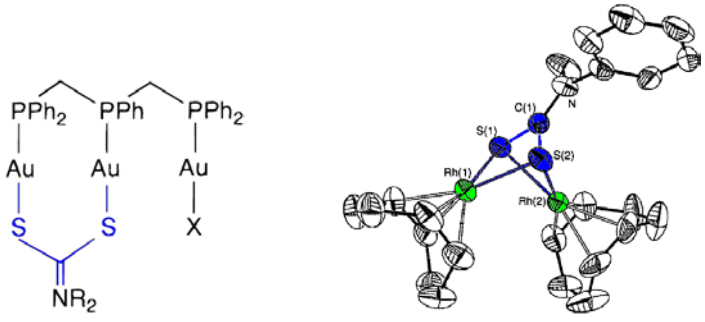

A **B**

Figure 3-7 η^1,η^1-bridging (A)[8] and η^2,η^2- bridging dithiocarbamates (B)[9] (Mode D and E respectively).

The first of the bridging coordination modes (F) is one in which one sulfur atom bridges two metal centers and the other is only coordinated to one metal center. The interesting feature is that all of the sulfur-metal bonds are similar in length (Figure 3-8).[10] This observation is not limited to single metal complexes, but is also observed for mixed metal systems. The second

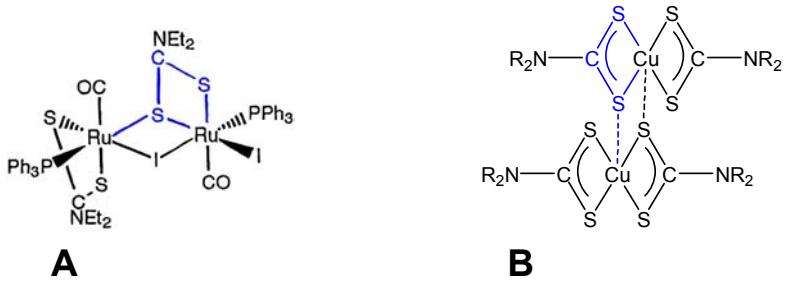

Figure 3-8 Synmetric η^2-bridging (A)[10] and asymmetric η^2-bridging dithiocarbamates (B)[11] (Modes F and G respectively).

bridging mode (G) is very similar to the previous one except the sulfur interactions are unsymmetrical. This interaction is typically observed when the DTCs are holding layers of metal complexes together (Figure 3-8).[11]

The final two coordination modes involve DTC as a "capping" ligand. Both of these modes are very uncommon and appear to be limited to late transition metal complexes. In coordination mode (H), the DTC binds to the metal centers in a η^1,η^2-manner (Figure 3-9).[3] Finally in coordination mode (I), the DTC binds in a η^2,η^2-manner (Figure 3-9).[3]

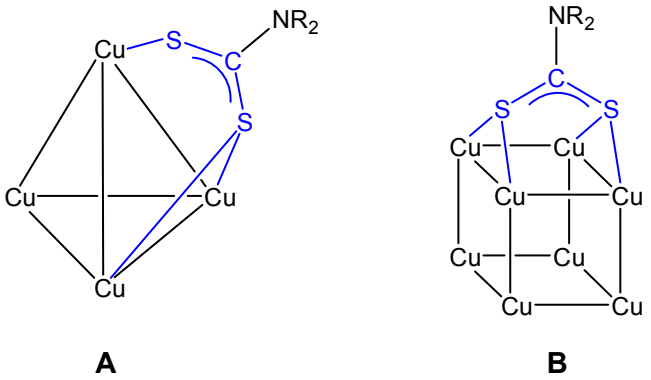

Figure 3-9 Capping a triangular metal face (A)[3] and a square metal face (B)[3] (Modes H and I respectively).

3.1.2 Remote Functionality of Hexamolybdate for Metal Coordination

Functionalized POMs have been studied and reviewed over the last few decades.[12,13,14] With this desire to create functionalized POMs, the Maatta group has focused on trying to obtain functionality that could coordinate to a metal centers. The first attempt was reported by Hill[15] where a vanadium organoimido complex (Figure 3-10) was synthesized with the imido substituent bearing a pyridine functionality. The pyridine was successful in coordinating to rhodium and tungsten metal complexes (Figure 3-10). This structure spurred the investigation of

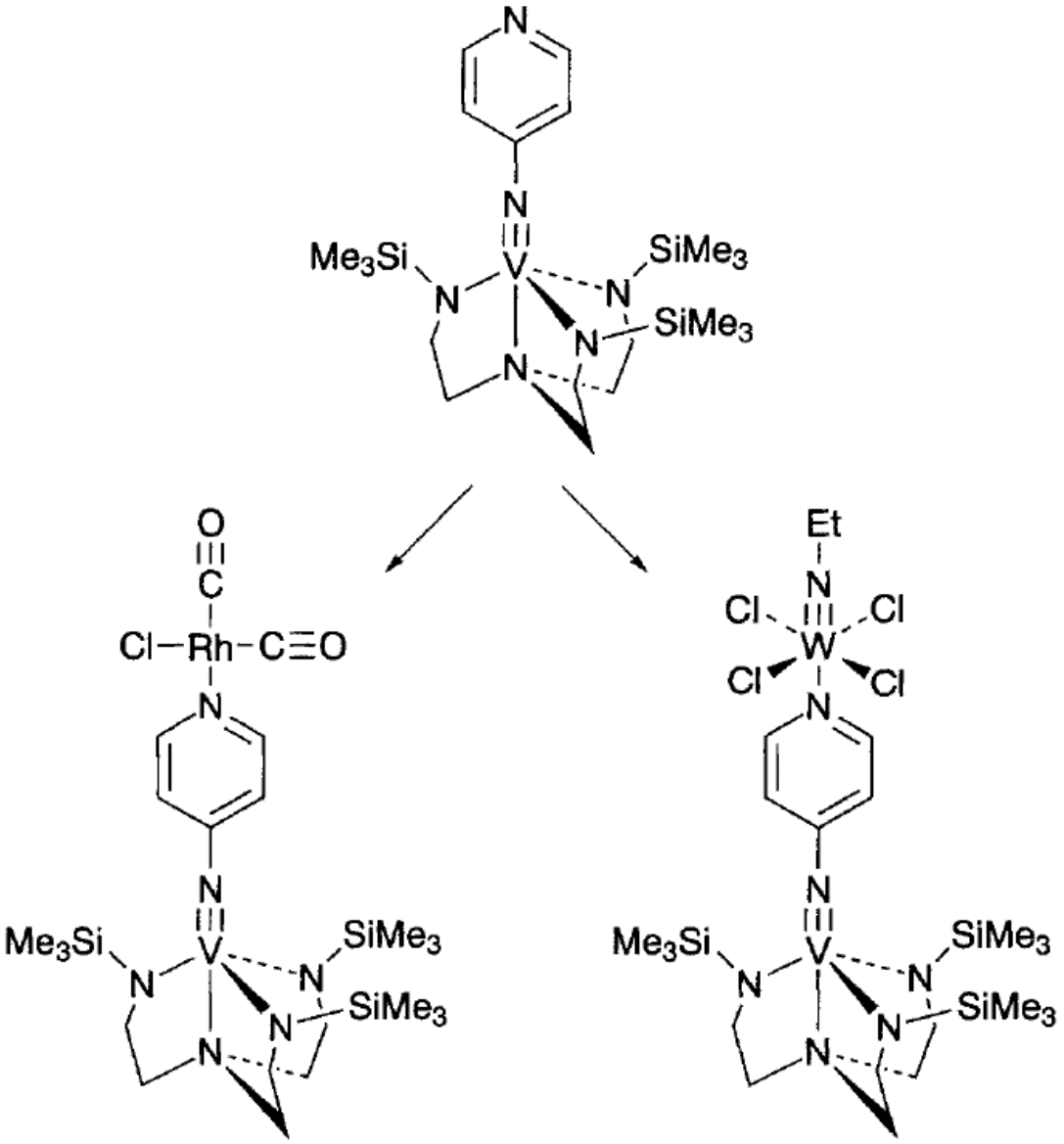

Figure 3-10 Reaction scheme of a vanadium pyridylimdo complex coordinating to a Rh and W metal.[15]

incorporating functionality through imido ligands to POMs and more specifically, hexamolybdate. Forster obtained a functionalized hexamolybdate barring a *m*-pyridyl group.[16] Expanding on this initial find, Moore characterized carboxylic acid-, *m*-methoxypyridyl-, and styryl-functionalized imido-hexamolybdates (Figure 3-11).[17] Kwen later reported a *p*-cyanophneyl imido hexamolybdate.[18]

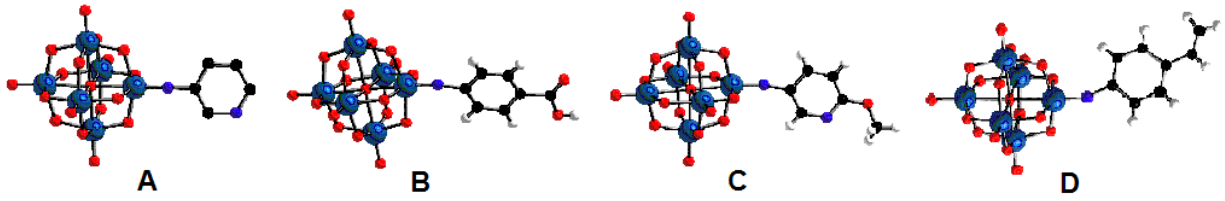

Figure 3-11 Substituted hexamolybdates with remote functionality: m-pyridine (A)[16], carboxylic acid (B)[17], 2-methoxypyridine (C)[17], and styrene (D)[17].

All of these functionalized POMs are designed for metal coordination. With this in mind, one could envision supermolecules that have one or more organoimido hexamolybdates coordinated to the same metal center. Our group has previously prepared hydrogen bonded dimers of hexamolybdate in the carboxylic acid functionalized hexamolybdate (Figure 3-12).[17]

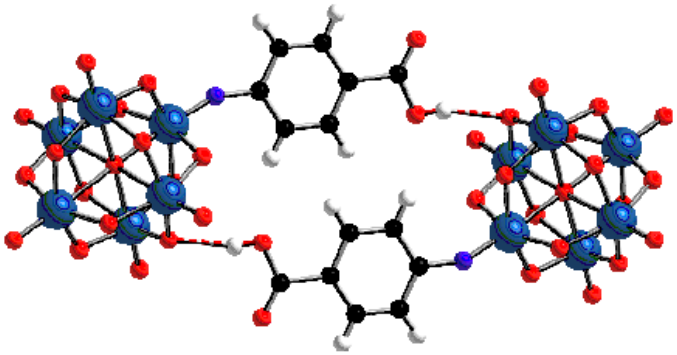

Figure 3-12 Carboxylic acid substituted hexamolybdate dimmer resulting from H-bonding interactions.[17]

Strong[19] described a hexamolybdate functionalized with six organoimido ligands, making possible the synthesis of a variety of supramolecular architectures (Figure 3-13). These discrete

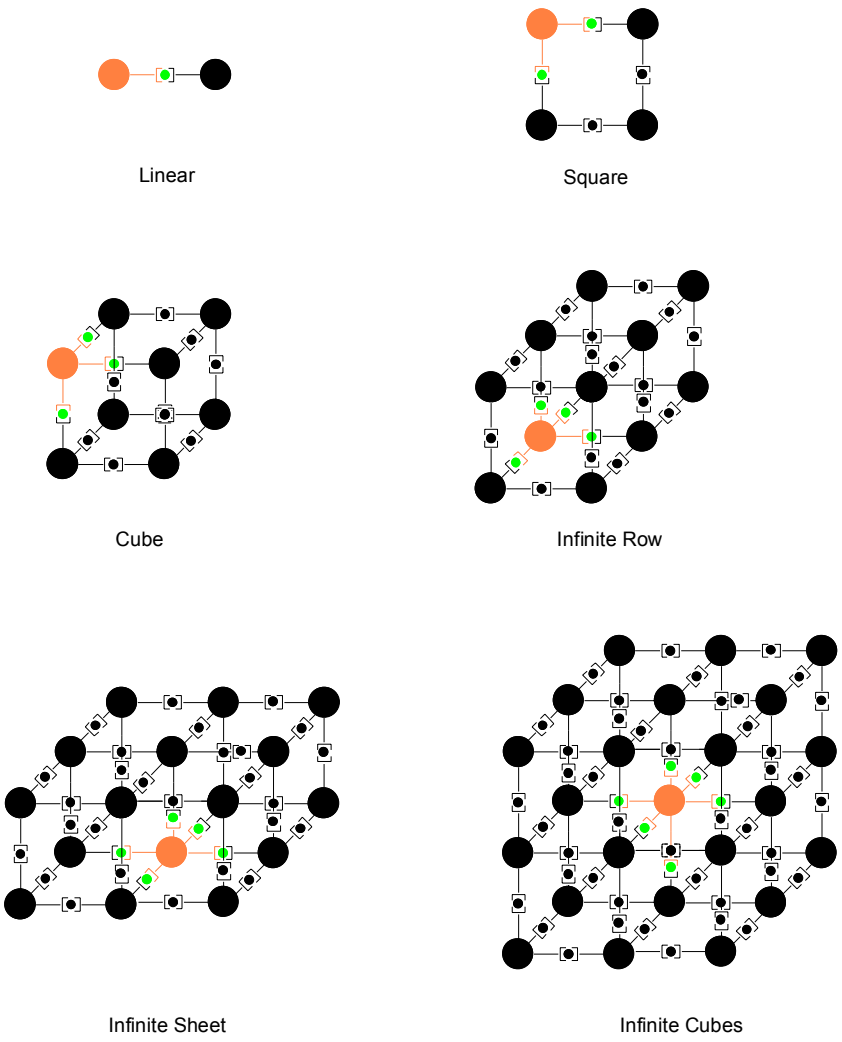

Figure 3-13 Possible supramolecular architectures based on the number of substituted terminal oxygens of hexamolybdate. Orange balls represent substituted hexamolybdate and green balls represent coordinated metal atoms.

supramolecular structures are possible due to the octahedral nature of hexamolybdate, where each terminal oxygen is either separated by 90 or 180 degrees. Also, the ability to control the number of imido ligands substituted onto hexamolybdate is key. Hexamolybdate will only form substituted species in one particular fashion. Figure 3-13 depicts the six possible supramolecular species. Unfortunately, all attempts to date to coordinate metals with functionalized hexamolybdates have been unsuccessful either because of the lack of synthetic reproducibility of the functionalized POM or their inability to bind metals. The inability to bind metals is widely believed to result from the electron withdrawing effect of hexamolybdate (Figure 3-14) that

renders the donor site non-basic. Kwen tried to overcome this obstacle by adding a "organic spacer".[18] The results are inconclusive and require further investigation.

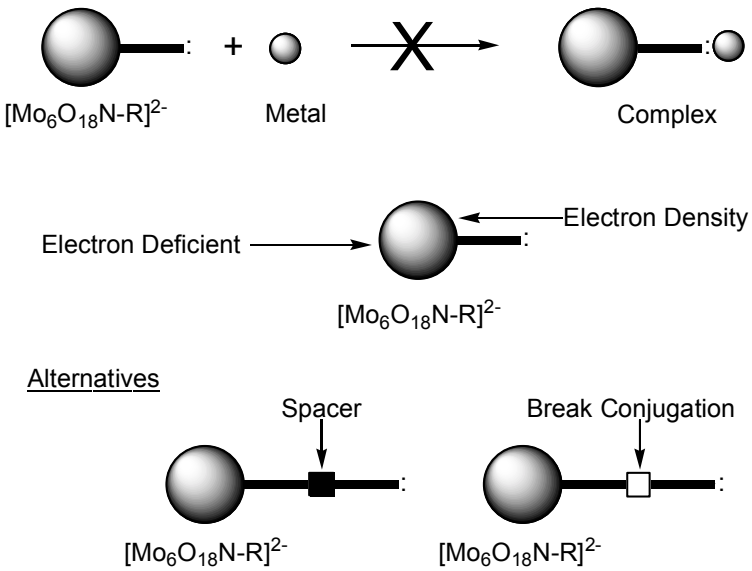

Figure 3-14 Possible explanation for the poor ability of substituted hexamolybdate to coordinate metals and two possible solutions.

Herein, I report the synthesis of a new series of dithiocarbamate metal complexes. The DTC complexes are derived from the reaction of 4-aminopiperidine, carbon disulfide, and a base. Attempts made to attach the DTC as well as the DTC metal complexes to the hexamolybdate cluster are described.

3.2 Results and Discussion

3.2.1 Synthesis of DTC ligand and Metal Complexes

All transition metals can form dithiocarbamate complexes. This ability of the DTC ligand makes it an attractive functionality to incorporate into hexamolybdate. If this were possible, the amount of POM/metal complexes would be enormous.

The synthesis of the target DTC ligand was prepared under normal synthetic conditions (Figure 3-15). 4-aminopiperidine was added to water. To this plum colored solution, carbon disulfide was added. Finally, sodium hydroxide was added and the mixture was allowed to stir at room temperature for a few hours. Upon removal of the water, a white precipitate was collected and washed with ether. As expected, this sodium salt was only soluble in water.

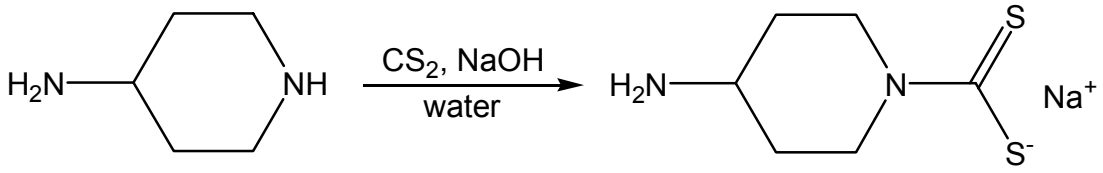

Figure 3-15 Reaction scheme for the formation of 4-aminopiperidine dithiocarbamate.

The synthesis of the transition metal complexes was very straightforward (Figure 3-16). The sodium DTC was dissolved in water. To this solution, a metal salt (nitrate or halide) was added. After two hours of stirring at room temperature, the resulting precipitate was

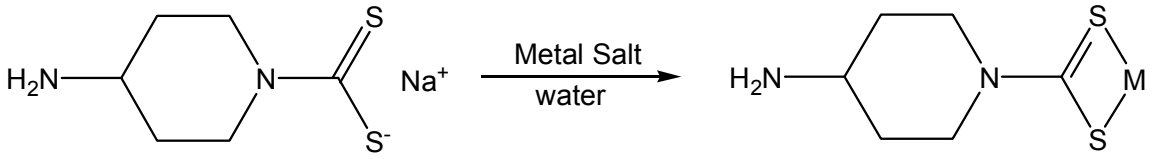

Figure 3-16 Reaction scheme for the formation of metal complexes with 4-aminopiperidine dithiocarbamate.

collected and used without further purification. IR was used to characterize these metal complexes. These results are summarized in Table 2. In one particular case, the diamagnetic Co^{III}DTC was analyzed with ^{1}H NMR. All hydrogens are accounted for and can be assigned to their respective peaks. Finally, a single crystal of Ni^{II}DTC was grown by slow diffusion of ether

into an acetonitrile solution. The structure obtained through X-ray analysis will be discussed later in this chapter.

Table 4 IR bands for the C=N stretch of the DTC metal complexes.

Metal DTC Complex	IR (cm^{-1}): ν(C=N)
Sodium (Na^{+})	1464
Silver (Ag^{+})	1473
Nickel (Ni^{2+})	1471
Manganese (Mn^{2+})	1471
Cobalt (Co^{3+})	1495
Iron (Fe^{3+})	1485

3.2.2 Attempts to Substitute Hexamolybdate

In order to incorporate the DTC complexes onto hexamolybdate, we attempted to convert the amino group into the corresponding phosphineimine (Figure 3-17) since phosphineimines

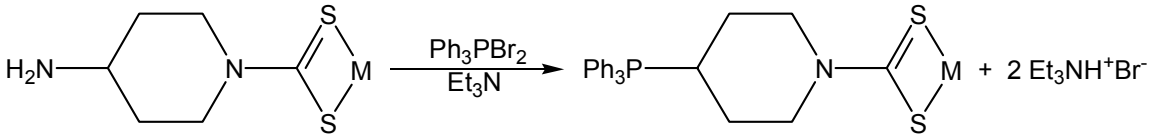

Figure 3-17 Reaction scheme for the formation of the phosphineimine.

have been reported to undergo oxo/imido exchange with hexamolybdate. Some unsuspected problems occurred in trying to prepare the phosphineimine DTCs, the first of which was solubility. As mentioned above, the sodium DTC was only soluble in water which makes the conversion to the phosphineimine unrealistic. The silver and manganese complexes, obtained from the precipitation from water, displayed slight solubility in dimethylsulfoxide (DMSO). These two complexes are not soluble in any other organic solvent. Unfortunately, DMSO is not an acceptable solvent for the phosphineimine conversion since rigorously dried solvents are required. The nickel DTC complex was sparingly soluble in acetonitrile and dichloromethane (DCM). This was very encouraging because these solvents are suitable for phosphineimine

synthesis. However, all attempts at converting the Ni DTC's amine to the phosphineimine were unsuccessful. An explanation was found in the crystal structure of the complex.

A single crystal of the nickel DTC complex was obtained by slow diffusion of ether into an acetonitrile solution. The green crystals obtained were analyzed by X-ray diffraction and

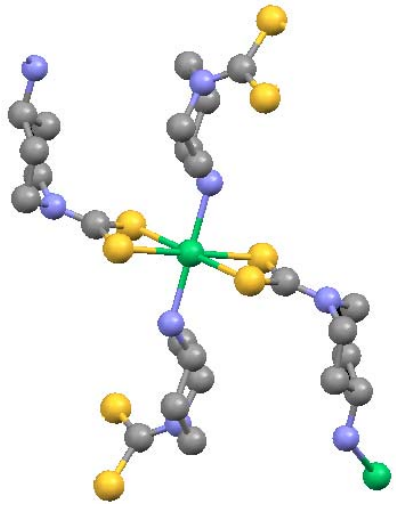

Figure 3-18 Ball and stick representation of Ni^{II} DTC complex.

yielded a structure with very interesting characteristics (Figure 3-18). The DTC ligand coordinated to the nickel in the expected mode, but the amino groups of adjacent complexes coordinated to the nickel as well. This unanticipated coordination of the amino groups prevented the reaction with the phosphine. Attempts to displace the amino groups by the addition of pyridine proved unsuccessful.

Nevertheless, this nickel DTC complex is interesting and will be discussed in depth. The DTC ligand coordinates to the nickel in the typical mode A (described in the introduction). One of the S-Ni bond lengths is 2.4229(8) Å while the other is 2.4426(9) Å, which suggests that the negative charge and double bond character is evenly dispersed over both sulfur atoms. Additional evidence for binding mode A comes from the identical S-C bond lengths (1.713(3) Å and 1.715(3) Å). The amino groups coordinated to the nickel have a bond length (N-Ni) of 2.124(3) Å. The nickel center has an pseudo-octahedral coordination environment. This is supported by the bond angles of N-Ni-S_1, N-Ni-S_2, N-Ni-N_2, S_1-Ni-S_1, and S_2-Ni-S_2 (84.54(8)º & 95.46(8)º, 87.91(9)º & 92.09(9)º, 179.999(1)º, 180.0º, 180.00(4)º respectively, Figure 3-19). The

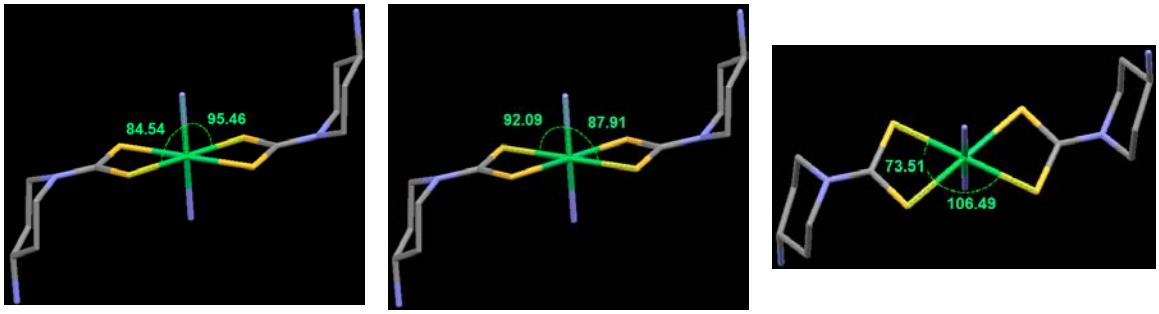

Figure 3-19 Stick representation of Ni^{II} DTC complex with selected angles.

sulfur atoms do not coordinate to the nickel in a true square planar fashion, but are very close as the bond angles for S_1-Ni-S_2 are 106.49(3)º & 73.51(3)º (Figure 3-19). If the nickel DTC structural view is expanded, an infinite 2D grid-like structure is revealed (Figure 3-20).

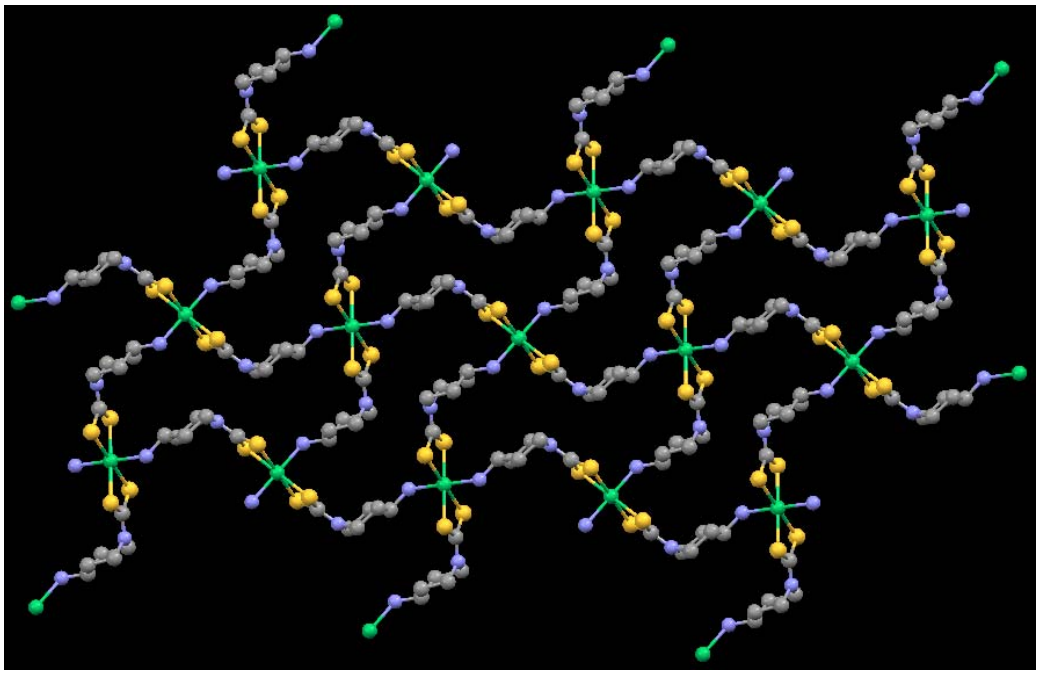

Figure 3-20 Ball and stick representation of Ni^{II} DTC complex showing the infinite 2D grid.

To combat this amine coordination problem, coordinatively saturated metal complexes, $M(DTC)_3$, have been synthesized. This approach should prevent the amine groups from interacting with the metals because all of the coordination sites would be occupied by the DTC lignads. Cobalt(III) was the first choice due to its geometry and NMR-friendly diamagnetism. This $Co(DTC)_3$ complex is slightly soluble in acetonitrile and dichloromethane. The $Co(DTC)_3$

complex has been characterized by IR, ^{1}H NMR, and mass spectrometry. The $Co(DTC)_3$ displayed the C-N stretch in the expected region (1495 cm^{-1}) and ^{1}H NMR experiments had all of the expected peaks. The mass spectrum observed agreed with the calculated value for $Co(DTC)_3$. However, the conversion of the amine to the phosphineimine has been unsuccessful. This may be attributed to the complexes sparse solubility. A $Fe^{III}(DTC)_3$ complex was also synthesized because of its octahedral geometry, but its solubility was poor and produced similar results as observed in the $Co(DTC)_3$ when attempting to convert the amine to the phosphineimine.

3.2.3 Conclusion

A new series of transition metal DTC complexes has been synthesized from 4-aminopiperidine and characterized. In the $Ni(DTC)_2$ complex, single crystal analysis revealed that the amine groups of adjacent DTC ligands are coordinating to the adjacent nickel atoms. These coordinated amine groups are inaccessible for subsequent conversion to phosphineimines. Experiments have been attempted to combat this problem, but are inconclusive at the present time. $Co(DTC)_3$ and $Fe(DTC)_3$ complexes have been synthesized in an effort to "free up" the amine groups. Initial results have been encouraging and a slight increase in solubility has been observed and further investigation is needed. Another experiment to pursue is to synthesize an ammonium or alkylammonium DTC complex, which typically are more soluble in organic solvents than the sodium analogue. This could lead to a DTC that could be converted to the phosphineimine because of greater solubility and then substituted onto hexamolybdate. Transition metals could then be coordinated to the DTC functionalized hexamolybdate.

3.3 Experimental

3.3.1 Instrumentation

All chemicals were purchased from Aldrich and used without further purification. ^{1}H NMR spectra were recorded on a Varian Unity Plus 400 MHz or 200 MHz spectrometer in CD_3CN or CD_3Cl. Compounds were prepared for infrared (IR) analysis on a Nicolet Protégé 460 as KBr pellets. Mass spectra, MALDI-TOF/ TOF-MS, were collected on a Bruker Daltonics Ultraflex TOF/TOF.

X-ray data was collected on a Bruker SMART 1000 four-circle CCD diffractometer at 203 K using a fine-focus molybdenum Kα tube. Data was collected using SMART.[20] Initial cell constants were found by small widely separated "matrix" runs. Generally, an entire hemisphere of reciprocal space was collected regardless of Laué symmetry. Scan speed and scan width was chosen based on scattering power and peak rocking curves.

Unit cell constants and orientation matrix was improved by least-squares refinement of reflections thresholded from the entire dataset. Integration was performed with SAINT,[21] using this improved unit cell as a starting point. Precise unit cell constants were calculated in SAINT from the final merged dataset. Lorenz and polarization corrections were applied. Laué symmetry, space group, and unit cell contents was found with XPREP. Absorption correction was applied as noted.

Data was reduced with SHELXTL.[22] The structure was solved in all cases by direct methods without incident. All hydrogens were assigned to idealized positions and were allowed to ride. All heavy atoms were refined with anisotropic thermal parameters.

The complex sits on an inversion center, giving octahedral geometry around the nickel(II) cation. Absorption correction was attempted but did not improve the fit. All hydrogens were assigned to idealized positions and were allowed to ride.

3.3.2 Synthesis

3.3.2.1 Preparation of Sodium 4-Aminopiperidine Dithiocarbamate (NaDTC) (1)

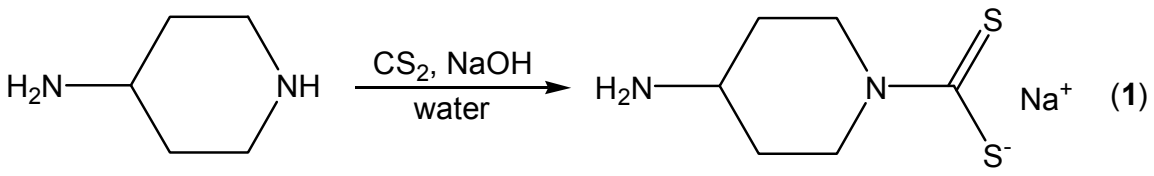

4-Aminopiperidine (1 g, 9.99 mmol) and carbon disulfide (0.60 mL, 9.99 mmol) were added to a flask containing 15 mL of water. NaOH (0.40 g, 9.99 mmol) was dissolved in 3 mL and added dropwise with a pipette to the mixture. This yellow solution was stirred at room temperature for 2 hours. The water was removed by rotary evaporation to yield an off white precipitate. Yield (1.1 g, 56%).

^{1}H NMR (D_2O): δ = 1.35 (m, 2H, CH_2), 1.89 (d, 2H, CH_2), 3.02 (m, 1H, CH), 3.29 (t, 2H, CH_2), 5.36 (d, 2H, CH_2). IR (KBr pellet, cm^{-1}): 1464 ν(C-N).

3.3.2.2 Preparation of Metal Dithiocarbamate Complexes

3.3.2.2.A Preparation of Nickel(II) Bis-Dithiocarbamate (2)

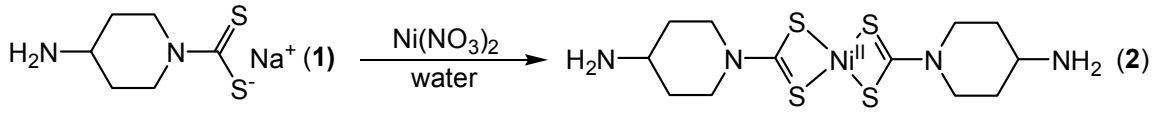

(**1**) (0.5 g, 2.52 mmol) and $Ni(NO_3)_2$ (0.366 g, 1.26 mmol) were dissolved in 15 mL of water. This mixture was allowed to stir at room temperature for two hours. A green precipitate was produced and collected on a frit. It was then washed with water and dried under vacuum. Yield (0.27 g, 52%).

^{1}H NMR (CD_2Cl): δ = 1.26 (s, 2H), 1.38 (m, 2H), 1.93 (m, 2H), 3.07 (m, 1H), 3.17 (m, 2H), 4.39 (m, 2H). IR (KBr pellet, cm^{-1}): 1471 ν(C-N). MS (MALDI): 409 calculated for ($C_{12}H_{22}N_4S_4Ni$)=409.28.

3.3.2.2.B Preparation of Silver(I) Dithiocarbamate (3)

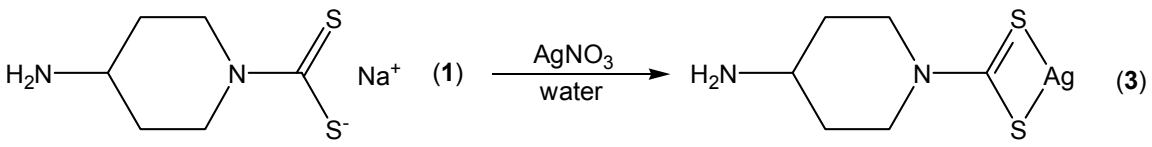

(**1**) (0.5 g, 2.52 mmol) and $Ag(NO_3)_2$ (0.214 g, 2.52 mmol) were dissolved in 15 mL of water. This mixture was allowed to stir at room temperature for two hours. A black precipitate was produced and collected on a frit. It was then washed with water and dried under vacuum. Yield (0.27 g, 38%).

IR (KBr pellet, cm^{-1}): 1473 ν(C-N).

3.3.2.2.C Preparation of Manganese(II) Bis-Dithiocarbamate (4)

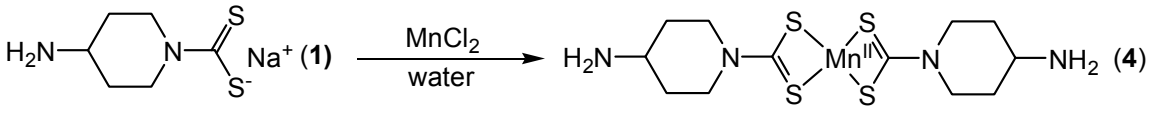

(**1**) (0.5 g, 2.52 mmol) and $MnCl_2$ (0.250 g, 1.26 mmol) were dissolved in 15 mL of water. This mixture was allowed to stir at room temperature for two hours. A brown precipitate was produced and collected on a frit. It was then washed with water and dried under vacuum. Yield (0.32 g, 64%).

IR (KBr pellet, cm^{-1}): 1471 ν(C-N).

3.3.2.2.D Preparation of Cobalt(III) Tris-Dithiocarbamate (5)

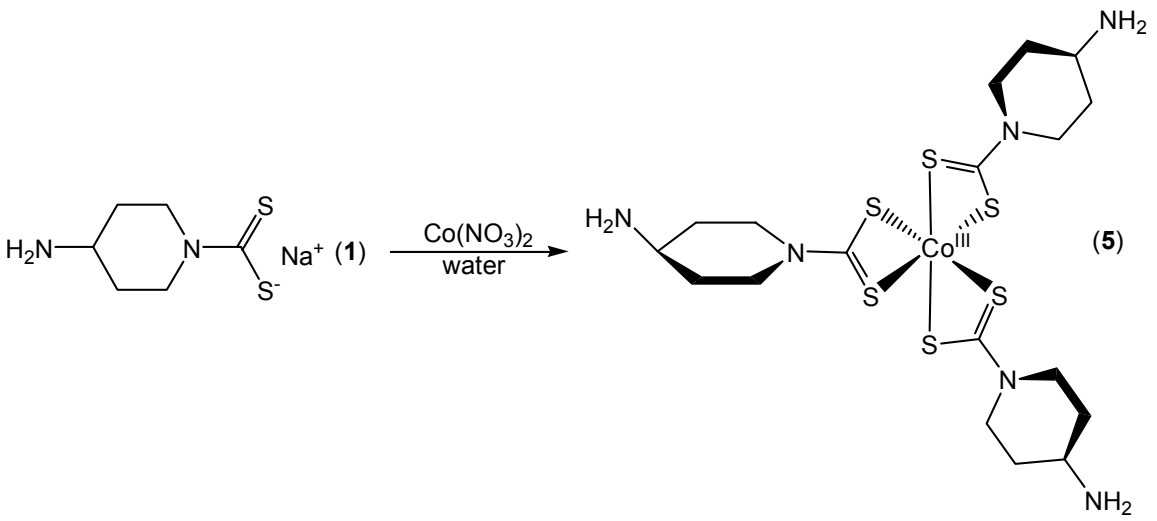

(**1**) (0.5 g, 2.52 mmol) and $Co(NO_3)_2$ (0.244 g, 0.841 mmol) were dissolved in 15 mL of water. This mixture was allowed to stir at room temperature for two hours. A green precipitate was produced and collected on a frit. It was then washed with water and dried under vacuum. Yield (0.36 g, 73%).

^{1}H NMR (CD_2Cl_2): δ = 1.32 (m, 2H, C*H*$_2$), 1.88 (d, 2H, C*H*$_2$), 3.00 (m, 1H, C*H*), 3.17 (m, 2H, C*H*$_2$), 4.49 (d, 2H, C*H*$_2$). IR (KBr pellet, cm^{-1}): 1495 ν(C-N). MS (MALDI): 584 calculated for ($C_{18}H_{33}N_6S_6Co$)= 584.82.

3.3.2.2.E Preparation of Iron(II)Tris-Dithiocarbamate (6)

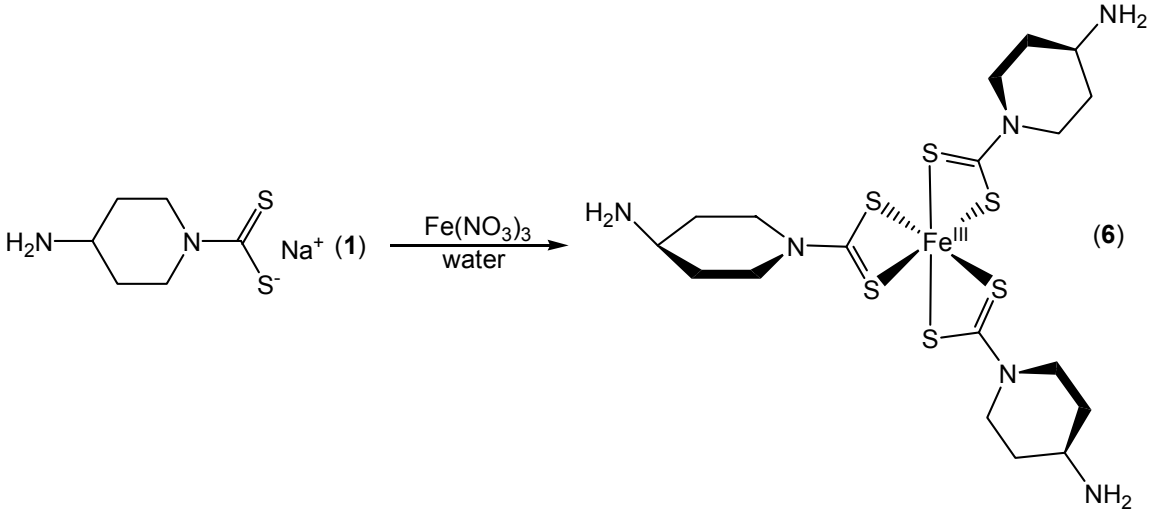

(**1**) (0.5 g, 2.52 mmol) and $Fe(NO_3)_3$ (0.339 g, 0.841 mmol) were dissolved in 15 mL of water. This mixture was allowed to stir at room temperature for two hours. A brown precipitate was produced and collected on a frit. It was then washed with water and dried under vacuum. Yield (0.12 g, 24%).

IR (KBr pellet, cm^{-1}): 1485 ν(C-N).

[1] Coucouvanis, D., *Prog. Inorg. Chem.*, **1970**, *11*, 233.
[2] Coucouvanis, D., *Prog. Inorg. Chem.*, **1979**, *26*, 301.
[3] Karlin, K., *Pro. Inorg. Chem.*, **2005**, *53*, 71.
[4] Debus, H., *Ann. Chem.*, **1850**, *73*, 26.
[5] Delepine, M., *Compt. Rend.*, **1907**, *144*, 1125.
[6] Cameron, B., Drakes, M., Baird, I., Skerlji, R., Santucci, L., Fricker, S., *Inorg. Chem.*, **2003**, *42*, 4102.
[7] Fernadez, E., Lopez-de-Luzuriaga, J., Monge, M., Olmos, E., Gimenu, M., Laguna, A., Jones, P., *Inorg Chem.*, **1998**, *37*, 5532.
[8] Bardji, M., Laguna, A., Jones, P., Fischer, A., *Inorg. Chem.*, **2000**, *39*, 3560.
[9] Elduque, A., Finestra, C., Lopez, J., Lahoz, F., Mercgan, F., Oro, L., Pinillos, M., *Inorg. Chem.*, **1998**, *37*, 824.
[10] Leung, W., Wu, M., Chim, J., Wong, W., *Inorg. Chem.*, **1996**, *35*, 4801.
[11] Hgo, S., Banger, K., DelaRosa, M., Toscano, P., Welch, J., *Polyhedron*, **2003**, *22*, 1575.
[12] M. T. Pope, "Heteropoly and Isopoly Oxometalates": Springer, Berlin, **1983**.
[13] J.J. Borras-Almenar, E. Coronado, A. Mueller, and M.T. Pope, "Polyoxometalate Molecular Science": Kluwer, Dordrecht, **2001**.
[14] *Chem. Rev.*, **1998**, *98*.
[15] Hill, P., Yap, G., Rheingold, A., Maatta, E.A., *Chem. Comm.*, **1995**, 737.
[16] Forster, G., Liable-Sands, L., Rheingold, A., Maatta, E.A., unpublished results.
[17] Moore, A., PhD Thesis, Kansas State University, **1998**.
[18] Kwen, H., PhD Thesis, Kansas State University, **2000**.
[19] Strong, J., Yap, G., Ostrander, R., Liable-Sands, L., Rheingold, A., Thouvenot, R., Gouzerh, P., Maatta, E.A., *J. Am. Chem. Soc.*, **2000**, *122*, 639.
[20] SMART v5.060, © 1997 - 1999, Bruker Analytical X-ray Systems, Madison, WI.
[21] SAINT v6.02, © 1997 - 1999, Bruker Analytical X-ray Systems, Madison, WI.
[22] SHELXTL v5.10, © 1997, , Bruker Analytical X-ray Systems, Madison, WI.

CHAPTER 4 - Copolymerization of Styrenylimido Hexamolybdate

4.1 Introduction

4.1.1 Chloromethylstyrene

A very common and useful monomer in polymer chemistry is chloromethlystyrene (CMS) (Figure 4-1). Its synthesis was first described by Clarke and Hammerschlag in 1957.[1] Since its inception, there have been thousands of articles and patents dealing with the chemical and physical properties of CMS polymers and copolymers.[2]

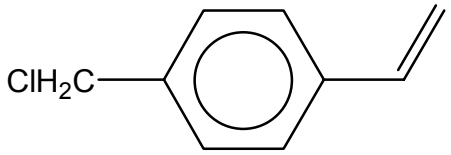

Figure 4-1 Representation of 4-chloromethylstyrene.

Because of the chemical reactivity of the benzylic chlorine of CMS, nucleophilic substitutions are by far the most reported procedure to modify CMS. In many cases, this modification can be done before polymerization leaving the vinyl substituent unchanged (Figure 4-2). There are also reports where bifunctional nucleophiles have been used to produce nonconjugated dienes (Figure 4-2).[2] With this general idea for nucleophilic substitution, there are roughly eight types of modified CMS that have been reported. These are the formation of carbon-oxygen bonds, either ether or ester functionality, carbon-nitrogen bonds, either amines or ureas, carbon-sulfur bonds, carbon-carbon bonds, and finally a small sampling of carbon-phosphorous, carbon-silicon, carbon-germanium, and carbon-tin bonds.[2] All of these modifications can be performed on CMS polymers and copolymers as long as steric effects do not hinder the availability of the chloromethyl group. A brief summary of the modified CMS will be presented below.

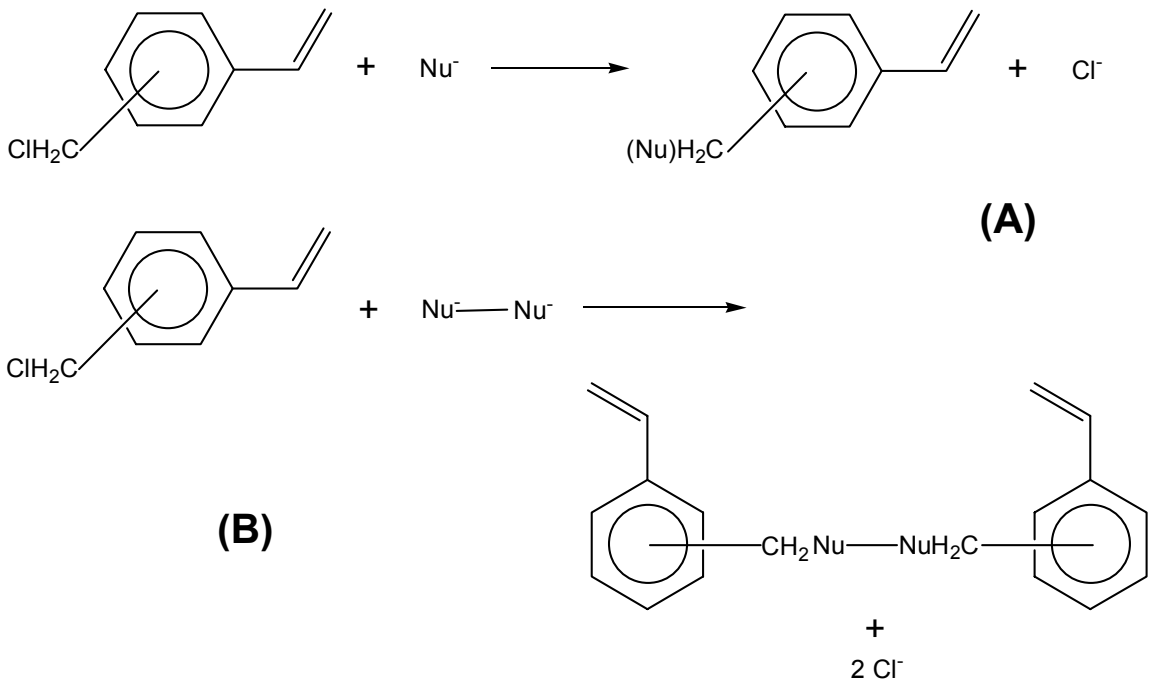

Figure 4-2 Two possible reaction schemes for the nucleophilic substitution of CMS.[2]

The formation of the carbon-oxygen bond through the reaction of either a hydroxyl group (OH) or a carboxylate group (COO^-) with CMS is by far the most reported modification. There are different procedures in which the final product is obtained, but to form an ether linkage, an alcohol or phenol is mixed with CMS in basic medium. The basic medium is generally sodium or potassium hydroxide in water or can be an alkali metal in anhydrous solvents. The ester formation is very similar to the ether formation procedure. In this case, a carboxylic acid is mixed with CMS in basic medium. Figure 4-3 shows select examples of the formation of a carbon-oxygen linkage using OH and COO groups with CMS.

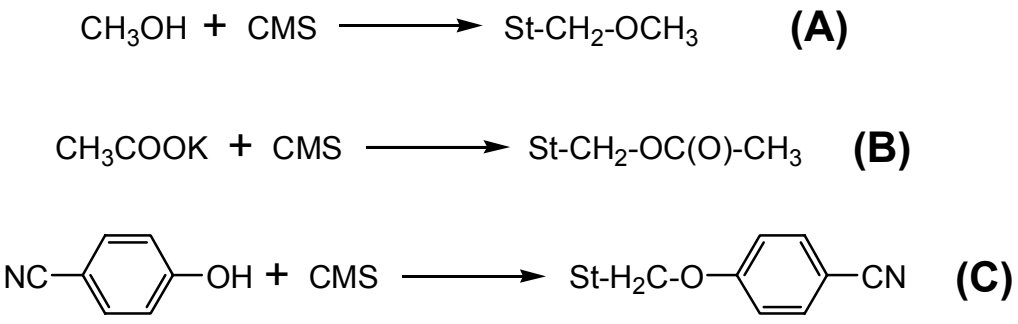

Figure 4-3 Examples of the formation of carbon-oxygen bonds with CMS (St=styryl). **A**=Methanol[3], **B**=Acetate[4], **C**=4-Cyanophenol[5].

The formation of the carbon-nitrogen bond generally involves either an amine or amide. The reaction of tertiary amines with CMS typically leads to ammonium salts. Primary and secondary amines have been reported to react with CMS producing secondary and tertiary amines respectively. Amides react in a similar fashion and produce a urea-like polymerizeable monomer. Examples of the carbon-nitrogen bond formation are shown in Figure 4-4.

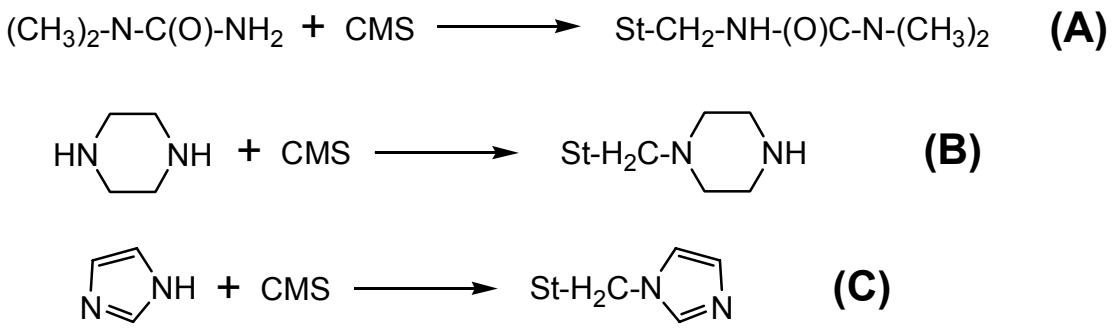

Figure 4-4 Examples of the formation of carbon-nitrogen bonds with CMS (St=styryl). **A**=Secondary amine[6], **B**=Piperazine[7], **C**=Imidazole[8].

Sulfur-carbon bonds are usually obtained from thiolates. These are analogues to the alcohol or phenol products. Dialkylsulfides react with CMS to produce sulfonium salts. These salts are analogues to the tertiary amines. Examples of the carbon-sulfur formation are shown in Figure 4-5.

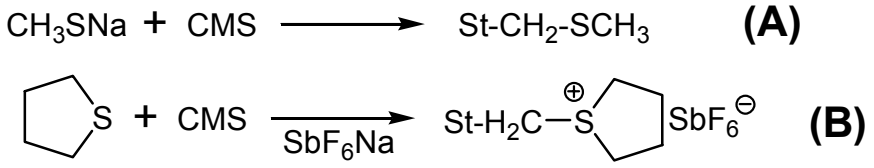

Figure 4-5 Examples of the formation of carbon-sulfur bonds with CMS (St=styryl). **A**=Methylthiolate[9], **B**=Tetrahydrothiophene[10].

Finally, carbon-carbon, carbon-silicon, carbon-germanium, and carbon-tin bonds are produced through Grignard conditions. The CMS Grignard is usually prepared and reacted with a halogenated species of the desired atom. Trialkyl and triaryl phosphines can react with CMS and form phosphonium salts. Examples are displayed in Figure 4-6.

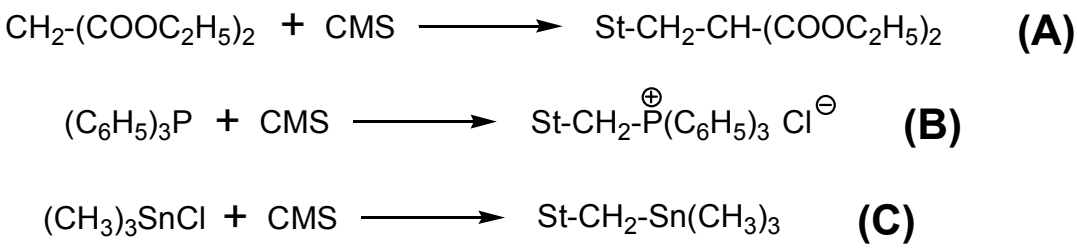

Figure 4-6 Examples of the formation of carbon-carbon, carbon-phosphorus, and carbon-tin bonds with CMS (St=styryl). **A**=Diethylmalonate[11], **B**=Triphenyl phosphine[12], **C**=Trimethyltin chloride[13].

CMS polymers and copolymers are used in a variety of applications. With the ability to substitute various substituents through the chlorine, ion exchange resins, catalyst supports, photosensitizers, and organometallic polymers have been reported.[2]

4.1.2 Styrylimido Hexamolybdate

It has long been a goal of POM chemists to prepare polymerizeable units incorporating POMs. Such a unit has been prepared by Judeinstein,[14] who was able to incorporate a silane group bearing styrene functionality into a lacunary Keggin (SiW_{11}) fragment. This functionalized Keggin was polymerized by radical initiation with benzoyl peroxide or AIBN. Similar compounds based on the divacant SiW_{10} POM have been prepared by Thouvenot.[15,16] Very recently, Proust and Thouvenot have described the synthesis of a vinyl containing Keggin (PW_{11}) system (Figure 4-7)[17]. However, there is only one example of a Lindqvist polymerizeable unit.[18]

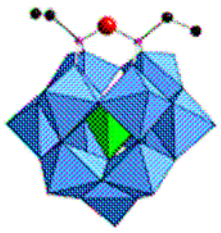

Figure 4-7 Polyhedron representation of $[PW_{11}O_{39}(Si\text{-}CH{=}CH_2)_2O]^{3-}$.[17]

The styrylimido hexamolybdate, $[TBA]_2[Mo_6O_{18}N\text{-}C_6H_4\text{-}C_2H_3]$, was synthesized first by Moore. Kwen was able to copolymerize this functionalized POM with 4-methylstyrene with AIBN as a radical initiator.[19] When each monomer was reacted in equimolar amounts, a green

copolymer was obtained in a 2.7 : 1 ratio of 4-methylstyrene to POM. Copolymers of varying ratios could be obtained simply be changing the starting molar amounts of 4-methylstyrene in the reaction. Kwen also performed experiments trying to obtain a cross-linked copolymer of styrylimido hexamolybdate, 4-methylstyrene, and divinylbenzene.[19] ^{1}H NMR studies supported a cross-linked polymer by exhibiting peaks with increased broadening in the aryl region as well as broadening of the TBA (tetrabutyl ammonium) counterion peaks suggesting that the TBAs are no longer free to rotate in solution.

Herein, I will report the synthesis and characterization of a new copolymer with styrylimido hexamolybdate and 4-chloroemthylstyrene (CMS). Also, I will describe the attempt to perform nucleophilic substitution of the copolymer with a ferrocene carboxylate as well as an attempted olefin metathesis using Grubbs' catalyst.

4.2 Results and Discussion

4.2.1 Synthesis of Monomer and Copolymer

The synthesis of styrylimido hexamolybdate involves reaction between a phosphineimine and hexamolybdate (Figure 4-8). This product has been fully characterized by NMR as well as

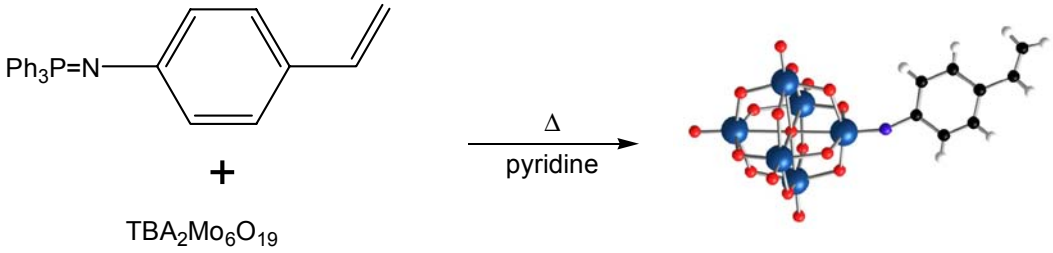

Figure 4-8 Reaction scheme to prepare styrylimido hexamolybdate.[18]

by single crystal X-ray analysis. I have introduced a modification that simplifies the purification of the material. As in most substitutions with phosphineimines, an oily precipitate is obtained. This oily precipitate is composed of the substituted hexamolybdate as well as the triphenylphosphine oxide by-product and any unreacted starting materials. The pure compound was previously obtained by the freeze-dry method. As described by Kwen, the oily precipitate is frozen in ether with liquid nitrogen and then warmed slowly to room temperature. The ether is then removed and this process is repeated if necessary. This technique for purification can be tedious and wasteful because of the amount of ether used. However, I found that all of the unwanted compounds can be removed in one step. When the oily precipitate is obtained, absolute ethanol is added to the reaction flask and stirred at room temperature for one hour. This produces an off-white solution that is filtered from the precipitate. After filtration, the product is obtained in a pure form as a rust colored precipitate. In some cases, multiple washing was required to obtain a pure product.

Using the initial results discovered by Kwen as a guideline, the copolymerization of styrylimido hexamolybdate and CMS was very straightforward. However, the polymerization yield seems to be dependent upon the amount of radical initiator, AIBN, used in the reaction. Under Kwen's copolymerization conditions, the amount of AIBN needed to obtain polymerization was 0.020 g. If this amount was used for the copolymerization with CMS, no

polymerization was observed by ^{1}H NMR. Polymerization was finally observed when the AIBN was increased to the amount of 0.200 g (Figure 4-9). After heating the reaction mixture

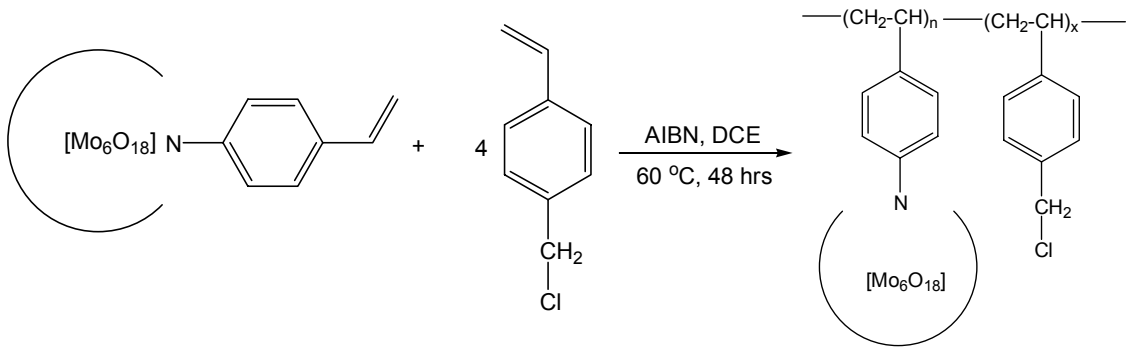

Figure 4-9 Reaction scheme for the copolmerization of 4-chloromethylsytrene and styrylimido hexamolybdate.

overnight, an unwanted precipitate is filtered and the resulting green solution is collected. The solvent is removed to yield a green precipitate. This precipitate was washed with ether and ethanol numerous times to produce the pure copolymer as a light green solid. The ^{1}H NMR spectrum of the copolymer had very broad peaks that are characteristic for the formation of polymers. The broadness is due to the protons inability to rotate freely. There are two broad peaks in the ^{1}H NMR of the copolymer with no signs of the vinylic protons of the starting materials. The four peaks corresponding to the counterion TBA, of styrylimido hexamolybdate, are broadened slightly. The two broad peaks result from the methylene protons of CMS and finally the combination of the aromatic protons of both CMS and the styrylimido hexamolybdate. By comparing integrated intensities of the methylene CMS and TBA N-CH_2 peaks, the ratio of CMS to styrylimido hexamolybdate can be obtained. This ratio was found to be 3.2:1. The copolymer was very soluble in acetonitrile, dichloromethane, and unreactive to water.

4.2.2 Ferrocene Substitution

As described above, there are many nucleophiles that have been reported that will substitute CMS. One goal is to observe an induced electron transfer between an electron donor metal atom, and the hexamolybdate cluster (Figure 4-10). The first approach to such a system

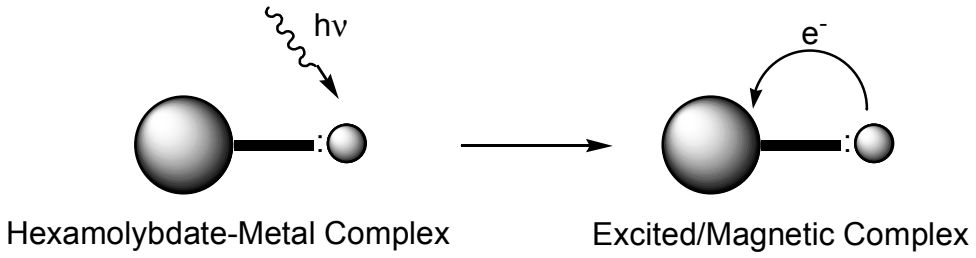

Figure 4-10 Pictorial of light-excited electron transfer between a metal and hexamolybdate.

was to try to substitute a ferrocene group onto the copolymer. Ferrocene was chosen because of previous success in the Maatta group. Ferrocene has been substituted directly onto hexamolybdate as an inido substituent and the complex was fully characterized. It was also observed that this compound transferred an electron from the ferrocene to the cluster with exposure to light. This resulted in a species with 6 unpaired electrons. The iron in ferrocene is d^6 and transfers one electron to the cluster and the remaining five electrons remain unpaired in the metal d-orbitals. However, this excited state is very short lived. With the hexamolybdate cluster now incorporated into a polymer, perhaps this electron transfer that was observed before will proceed again if the ferrocene can be incorporated into the polymer and the excited state observed for longer times since the two are no longer directly connected to one another.

In order to incorporate a ferrocene unit into the polymer, the starting ferrocenyl monocarboxylic acid was converted to the carboxylate salt (Figure 4-11). This had to be done

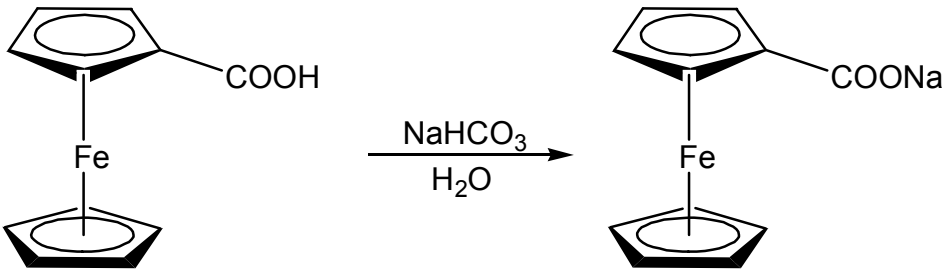

Figure 4-11 Reaction scheme for the formation of sodium ferrocenecarboxylate.

first because nucleophilic substitution of CMS requires base with a carboxylic acid and many POMs are not stable under basic conditions. Sodium bicarbonate was stirred in a water suspension of ferrocene monocarboxylic acid. After a few hours, there was no longer a suspension and all of the ferrocene was dissolved into the water. The water was removed and

yielded the carboxylate salt. Now nucleophilic substitution can be attempted without the use of base with the copolymer (Figure 4-12).

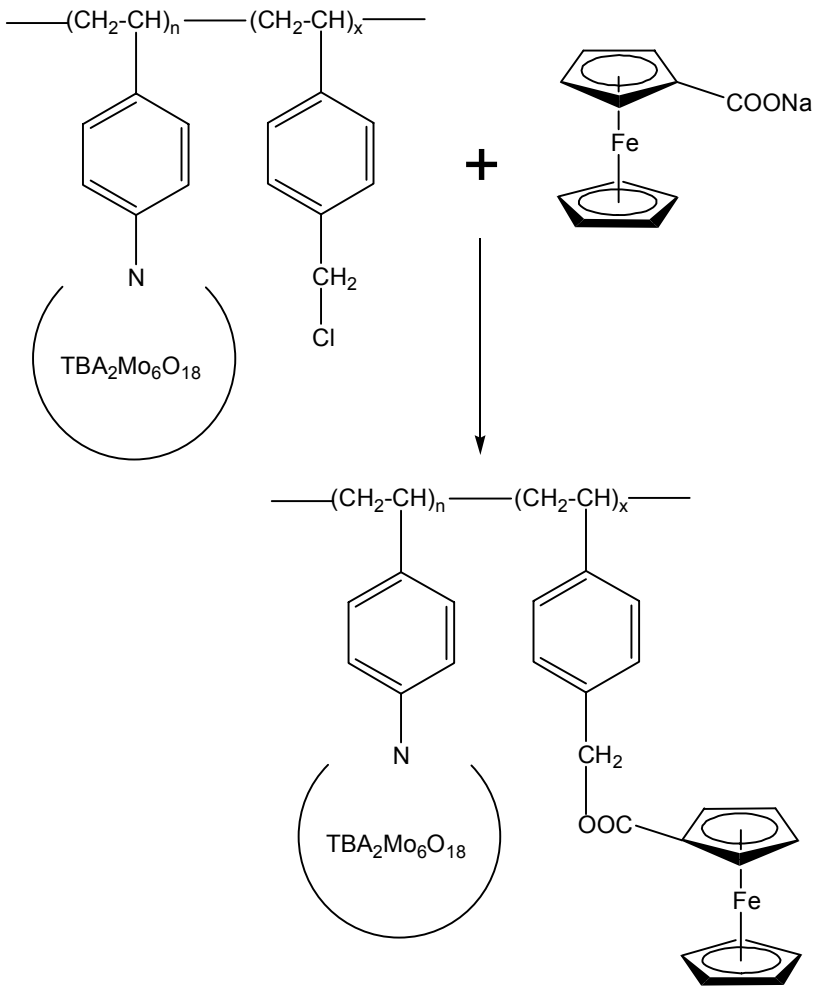

Figure 4-12 Attempted reaction for the nucleophilic substitution of the copolymer.

The copolymer was dissolved in acetonitrile and the ferrocene carboxylate was dissolved in a minimal amount of water and stirred at room temperature. After 1 day, the solvent was removed to leave a very deep red colored solid. This solid was dissolved into acetonitrile and analyzed by ^{1}H NMR. The broad peaks associated with the copolymer were still present, but the methylene protons for CMS were not shifted. This suggests that the substitution did not proceed. Temperature, molar amounts, and solvent systems were modified to combat the problem, but still no shift of the methylene protons was observed in the ^{1}H NMR. Further experiments are needed to fully understand these problems as well as other carboxylates need to be studied.

4.2.3 Olefin Metathesis using Grubbs catalyst

Another potential application for styrylimido hexamolybdate is olefin metathesis.[20] This could be very interesting because remote functionality could be introduced into the hexamolybdate species. With the previous discussion on how the POM cluster acts as an "electron sponge", the styrene group could be used as a spacer. In using a spacer, the idea is that the electron withdrawing effect of the cluster will be diminished because of the greater distance between the coordinating functionality and the cluster. This was first attempted using 4-vinyl pyridine.

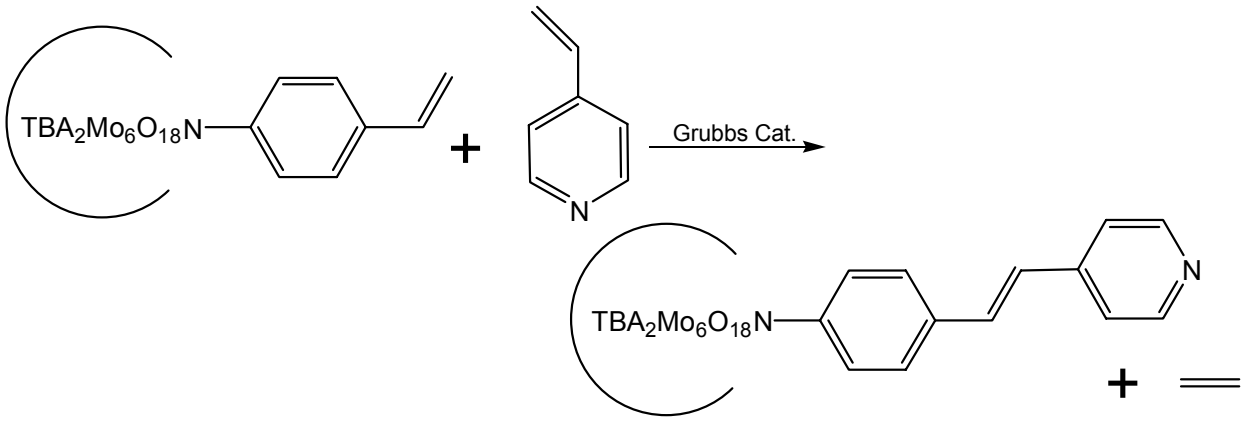

Figure 4-13 Schematic of olefin metathesis using a Grubbs catalyst.

The experimental conditions were very standard[21] (Figure 4-13). The 4-vinyl pyridine amounts and styrylimido hexamolybdate amounts are dissolved in dichloromethane and 50 mg of the 2nd generation Grubbs catalyst is added and stirred at 80 ºC for overnight. The workup is simple recrystallation by slow diffusion of ether into an acetonitrile solution. Attempts to extract the product into dichloromethane was performed, but yielded no product. The ^{1}H NMR analysis of some of the crystals suggested that the metathesis did in fact work as peaks were observed that are consistent with the formation of the product, but there were still too many impurities in the NMR. Further recrystallation was attempted, but yielded inconclusive results. To help improve the results, other catalysts were used. 2nd generation Grubbs as well as 2nd generation Hoveyda-Grubbs were tried (Figure 4-14). All produced similar results according to ^{1}H NMR. Finally, 4-

vinyl boronic acid was investigated under the same conditions. This yielded no reaction. Second generation and Helvetica Grubbs catalysts were used, but still no observable product formation was detected. Further investigation into olefin metathesis needs to be done because this is a very promising approach to functionalized hexamolybdates.

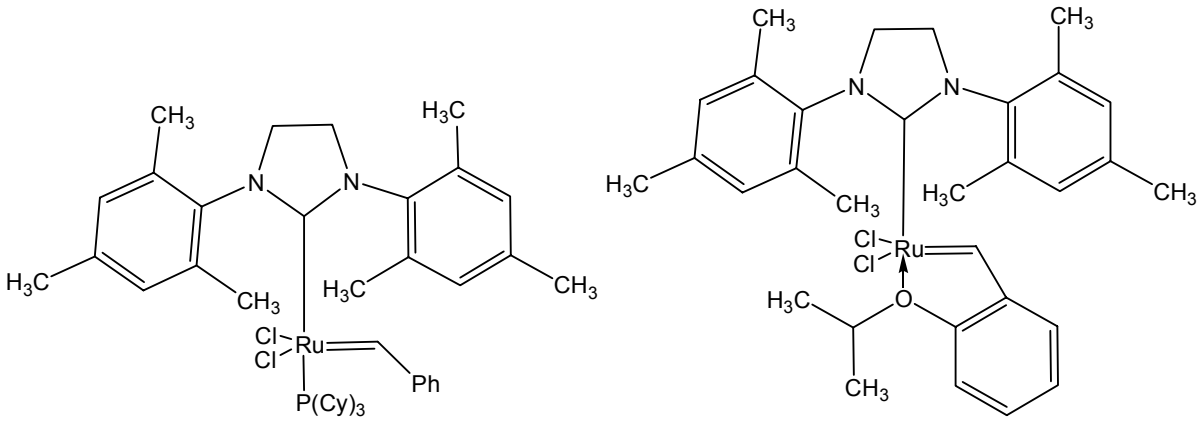

Figure 4-14 2nd generation Grubbs (left) and 2nd generation Hoveyda-Grubbs catalyst (right).

4.2.4 Conclusions

A new copolymer consisting of an imido hexamolybdate and 4-chloromethylstyrene has been synthesized and characterized by ^{1}H NMR. This copolymer should have the ability to incorporate new organic functionality through reaction of the chloromethyl group. An attempt to achieve this has only been attempted with a ferrocene carboxylate. To this point, all attempts to substitute the ferrocene unit onto the polymer have been unsuccessful. However, many other avenues are available in which other transition metal centers can be incorporated into the copolymer. Also, the reactivity of the styrylimido hexamolybdate was investigated in olefin metathesis in the presence of a Grubbs catalyst. Results were inconclusive as to whether the metathesis occurred and perhaps less exotic olefins need to be tested.

4.3 Experimental

4.3.1 Instrumentation

All starting materials were purchased from Aldrich and used without further purification. Et_3N and toluene were purchased from Aldrich in a Sure-Seal bottle and used without further drying. Pyridine was dried over CaH_2. ^1H NMR spectra were recorded on a Varian Unity plus 400 MHz or 200 MHz spectrometer in CD_3CN or CD_3Cl. Compounds were prepared for infrared (IR) analysis on a Nicolet Protégé 460 as KBr pellets. Mass spectra, MALDI-TOF/ TOF-MS, were collected on a Bruker Daltonics Ultraflex TOF/TOF.

4.3.2 Synthesis

4.3.2.1 Preparation of Tetrabutylammonium Hexamolybdate (1)[22]

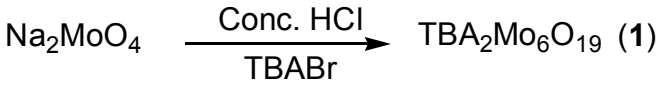

Concentrated HCl (18 mL, 216 mmol) was added dropwise with a separatory funnel to a suspension of Na_2MoO_4 (25 g, 121 mmol) in 30 mL of DMF with vigorous stirring. During the addition, a yellow solution and white precipitate were obtained. After stirring an additional 5 minutes upon complete addition of HCl, the white precipitate was removed by filtration. In another beaker, TBABr (13.05 g, 40.5 mmol) was dissolved in 15 mL of DMF. This solution was added to the yellow filtrate and a yellow precipitate formed. The yellow precipitate was collected on a frit and washed several times with diethyl ether. The final product was obtained by recrystalization using hot acetonitrile. The resulting yellow solution was decanted to another beaker and placed in the refrigerator overnight to complete the recrystalization. The yellow crystals was collected and dried under vacuum. Yield 13.12 g (48%).

^{1}H NMR (CD_3CN): δ = 0.97 (m, 24H, C*H*$_3$), 1.36 (m, 16H, C*H*$_2$), 1.61 (m, 16H, C*H*$_2$), 3.11 (m, 16H, N-C*H*$_2$). IR (KBr pellet cm^{-1}): 956 (s) and 800 (s).

4.3.2.2 Preparation of Styrenylphosphineimine (2)

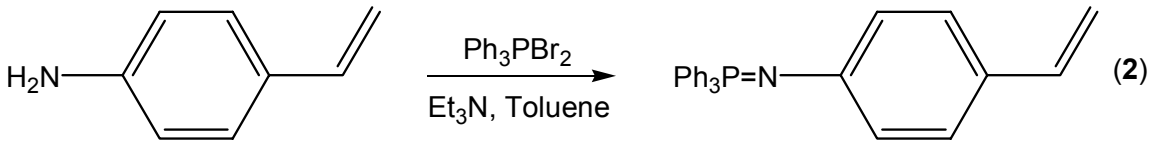

4-Vinylaniline (1 g, 8.39 mmol) and Ph_3PBr_2 (3.70 g, 8.77 mmol) was added together in a two necked flask along with 30 mL of dry toluene inside the glovebox. This suspension was removed from the glovebox. Dry Et_3N (2.5 mL, 18.7 mmol) was syringed into the reaction flask. This mixture was stirred at room temperature for overnight. The white precipitate ($Et_3NH^+Br^-$)

was removed by filtration and the solvent was removed under vacuum. The light brown tacky precipitate of (Ph_3P=N-C_6H_4CH=CH_2) was used as is in the following step. Yield (2.2 g, 69%). ^{1}H NMR (CD_3CN): δ = 4.92 (m, 1H, CH_2=), 5.45 (m, 1H, CH_2=), 6.55 (m, 1H, C*H*), 6.24 (m, 2H, aryl-H), 7.04 (m, 2H, aryl-H), 7.48-7.67 & 7.72-7.80 (m, 15H, P-(C_6H_5)$_3$).

4.3.2.3 Preparation of Styrenylimido Hexamolybdate (3)

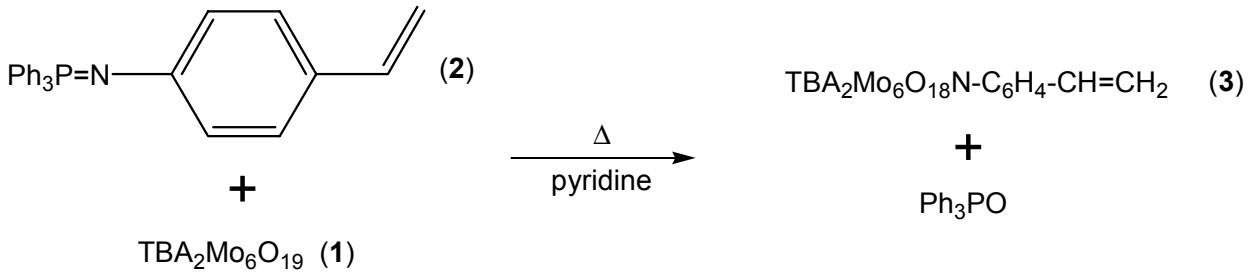

Ph_3P=N-C_6H_4CH=CH_2 (**2**) (2.2 g, 5.79 mmol) and $TBA_2Mo_6O_{19}$ (**1**) (5.27 g, 3.86 mmol) was added together in a two necked flask. 20 mL of dry pyridine was added to the flask and the solution was stirred at 90^{o}C for 5 days. The solvent was then removed under vacuum to yield a tacky orange precipitate. 30 mL of ethanol was added to the tacky precipitate and stirred. The ethanol was decanted and this step was repeated until a red-orange powder was obtained. Yield (5.65 g, 99%).

^{1}H NMR (CD_3CN): δ = 0.97 (m, 24H, CH_3), 1.36 (m, 16H, CH_2), 1.61 (m, 16H, CH_2), 3.11 (m, 16H, N-CH_2), 5.26 (d, 1H, =CH_2), 5.79 (d, 1H, =CH_2), 6.77 (m, 1H, C*H*), 7.49, 7.47, 7.21, 7.19 (AA'BB', 4H, C_6H_4). IR (KBr Pellet, cm^{-1}): 1605 (w), 975 (sh), and 952 (s).

4.3.2.4 Copolymerization of Styrenylimido Hexamolybdate with 4-Chloromethylstyrene (4)

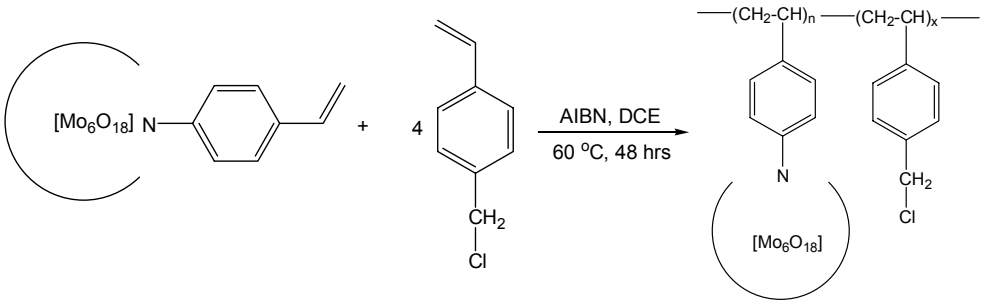

(**3**) (1 g, 0.682 mmol) was added to 10 mL of 1,2-dichloroethane and heated in an oil bath to 60 ºC. When (**3**) was almost dissolved, 4-chlormethylstyrene (0.410 mL, 2.4 mmol) was added with a syringe. AIBN (0.040 g) was dissolved in a minimal amount of DCM and this solution was then added to the heated DCM solution with a pipette. This red solution was heated at 60 ºC overnight. The solvent was removed under vacuum producing an oily green precipitate. This green precipitate was washed several times with ether and ethanol until a clean green powder was obtained. Yield (0.93 g).

^{1}H NMR (CD_3CN): δ = 0.97 (m, 24H, C*H*$_3$), 1.36 (m, 16H, C*H*$_2$), 1.61 (m, 16H, C*H*$_2$), 3.11 (m, 16H, N-C*H*$_2$), 4.62 (4H, br, Cl-C*H*$_2$-), 7.5-6.3 (12H, br aryl-*H*). IR (KBr pellet, cm^{-1}): 975 (sh) and 952 (s).

4.3.2.5 Preparation of Sodium Ferrocenecarboxylate (6)

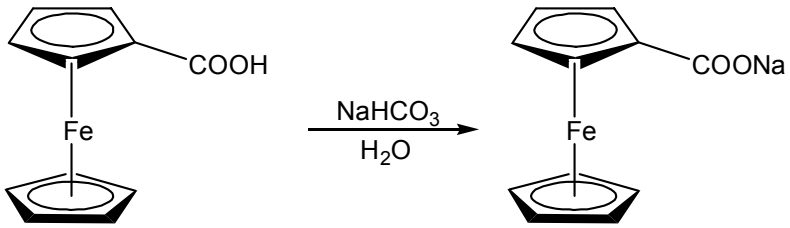

(**5**) (**6**)

Monocarboxylic acid ferrocene **(5)** (0.5 g, 2.17 mmol) was suspended in 30 mL of distilled water. $NaHCO_3$ (0.182 g, 2.17 mmol) was added next and the mixture was allowed to stir at room temperature for ~10 hours. The reaction was filtered through a frit to remove any insoluble precipitates and the water was removed by rotary-evaporation. This yielded a red-brown solid that was used without further purification. Yield (0.45 g, 82%).

IR (KBr pellet, cm^{-1}): 1531 (s).

4.3.2.6 Preparation of Ferrocene substituted copolymer (7)

(6) (0.2g, 0.794 mmol) was dissolved in a minimal amount of water. This dark red solution was added to an acetonitrile solution of copolymer **(4)** (0.701g, 0.397 mmol). This mixture was stirred at room temperature for 24 hours. After removing the solvent, a red-brown precipitate was obtained. This was then washed with ether and ethanol. Yield (0.52g)
^{1}H NMR (CD_3CN): δ = 0.97 (m, CH_3), 1.36 (m, CH_2), 1.61 (m, CH_2), 3.11 (m, N-CH_2), 4.62 (br m, Cl-CH_2-), 7.5-6.3 (br aryl-*H*).

[1] Clark, J., Hammerschlag, A., *Chem. Abstr.*, **1957**, *51*, 12144.
[2] Montheard, J., Jegot, C., Lamps, M., *J.M.S.-Rev. Macromol. Chem. Phys.***, 1999,** *C39*, 135.
[3] Fukuda, H., Nakashima, Y., *J. Polym. Sci. Polym. Chem. Ed.*, **1983**, *21*, 1423.
[4] Amadei, H., Montheard, J., Boiteux, G., Seytre, G., *J. Polym. Mater.*, **1986**, *3*, 5.
[5] Hayashi, A., Goto, Y., Nakayama, M., Kaluzynski, K., Sato, H., Kata, K., Kondo, K., Watanabe, T., Miyata, S., *Chem. Mater.*, **1992**, *4*, 555.
[6] Kondo, S., Minafujii, M., Inagki, Y., Tsuda, K., *Polym. Bull.*, **1986**, *15*, 77.
[7] Gross, A., Maier, G., Nuyken, O., *Macromol. Chem. Phys.*, **1996**, *197*, 2811.
[8] Kondo, S., Kawasoe, S., Kunisada, H., Yuki, Y., *J. Macromol. Sci. Pure Appl. Chem.*, **1993**, *A30*, 413.
[9] Yamashita, K., Yamada, A., Goto, T., Lida, K., Higashi, K., Nango, N., Tsuds, K., *Reac. Polym.*, **1994**, *22*, 65.
[10] Tagashi, H., Endo, T., *J. Polym. Sci. Part C: Polym. Lett.*, **1988**, *26*, 77.
[11] Endo, T., Marnoka, S., Yokozawa, T., *J. Polym. Sco. Part A: Polym. Chem. Ed.*, **1987**, *20*, 2575.
[12] Ruckenstein, E., Hong, L., *Macromolecules*, **1993**, *26*, 1363.
[13] Kawakami, Y., Hisada, H., Yamashita, Y., *J. Polym. Sci. Part A: Polym. Chem.*, **1988**, *26*, 1307.
[14] Judeinstein, P., *Chem. Mater.*, **1992**, *4*, 4.
[15] Mayer, C., Cabuil, V., Latol, T., Thouvenot, R., *Angew. Chem. Int. Ed.*, **1999**, *38*, 3672.
[16] Mayer, C., Thouvenot, R., Latot, T., *Chem. Mater.*, **2000**, *12*, 257.
[17] Agustin, D., Dallery, J., Coelho, C., Proust, A., Thouvenot, R., *J. Organometallic Chem.*, **2007**, *692*, 746.
[18] Moore, A., Kwen, H., Beatty, A., Maatta, E.A., *Chem. Comm.*, **2000**, 1793.
[19] Kwen, H., PhD Thesis, Kansas State University, **2000**.
[20] Trnka, T., Grubbs, R., *Acc. Chem. Res.*, **2001**, *34*, 18.
[21] Malaise, G., Bonrath, W., Breuninger, M., Netscher, T., *Helvetica Chim. Acta*, **2006**, *89*, 797.
[22] Hur, N., Klemperer, W., Wang, R., *Inorg. Synth.*, **1990**, *27*, 77.

CHAPTER 5 - 4-Iodophenylimido Hexamolybdate, 4-Nitro-, and 4-Amino-2,2'-Bipyridines

5.1 Introduction

Hexamolybdate is a very intriguing POM because of its ability to exchange its terminal oxygens for imido ligands[1,2]. This capability has led many chemists to investigate new imido ligands for the direct functionalization of hexamolybdate. As discussed in Chapter 1, there are currently three procedures that are commonly employed. The first two were discovered by the Maatta group[3,4] and involved either a phosphineimine or isocyanate. It is thought to undergo a

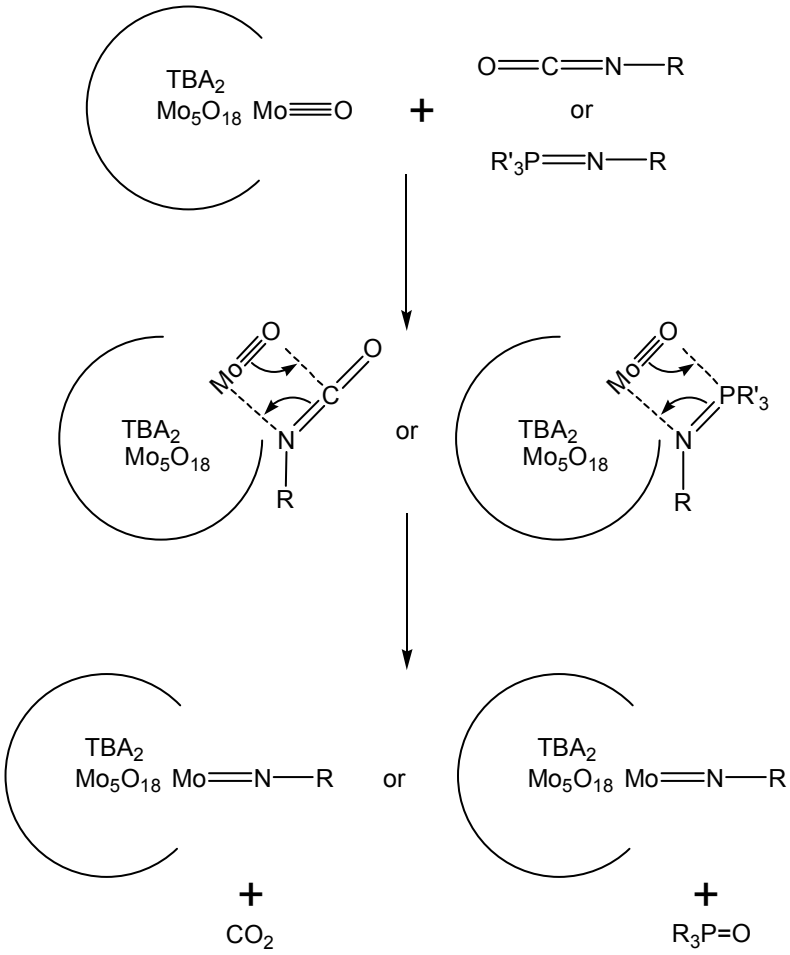

Figure 5-1 Schematic representation of the proposed four member intermediates in the substitution of hexamolybdate.

"Wittig-like" [2+2] exchange process (Figure 5-1). The third method, developed by Peng[5], uses an aromatic amine and an initiator dicyclohexylcarbodiimide (DCC). There are also reports of functionalized hexamolybdates being obtained from the reaction of octamolybdate, $[Mo_8O_{26}]^{4-}$, and the hydrogen chloride salt of an amine.[6] The formation of the substituted hexamolybdate is thought to be the result of a cluster rearrangement. However, there are not many examples of this rearrangement in the literature.

With these procedures in hand, the goal of obtaining an organic functionalized hexamolybdate is possible. As mentioned in Chapter 1, the Maatta group has successfully synthesized and characterized many substituted hexamolybdates. Most of the compounds were developed for metal coordination in hopes that electron transfer would occur between the coordinated metal and hexamolybdate cluster. Unfortunately, the imido ligands were not successful in metal coordination because of the large electron withdrawing effect of the cluster. One approach to combat this problem is to extend the coordinating site away from the cluster (Figure 5-2). Another idea was to synthesize more efficient imido ligands for metal

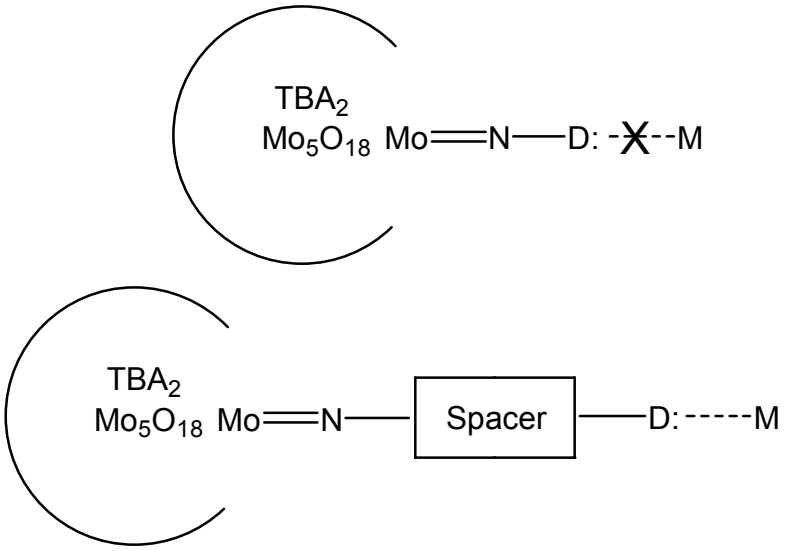

Figure 5-2 Schematic representation of the effect of adding an organic spacer between the hexamolybdate cluster and the donor site for metal coordination.

coordination. Instead of synthesizing imido ligands bearing only one site capable for metal coordination, imido ligands that can act as bidentate ligands are desired. This may not solve the

electron withdrawing effect, but should result in a more favorable environment for the metal atom.

Herein, I will describe the synthesis and characterization of an iodophenylimido hexamolybdate. Also, the synthesis and single crystal analysis of 4-nitro- and 4-amino-2,2'bipyridine will be described.

5.2 Results and Disscussion

5.2.1 Iodophenylimido Hexamolybdate

We wished to incorporate an iodo function into the hexamolybdate cluster. Halogens are very reactive groups and can be used in a variety of coupling reactions. The synthesis of the desired hexamolybdate utilized 4-iodophenyl isocyanate reacting with hexamolybdate dissolved in pyridine (Figure 5-3). The orange solution was heated for 1 day at 80 ºC and filtered through

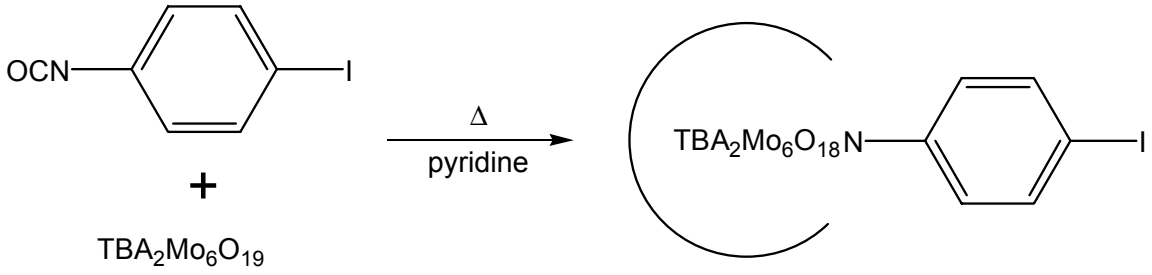

Figure 5-3 Reaction scheme for the formation of iodophenylimido hexamolybdate.

a frit to remove any precipitates. The product was obtained after removing the solvent to yield an orange precipitate. Single crystals were grown for x-ray analysis by vapor diffusion of ether into acetonitrile.

The structure is displayed in Figure 5-4 and reveals the substituted hexamolybdate cluster, one TBA, and one disordered TBA in the unit cell. The Mo-N bond distance is 1.737 Å and is slightly longer than those of the terminal oxygens (1.68 Å), but is shorter than the bridging oxygens (1.9 Å) which implies multiple bond character. The Mo-N-C unit is not completely linear, which is consistent with other substituted hexamolybdate structures, with the angle being 156.4º. Other bond lengths and angles can be found in Appendix B.

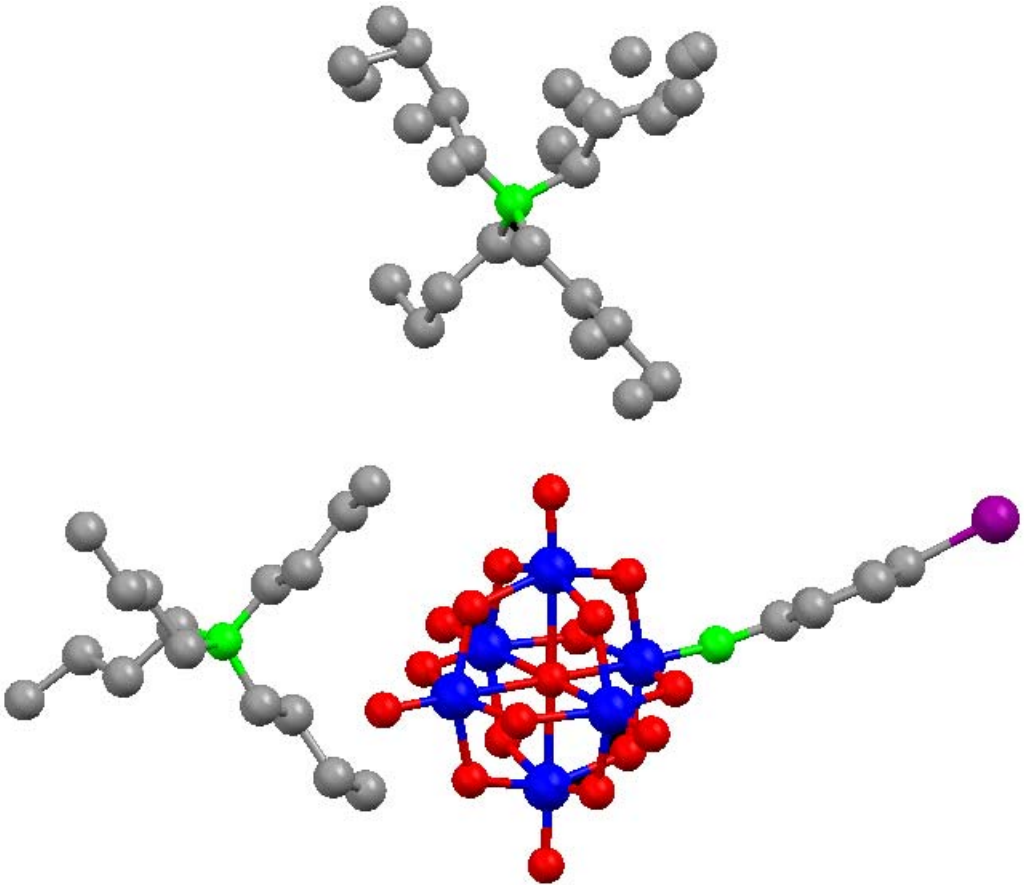

Figure 5-4 Ball and stick representation of the unit cell for iodophenylimido hexamolybdate (hydrogens are omitted for clarity).

This particular substituted hexamolybdate was synthesized in the hope that it would lead to further extended clusters. The goal was to perform Suzuki couplings[7] with the iodo functionality and form new carbon-carbon bonds (Figure 5-5). As discussed earlier in Chapter 3,

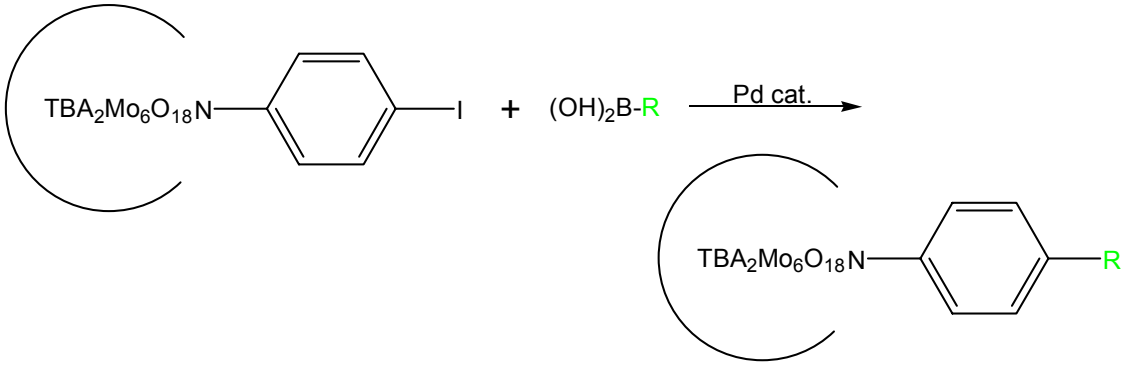

Figure 5-5 Scheme representing the possible Suzuki coupling reaction, R = organic fragment.

these extended systems could help diminish the electron withdrawing effect of the cluster and hence increase the ability to bind a metal. Also, the iodo could be reacted with amines and yield a new carbon-nitrogen bond[8] as described in Figure 5-6.

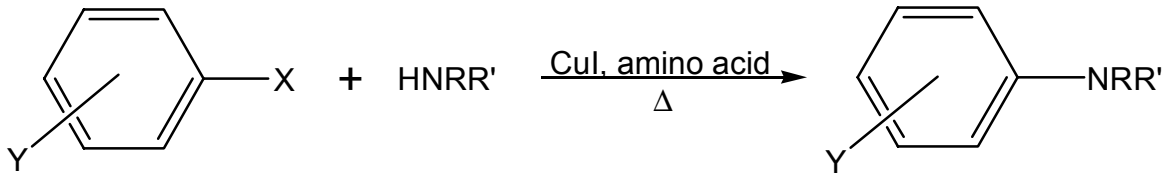

Figure 5-6 Reaction scheme for the formation of a C-N bond with an amine and halogen. (Y,R, and R' = organic substituent, X = I or Br, amino aicd = N-methylglycine, L-proline, or N,N-dimethylglycine)

One final objective for the iodophenylimido hexamolybdate was to investigate its ability to form halogen bond interactions.[9] This was thought to be very promising because of the electron withdrawing effect of the cluster making the iodo group very "active" for halogen bond interactions. The loss of electron density should encourage the iodine atom to interact with a lone pair of electrons from a suitable donor. For example, the nitrogen in pyrazine would be ideal for such a case. In an effort to observe this, iodophenylimido hexamolybdate was mixed in a 1:2 ratio with tetramethylpyrazine and 4,4'-bipyridine in solution in the hopes of creating cocrystals (Figure 5-7). Preliminary results produced one crystal, but it was unsuitable for x-ray analysis. Further investigation is needed.

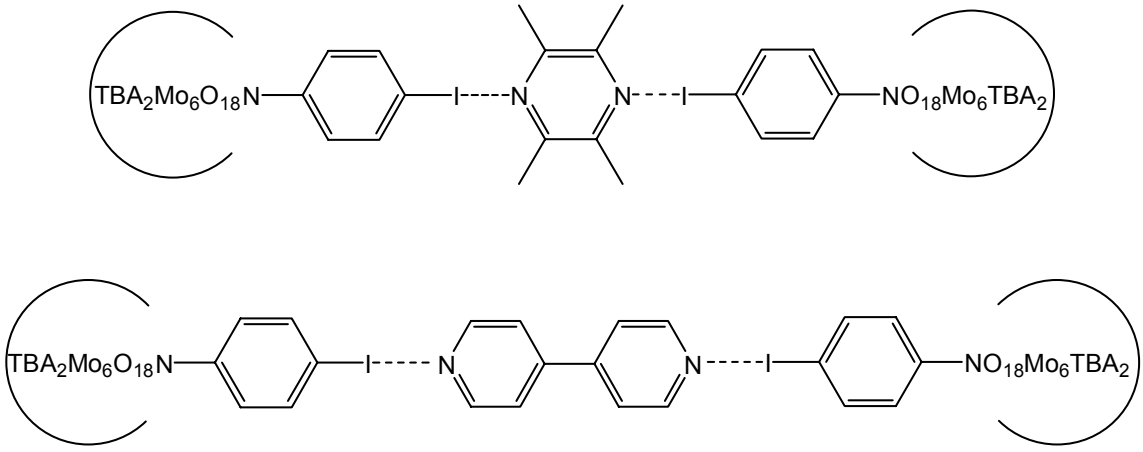

Figure 5-7 Representation of the possible halogen-nitrogen interactions.

5.2.3 4-Amino- and 4-Nitro- 2,2'-Bipyridine[10]

With the goal of coordinating a metal with a functionalized hexamolybdate, a bipyridine seemed to be an appropriate choice for a ligand. Herein, the synthesis and characterization of 4-amino-2,2'-bipyridine will be described.

In an effort to synthesize 4-amino-2,2'bipyridine, the procedure reported by Zhang[10] was followed. In the first step, 2-trimethylstannylpyridine was synthesized. This was done by reacting n-butyl lithium with 2-bromopyridine and trimethyltin chloride. This was then coupled

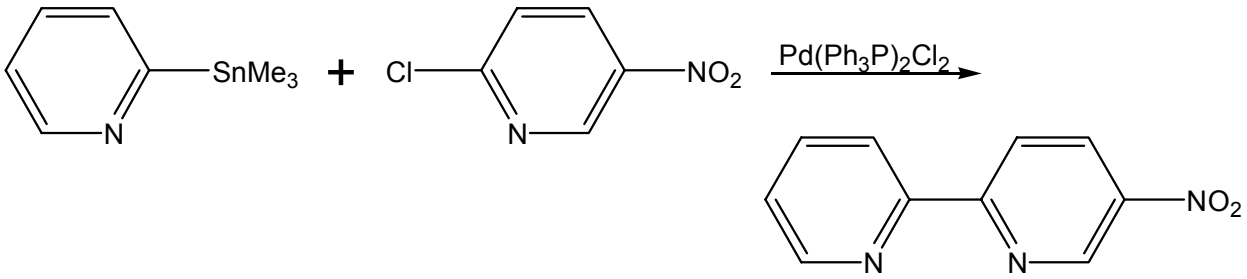

Figure 5-8 Reaction scheme for the formation of 4-nitro-2,2'-bipyridine.[10]

with 2-chloro-5-nitropyridine in a Stille reaction[10] (Figure 5-8). Following purification, single crystals were obtained by slow evaporation of a dichloromethane solution. From the X-ray analysis of the crystal, only one molecule is found in the unit cell and typical features of bipyridine compounds are observed (Figure 5-9). The nitrogen of the pyridine rings are aligned opposite from each other. The rings are nearly planar as seen by the torsion angle between the rings of 179.96º. The nitro group is as expected with N-O bond lengths of 1.217 Å and 1.218 Å. Other bond lengths and angles can be found in Appendix B.

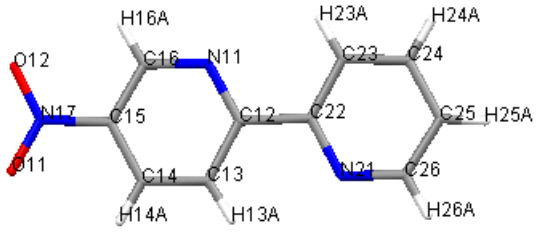

Figure 5-9 Stick representation of the unit cell for 4-nitro-2,2'-bipyridine.

To obtain the amino derivative, the nitro group must be reduced. This was accomplished by the reaction of nitro-bipyridine with sodium borohydride and palladium on carbon as a

catalyst (Figure 5-10). Single crystals were obtained by slow evaporation of a dichloromethane solution which was used for x-ray analysis. It was determined that two molecules of amino-

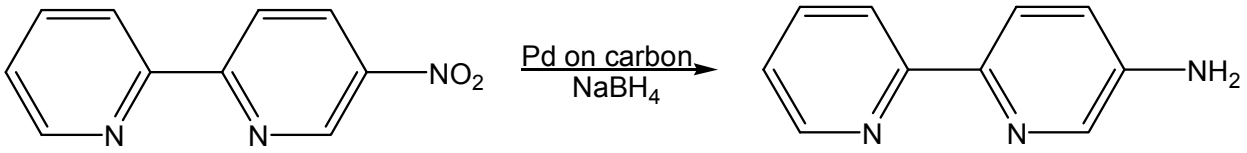

Figure 5-10 Reaction scheme for the formation of 4-amino-2,2'-bipyridine.

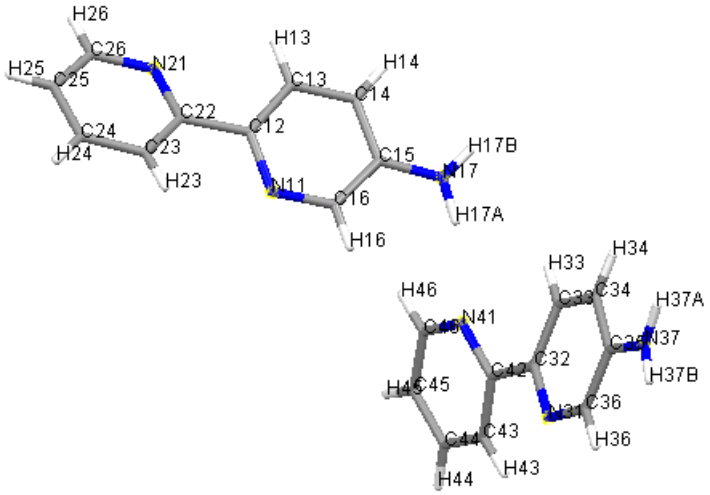

Figure 5-11 Stick representation of the unit cell for 4-amino-2,2'-bipyridine.

bipyridine are found in the unit cell (Figure 5-11). Again, the nitrogen of the pyridine rings are opposite to one another. The ring containing the amino group is nearly planar as seen by the torsion angle (179.5º). The two pyridine rings of the bipyridine molecules are not planar due to self complementary H-bonding (Figure 5-12). The amino group of one bipyridine is H-bonded to a pyridine of another bipyridine which does not bear the amino functionality. This results in a torsion angle between connected pyridine rings of 158.2º. The N-H-N bond lengths are 2.15 Å and 2.14 Å respectively. This is drastically different than the nitro-bipyridine crystal structure which displayed no H-bonding and nearly planar rings. All other bond angles and lengths can be found in Appendix B.

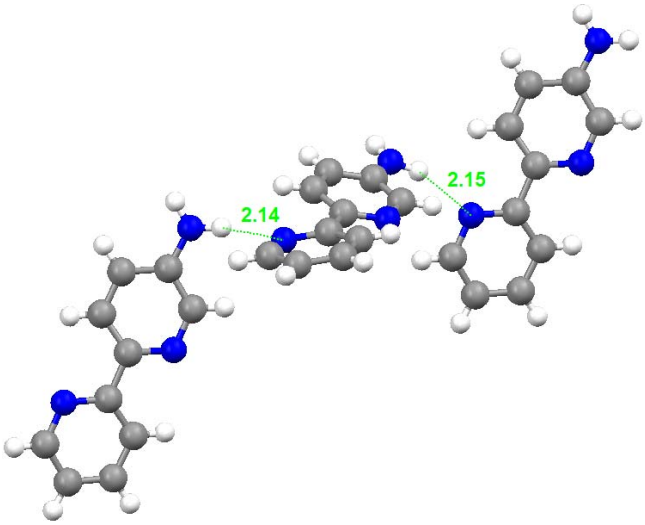

Figure 5-12 H-bonds interactions and bond lengths (**Å**) in 4-amino-2,2'-bipyridine.

5.2.4 Conclusions

A new functionalized hexamolybdate was synthesized using an isocyanate bearing an iodo functionality. It was characterized through ^{1}H NMR, IR, and single crystal x-ray diffraction. Attempts to couple the iodo with boronic acids produced varying results. ^{1}H NMR experiments suggest that the carbon-carbon coupling between the iodophenylimido hexamolybdate and a boronic acid worked, but the product was contaminated with impurities that could not be removed. In most cases, however, the imido bond was cleaved and only nonsubstituted hexamolybdate was retrieved. However, only a few experimental conditions have been tested as well as only a few catalyst tried. Much more investigation needs to be done with this very promising POM.

Single crystals have been grown and analyzed of 4-nitro and 4-amino-2,2'-bipyridine. The 4-amino-2,2'-bipyridine was synthesized in an attempt to substitute this molecule onto hexamolybdate through a phosphineimine reaction. Unfortunately, the substitution was not accomplished, but a crystal structure for the 4-nitro-2,2'-bipyridine was obtained and reported for the first time.

5.3 Experimental

5.3.1 Instrumentation

All chemicals were purchased from Aldrich and used without further purification. ^{1}H NMR spectra were recorded on a Varian Unity plus 400 MHz or 200 MHz spectrometer in CD_3CN or CD_3Cl. Compounds were prepared for infrared (IR) analysis on a Nicolet Protégé 460 as KBr pellets. Mass spectra, MALDI-TOF/ TOF-MS, were collected on a Bruker Daltonics Ultraflex TOF/TOF.

X-ray data was collected on a Bruker SMART 1000 four-circle CCD diffractometer at 203 K for 4-nitro-2,2'-bipyridine and 4-amino-2,2'-bipyridine and SMART APEX CCD diffractometer at 100 K for iodophenylimido hexamolybdate using a fine-focus molybdenum Kα tube. Data was collected using SMART.[11] Initial cell constants were found by small widely separated "matrix" runs. Generally, an entire hemisphere of reciprocal space was collected regardless of Laué symmetry. Scan speed and scan width were chosen based on scattering power and peak rocking curves.

Unit cell constants and orientation matrix were improved by least-squares refinement of reflections thresholded from the entire dataset. Integration was performed with SAINT,[12] using this improved unit cell as a starting point. Precise unit cell constants were calculated in SAINT from the final merged dataset. Lorenz and polarization corrections were applied. Laué symmetry, space group, and unit cell contents were found with XPREP. Absorption correction was applied as noted.

Data was reduced with SHELXTL.[13] The structures were solved in all cases by direct methods without incident. All hydrogens were assigned to idealized positions and were allowed to ride. Orientation of methyl groups was allowed to rotate using the "AFIX 137" command. All heavy atoms were refined with anisotropic thermal parameters.

Data for 4-nitro-2,2'-bipyridine was not corrected for absorption.

For iodophenylimido hexamolybdate, the asymmetric unit contained one metal cluster, one fully ordered, well behaved Bu_4N cation, and one partially disordered Bu_4N cation. The latter counterion contained three disordered n-butyl chains. The first (C51A-C54A / C51B-C54B) was treated as a pair of species, with total occupancy constrained to 100%, and with geometry idealized with distance restraints, pairwise shared anisotropic thermal parameters for

C51A/C51B, C52A/C52B, and C53A/C53B, and independent thermal parameters for C54A and C54B. The second (C61A-C64A / C61B-C64B / C61A-C64C) was treated as a triplet of species, with total occupancy constrained to 100% (using free variables and the SUMP command), and with geometry idealized with distance restraints, shared anisotropic thermal parameters for each triplet C51A/C51B/C51C, C52A/C52B/C52C, C53A/C53B/C53C, and C54A/C54B/C54C. The third (C73A/C73B, C74A/C74B) was disordered over two of the four carbon atoms and was treated as a pair of species, with total occupancy constrained to 100%, and with geometry idealized with distance restraints, pairwise shared anisotropic thermal parameters for C72A/C72B, C73A/C73B, and C74A/C74B. The nearest unsplit atom (C72) was artificially split into 2 atoms in the two PARTs (C72A/C72B) with identical coordinates and thermal parameters, so that pairs of hydrogen atoms could be inserted relative to the disordered chain.

5.3.2 Synthesis

5.3.2.1 Preparation of Iodophenylimido Hexamolybdate (1)

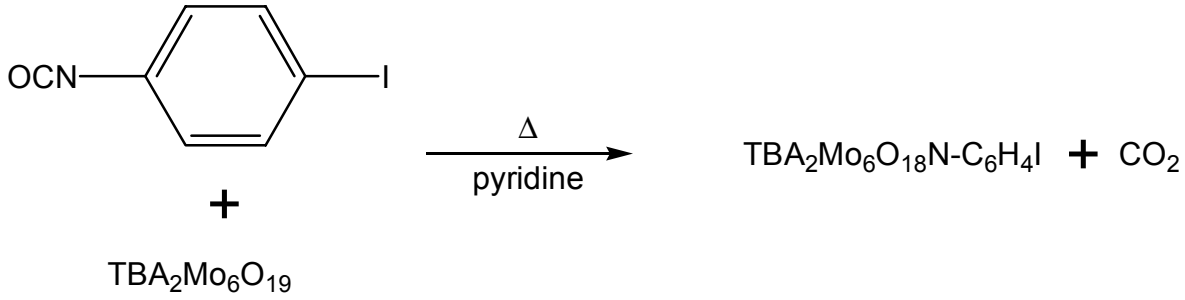

$TBA_2Mo_6O_{19}$ (2.95 g, 2.16 mmol) and 4-iodophenyl isocyanate (0.5 g, 2.16 mmol) were added to a flask inside the glovebox. Dry acetonitrile (20 mL) was added and this mixture was stirred at 90°C for 24 hours. The solvent was removed under vacuum to yield an orange precipitate. A pure product was obtained by slow evaporation of ether into acetonitrile to yield red/orange crystals. Yield (1.35 g, 40%).

^{1}H NMR (CD_3CN): δ = 0.97 (m, 24H, CH_3), 1.36 (m, 16H, CH_2), 1.61 (m, 16H, CH_2), 3.11 (m, 16H, N-CH_2), 6.47 (d, 2H, aryl), and 7.43 (d, 2H, aryl). IR (KBr pellet, cm^{-1}): 975 (sh) and 952 (s).

5.3.2.2 Preparation of 2-trimethylstannylpyridine (2)[10]

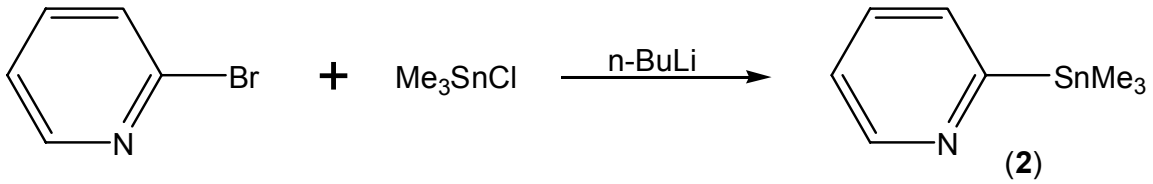

20 mL of a 2.5 M (hexanes) n-BuLi solution was diluted with 25 mL of dry ether at -78 ºC. To this solution, 4.8 mL (50 mmol) of 2-bromopyridine dissolved in 50 mL of dry ether at -78 ºC and canulated to the reaction flask dropwise. The organic solution was stirred for one hour at -78 ºC. A solution of 10.9g (54 mmol) trimethyltin chloride dissolved in 10 mL of THF was added dropwise by syringe. The cold bath was removed and the mixture was allowed to warm to

room temperature. The reaction was quenched with a saturated NH_4Cl solution and the organic layer washed with water, brine, and dried with $MgSO_4$. After removal of the solvent, the product was obtained by short path distillation to yield a colorless liquid. Yield 3.71 g (31%).
^1H NMR ($CDCl_3$): δ = 0.37 (t, 9H, CH_3), 7.13 (m, 1H, aryl), 7.48 (m, 2H, aryl), 8.75 (m, 1H, aryl).

5.3.2.3 Preparation of 4-nitro-2,2-bipyridine (3)[10]

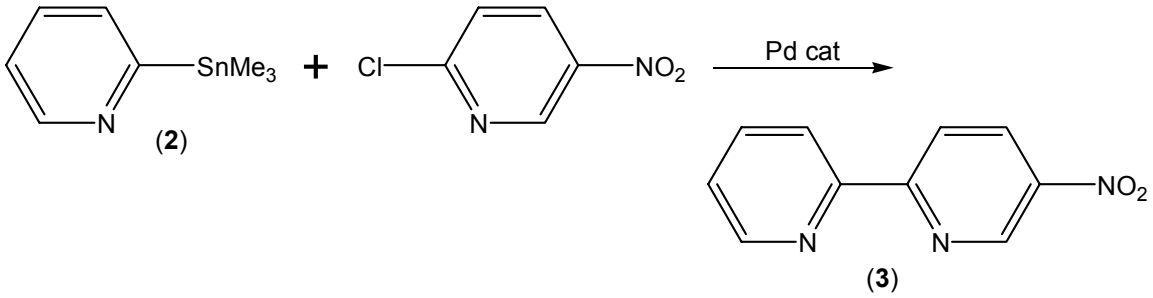

A solution of 2-chloro-5-nitropyridine (1 g, 6.3 mmol), (**2**) (1.65 g, 6.8 mmol), and $Pd(Ph_3P)_2Cl_2$ (0.25 g, 0.34 mmol) in 20 mL of dry THF. This solution was refluxed under an inert atmosphere for 24 hours. The reaction mixture was allowed to cool to room temperature and diluted with 20 mL of ether. The solution was filtered through a small plug of silica gel/celite and eluted with dichloromethane. The solvent was removed to yield a dark red precipitate. This precipitate was dissolved in a minimal amount of dichloromethane and passed through a small plug of silica gel with dichloromethane as the elutent. The final product is yellow in color and crystals are grown by slow evaporation of the solvent. Yield 0.75 g (59%).
^1H NMR ($CDCl_3$): δ = 7.43 (m, 1H, aryl), 7.91 (m, 1H, aryl), 8.53 (t, 1H, aryl), 8.59 (d, 1H, aryl), 8.68 (d, 1H, aryl), 8.75 (d, 2H, aryl), 9.49 (d, 1H, aryl).

5.3.2.4 Preparation of 4-amino-2,2'-bipyridine (4)[10]

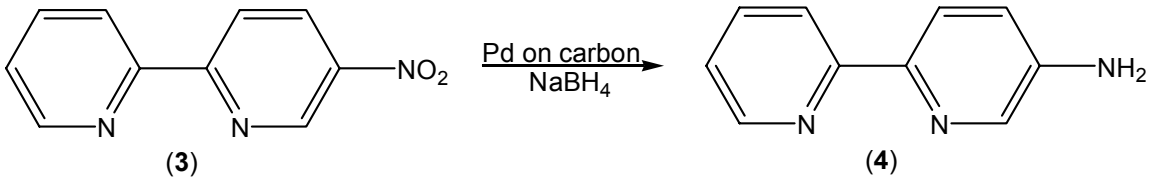

(**3**) (**4**)

4-nitro-2,2'-bipyridine (0.13 g, 0.6467 mmol) was dissolved in 50 mL of methanol. This solution was degassed for 30 minutes with argon. Pd on activated carbon (0.03 g, 10%) was added and the solution was cooled with an ice bath. 0.4 g of sodium borohydride was then added in small increments. The ice bath was removed and the reaction mixture was stirred at room temperature for 5 hours. The Pd was removed by filtration using a Celite bed. The solvent was removed and then 50 mL of water was added to the reaction flask. The product is then extracted with dichloromethane. The organic layer is then dried with $MgSO_4$. Crystals were grown by slow evaporation of a dichloromethane solution. Yield 0.07 g (63%).

^{1}H NMR ($CDCl_3$): δ = 3.85 (br, 2H, NH_2), 7.11 (d, 1H, aryl), 7.22 (m, 1H, aryl), 7.76 (t, 1H, aryl), 8.16 (d, 1H, aryl), 8.21 (d, 1H, aryl), 8.26 (d,1H, aryl), 8.62 (d, 1H, aryl).

[1] J.J. Borras-Almenar, E. Coronado, A. Muller, and M. Pope, Polyoxometalate Molecular Science: Kluwer, Dordrecht, 2001.
[2] Gouzerh, P., and Proust, A., *Chem. Rev.*, **1998**, *98*, 77.
[3] Du, Y., Rheingold, A., Maatta, E.A., *J. Am. Chem. Soc.*, **1992**, *114*, 345.
[4] Strong, J., Ostrander, R., Rheingold, A., Maatta, E.A., *J. Am. Chem. Soc.*, **1994**, *116*, 3601.
[5] Wei, Y., Xu, B., Barnes, C., Peng, Z., *J. Am. Chem. Soc.*, **2001**, *123*, 4083.
[6] Li, Q., Wu, P., Xia, Y., Wei, Y., Guo, H., *Journal of Organometallic Chemistry*, **2006**, *691*, 1223.
[7] Felpin, F., Ayad, T., Mitra, S., *Eur, J. Org. Chem.*, **2006**, 2679.
[8] Zhang, H., Cai, Q., Ma, D., *J. Org. Chen.*, **2005**, *70*, 5164.
[9] Metranglo, P., Neukirch, H., Pilati, T., Resnati, G., *Acc. Chem. Res.*, **2005**, *38*, 386.
[10] Zhang, B., and Braslow, R., *J. Am. Chem. Soc.*, **1997**, *119*, 1676.
[11] SMART v5.060, © 1997 - 1999, Bruker Analytical X-ray Systems, Madison, WI.
[12] SAINT v6.02, © 1997 - 1999, Bruker Analytical X-ray Systems, Madison, WI.
[13] SHELXTL v5.10, © 1997, , Bruker Analytical X-ray Systems, Madison, WI.

Appendix A - NMR, IR, & Mass Spectra

Chapter 2

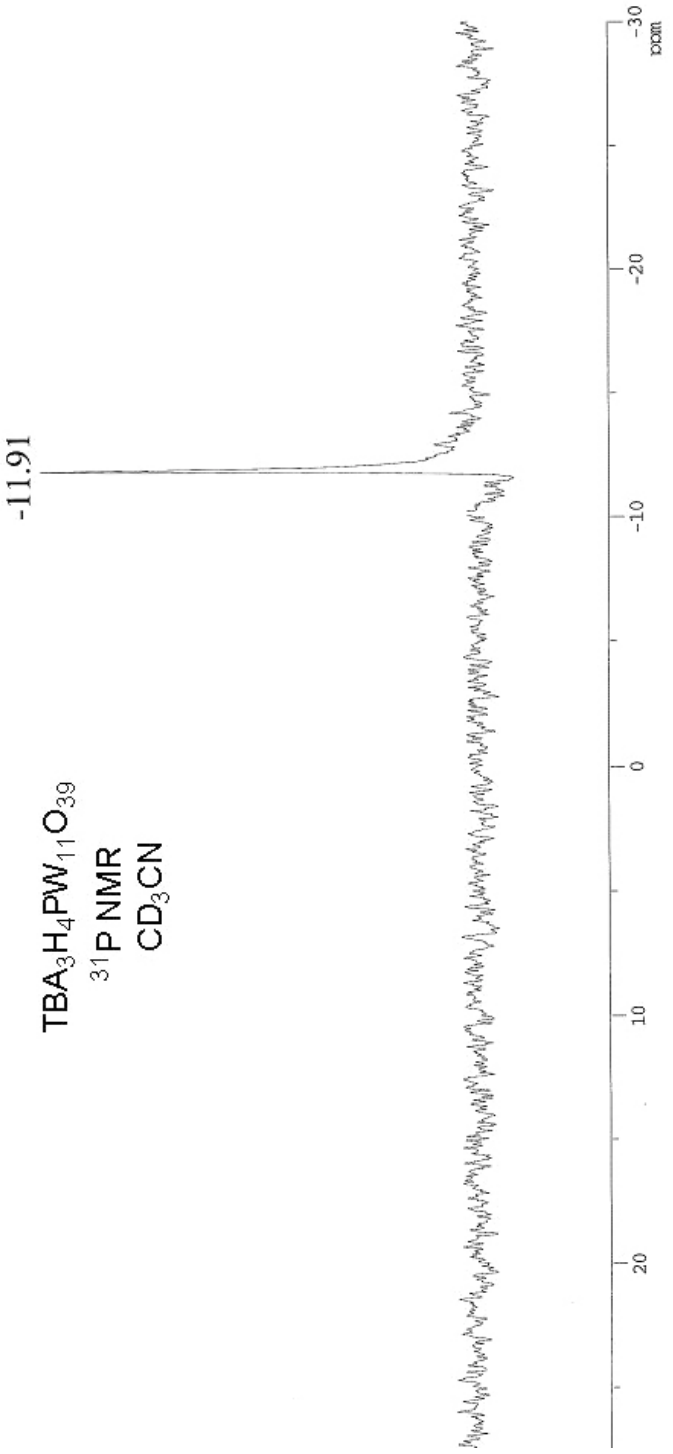

Figure A- 1 ^{31}P NMR of $TBA_3H_4PW_{11}O_{39}$

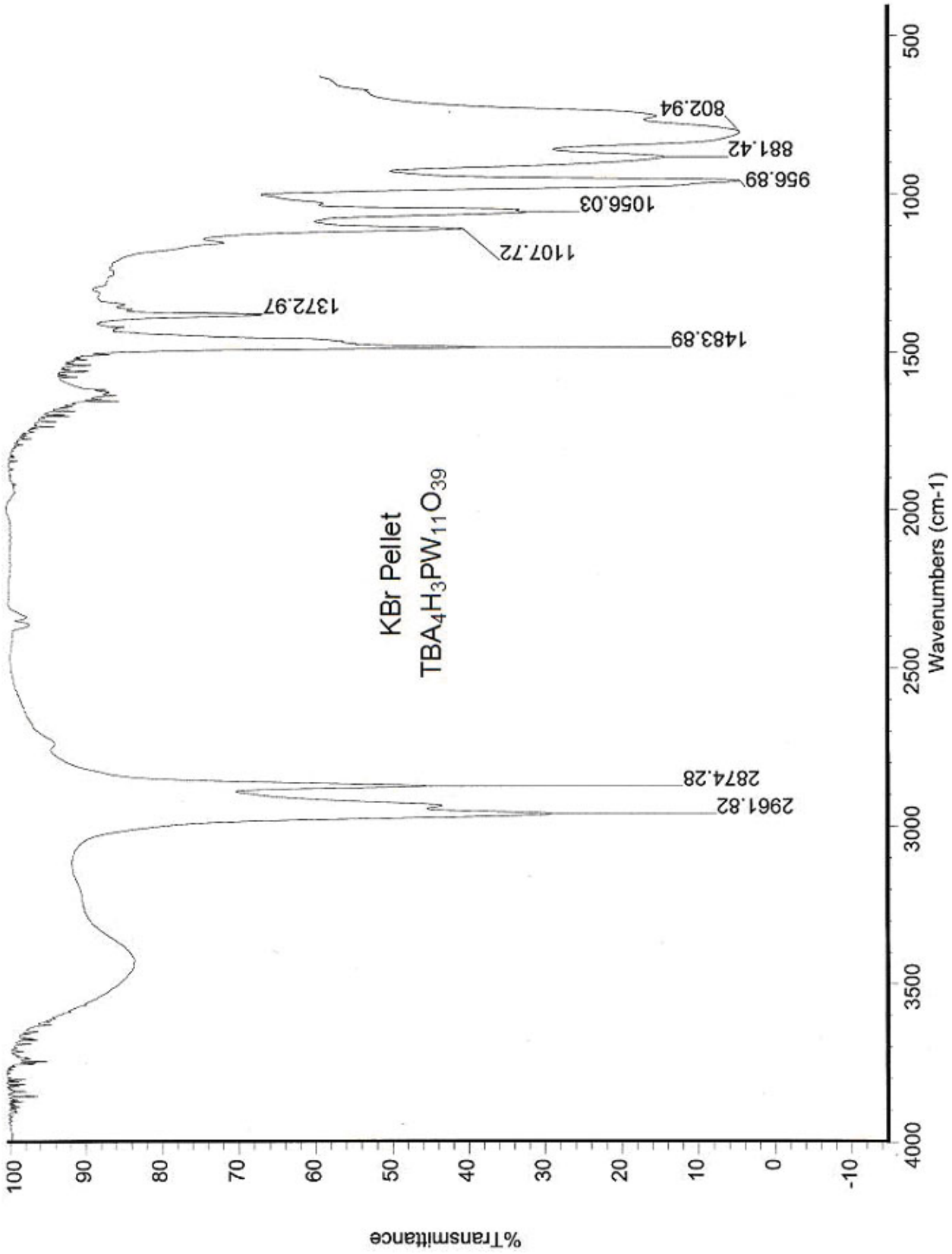

Figure A- 2 IR of $TBA_3H_4PW_{11}O_{39}$

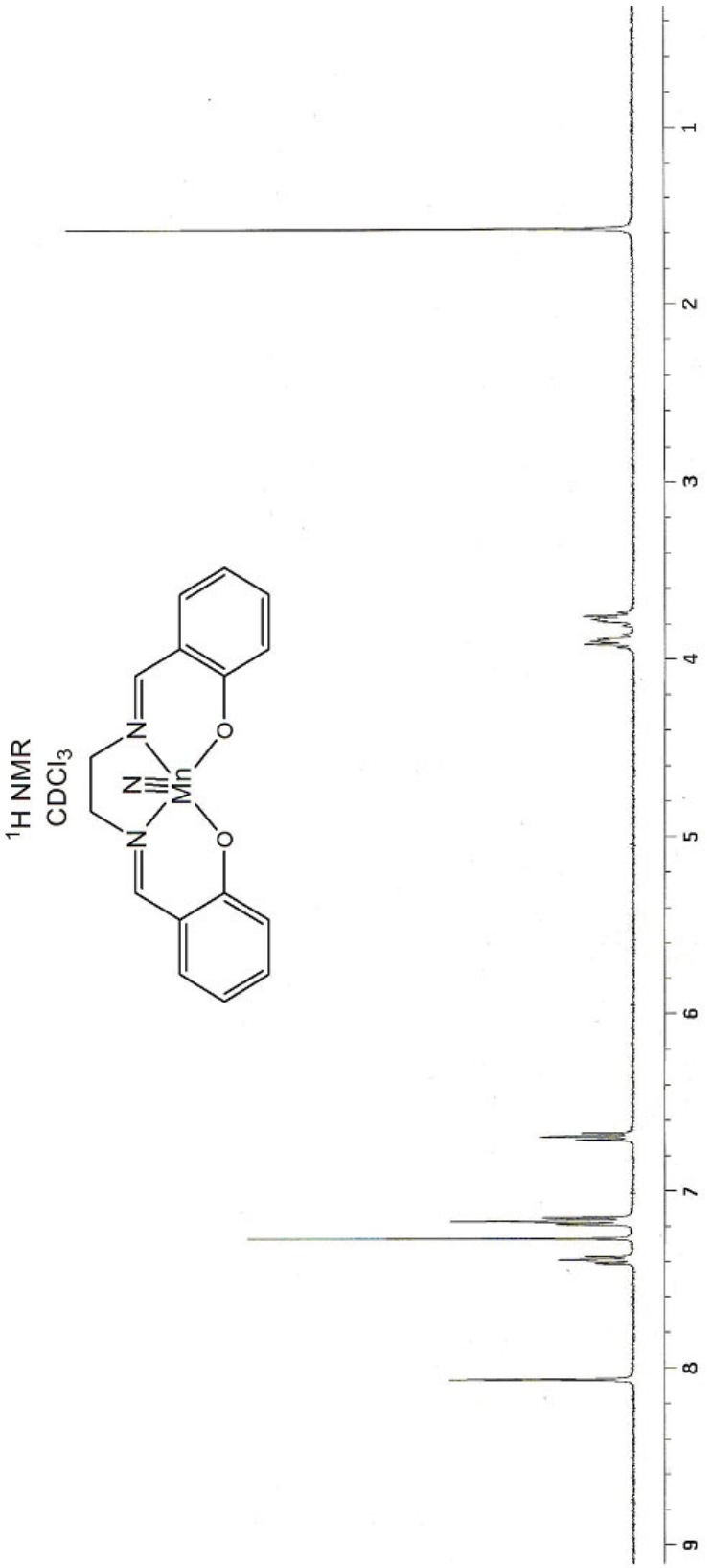

Figure A- 3 ^{1}H NMR of Mn(N) Salen

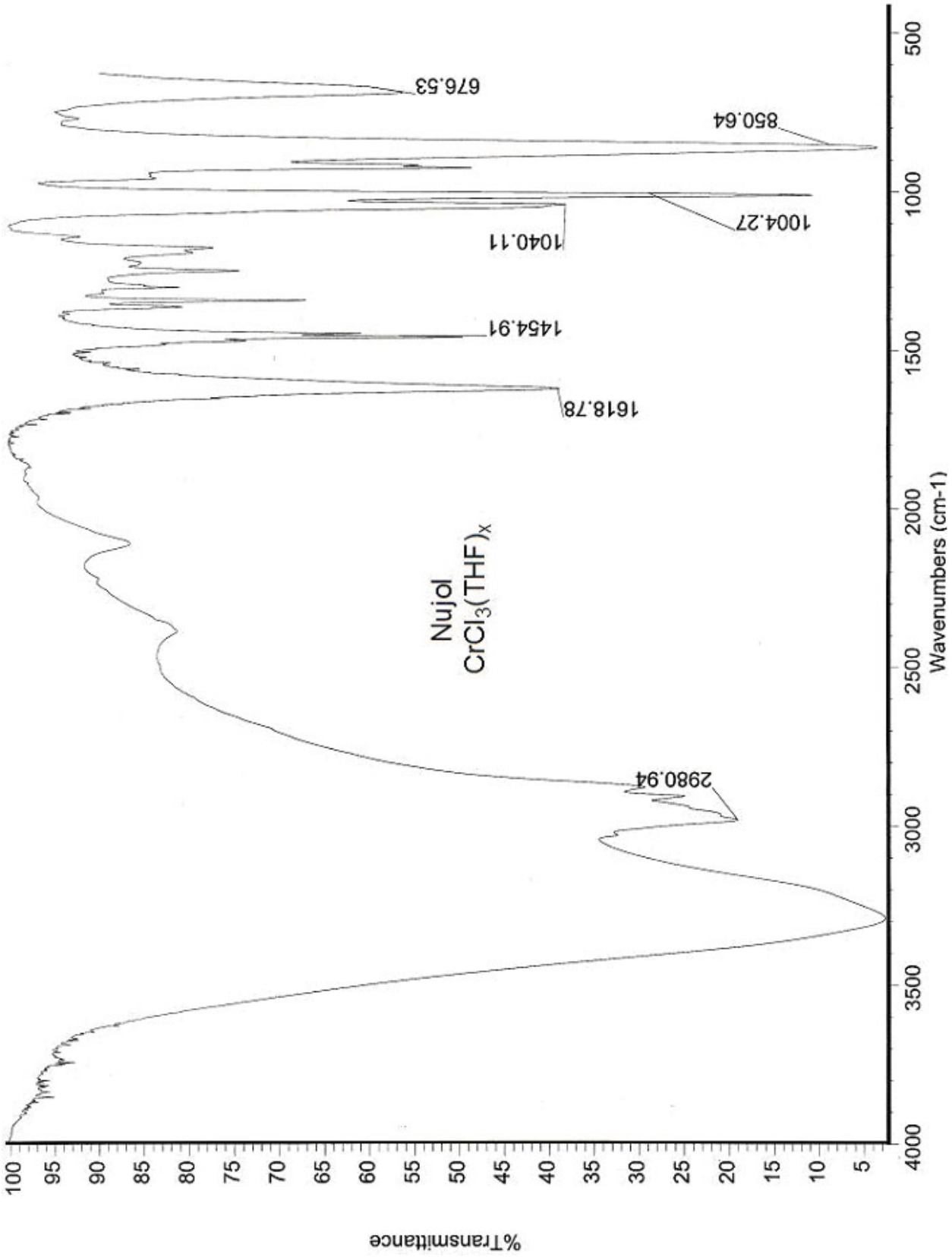

Figure A- 4 IR of $CrCl_3(THF)_x$

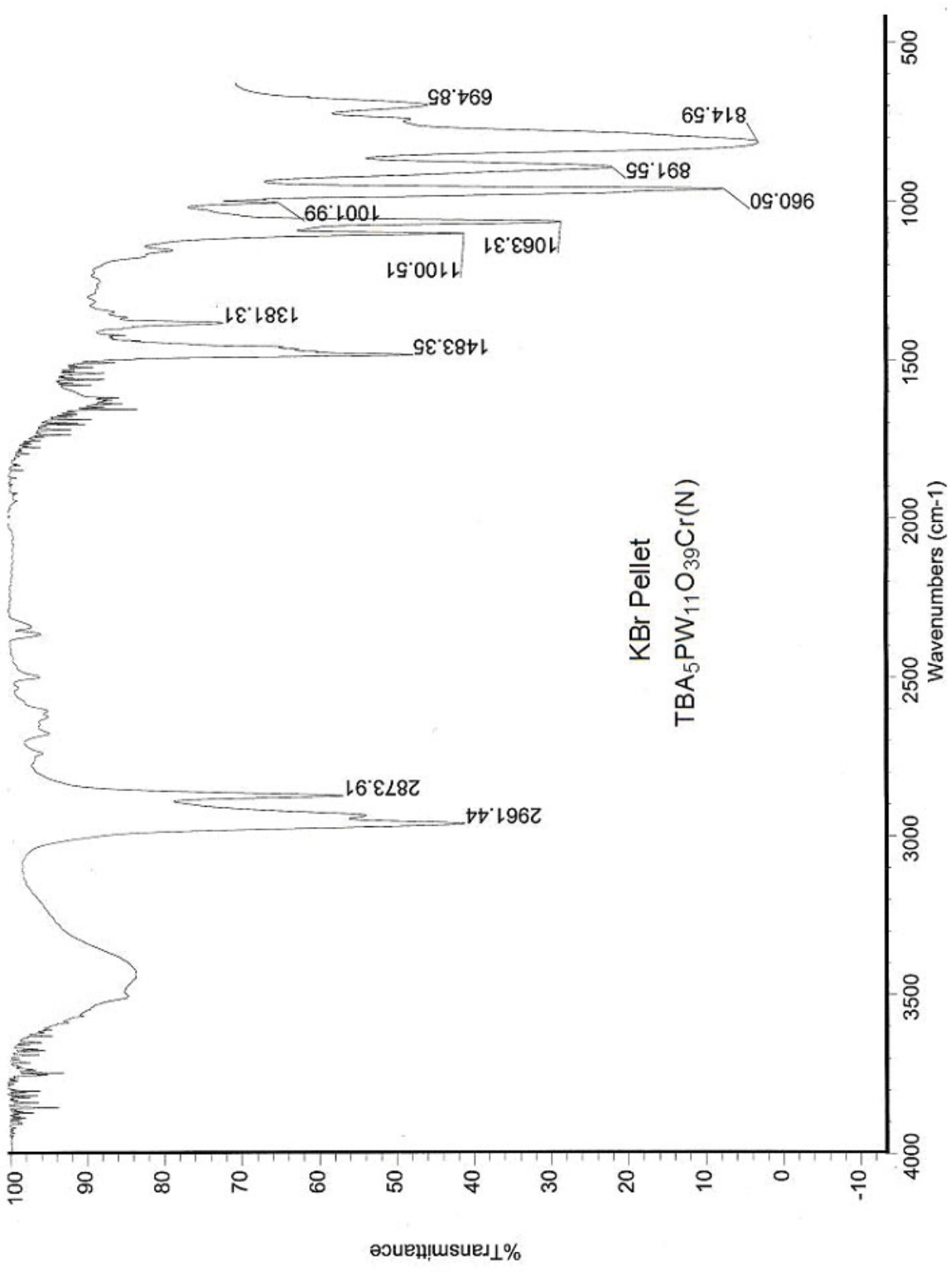

Figure A- 5 IR of $TBA_5PW_{11}O_{39}Cr(N)$

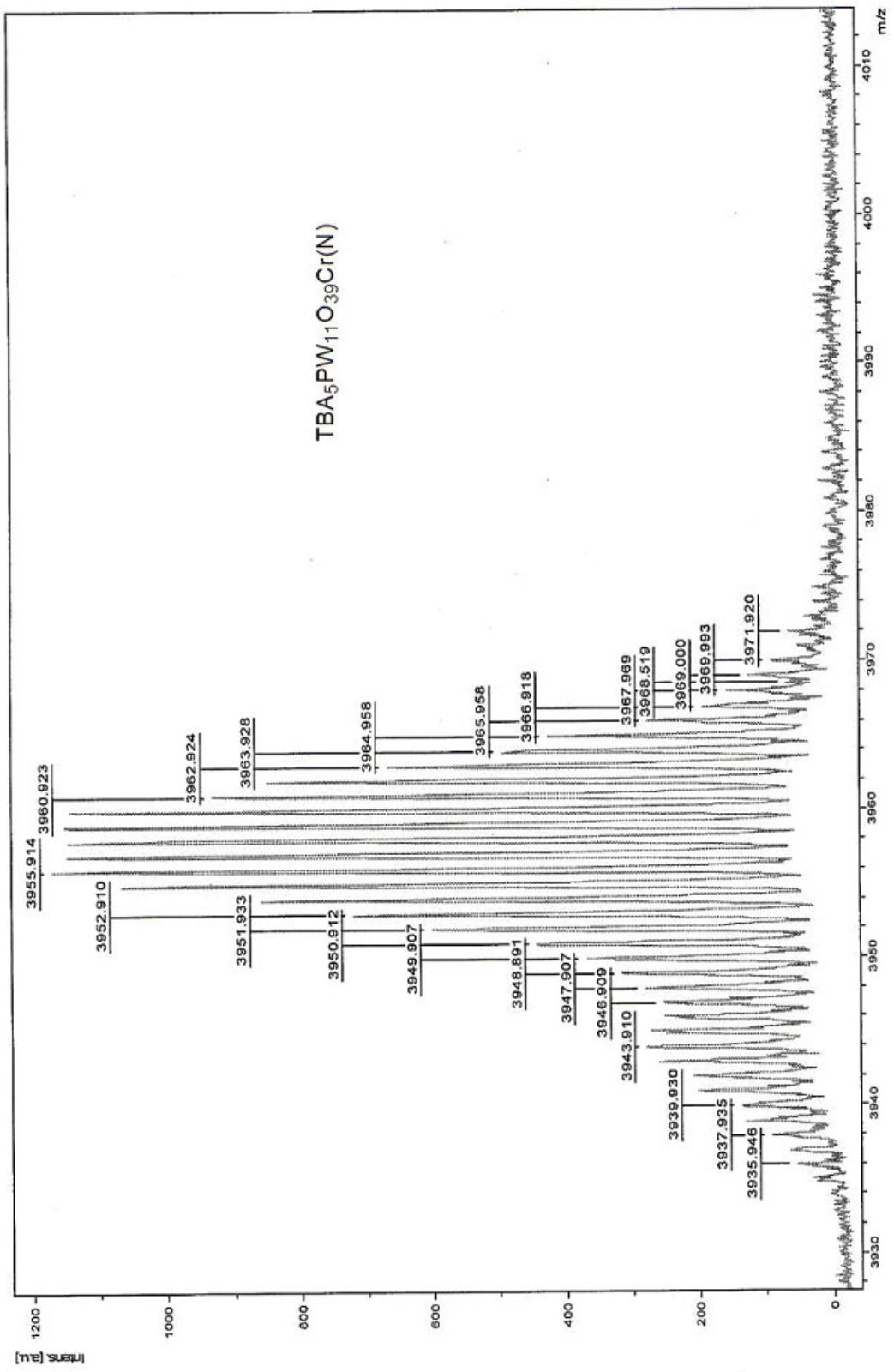

Figure A- 6 Observed mass spectrum of $TBA_5PW_{11}O_{39}Cr(N)$

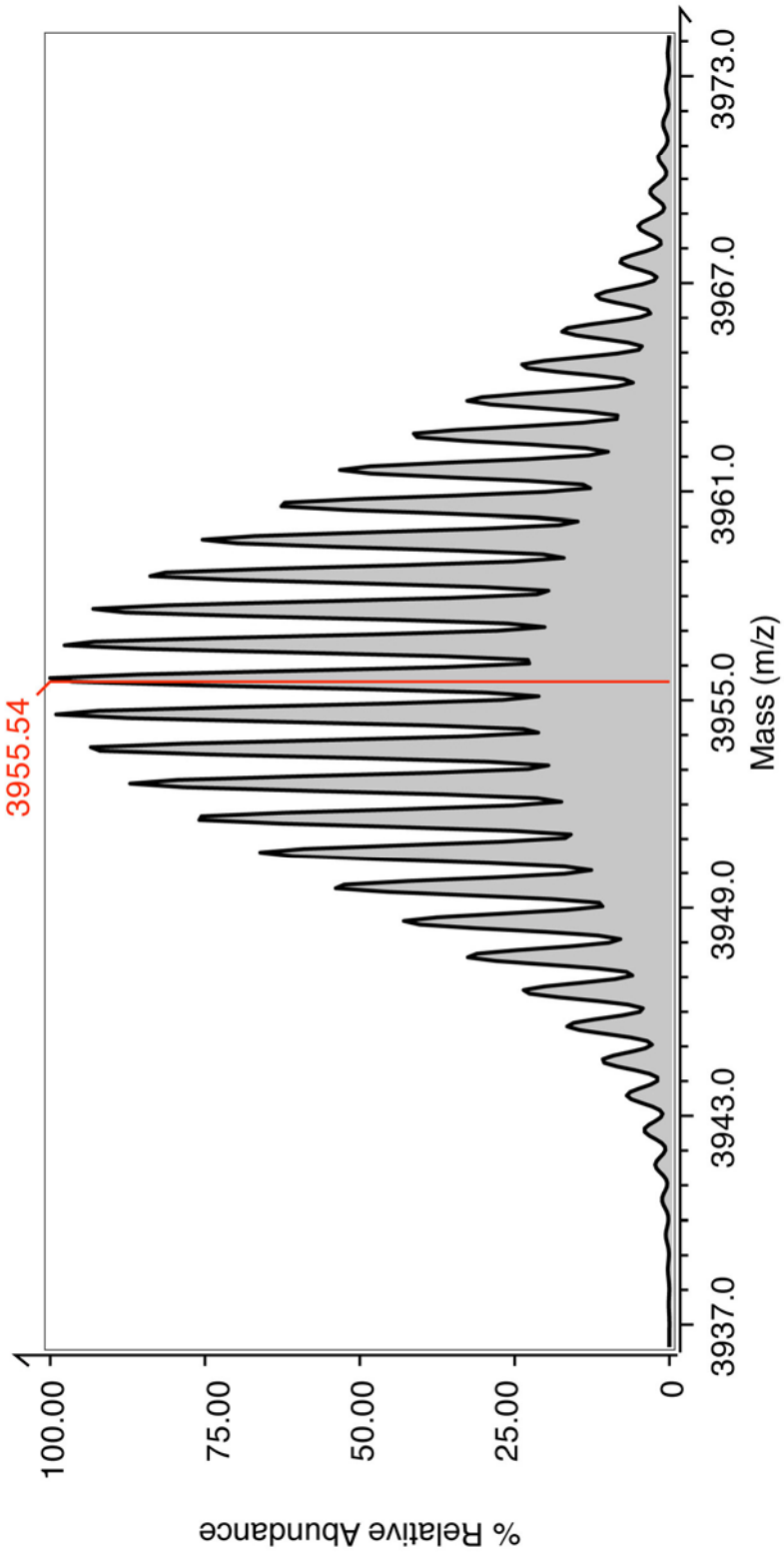

Figure A- 7 Simulated mass spectrum of $[TBA]_5[PW_{11}Cr^{V}N]$.

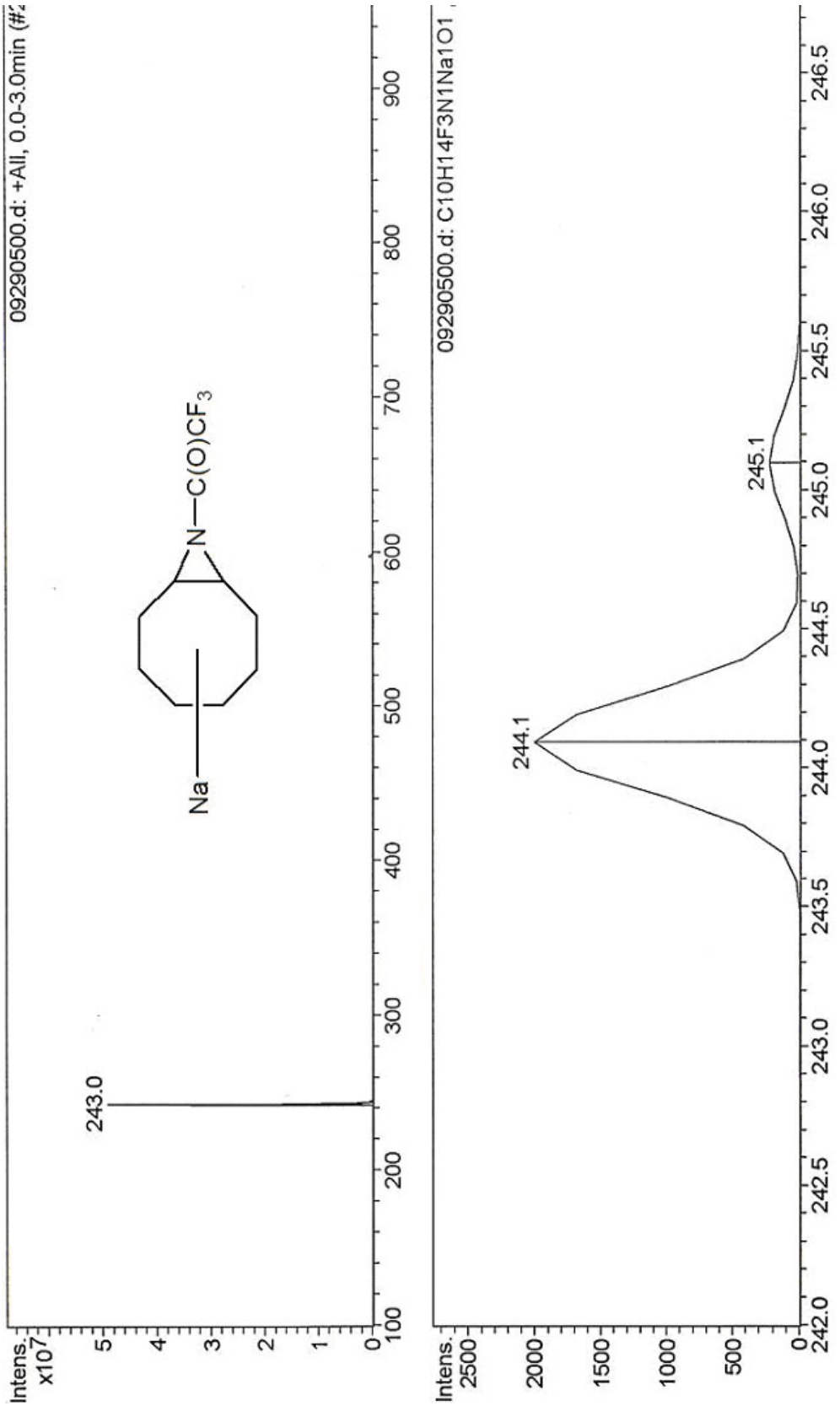

Figure A- 8 Mass Spec. of Aziridine product

Chapter 3

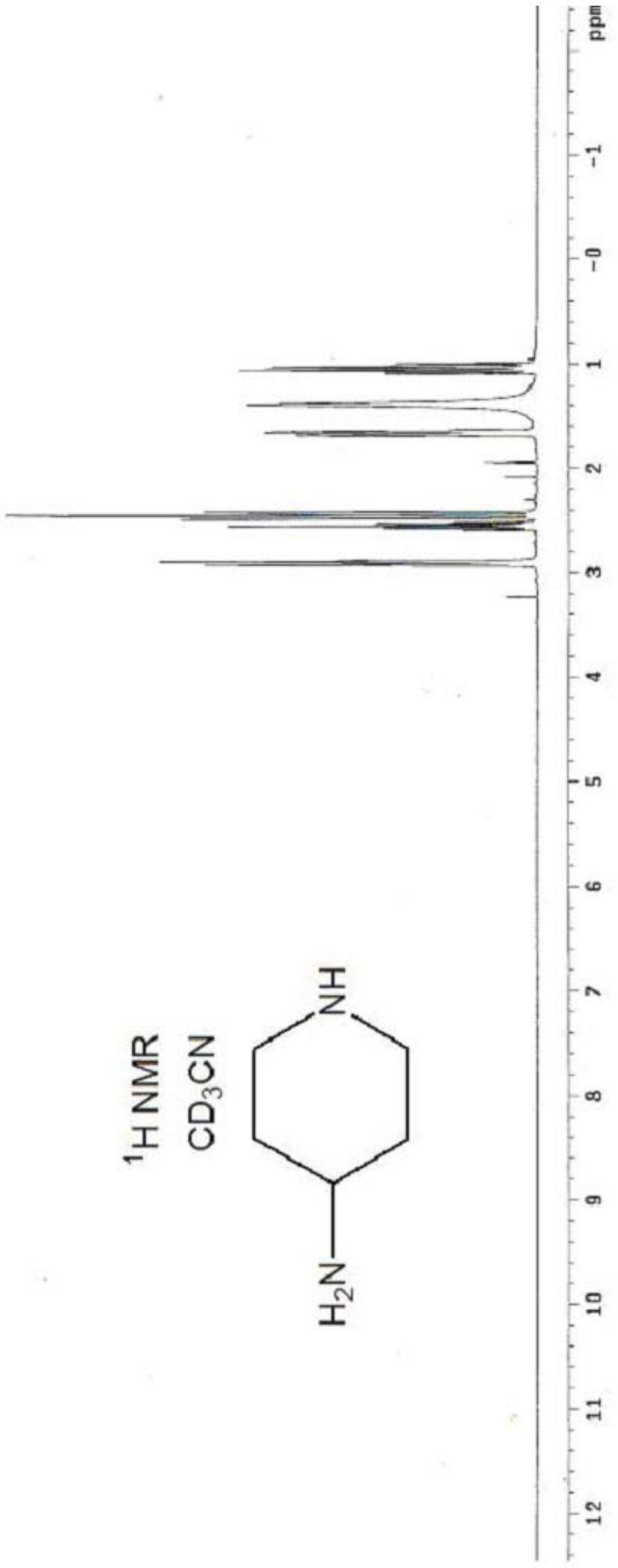

Figure A- 9 ^{1}H NMR of 4-aminopiperidine

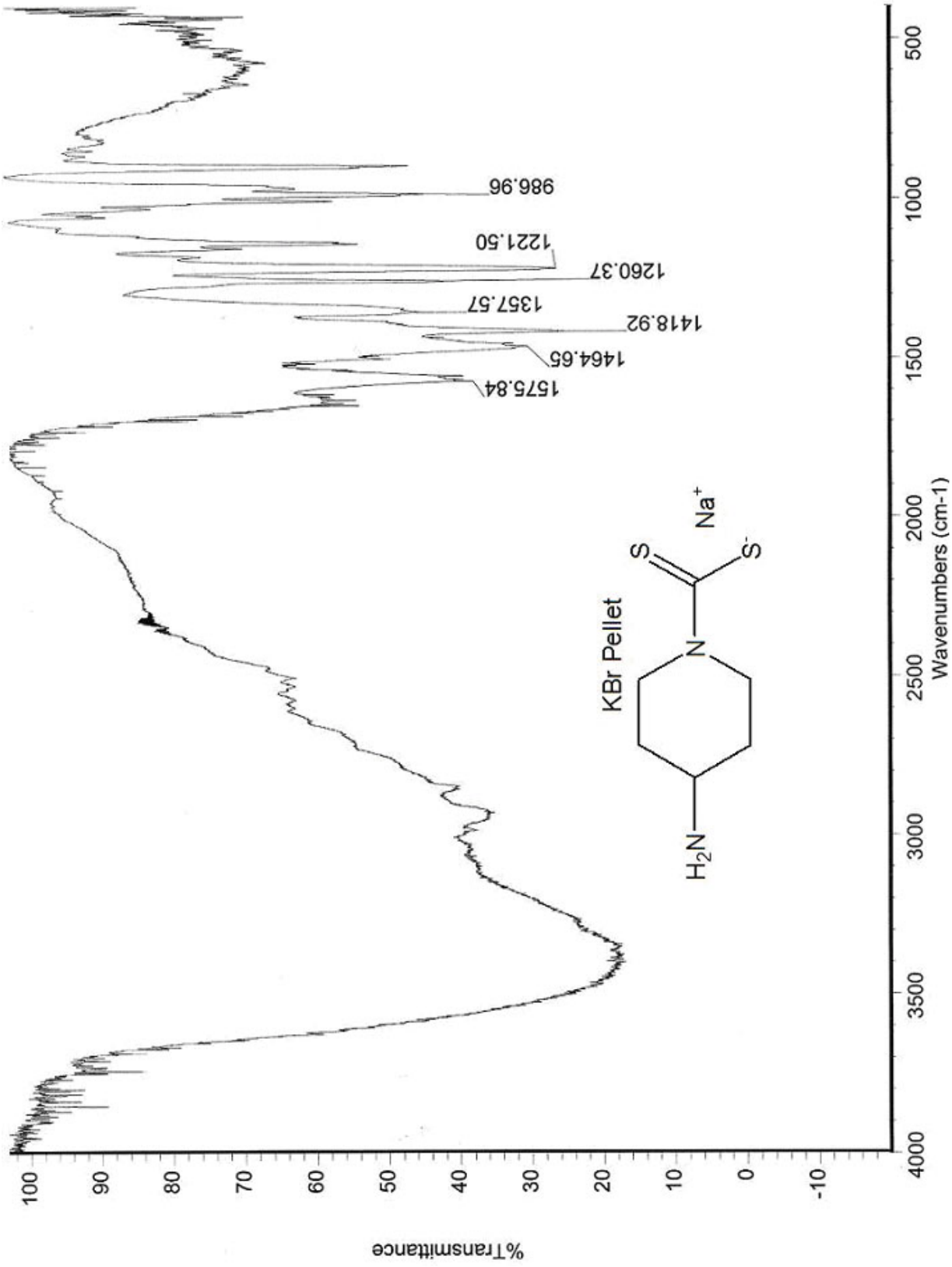

Figure A- 10 IR of Na(DTC)

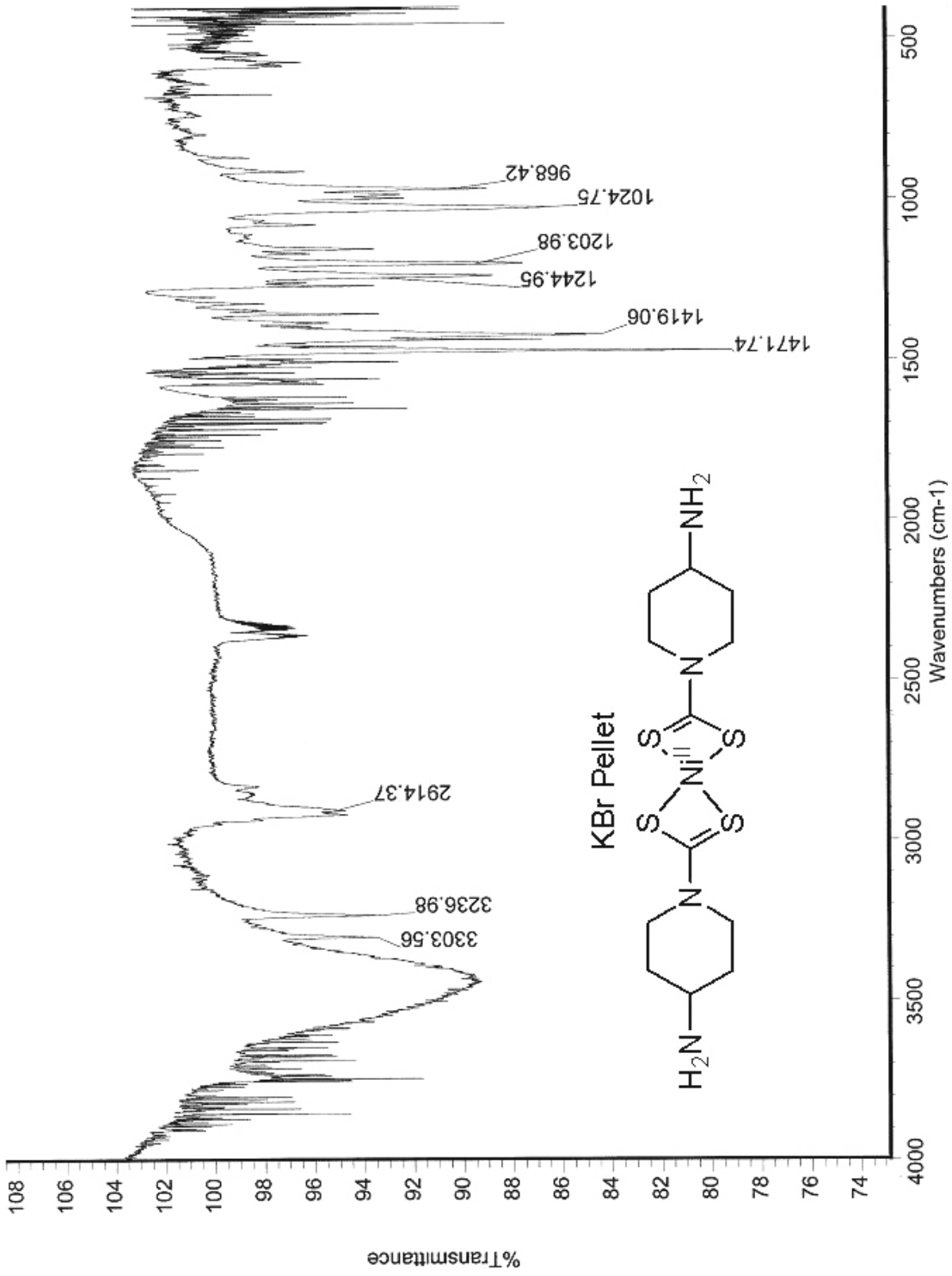

Figure A- 11 IR of Ni^{II}(DTC)

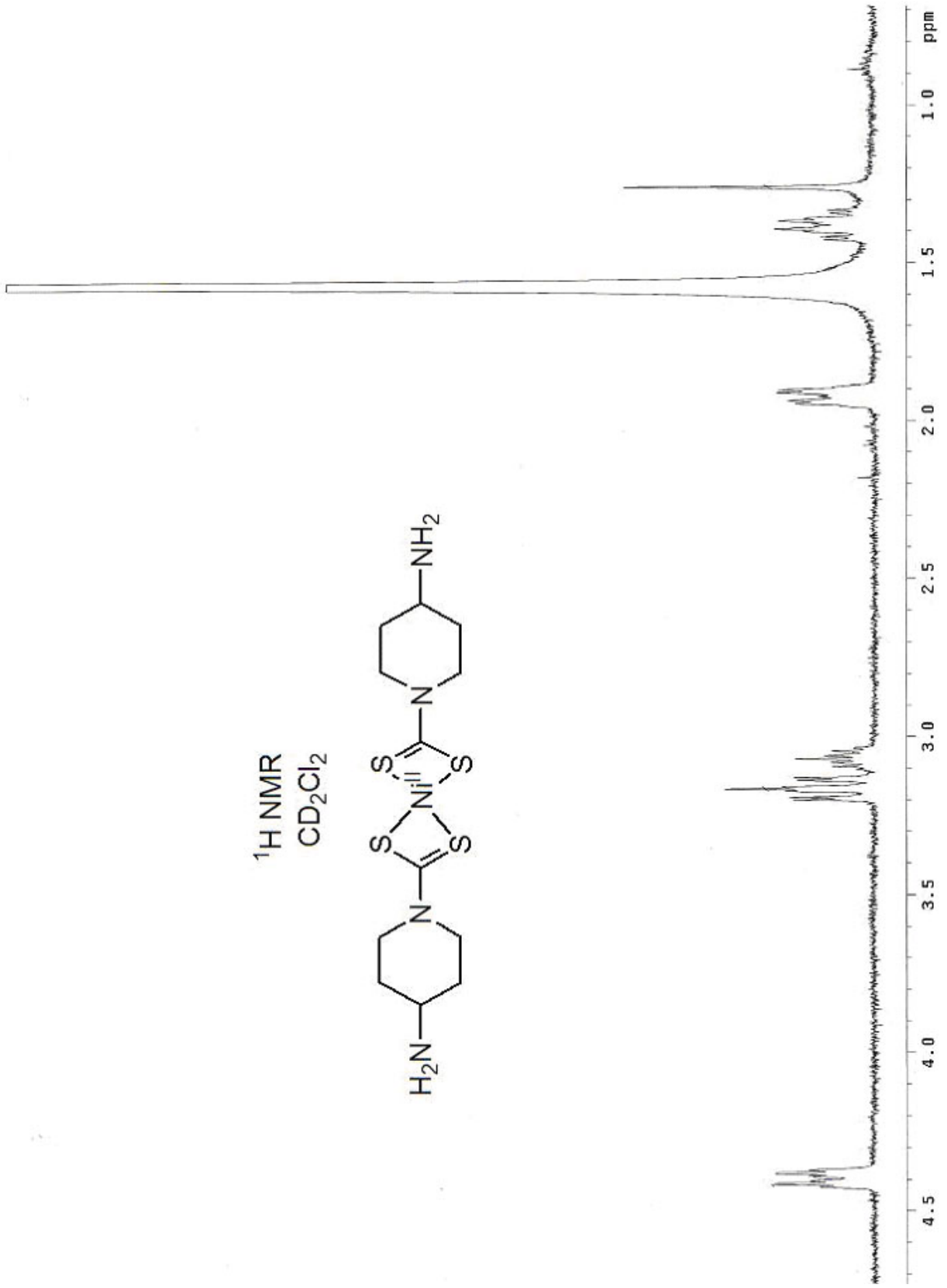

Figure A- 12 ^{1}H NMR of Ni^{II}(DTC)

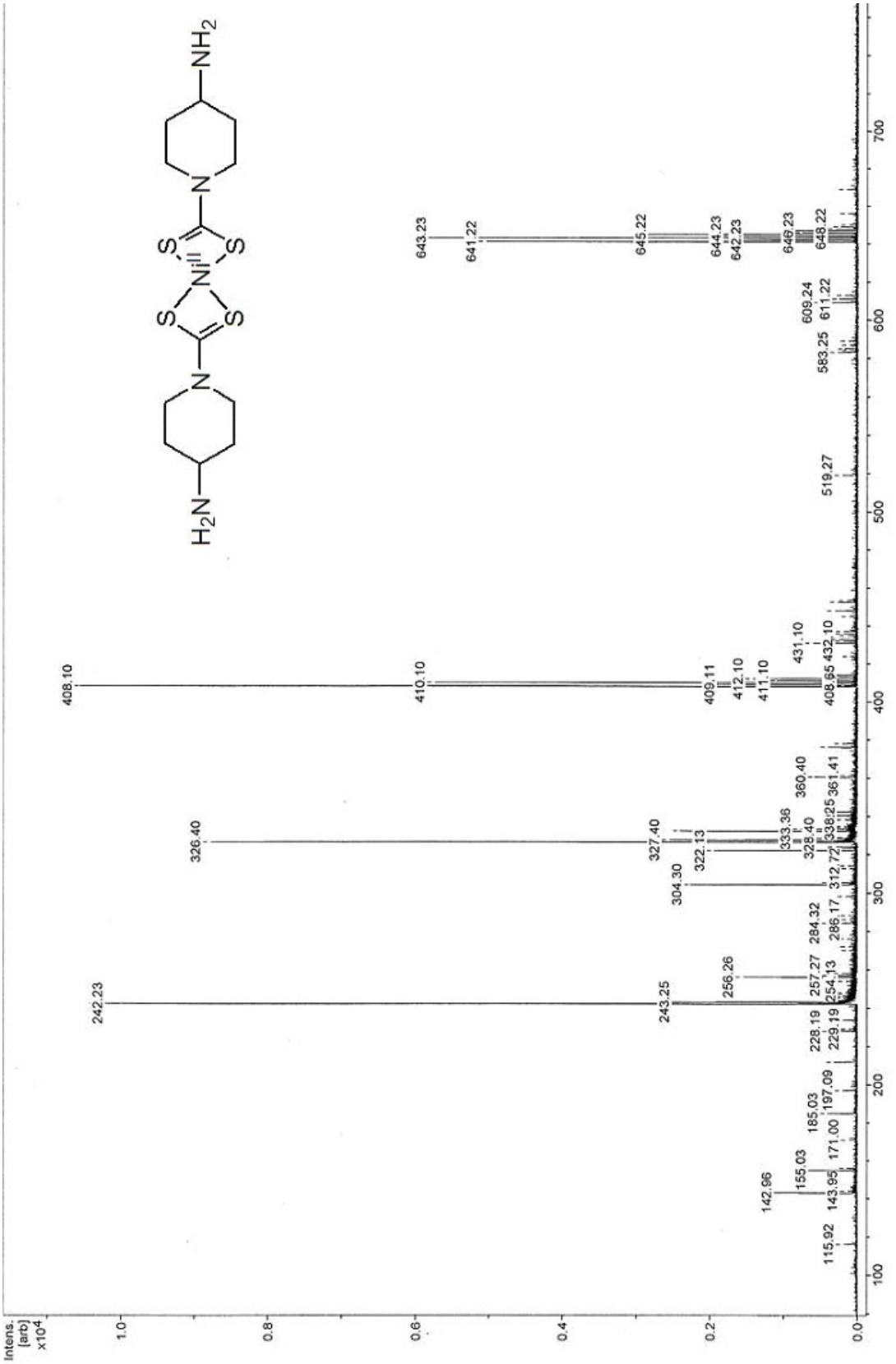

Figure A- 13 Mass Spec. of Ni^{II}(DTC)

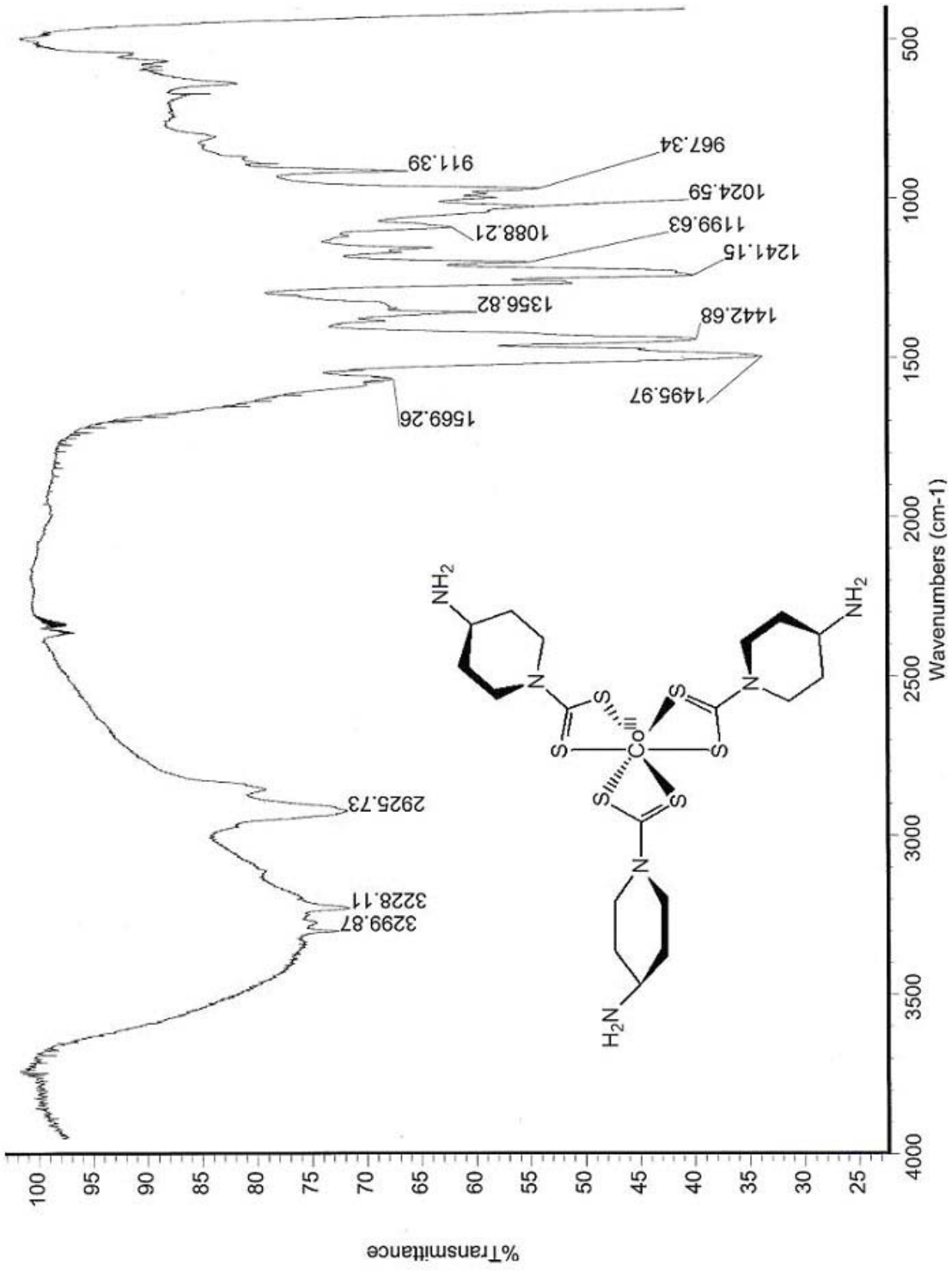

Figure A- 14 IR of Co^{III}(DTC)

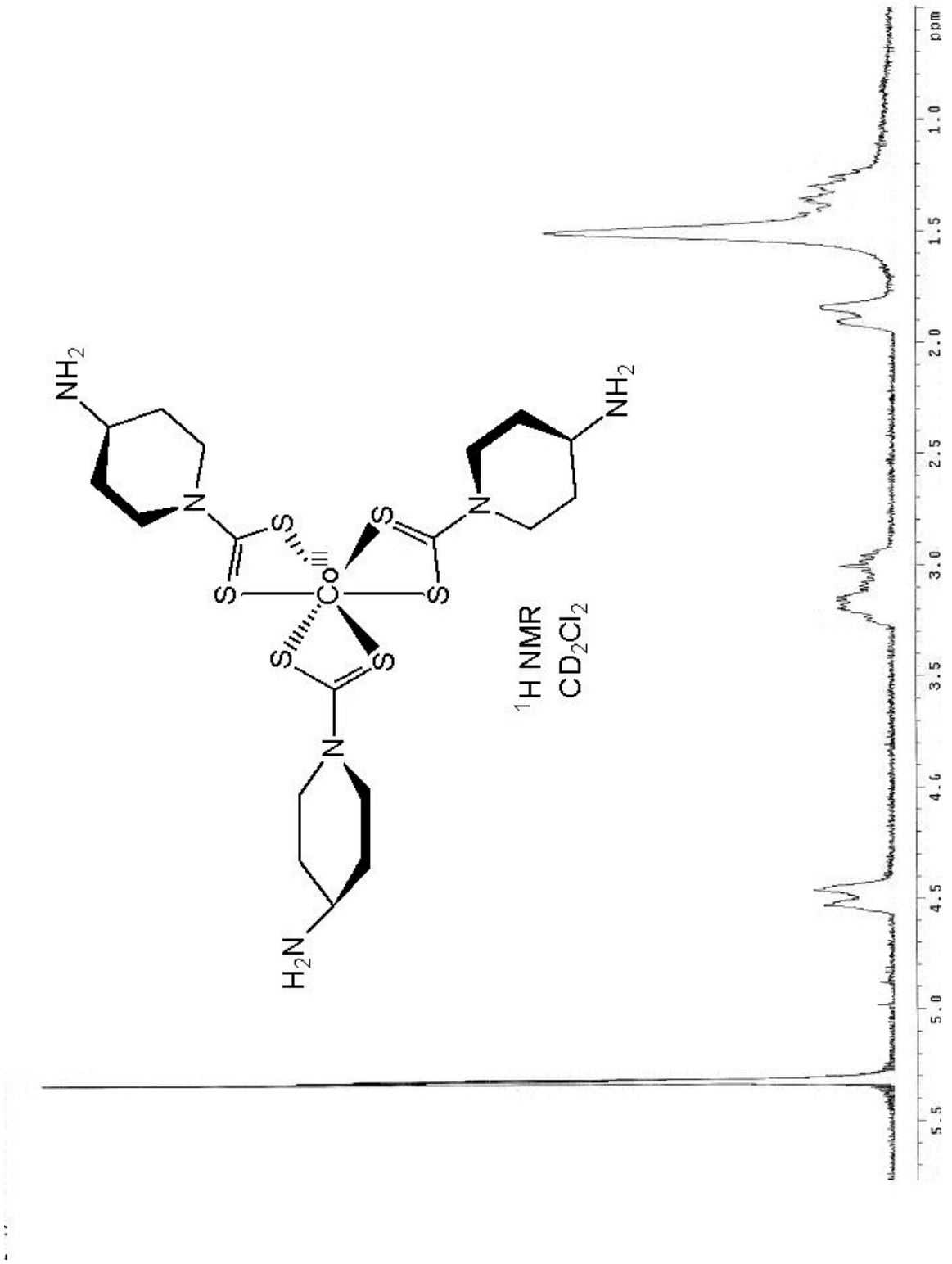

Figure A- 15 ^{1}H NMR of Co^{III}(DTC)

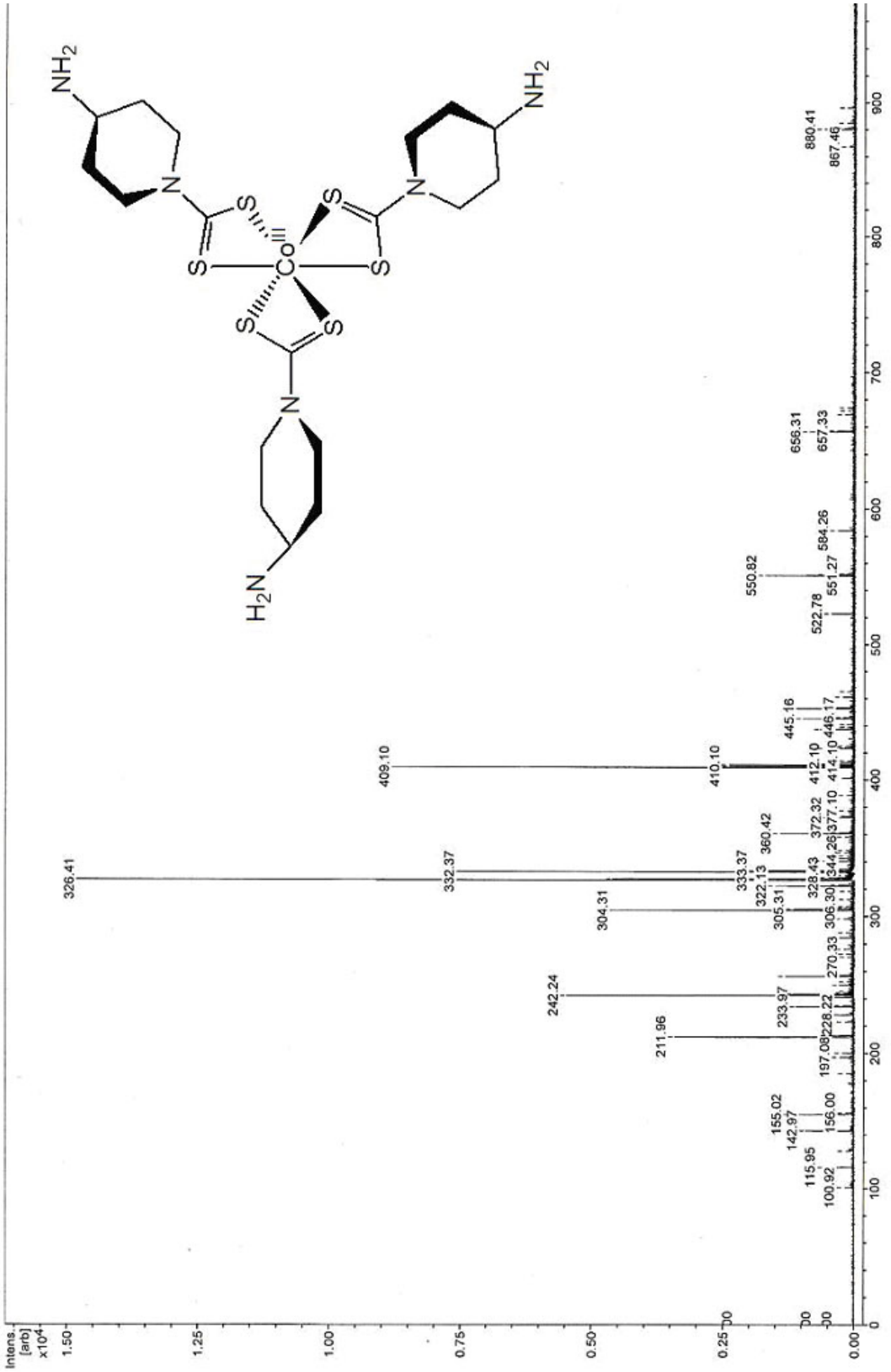

Figure A- 16 Mass Spec. of Co^{III}(DTC)

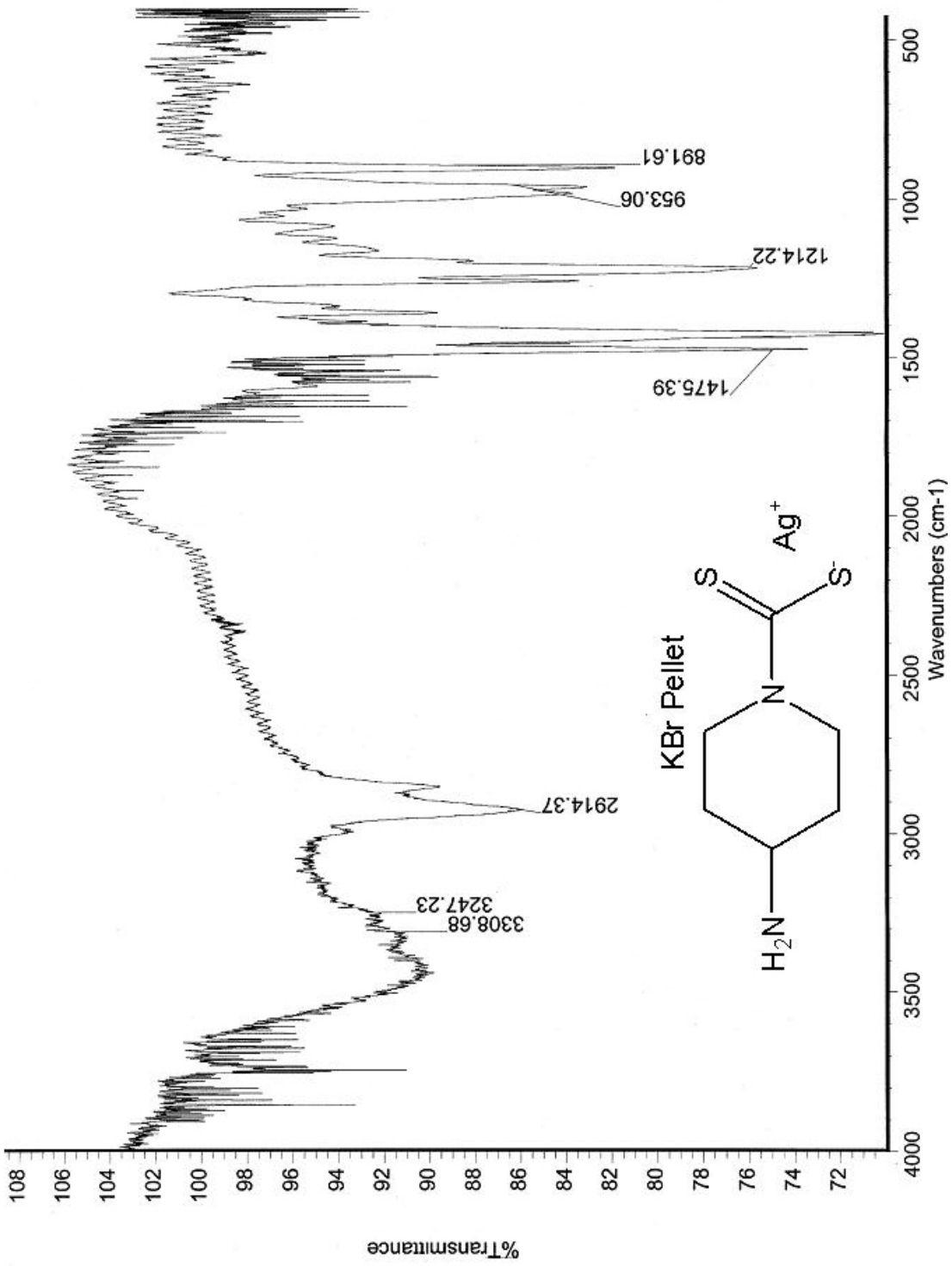

Figure A- 17 IR of Ag^{I}(DTC)

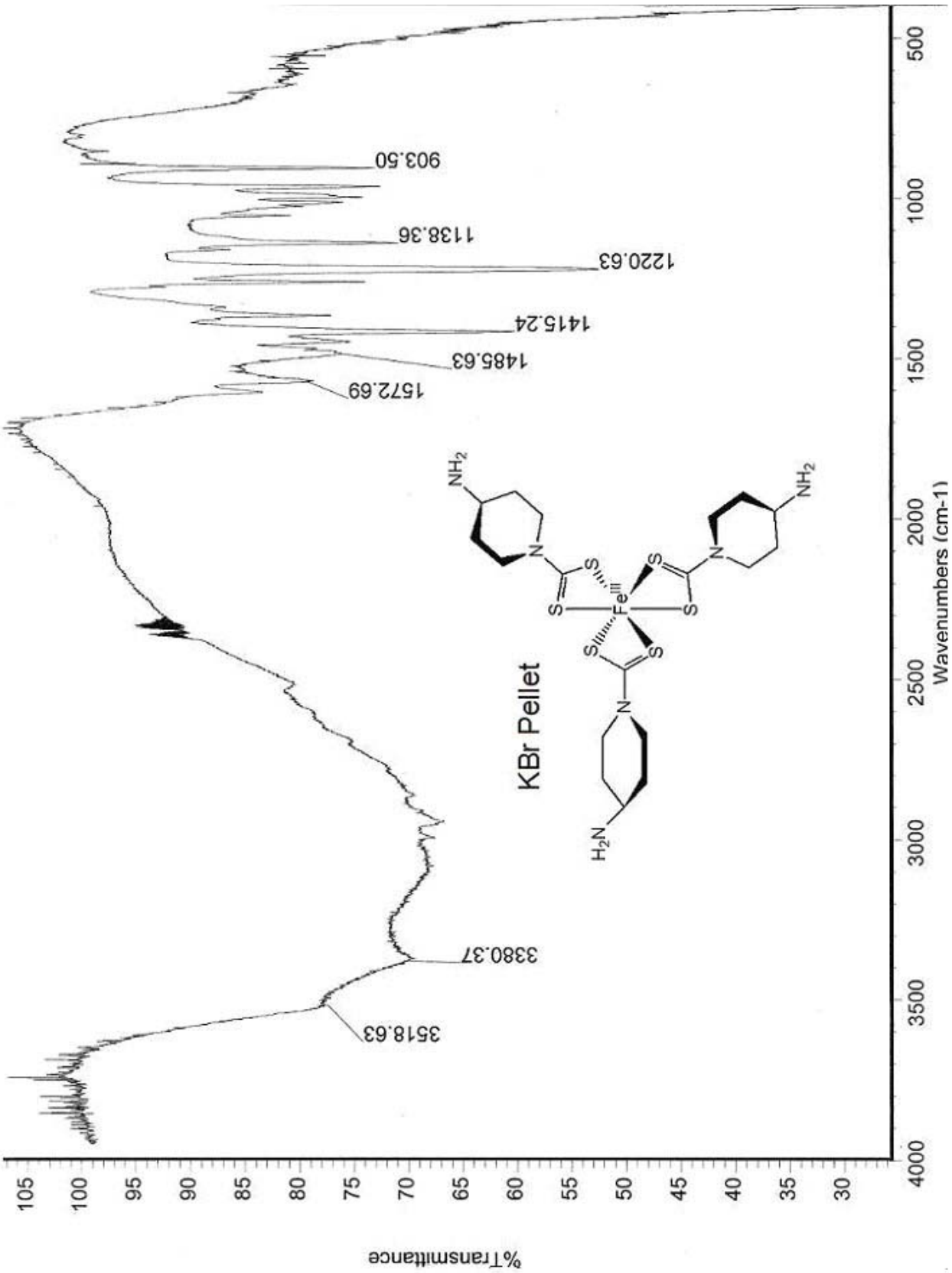

Figure A- 18 IR of Fe^{III}(DTC)

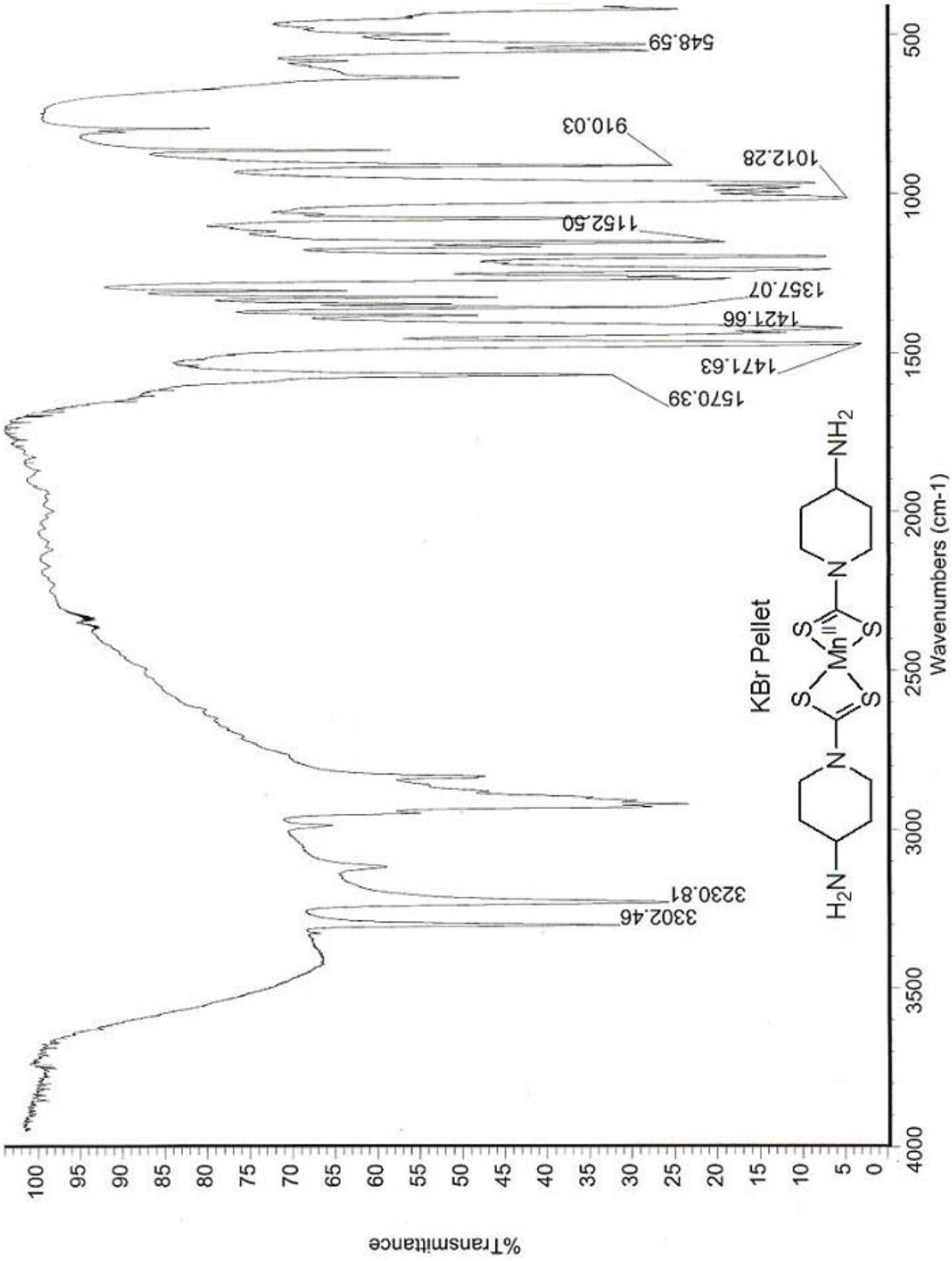

Figure A- 19 IR of Mn^{II}(DTC)

Chapter 4

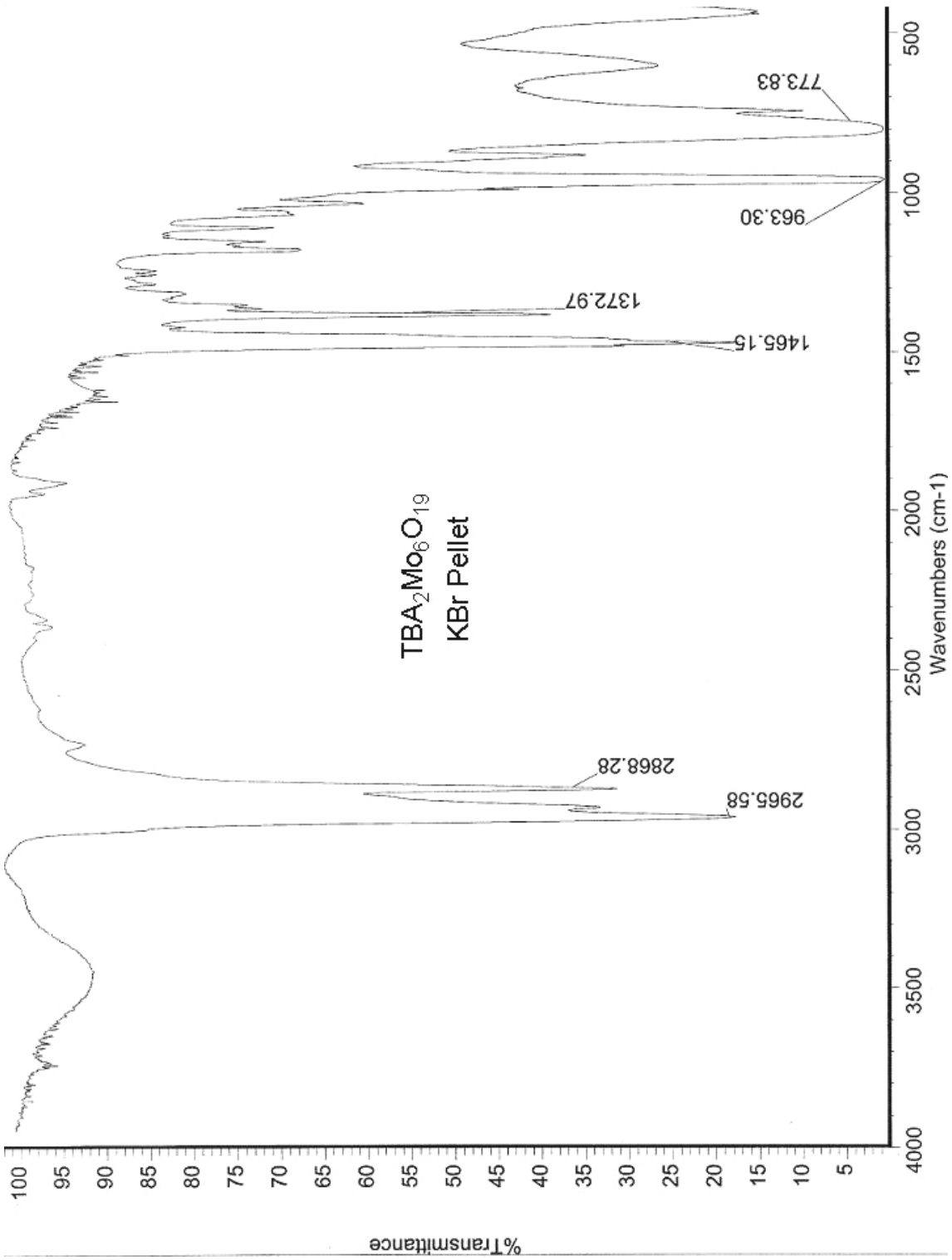

Figure A- 20 IR of $TBA_2Mo_6O_{19}$

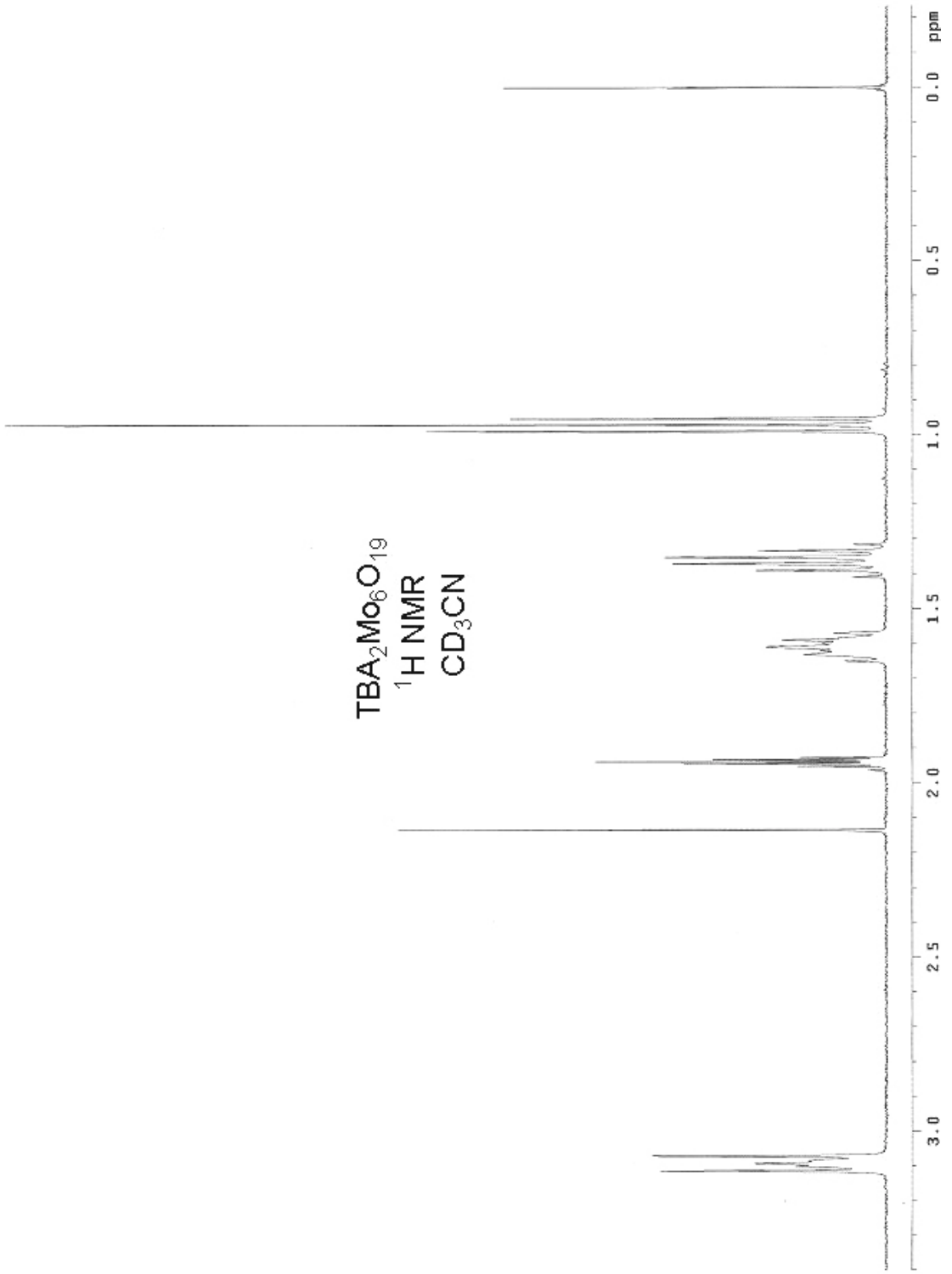

Figure A- 21 ^{1}H NMR of $TBA_2Mo_6O_{19}$

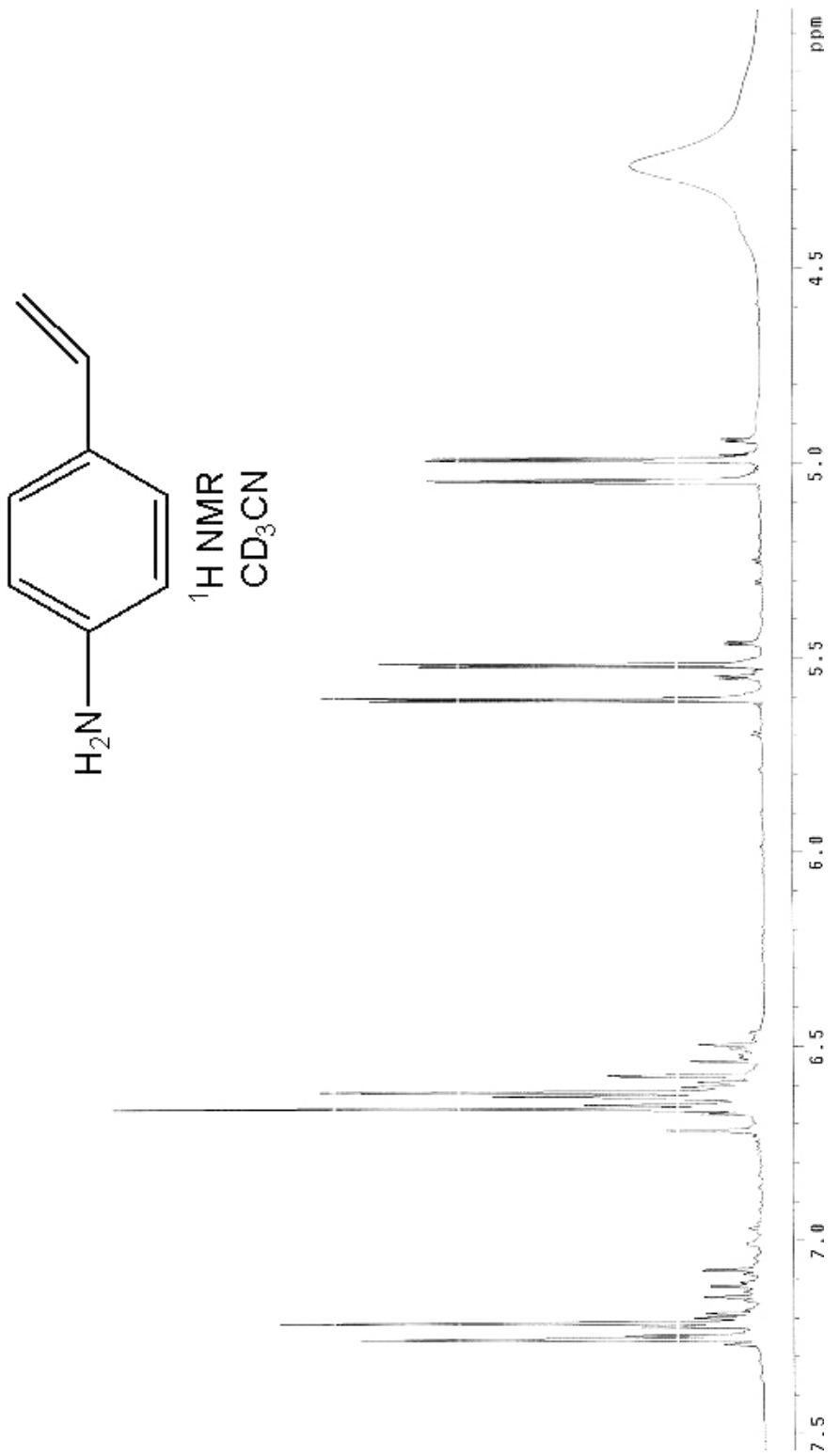

Figure A- 22 ^{1}H NMR of 4-aminostyrene

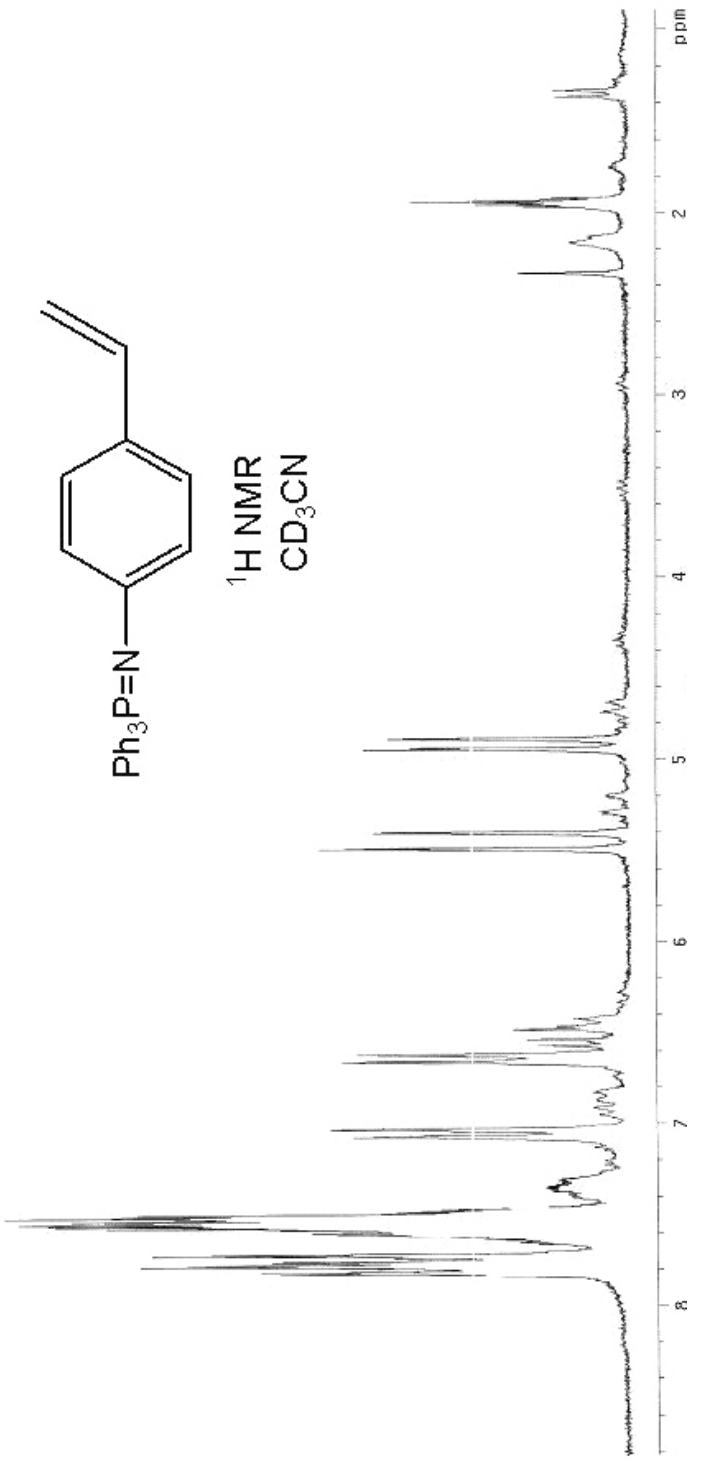

Figure A- 23 ^{1}H NMR of Styrylphosphineimine

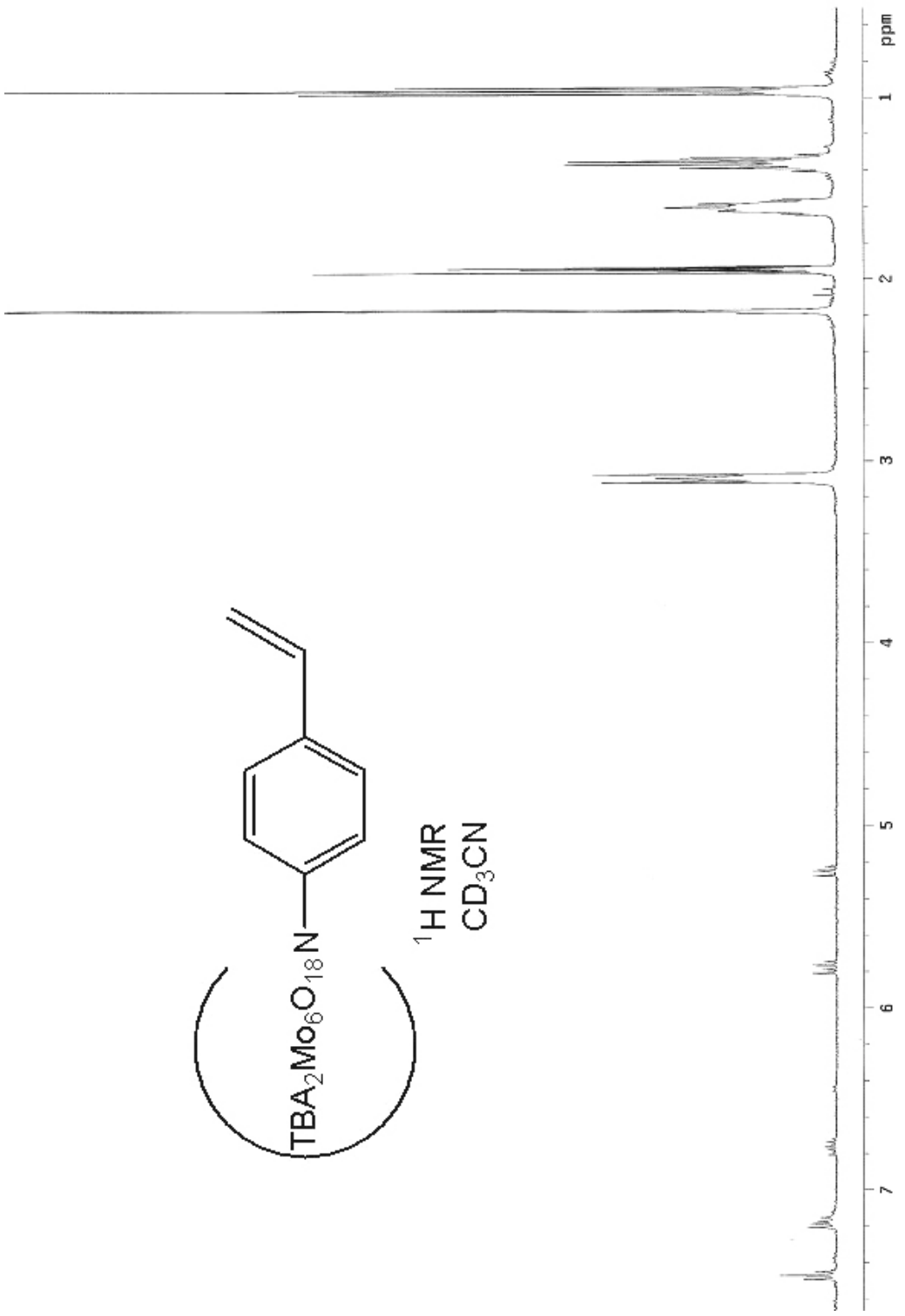

Figure A- 24 ^{1}H NMR of Styrylimido hexamolybdate

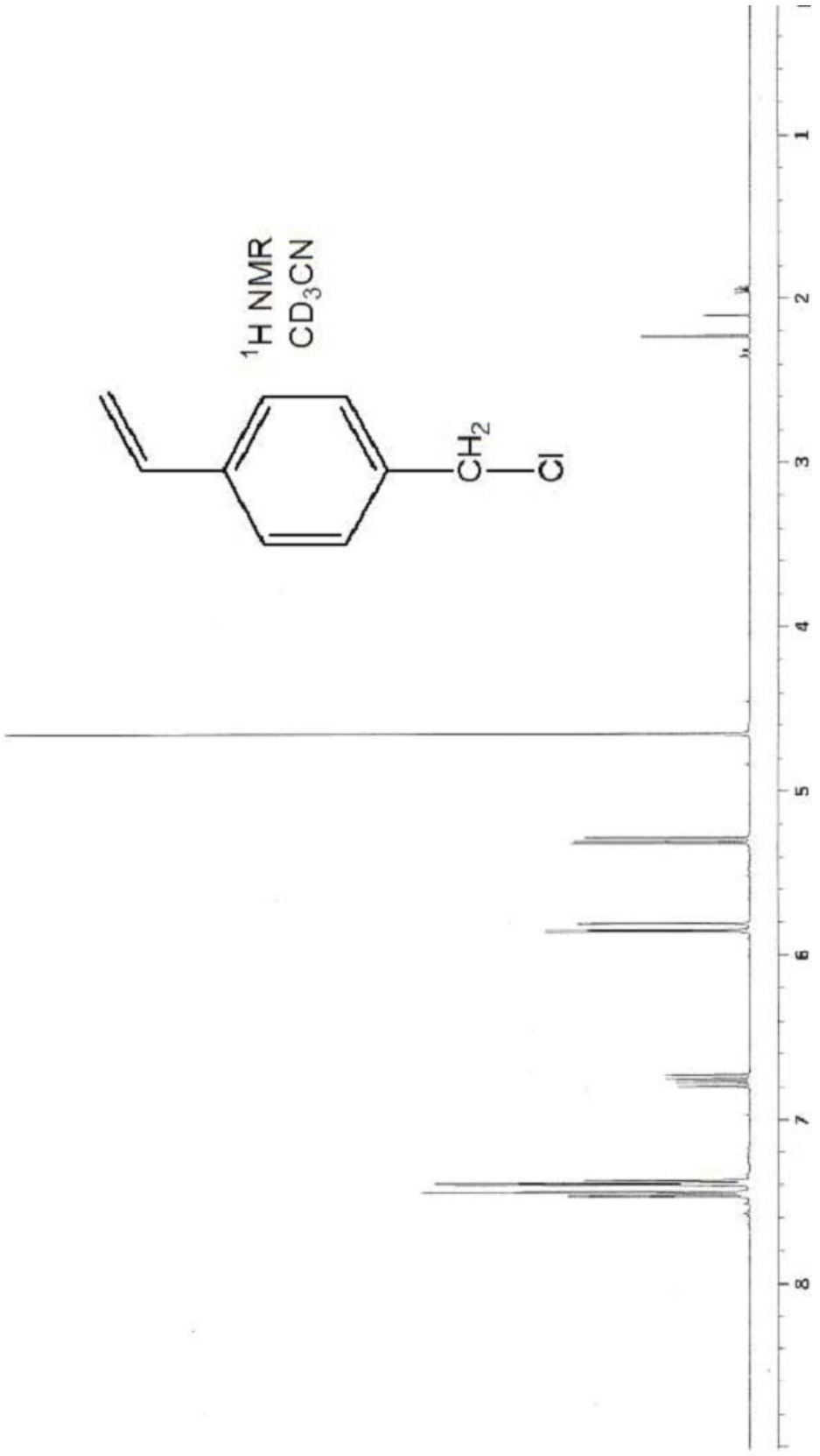

Figure A- 25 ^{1}H NMR of 4-chloromethyl styrene

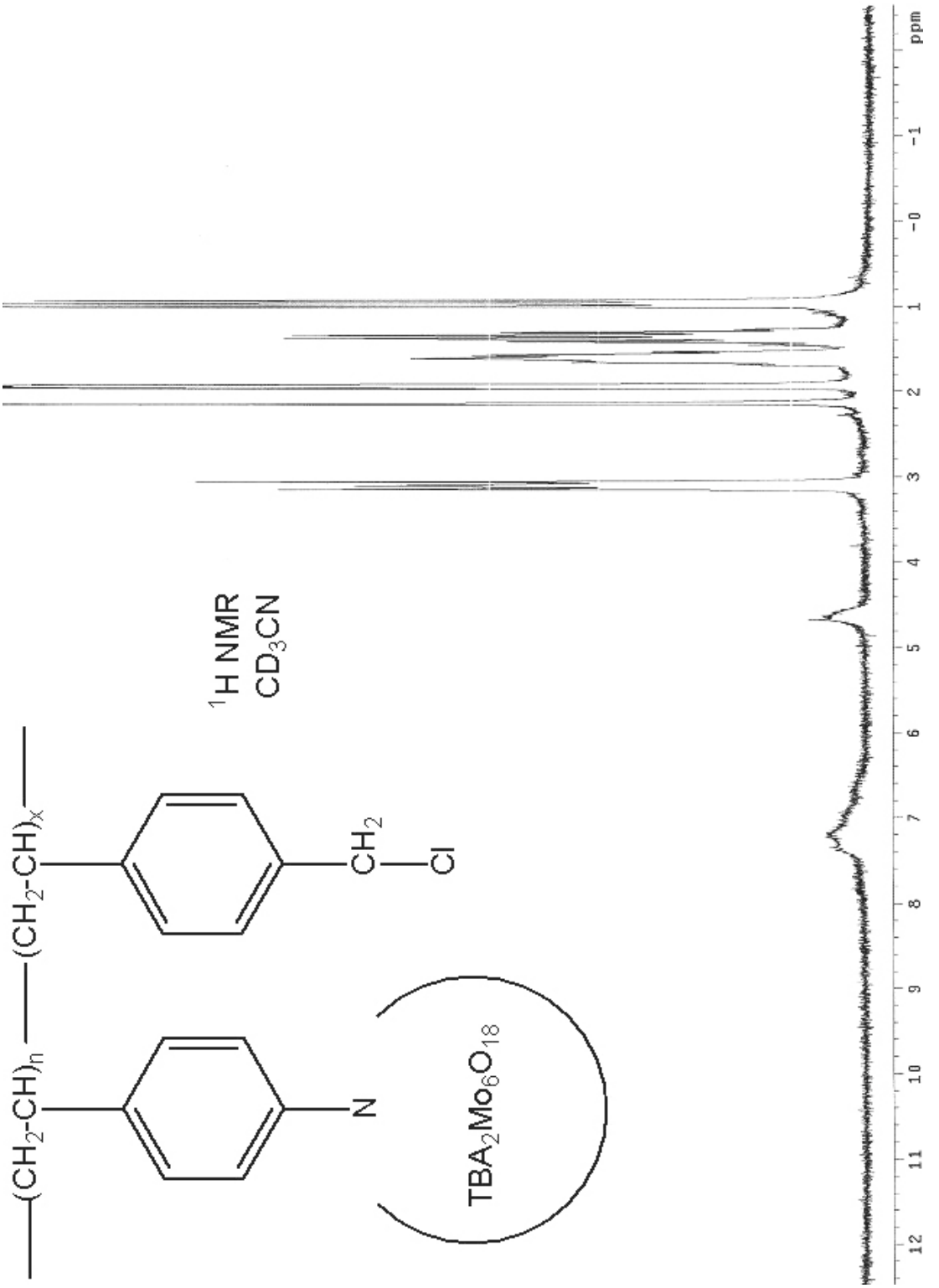

Figure A- 26 ^{1}H NMR of copolymer

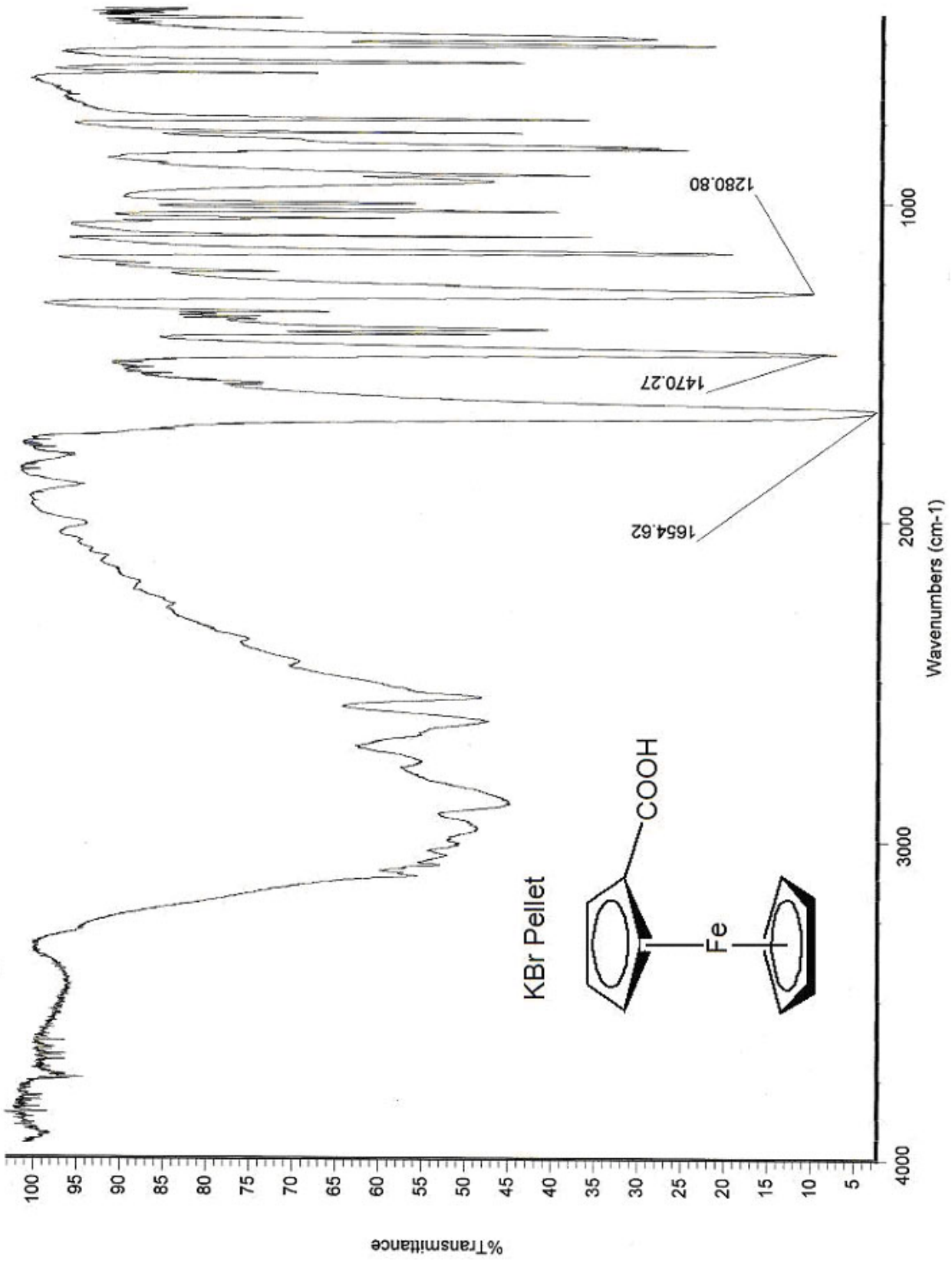

Figure A- 27 IR of Ferrocene monocarboxylic acid

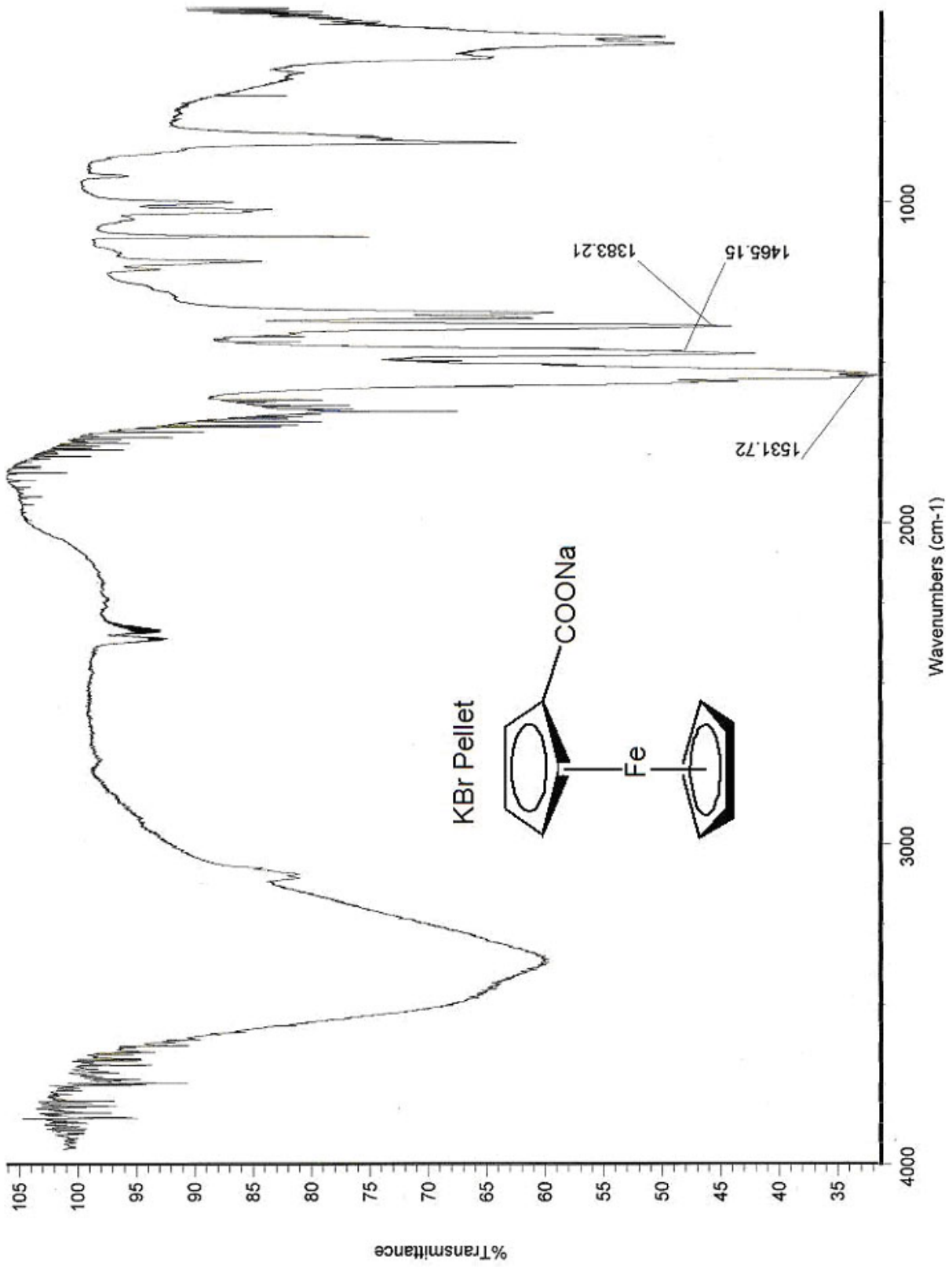

Figure A- 28 IR of Ferrocene carboxylate

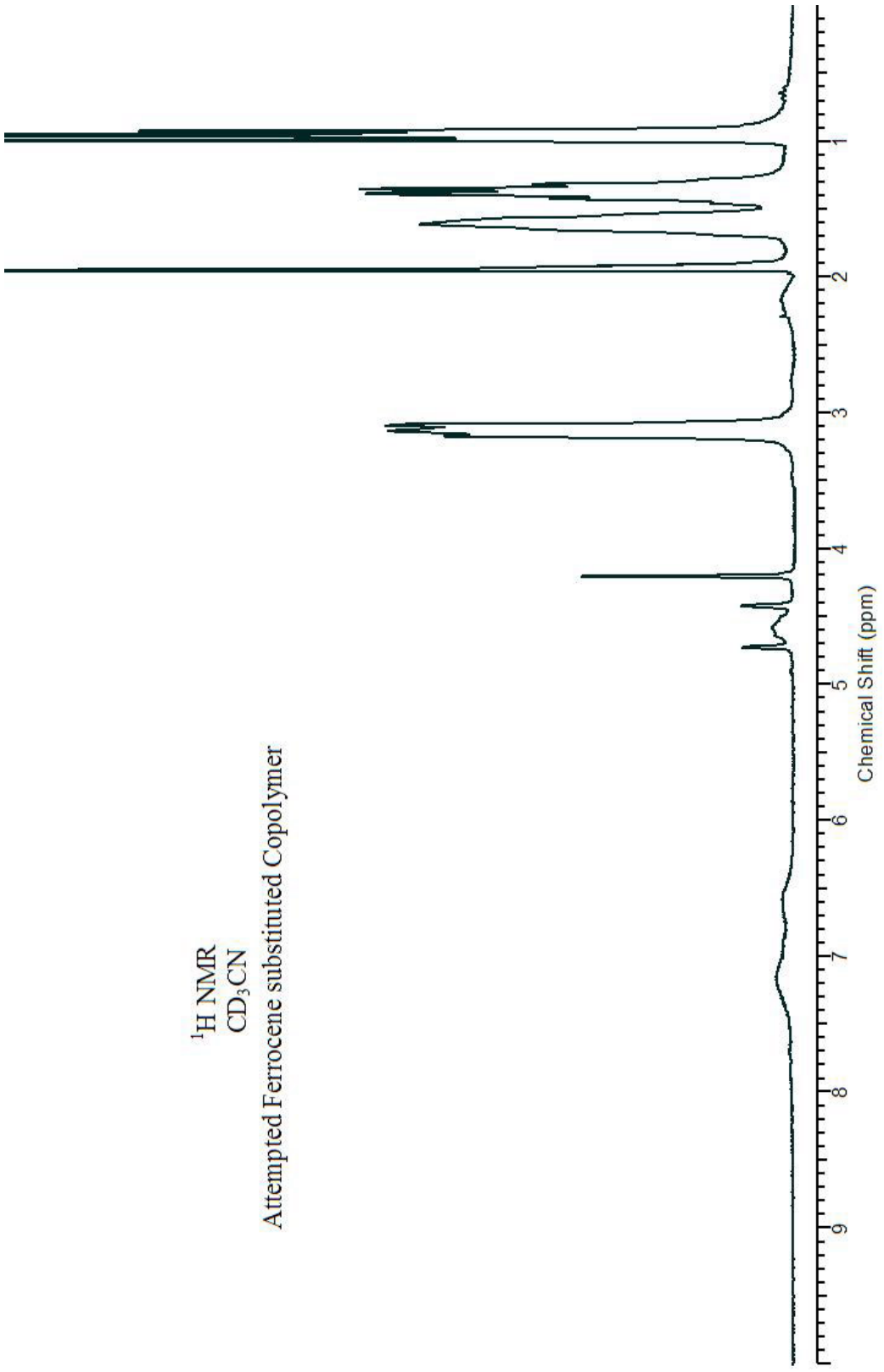

Figure A- 29 ^{1}H NMR of the attempted substitution of the copolymer with Ferrocene carboxylate

Chapter 5

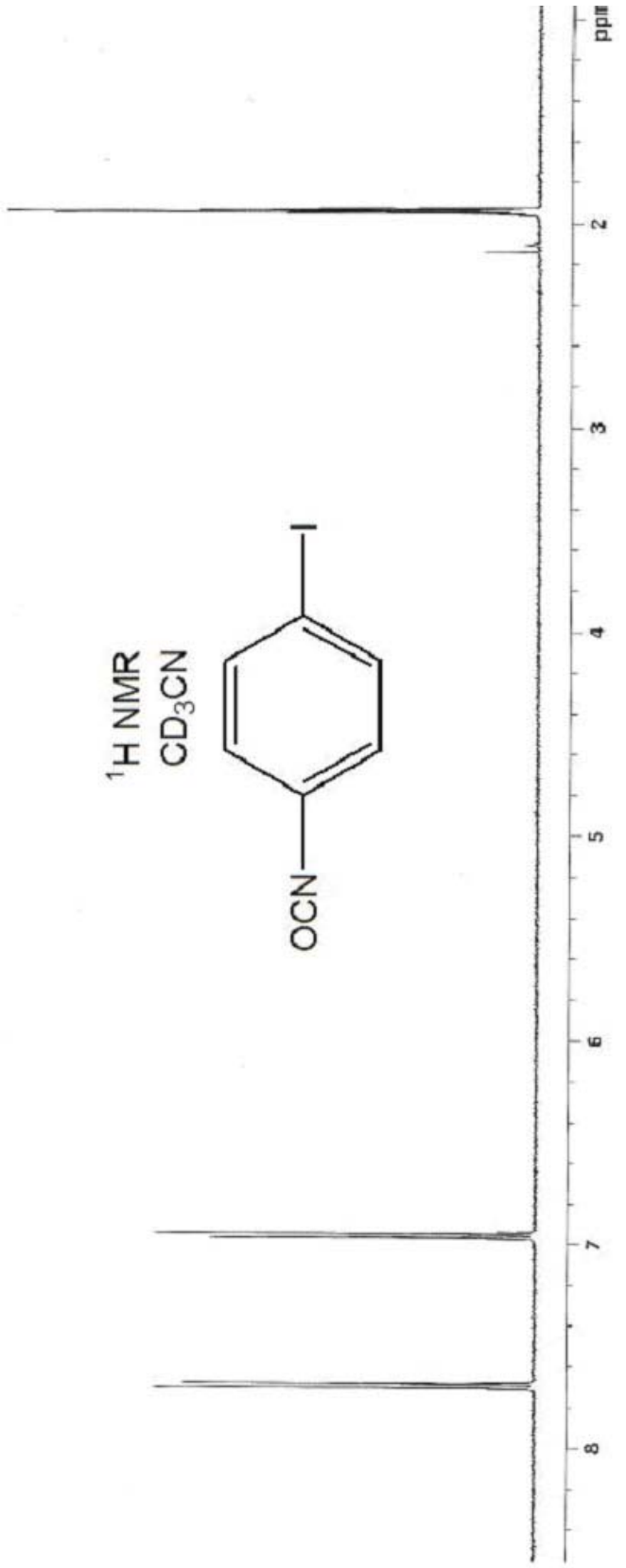

Figure A- 30 ^{1}H NMR of 4-iodophenyl isocyanate

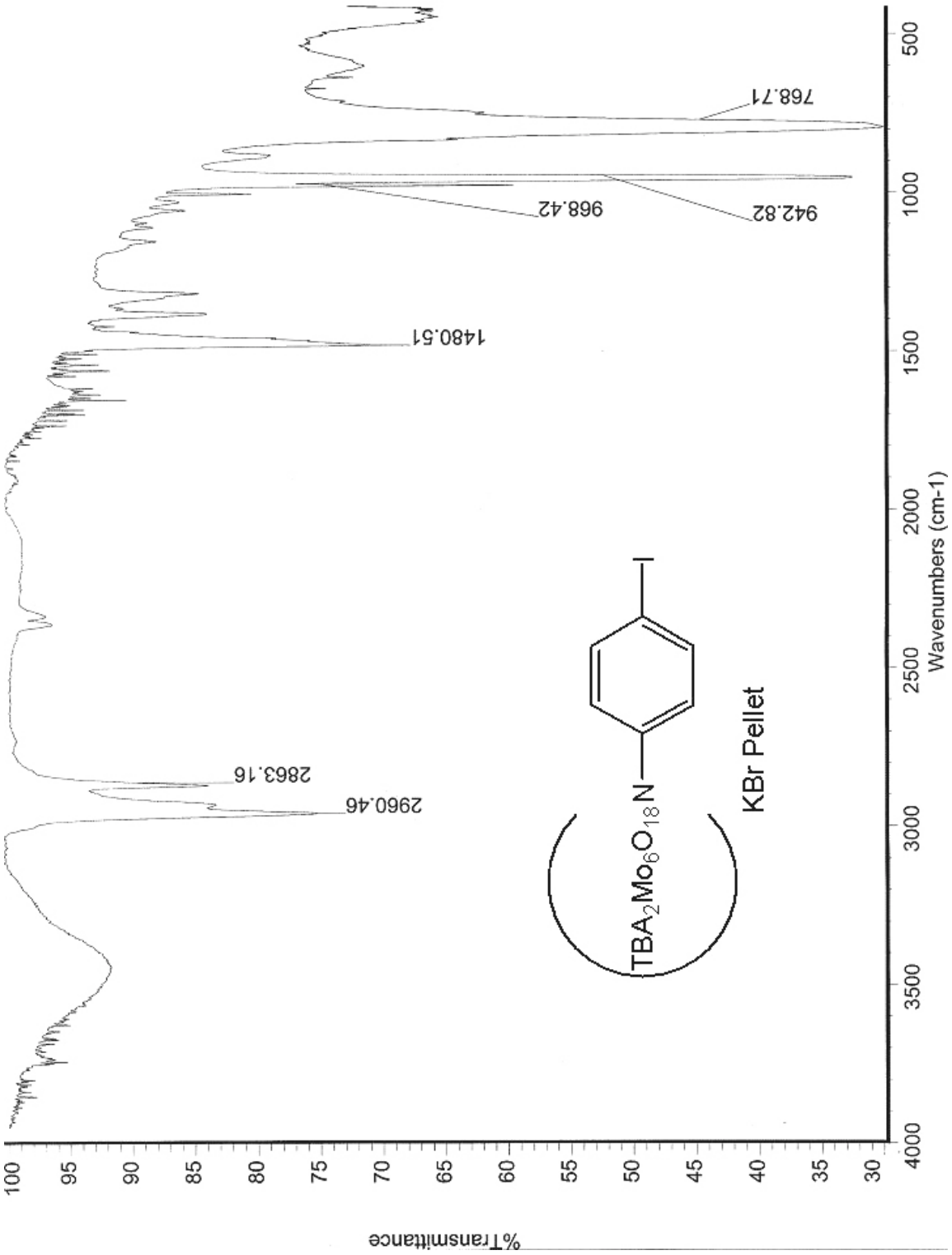

Figure A- 31 IR of iodophenylimido hexamolybdate

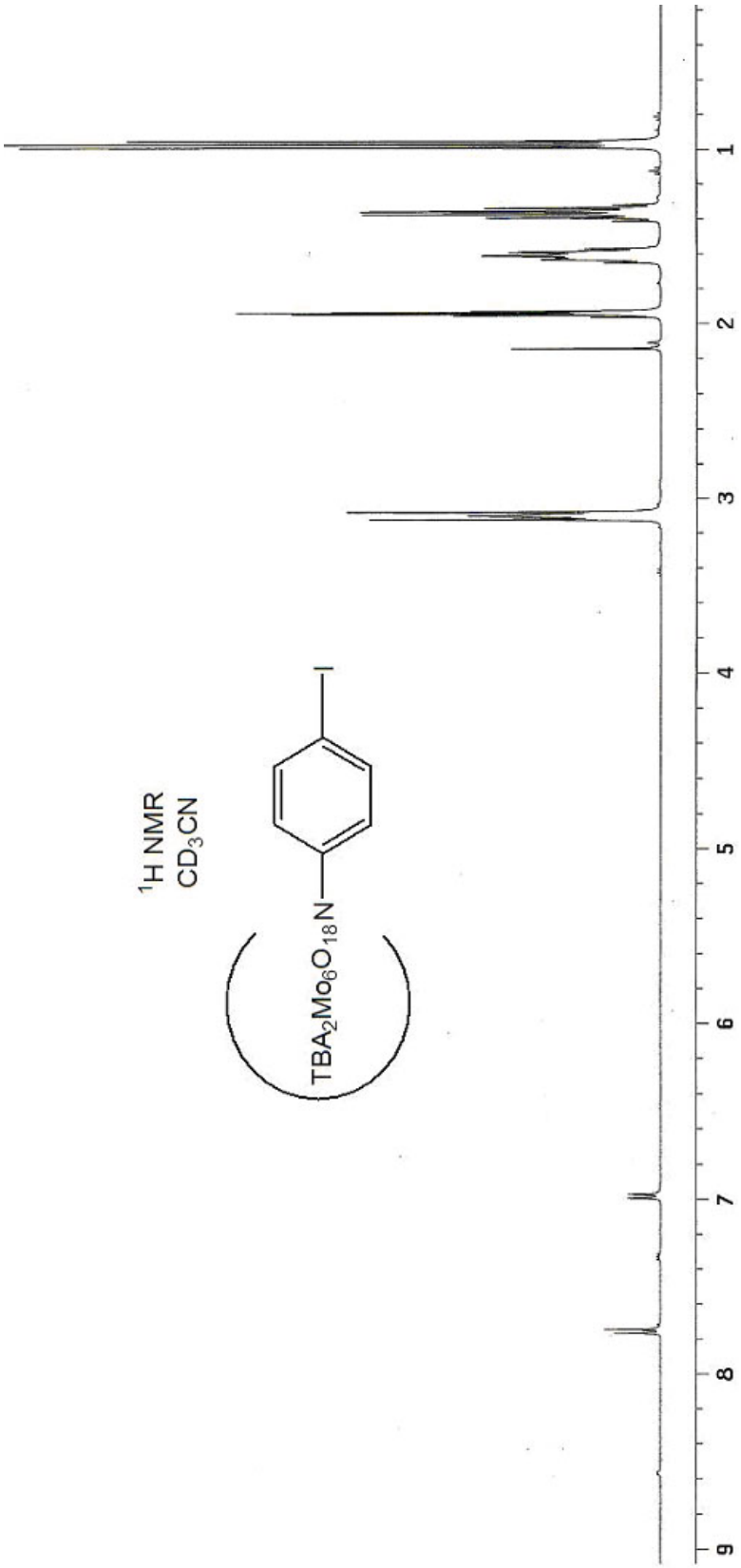

Figure A- 32 ^{1}H NMR of 4-iodophenylimido hexamolybdate

Figure A- 33 ^{1}H NMR of 4-nitro-2,2'-bipyridine

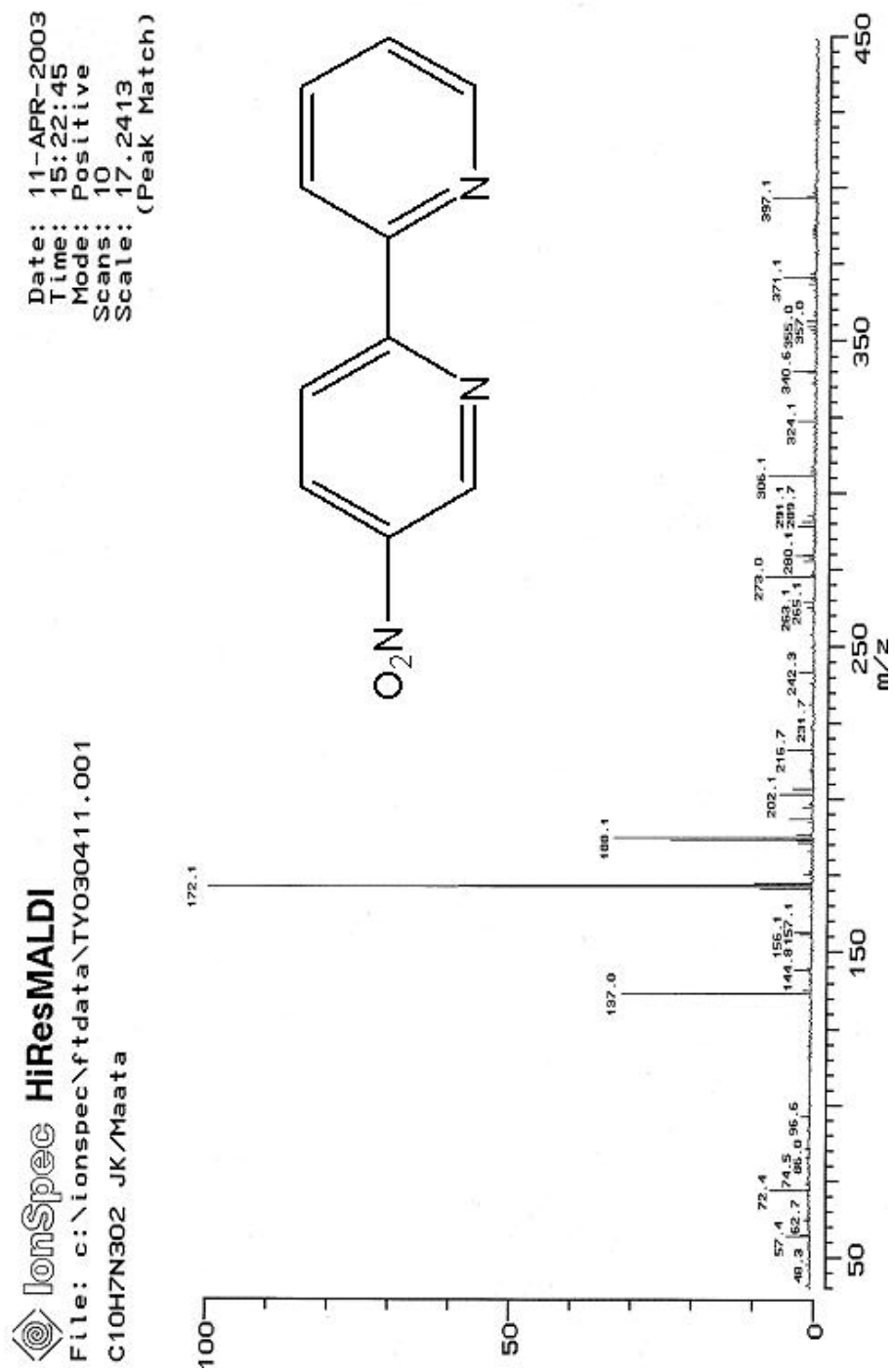

Figure A- 34 Mass spec. for 4-nitro-2,2'-bipyridine

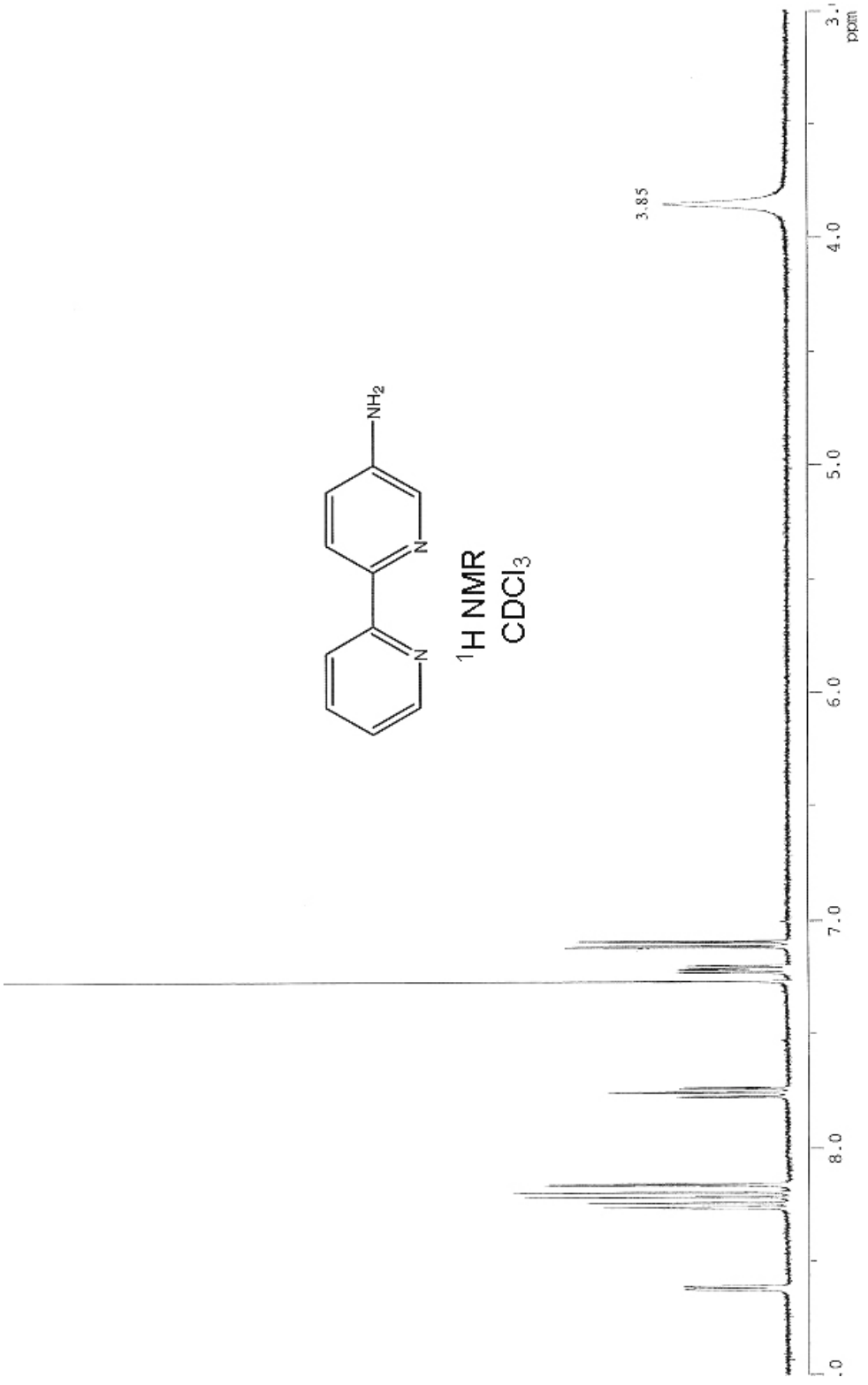

Figure A- 35 ^{1}H NMR of 4-amino-2,2'-bipyridine

Appendix B - Crystallographic Data

Nickel(II) Dithiocarbamate

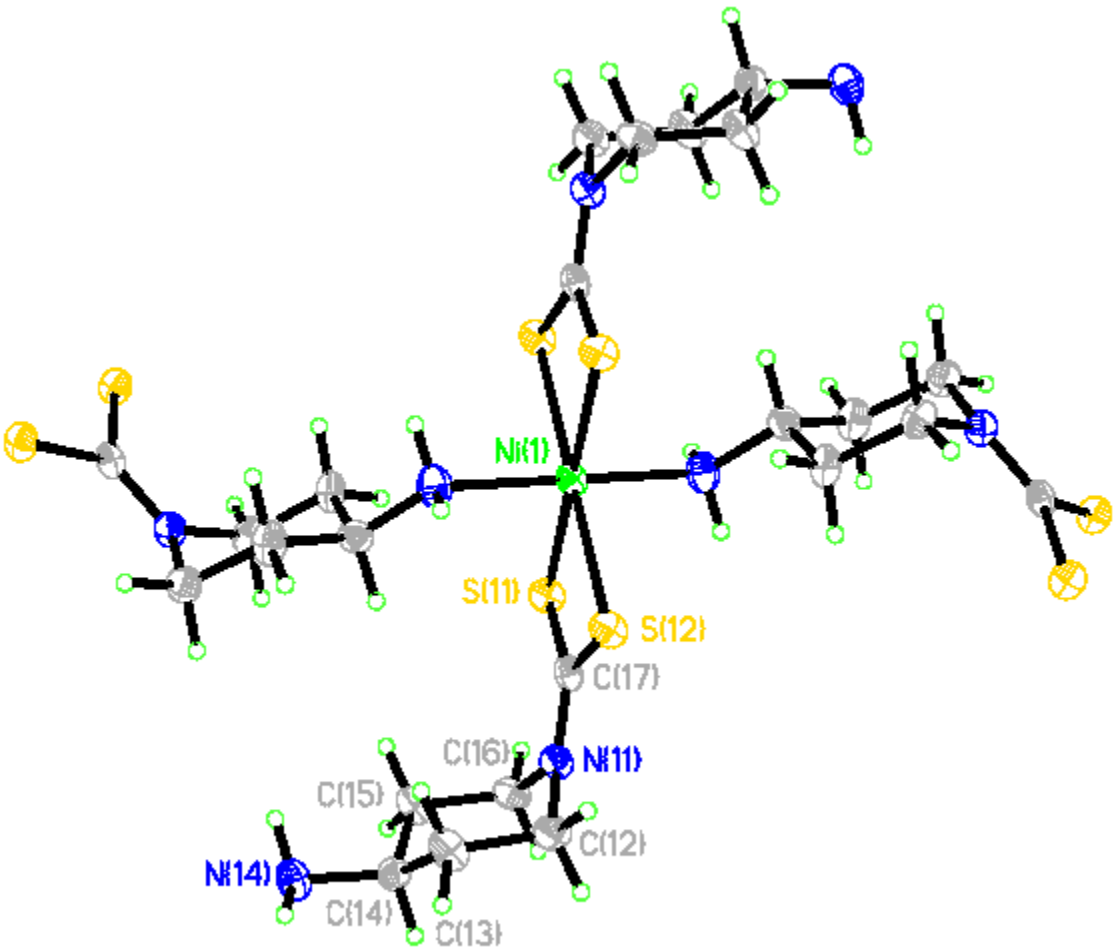

Figure B-1 ORTEP drawing for Ni^{II} DTC

Table 1. Crystal data and structure refinement for Ni^{II} DTC.

Identification code	jk0602m	
Empirical formula	C12 H22 N4 Ni S4	
Formula weight	409.29	
Temperature	173(2) K	
Wavelength	0.71073 Å	
Crystal system	Monoclinic	
Space group	P2(1)/n	
Unit cell dimensions	a = 6.1306(5) Å	α= 90°.
	b = 14.5111(11) Å	β= 106.756(5)°.
	c = 9.5128(8) Å	γ = 90°.
Volume	810.34(11) $Å^3$	
Z	2	
Density (calculated)	1.677 g/cm^3	
Absorption coefficient	1.710 mm^{-1}	
F(000)	428	
Crystal size	0.45 x 0.1 x 0.1 mm^3	
Theta range for data collection	2.64 to 28.33°.	
Index ranges	-8<=h<=8, -17<=k<=18, -12<=l<=11	
Reflections collected	5865	
Independent reflections	1904 [R(int) = 0.1110]	
Completeness to theta = 28.33°	94.2 %	
Absorption correction	None	
Refinement method	Full-matrix least-squares on F^2	
Data / restraints / parameters	1904 / 0 / 97	
Goodness-of-fit on F^2	1.046	
Final R indices [I>2sigma(I)]	R1 = 0.0535, wR2 = 0.1350	
R indices (all data)	R1 = 0.0675, wR2 = 0.1431	
Largest diff. peak and hole	0.909 and -0.529 $e.Å^{-3}$	

Table 2. Atomic coordinates (x 10^4) and equivalent isotropic displacement parameters ($Å^2$x 10^3) for Ni^{II} DTC. U(eq) is defined as one third of the trace of the orthogonalized U^{ij} tensor.

	x	y	z	U(eq)
Ni(1)	5000	5000	10000	20(1)
S(11)	1290(1)	4344(1)	8816(1)	24(1)
N(11)	863(5)	4034(2)	5989(3)	24(1)
C(12)	1793(6)	3879(2)	4753(4)	29(1)
S(12)	4604(1)	4980(1)	7371(1)	25(1)
C(13)	2679(6)	2901(2)	4840(4)	30(1)
C(14)	859(6)	2194(2)	4918(4)	25(1)
N(14)	1806(5)	1264(2)	5170(4)	29(1)
C(15)	-279(6)	2441(2)	6090(4)	27(1)
C(16)	-1063(5)	3423(2)	5921(4)	26(1)
C(17)	2104(5)	4409(2)	7241(4)	22(1)

Table 3. Bond lengths [Å] and angles [°] for Ni^{II} DTC.

Ni(1)-N(14)#1	2.124(3)
Ni(1)-N(14)#2	2.124(3)
Ni(1)-S(11)	2.4229(8)
Ni(1)-S(11)#3	2.4229(8)
Ni(1)-S(12)	2.4426(9)
Ni(1)-S(12)#3	2.4427(9)
S(11)-C(17)	1.713(3)
N(11)-C(17)	1.331(4)
N(11)-C(16)	1.463(4)
N(11)-C(12)	1.464(4)
C(12)-C(13)	1.513(5)
C(12)-H(12A)	0.9900
C(12)-H(12B)	0.9900
S(12)-C(17)	1.715(3)
C(13)-C(14)	1.533(4)
C(13)-H(13A)	0.9900
C(13)-H(13B)	0.9900
C(14)-N(14)	1.462(4)
C(14)-C(15)	1.518(4)
C(14)-H(14)	1.0000
N(14)-Ni(1)#4	2.124(3)
N(14)-H(14A)	0.9200
N(14)-H(14B)	0.9200
C(15)-C(16)	1.498(5)
C(15)-H(15A)	0.9900
C(15)-H(15B)	0.9900
C(16)-H(16A)	0.9900
C(16)-H(16B)	0.9900

N(14)#1-Ni(1)-N(14)#2	179.999(1)
N(14)#1-Ni(1)-S(11)	84.54(8)
N(14)#2-Ni(1)-S(11)	95.46(8)
N(14)#1-Ni(1)-S(11)#3	95.46(8)
N(14)#2-Ni(1)-S(11)#3	84.54(8)

S(11)-Ni(1)-S(11)#3 180.0
N(14)#1-Ni(1)-S(12) 92.09(9)
N(14)#2-Ni(1)-S(12) 87.91(9)
S(11)-Ni(1)-S(12) 73.51(3)
S(11)#3-Ni(1)-S(12) 106.49(3)
N(14)#1-Ni(1)-S(12)#3 87.91(9)
N(14)#2-Ni(1)-S(12)#3 92.09(9)
S(11)-Ni(1)-S(12)#3 106.49(3)
S(11)#3-Ni(1)-S(12)#3 73.51(3)
S(12)-Ni(1)-S(12)#3 180.00(4)
C(17)-S(11)-Ni(1) 85.07(11)
C(17)-N(11)-C(16) 122.2(3)
C(17)-N(11)-C(12) 121.8(3)
C(16)-N(11)-C(12) 111.6(3)
N(11)-C(12)-C(13) 108.5(3)
N(11)-C(12)-H(12A) 110.0
C(13)-C(12)-H(12A) 110.0
N(11)-C(12)-H(12B) 110.0
C(13)-C(12)-H(12B) 110.0
H(12A)-C(12)-H(12B) 108.4
C(17)-S(12)-Ni(1) 84.41(12)
C(12)-C(13)-C(14) 112.1(3)
C(12)-C(13)-H(13A) 109.2
C(14)-C(13)-H(13A) 109.2
C(12)-C(13)-H(13B) 109.2
C(14)-C(13)-H(13B) 109.2
H(13A)-C(13)-H(13B) 107.9
N(14)-C(14)-C(15) 110.0(3)
N(14)-C(14)-C(13) 111.4(3)
C(15)-C(14)-C(13) 111.9(3)
N(14)-C(14)-H(14) 107.8
C(15)-C(14)-H(14) 107.8
C(13)-C(14)-H(14) 107.8
C(14)-N(14)-Ni(1)#4 127.7(2)
C(14)-N(14)-H(14A) 105.4
Ni(1)#4-N(14)-H(14A) 105.4

C(14)-N(14)-H(14B) 105.4

Ni(1)#4-N(14)-H(14B) 105.4

H(14A)-N(14)-H(14B) 106.0

C(16)-C(15)-C(14) 110.2(3)

C(16)-C(15)-H(15A) 109.6

C(14)-C(15)-H(15A) 109.6

C(16)-C(15)-H(15B) 109.6

C(14)-C(15)-H(15B) 109.6

H(15A)-C(15)-H(15B) 108.1

N(11)-C(16)-C(15) 110.0(3)

N(11)-C(16)-H(16A) 109.7

C(15)-C(16)-H(16A) 109.7

N(11)-C(16)-H(16B) 109.7

C(15)-C(16)-H(16B) 109.7

H(16A)-C(16)-H(16B) 108.2

N(11)-C(17)-S(11) 121.7(2)

N(11)-C(17)-S(12) 122.0(2)

S(11)-C(17)-S(12) 116.3(2)

Symmetry transformations used to generate equivalent atoms:

#1 -x+1/2,y+1/2,-z+3/2 #2 x+1/2,-y+1/2,z+1/2

#3 -x+1,-y+1,-z+2 #4 -x+1/2,y-1/2,-z+3/2

Table 4. Anisotropic displacement parameters ($Å^2 x\ 10^3$) for Ni^{II} DTC. The anisotropic displacement factor exponent takes the form: $-2\pi^2[\ h^2\ a^{*2}U^{11} + ...\ + 2\ h\ k\ a^*\ b^*\ U^{12}\ ]$

U^{11}	U^{22}	U^{33}	U^{23}	U^{13}	U^{12}
Ni(1)20(1)	20(1)	23(1)	-1(1)	10(1)	-3(1)
S(11)22(1)	28(1)	26(1)	-2(1)	12(1)	-4(1)
N(11)27(1)	23(1)	24(2)	-1(1)	13(1)	-2(1)
C(12)37(2)	29(2)	24(2)	0(2)	14(2)	-7(1)
S(12)26(1)	27(1)	27(1)	-2(1)	14(1)	-7(1)
C(13)29(2)	28(2)	37(2)	-5(2)	19(2)	-6(1)
C(14)29(2)	24(2)	23(2)	1(1)	10(1)	2(1)
N(14)29(1)	24(1)	38(2)	-2(1)	15(1)	0(1)
C(15)29(2)	22(2)	35(2)	-6(1)	16(2)	-4(1)
C(16)22(2)	29(2)	28(2)	-5(1)	8(1)	-4(1)
C(17)22(2)	17(1)	29(2)	1(1)	13(1)	1(1)

Table 5. Hydrogen coordinates (x 10^4) and isotropic displacement parameters ($Å^2$x 10^3) for Ni^{II} DTC .

	x	y	z	U(eq)
H(12A)	3044	4320	4799	35
H(12B)	591	3974	3815	35
H(13A)	4007	2837	5721	36
H(13B)	3198	2772	3966	36
H(14)	-340	2196	3949	30
H(14A)	2787	1272	6107	35
H(14B)	2706	1204	4551	35
H(15A)	-1599	2029	6005	32
H(15B)	812	2351	7074	32
H(16A)	-2241	3502	4967	31
H(16B)	-1747	3584	6712	31

Table 6. Torsion angles [°] for Ni^{II} DTC.

N(14)#1-Ni(1)-S(11)-C(17)	98.97(13)
N(14)#2-Ni(1)-S(11)-C(17)	-81.03(13)
S(11)#3-Ni(1)-S(11)-C(17)	-114(3)
S(12)-Ni(1)-S(11)-C(17)	5.15(10)
S(12)#3-Ni(1)-S(11)-C(17)	-174.85(10)
C(17)-N(11)-C(12)-C(13)	94.6(3)
C(16)-N(11)-C(12)-C(13)	-62.3(4)
N(14)#1-Ni(1)-S(12)-C(17)	-88.83(12)
N(14)#2-Ni(1)-S(12)-C(17)	91.17(12)
S(11)-Ni(1)-S(12)-C(17)	-5.15(10)
S(11)#3-Ni(1)-S(12)-C(17)	174.85(10)
S(12)#3-Ni(1)-S(12)-C(17)	127(5)
N(11)-C(12)-C(13)-C(14)	54.3(4)
C(12)-C(13)-C(14)-N(14)	-173.5(3)
C(12)-C(13)-C(14)-C(15)	-49.9(4)
C(15)-C(14)-N(14)-Ni(1)#4	67.1(4)
C(13)-C(14)-N(14)-Ni(1)#4	-168.2(2)
N(14)-C(14)-C(15)-C(16)	174.8(3)
C(13)-C(14)-C(15)-C(16)	50.4(4)
C(17)-N(11)-C(16)-C(15)	-92.0(4)
C(12)-N(11)-C(16)-C(15)	64.8(4)
C(14)-C(15)-C(16)-N(11)	-57.1(4)
C(16)-N(11)-C(17)-S(11)	-9.9(4)
C(12)-N(11)-C(17)-S(11)	-164.3(2)
C(16)-N(11)-C(17)-S(12)	169.9(2)
C(12)-N(11)-C(17)-S(12)	15.5(4)
Ni(1)-S(11)-C(17)-N(11)	172.0(3)
Ni(1)-S(11)-C(17)-S(12)	-7.87(15)
Ni(1)-S(12)-C(17)-N(11)	-172.0(3)
Ni(1)-S(12)-C(17)-S(11)	7.81(15)

Symmetry transformations used to generate equivalent atoms:

#1 -x+1/2,y+1/2,-z+3/2 #2 x+1/2,-y+1/2,z+1/2

#3 -x+1,-y+1,-z+2 #4 -x+1/2,y-1/2,-z+3/2

Iodophenylimido Hexamolybdate

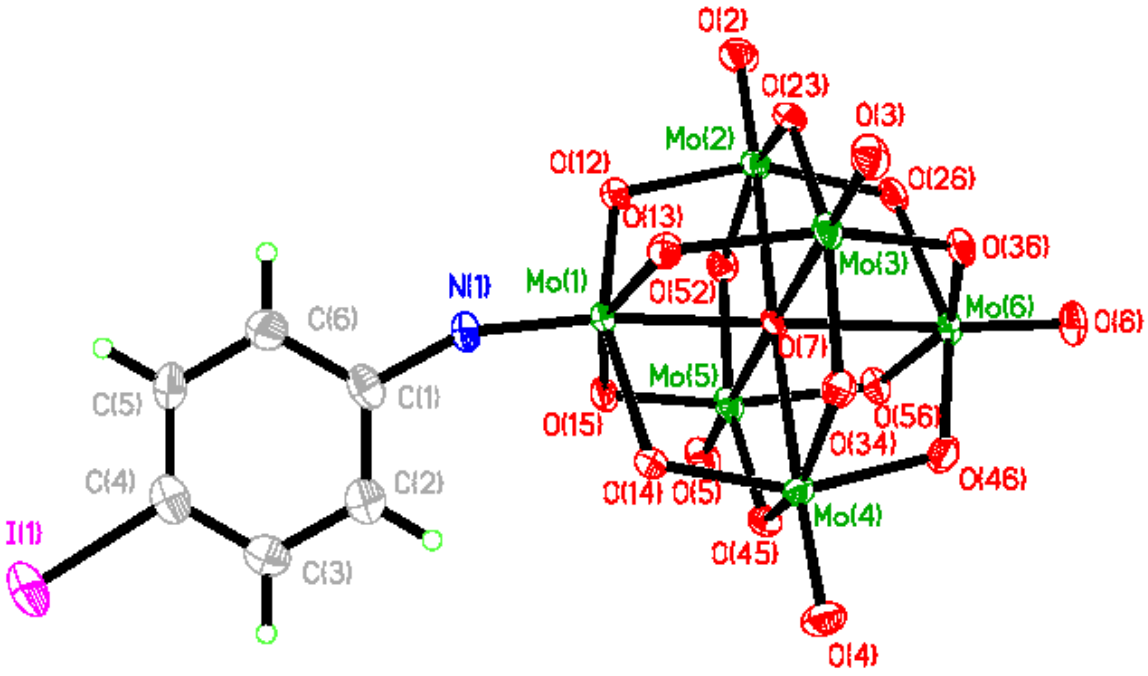

Figure B-2 ORTEP drawing of Iodophenylimido Hexamolybdate

Table 1. Crystal data and structure refinement for Iodophenylimido Hexamolybdate.

Identification code	jk0501	
Empirical formula	C38 H76 I Mo6 N3 O18	
Formula weight	1565.56	
Temperature	100(2) K	
Wavelength	0.71073 Å	
Crystal system	Monoclinic	
Space group	P2(1)/n	
Unit cell dimensions	a = 17.4333(10) Å	α= 90°.
	b = 15.2988(9) Å	β= 104.9830(10)°.
	c = 20.4778(12) Å	γ = 90°.
Volume	5275.9(5) Å^3	
Z	4	
Density (calculated)	1.971 g/cm^3	
Absorption coefficient	2.036 mm^{-1}	
F(000)	3096	
Crystal size	0.48 x 0.32 x 0.22 mm^3	
Theta range for data collection	1.78 to 28.27°.	
Index ranges	-22<=h<=23, -20<=k<=20, -27<=l<=26	
Reflections collected	46094	
Independent reflections	12652 [R(int) = 0.0260]	
Completeness to theta = 28.27°	96.8 %	
Absorption correction	Semi-empirical from equivalents	
Max. and min. transmission	1.000 and 0.784	
Refinement method	Full-matrix least-squares on F^2	
Data / restraints / parameters	12652 / 36 / 660	
Goodness-of-fit on F^2	1.199	
Final R indices [I>2sigma(I)]	R1 = 0.0481, wR2 = 0.1169	
R indices (all data)	R1 = 0.0508, wR2 = 0.1182	
Largest diff. peak and hole	3.049 and -3.512 e.Å^{-3}	

Table 2. Atomic coordinates (x 10^4) and equivalent isotropic displacement parameters ($Å^2$x 10^3) for Iodophenylimido Hexamolybdate. U(eq) is defined as one third of the trace of the orthogonalized U^{ij} tensor.

	x	y	z	U(eq)
Mo(1)	4540(1)	1336(1)	7372(1)	14(1)
N(1)	4322(3)	343(3)	6954(2)	19(1)
C(1)	4321(4)	-284(4)	6455(3)	26(1)
C(2)	4859(5)	-193(5)	6055(4)	38(2)
C(3)	4838(5)	-787(5)	5544(4)	39(2)
C(4)	4282(4)	-1447(4)	5408(3)	30(1)
I(1)	4234(1)	-2241(1)	4563(1)	36(1)
C(5)	3763(4)	-1552(4)	5815(3)	28(1)
C(6)	3778(4)	-978(4)	6334(3)	29(1)
Mo(2)	3652(1)	2846(1)	8014(1)	18(1)
O(2)	2745(2)	2951(3)	8159(2)	26(1)
Mo(3)	5378(1)	2050(1)	8867(1)	17(1)
O(3)	5735(2)	1600(3)	9640(2)	23(1)
Mo(4)	6137(1)	2512(1)	7589(1)	17(1)
O(4)	7054(2)	2436(3)	7463(2)	25(1)
Mo(5)	4406(1)	3291(1)	6725(1)	19(1)
O(5)	4063(3)	3777(3)	5966(2)	26(1)
Mo(6)	5268(1)	4048(1)	8248(1)	16(1)
O(6)	5505(2)	5038(3)	8603(2)	24(1)
O(7)	4897(2)	2650(2)	7796(2)	13(1)
O(12)	3592(2)	1699(3)	7571(2)	19(1)
O(13)	5026(2)	1038(2)	8284(2)	17(1)
O(14)	5635(2)	1477(2)	7246(2)	18(1)
O(15)	4245(2)	2108(2)	6551(2)	19(1)
O(26)	4173(2)	3881(2)	8347(2)	18(1)
O(36)	5540(2)	3260(3)	9034(2)	18(1)
O(46)	6195(2)	3665(3)	8038(2)	21(1)
O(56)	4788(2)	4290(2)	7340(2)	19(1)
O(23)	4266(2)	2243(3)	8805(2)	17(1)
O(34)	6290(2)	2044(2)	8497(2)	17(1)

O(45)	5537(2)	3123(3)	6791(2)	18(1)
O(52)	3501(2)	3308(3)	7107(2)	19(1)
N(2)	3277(3)	6115(3)	9025(2)	14(1)
C(11)	2519(3)	6285(4)	9240(3)	16(1)
C(12)	2616(3)	6609(4)	9958(3)	19(1)
C(13)	1797(3)	6731(4)	10087(3)	24(1)
C(14)	1844(4)	7114(5)	10781(3)	31(1)
C(21)	3785(3)	5409(3)	9454(3)	17(1)
C(22)	3363(3)	4570(3)	9550(3)	19(1)
C(23)	3967(4)	3894(4)	9925(3)	22(1)
C(24)	3573(4)	3050(4)	10055(3)	33(1)
C(31)	3023(3)	5828(3)	8288(2)	15(1)
C(32)	3610(3)	6002(4)	7861(2)	17(1)
C(33)	3250(3)	5670(4)	7140(3)	21(1)
C(34)	3726(4)	5979(4)	6658(3)	29(1)
C(41)	3781(3)	6936(3)	9115(3)	17(1)
C(42)	3361(3)	7736(3)	8744(3)	18(1)
C(43)	3973(4)	8403(4)	8641(3)	24(1)
C(44)	3583(4)	9207(4)	8251(3)	31(1)
N(3)	2156(3)	5545(4)	3427(3)	30(1)
C(51A)	1820(10)	6369(16)	3168(11)	24(3)
C(52A)	911(8)	6369(9)	2950(8)	33(2)
C(53A)	596(9)	7174(9)	2514(8)	41(3)
C(54A)	848(14)	8036(9)	2883(14)	63(8)
C(51B)	1883(9)	6549(13)	3342(9)	24(3)
C(52B)	1000(7)	6739(8)	3228(7)	33(2)
C(53B)	799(10)	7686(10)	3013(8)	41(3)
C(54B)	849(9)	7891(13)	2298(8)	55(5)
C(61A)	1965(9)	4864(11)	2842(6)	27(3)
C(62A)	2133(13)	5155(11)	2179(8)	39(4)
C(63A)	2135(9)	4397(10)	1707(7)	36(3)
C(64A)	2320(30)	4660(20)	1051(12)	44(4)
C(61B)	1700(30)	5050(30)	2830(20)	27(3)
C(62B)	1910(30)	5320(30)	2180(20)	39(4)
C(63B)	2310(20)	4570(30)	1890(19)	36(3)
C(64B)	2330(90)	4740(60)	1160(30)	44(4)

C(61C)	1710(50)	5160(40)	2760(20)	27(3)
C(62C)	1720(30)	5640(20)	2100(20)	39(4)
C(63C)	1640(20)	4980(30)	1520(18)	36(3)
C(64C)	2430(30)	4520(40)	1550(30)	44(4)
C(71)	3050(3)	5596(4)	3605(3)	27(1)
C(72A)	3481(4)	4748(5)	3875(4)	47(2)
C(73A)	4339(10)	4740(16)	3849(14)	45(5)
C(74A)	4737(14)	3881(17)	4163(14)	52(4)
C(72B)	3481(4)	4748(5)	3875(4)	47(2)
C(73B)	4388(7)	4938(12)	4053(10)	45(5)
C(74B)	4891(9)	4194(13)	4421(10)	52(4)
C(81)	1870(4)	5169(4)	4005(3)	29(1)
C(82)	2169(5)	5661(5)	4675(4)	38(2)
C(83)	1800(4)	5286(5)	5219(4)	39(2)
C(84)	931(5)	5488(5)	5098(4)	40(2)

Table 3. Bond lengths [Å] and angles [°] for Iodophenylimido Hexamolybdate.

Mo(1)-N(1)	1.737(5)
Mo(1)-O(12)	1.884(4)
Mo(1)-O(13)	1.896(4)
Mo(1)-O(14)	2.004(4)
Mo(1)-O(15)	2.011(4)
Mo(1)-O(7)	2.214(3)
N(1)-C(1)	1.403(7)
C(1)-C(6)	1.402(9)
C(1)-C(2)	1.402(9)
C(2)-C(3)	1.380(9)
C(2)-H(2A)	0.9500
C(3)-C(4)	1.377(10)
C(3)-H(3A)	0.9500
C(4)-C(5)	1.389(9)
C(4)-I(1)	2.098(6)
C(5)-C(6)	1.375(9)
C(5)-H(5A)	0.9500
C(6)-H(6A)	0.9500
Mo(2)-O(2)	1.690(4)
Mo(2)-O(26)	1.865(4)
Mo(2)-O(23)	1.931(4)
Mo(2)-O(52)	1.941(4)
Mo(2)-O(12)	1.965(4)
Mo(2)-O(7)	2.345(3)
Mo(3)-O(3)	1.691(4)
Mo(3)-O(36)	1.890(4)
Mo(3)-O(34)	1.929(4)
Mo(3)-O(23)	1.933(4)
Mo(3)-O(13)	1.954(4)
Mo(3)-O(7)	2.326(3)
Mo(4)-O(4)	1.688(4)
Mo(4)-O(14)	1.856(4)
Mo(4)-O(45)	1.937(4)
Mo(4)-O(34)	1.946(4)

Mo(4)-O(46)	1.979(4)
Mo(4)-O(7)	2.317(3)
Mo(5)-O(5)	1.686(4)
Mo(5)-O(15)	1.853(4)
Mo(5)-O(52)	1.933(4)
Mo(5)-O(45)	1.957(4)
Mo(5)-O(56)	1.983(4)
Mo(5)-O(7)	2.352(3)
Mo(6)-O(6)	1.685(4)
Mo(6)-O(56)	1.868(4)
Mo(6)-O(46)	1.871(4)
Mo(6)-O(36)	1.968(4)
Mo(6)-O(26)	1.986(4)
Mo(6)-O(7)	2.353(3)
N(2)-C(41)	1.517(7)
N(2)-C(11)	1.519(6)
N(2)-C(21)	1.524(6)
N(2)-C(31)	1.524(6)
C(11)-C(12)	1.519(7)
C(11)-H(11A)	0.9900
C(11)-H(11B)	0.9900
C(12)-C(13)	1.530(7)
C(12)-H(12A)	0.9900
C(12)-H(12B)	0.9900
C(13)-C(14)	1.520(8)
C(13)-H(13A)	0.9900
C(13)-H(13B)	0.9900
C(14)-H(14A)	0.9800
C(14)-H(14B)	0.9800
C(14)-H(14C)	0.9800
C(21)-C(22)	1.517(8)
C(21)-H(21A)	0.9900
C(21)-H(21B)	0.9900
C(22)-C(23)	1.533(7)
C(22)-H(22A)	0.9900
C(22)-H(22B)	0.9900

C(23)-C(24)	1.518(9)
C(23)-H(23A)	0.9900
C(23)-H(23B)	0.9900
C(24)-H(24A)	0.9800
C(24)-H(24B)	0.9800
C(24)-H(24C)	0.9800
C(31)-C(32)	1.530(7)
C(31)-H(31A)	0.9900
C(31)-H(31B)	0.9900
C(32)-C(33)	1.535(7)
C(32)-H(32A)	0.9900
C(32)-H(32B)	0.9900
C(33)-C(34)	1.520(8)
C(33)-H(33A)	0.9900
C(33)-H(33B)	0.9900
C(34)-H(34A)	0.9800
C(34)-H(34B)	0.9800
C(34)-H(34C)	0.9800
C(41)-C(42)	1.525(7)
C(41)-H(41A)	0.9900
C(41)-H(41B)	0.9900
C(42)-C(43)	1.530(8)
C(42)-H(42A)	0.9900
C(42)-H(42B)	0.9900
C(43)-C(44)	1.527(8)
C(43)-H(43A)	0.9900
C(43)-H(43B)	0.9900
C(44)-H(44A)	0.9800
C(44)-H(44B)	0.9800
C(44)-H(44C)	0.9800
N(3)-C(51A)	1.43(2)
N(3)-C(61B)	1.48(5)
N(3)-C(61C)	1.50(6)
N(3)-C(71)	1.508(8)
N(3)-C(81)	1.511(7)
N(3)-C(61A)	1.557(15)

N(3)-C(51B)	1.604(19)
C(51A)-C(52A)	1.531(16)
C(51A)-H(51A)	0.9900
C(51A)-H(51B)	0.9900
C(52A)-C(53A)	1.536(14)
C(52A)-H(52A)	0.9900
C(52A)-H(52B)	0.9900
C(53A)-C(54A)	1.526(16)
C(53A)-H(53A)	0.9900
C(53A)-H(53B)	0.9900
C(54A)-H(54A)	0.9800
C(54A)-H(54B)	0.9800
C(54A)-H(54C)	0.9800
C(51B)-C(52B)	1.525(14)
C(51B)-H(51C)	0.9900
C(51B)-H(51D)	0.9900
C(52B)-C(53B)	1.528(14)
C(52B)-H(52C)	0.9900
C(52B)-H(52D)	0.9900
C(53B)-C(54B)	1.522(15)
C(53B)-H(53C)	0.9900
C(53B)-H(53D)	0.9900
C(54B)-H(54D)	0.9800
C(54B)-H(54E)	0.9800
C(54B)-H(54F)	0.9800
C(61A)-C(62A)	1.527(12)
C(61A)-H(61A)	0.9900
C(61A)-H(61B)	0.9900
C(62A)-C(63A)	1.510(14)
C(62A)-H(62A)	0.9900
C(62A)-H(62B)	0.9900
C(63A)-C(64A)	1.513(15)
C(63A)-H(63A)	0.9900
C(63A)-H(63B)	0.9900
C(64A)-H(64A)	0.9800
C(64A)-H(64B)	0.9800

C(64A)-H(64C)	0.9800
C(61B)-C(62B)	1.537(19)
C(61B)-H(61C)	0.9900
C(61B)-H(61D)	0.9900
C(62B)-C(63B)	1.530(19)
C(62B)-H(62C)	0.9900
C(62B)-H(62D)	0.9900
C(63B)-C(64B)	1.53(2)
C(63B)-H(63C)	0.9900
C(63B)-H(63D)	0.9900
C(64B)-H(64D)	0.9800
C(64B)-H(64E)	0.9800
C(64B)-H(64F)	0.9800
C(61C)-C(62C)	1.55(2)
C(61C)-H(61E)	0.9900
C(61C)-H(61F)	0.9900
C(62C)-C(63C)	1.539(19)
C(62C)-H(62E)	0.9900
C(62C)-H(62F)	0.9900
C(63C)-C(64C)	1.53(2)
C(63C)-H(63E)	0.9900
C(63C)-H(63F)	0.9900
C(64C)-H(64G)	0.9800
C(64C)-H(64H)	0.9800
C(64C)-H(64I)	0.9800
C(71)-C(72A)	1.529(8)
C(71)-H(71A)	0.9900
C(71)-H(71B)	0.9900
C(72A)-C(73A)	1.510(16)
C(72A)-H(72A)	0.9900
C(72A)-H(72B)	0.9900
C(73A)-C(74A)	1.546(17)
C(73A)-H(73A)	0.9900
C(73A)-H(73B)	0.9900
C(74A)-H(74A)	0.9800
C(74A)-H(74B)	0.9800

C(74A)-H(74C)	0.9800
C(73B)-C(74B)	1.512(14)
C(73B)-H(73C)	0.9900
C(73B)-H(73D)	0.9900
C(74B)-H(74D)	0.9800
C(74B)-H(74E)	0.9800
C(74B)-H(74F)	0.9800
C(81)-C(82)	1.535(9)
C(81)-H(81A)	0.9900
C(81)-H(81B)	0.9900
C(82)-C(83)	1.536(9)
C(82)-H(82A)	0.9900
C(82)-H(82B)	0.9900
C(83)-C(84)	1.502(10)
C(83)-H(83A)	0.9900
C(83)-H(83B)	0.9900
C(84)-H(84A)	0.9800
C(84)-H(84B)	0.9800
C(84)-H(84C)	0.9800

N(1)-Mo(1)-O(12)	105.7(2)
N(1)-Mo(1)-O(13)	105.09(19)
O(12)-Mo(1)-O(13)	92.95(16)
N(1)-Mo(1)-O(14)	97.19(19)
O(12)-Mo(1)-O(14)	156.11(16)
O(13)-Mo(1)-O(14)	87.43(16)
N(1)-Mo(1)-O(15)	97.19(19)
O(12)-Mo(1)-O(15)	87.63(16)
O(13)-Mo(1)-O(15)	156.64(16)
O(14)-Mo(1)-O(15)	82.84(16)
N(1)-Mo(1)-O(7)	172.22(18)
O(12)-Mo(1)-O(7)	79.72(15)
O(13)-Mo(1)-O(7)	79.85(14)
O(14)-Mo(1)-O(7)	76.84(14)
O(15)-Mo(1)-O(7)	77.28(14)
C(1)-N(1)-Mo(1)	156.4(4)

C(6)-C(1)-C(2)	119.7(6)
C(6)-C(1)-N(1)	121.3(6)
C(2)-C(1)-N(1)	118.9(6)
C(3)-C(2)-C(1)	119.2(7)
C(3)-C(2)-H(2A)	120.4
C(1)-C(2)-H(2A)	120.4
C(4)-C(3)-C(2)	121.0(7)
C(4)-C(3)-H(3A)	119.5
C(2)-C(3)-H(3A)	119.5
C(3)-C(4)-C(5)	119.9(6)
C(3)-C(4)-I(1)	117.9(5)
C(5)-C(4)-I(1)	122.2(5)
C(6)-C(5)-C(4)	120.3(6)
C(6)-C(5)-H(5A)	119.8
C(4)-C(5)-H(5A)	119.8
C(5)-C(6)-C(1)	119.8(6)
C(5)-C(6)-H(6A)	120.1
C(1)-C(6)-H(6A)	120.1
O(2)-Mo(2)-O(26)	104.12(19)
O(2)-Mo(2)-O(23)	103.81(19)
O(26)-Mo(2)-O(23)	89.22(16)
O(2)-Mo(2)-O(52)	103.45(19)
O(26)-Mo(2)-O(52)	88.50(17)
O(23)-Mo(2)-O(52)	152.36(16)
O(2)-Mo(2)-O(12)	103.06(19)
O(26)-Mo(2)-O(12)	152.81(16)
O(23)-Mo(2)-O(12)	84.97(16)
O(52)-Mo(2)-O(12)	84.59(16)
O(2)-Mo(2)-O(7)	177.96(18)
O(26)-Mo(2)-O(7)	77.92(14)
O(23)-Mo(2)-O(7)	76.05(14)
O(52)-Mo(2)-O(7)	76.53(14)
O(12)-Mo(2)-O(7)	74.91(14)
O(3)-Mo(3)-O(36)	103.20(18)
O(3)-Mo(3)-O(34)	102.96(18)
O(36)-Mo(3)-O(34)	88.63(16)

O(3)-Mo(3)-O(23)	104.13(18)
O(36)-Mo(3)-O(23)	87.87(16)
O(34)-Mo(3)-O(23)	152.77(15)
O(3)-Mo(3)-O(13)	103.32(18)
O(36)-Mo(3)-O(13)	153.48(15)
O(34)-Mo(3)-O(13)	85.27(16)
O(23)-Mo(3)-O(13)	85.91(16)
O(3)-Mo(3)-O(7)	179.01(17)
O(36)-Mo(3)-O(7)	77.56(14)
O(34)-Mo(3)-O(7)	76.38(14)
O(23)-Mo(3)-O(7)	76.49(14)
O(13)-Mo(3)-O(7)	75.92(14)
O(4)-Mo(4)-O(14)	104.83(19)
O(4)-Mo(4)-O(45)	103.33(19)
O(14)-Mo(4)-O(45)	89.63(17)
O(4)-Mo(4)-O(34)	102.69(18)
O(14)-Mo(4)-O(34)	89.03(16)
O(45)-Mo(4)-O(34)	153.40(16)
O(4)-Mo(4)-O(46)	101.28(19)
O(14)-Mo(4)-O(46)	153.88(16)
O(45)-Mo(4)-O(46)	85.02(16)
O(34)-Mo(4)-O(46)	84.58(16)
O(4)-Mo(4)-O(7)	177.85(18)
O(14)-Mo(4)-O(7)	77.10(14)
O(45)-Mo(4)-O(7)	77.53(14)
O(34)-Mo(4)-O(7)	76.28(14)
O(46)-Mo(4)-O(7)	76.79(14)
O(5)-Mo(5)-O(15)	104.68(19)
O(5)-Mo(5)-O(52)	103.53(19)
O(15)-Mo(5)-O(52)	89.49(17)
O(5)-Mo(5)-O(45)	103.54(19)
O(15)-Mo(5)-O(45)	89.13(17)
O(52)-Mo(5)-O(45)	152.34(15)
O(5)-Mo(5)-O(56)	103.11(18)
O(15)-Mo(5)-O(56)	152.20(16)
O(52)-Mo(5)-O(56)	84.70(16)

O(45)-Mo(5)-O(56)	83.75(16)
O(5)-Mo(5)-O(7)	178.46(17)
O(15)-Mo(5)-O(7)	76.85(14)
O(52)-Mo(5)-O(7)	76.48(14)
O(45)-Mo(5)-O(7)	76.30(14)
O(56)-Mo(5)-O(7)	75.36(14)
O(6)-Mo(6)-O(56)	104.32(19)
O(6)-Mo(6)-O(46)	104.52(19)
O(56)-Mo(6)-O(46)	91.38(17)
O(6)-Mo(6)-O(36)	102.60(18)
O(56)-Mo(6)-O(36)	152.44(16)
O(46)-Mo(6)-O(36)	87.48(17)
O(6)-Mo(6)-O(26)	101.94(18)
O(56)-Mo(6)-O(26)	86.12(17)
O(46)-Mo(6)-O(26)	153.20(16)
O(36)-Mo(6)-O(26)	82.71(16)
O(6)-Mo(6)-O(7)	176.93(17)
O(56)-Mo(6)-O(7)	77.38(14)
O(46)-Mo(6)-O(7)	77.89(14)
O(36)-Mo(6)-O(7)	75.46(14)
O(26)-Mo(6)-O(7)	75.53(14)
Mo(1)-O(7)-Mo(4)	91.52(12)
Mo(1)-O(7)-Mo(3)	90.42(13)
Mo(4)-O(7)-Mo(3)	90.57(12)
Mo(1)-O(7)-Mo(2)	90.58(12)
Mo(4)-O(7)-Mo(2)	177.87(17)
Mo(3)-O(7)-Mo(2)	89.82(12)
Mo(1)-O(7)-Mo(5)	90.91(12)
Mo(4)-O(7)-Mo(5)	89.96(12)
Mo(3)-O(7)-Mo(5)	178.56(17)
Mo(2)-O(7)-Mo(5)	89.60(12)
Mo(1)-O(7)-Mo(6)	179.58(18)
Mo(4)-O(7)-Mo(6)	88.90(12)
Mo(3)-O(7)-Mo(6)	89.53(11)
Mo(2)-O(7)-Mo(6)	89.00(12)
Mo(5)-O(7)-Mo(6)	89.14(12)

Mo(1)-O(12)-Mo(2)	114.68(19)
Mo(1)-O(13)-Mo(3)	113.65(18)
Mo(4)-O(14)-Mo(1)	114.47(18)
Mo(5)-O(15)-Mo(1)	114.80(18)
Mo(2)-O(26)-Mo(6)	117.50(18)
Mo(3)-O(36)-Mo(6)	117.32(18)
Mo(6)-O(46)-Mo(4)	116.30(19)
Mo(6)-O(56)-Mo(5)	118.04(19)
Mo(2)-O(23)-Mo(3)	117.22(18)
Mo(3)-O(34)-Mo(4)	116.77(18)
Mo(4)-O(45)-Mo(5)	115.90(18)
Mo(5)-O(52)-Mo(2)	117.37(18)
C(41)-N(2)-C(11)	110.0(4)
C(41)-N(2)-C(21)	106.6(4)
C(11)-N(2)-C(21)	111.9(4)
C(41)-N(2)-C(31)	111.7(4)
C(11)-N(2)-C(31)	106.6(4)
C(21)-N(2)-C(31)	110.2(4)
N(2)-C(11)-C(12)	116.7(4)
N(2)-C(11)-H(11A)	108.1
C(12)-C(11)-H(11A)	108.1
N(2)-C(11)-H(11B)	108.1
C(12)-C(11)-H(11B)	108.1
H(11A)-C(11)-H(11B)	107.3
C(11)-C(12)-C(13)	109.4(4)
C(11)-C(12)-H(12A)	109.8
C(13)-C(12)-H(12A)	109.8
C(11)-C(12)-H(12B)	109.8
C(13)-C(12)-H(12B)	109.8
H(12A)-C(12)-H(12B)	108.2
C(14)-C(13)-C(12)	112.4(5)
C(14)-C(13)-H(13A)	109.1
C(12)-C(13)-H(13A)	109.1
C(14)-C(13)-H(13B)	109.1
C(12)-C(13)-H(13B)	109.1
H(13A)-C(13)-H(13B)	107.9

C(13)-C(14)-H(14A) 109.5
C(13)-C(14)-H(14B) 109.5
H(14A)-C(14)-H(14B) 109.5
C(13)-C(14)-H(14C) 109.5
H(14A)-C(14)-H(14C) 109.5
H(14B)-C(14)-H(14C) 109.5
C(22)-C(21)-N(2) 116.4(4)
C(22)-C(21)-H(21A) 108.2
N(2)-C(21)-H(21A) 108.2
C(22)-C(21)-H(21B) 108.2
N(2)-C(21)-H(21B) 108.2
H(21A)-C(21)-H(21B) 107.3
C(21)-C(22)-C(23) 110.0(5)
C(21)-C(22)-H(22A) 109.7
C(23)-C(22)-H(22A) 109.7
C(21)-C(22)-H(22B) 109.7
C(23)-C(22)-H(22B) 109.7
H(22A)-C(22)-H(22B) 108.2
C(24)-C(23)-C(22) 112.2(5)
C(24)-C(23)-H(23A) 109.2
C(22)-C(23)-H(23A) 109.2
C(24)-C(23)-H(23B) 109.2
C(22)-C(23)-H(23B) 109.2
H(23A)-C(23)-H(23B) 107.9
C(23)-C(24)-H(24A) 109.5
C(23)-C(24)-H(24B) 109.5
H(24A)-C(24)-H(24B) 109.5
C(23)-C(24)-H(24C) 109.5
H(24A)-C(24)-H(24C) 109.5
H(24B)-C(24)-H(24C) 109.5
N(2)-C(31)-C(32) 116.7(4)
N(2)-C(31)-H(31A) 108.1
C(32)-C(31)-H(31A) 108.1
N(2)-C(31)-H(31B) 108.1
C(32)-C(31)-H(31B) 108.1
H(31A)-C(31)-H(31B) 107.3

C(31)-C(32)-C(33)	108.9(4)
C(31)-C(32)-H(32A)	109.9
C(33)-C(32)-H(32A)	109.9
C(31)-C(32)-H(32B)	109.9
C(33)-C(32)-H(32B)	109.9
H(32A)-C(32)-H(32B)	108.3
C(34)-C(33)-C(32)	111.5(5)
C(34)-C(33)-H(33A)	109.3
C(32)-C(33)-H(33A)	109.3
C(34)-C(33)-H(33B)	109.3
C(32)-C(33)-H(33B)	109.3
H(33A)-C(33)-H(33B)	108.0
C(33)-C(34)-H(34A)	109.5
C(33)-C(34)-H(34B)	109.5
H(34A)-C(34)-H(34B)	109.5
C(33)-C(34)-H(34C)	109.5
H(34A)-C(34)-H(34C)	109.5
H(34B)-C(34)-H(34C)	109.5
N(2)-C(41)-C(42)	114.6(4)
N(2)-C(41)-H(41A)	108.6
C(42)-C(41)-H(41A)	108.6
N(2)-C(41)-H(41B)	108.6
C(42)-C(41)-H(41B)	108.6
H(41A)-C(41)-H(41B)	107.6
C(41)-C(42)-C(43)	110.0(4)
C(41)-C(42)-H(42A)	109.7
C(43)-C(42)-H(42A)	109.7
C(41)-C(42)-H(42B)	109.7
C(43)-C(42)-H(42B)	109.7
H(42A)-C(42)-H(42B)	108.2
C(44)-C(43)-C(42)	112.2(5)
C(44)-C(43)-H(43A)	109.2
C(42)-C(43)-H(43A)	109.2
C(44)-C(43)-H(43B)	109.2
C(42)-C(43)-H(43B)	109.2
H(43A)-C(43)-H(43B)	107.9

C(43)-C(44)-H(44A) 109.5
C(43)-C(44)-H(44B) 109.5
H(44A)-C(44)-H(44B) 109.5
C(43)-C(44)-H(44C) 109.5
H(44A)-C(44)-H(44C) 109.5
H(44B)-C(44)-H(44C) 109.5
C(51A)-N(3)-C(61B) 94(2)
C(51A)-N(3)-C(61C) 87(3)
C(61B)-N(3)-C(61C) 8(3)
C(51A)-N(3)-C(71) 110.0(9)
C(61B)-N(3)-C(71) 122.0(19)
C(61C)-N(3)-C(71) 120(3)
C(51A)-N(3)-C(81) 116.0(11)
C(61B)-N(3)-C(81) 103.6(16)
C(61C)-N(3)-C(81) 111(2)
C(71)-N(3)-C(81) 111.1(5)
C(51A)-N(3)-C(61A) 108.6(10)
C(61B)-N(3)-C(61A) 20.4(19)
C(61C)-N(3)-C(61A) 23(3)
C(71)-N(3)-C(61A) 102.9(7)
C(81)-N(3)-C(61A) 107.4(7)
C(51A)-N(3)-C(51B) 15.4(10)
C(61B)-N(3)-C(51B) 108(2)
C(61C)-N(3)-C(51B) 102(3)
C(71)-N(3)-C(51B) 103.6(7)
C(81)-N(3)-C(51B) 107.5(9)
C(61A)-N(3)-C(51B) 123.9(9)
N(3)-C(51A)-C(52A) 113.6(17)
N(3)-C(51A)-H(51A) 108.8
C(52A)-C(51A)-H(51A)108.8
N(3)-C(51A)-H(51B) 108.8
C(52A)-C(51A)-H(51B)108.8
H(51A)-C(51A)-H(51B)107.7
C(51A)-C(52A)-C(53A)111.0(12)
C(51A)-C(52A)-H(52A)109.4
C(53A)-C(52A)-H(52A)109.4

C(51A)-C(52A)-H(52B)109.4
C(53A)-C(52A)-H(52B)109.4
H(52A)-C(52A)-H(52B)108.0
C(54A)-C(53A)-C(52A)113.0(13)
C(54A)-C(53A)-H(53A)109.0
C(52A)-C(53A)-H(53A)109.0
C(54A)-C(53A)-H(53B)109.0
C(52A)-C(53A)-H(53B)109.0
H(53A)-C(53A)-H(53B)107.8
C(52B)-C(51B)-N(3) 117.3(14)
C(52B)-C(51B)-H(51C)108.0
N(3)-C(51B)-H(51C) 108.0
C(52B)-C(51B)-H(51D)108.0
N(3)-C(51B)-H(51D) 108.0
H(51C)-C(51B)-H(51D)107.2
C(51B)-C(52B)-C(53B)111.8(11)
C(51B)-C(52B)-H(52C)109.3
C(53B)-C(52B)-H(52C)109.3
C(51B)-C(52B)-H(52D)109.3
C(53B)-C(52B)-H(52D)109.3
H(52C)-C(52B)-H(52D)107.9
C(54B)-C(53B)-C(52B)114.0(12)
C(54B)-C(53B)-H(53C)108.8
C(52B)-C(53B)-H(53C)108.8
C(54B)-C(53B)-H(53D)108.8
C(52B)-C(53B)-H(53D)108.8
H(53C)-C(53B)-H(53D)107.7
C(53B)-C(54B)-H(54D)109.5
C(53B)-C(54B)-H(54E)109.5
H(54D)-C(54B)-H(54E)109.5
C(53B)-C(54B)-H(54F)109.5
H(54D)-C(54B)-H(54F)109.5
H(54E)-C(54B)-H(54F)109.5
C(62A)-C(61A)-N(3) 115.8(11)
C(62A)-C(61A)-H(61A)108.3
N(3)-C(61A)-H(61A) 108.3

C(62A)-C(61A)-H(61B)108.3
N(3)-C(61A)-H(61B) 108.3
H(61A)-C(61A)-H(61B)107.4
C(63A)-C(62A)-C(61A)112.1(11)
C(63A)-C(62A)-H(62A)109.2
C(61A)-C(62A)-H(62A)109.2
C(63A)-C(62A)-H(62B)109.2
C(61A)-C(62A)-H(62B)109.2
H(62A)-C(62A)-H(62B)107.9
C(62A)-C(63A)-C(64A)113.6(13)
C(62A)-C(63A)-H(63A)108.8
C(64A)-C(63A)-H(63A)108.8
C(62A)-C(63A)-H(63B)108.8
C(64A)-C(63A)-H(63B)108.8
H(63A)-C(63A)-H(63B)107.7
N(3)-C(61B)-C(62B) 112(4)
N(3)-C(61B)-H(61C) 109.1
C(62B)-C(61B)-H(61C)109.1
N(3)-C(61B)-H(61D) 109.1
C(62B)-C(61B)-H(61D)109.1
H(61C)-C(61B)-H(61D)107.9
C(63B)-C(62B)-C(61B)111.6(19)
C(63B)-C(62B)-H(62C)109.3
C(61B)-C(62B)-H(62C)109.3
C(63B)-C(62B)-H(62D)109.3
C(61B)-C(62B)-H(62D)109.3
H(62C)-C(62B)-H(62D)108.0
C(62B)-C(63B)-C(64B)112(2)
C(62B)-C(63B)-H(63C)109.1
C(64B)-C(63B)-H(63C)109.1
C(62B)-C(63B)-H(63D)109.1
C(64B)-C(63B)-H(63D)109.1
H(63C)-C(63B)-H(63D)107.9
C(63B)-C(64B)-H(64D)109.5
C(63B)-C(64B)-H(64E)109.5
H(64D)-C(64B)-H(64E)109.5

C(63B)-C(64B)-H(64F)109.5
H(64D)-C(64B)-H(64F)109.5
H(64E)-C(64B)-H(64F)109.5
N(3)-C(61C)-C(62C) 119(5)
N(3)-C(61C)-H(61E) 107.5
C(62C)-C(61C)-H(61E)107.5
N(3)-C(61C)-H(61F) 107.5
C(62C)-C(61C)-H(61F)107.5
H(61E)-C(61C)-H(61F)107.0
C(63C)-C(62C)-C(61C)110.2(19)
C(63C)-C(62C)-H(62E)109.6
C(61C)-C(62C)-H(62E)109.6
C(63C)-C(62C)-H(62F)109.6
C(61C)-C(62C)-H(62F)109.6
H(62E)-C(62C)-H(62F)108.1
C(64C)-C(63C)-C(62C)111.8(19)
C(64C)-C(63C)-H(63E)109.3
C(62C)-C(63C)-H(63E)109.3
C(64C)-C(63C)-H(63F)109.3
C(62C)-C(63C)-H(63F)109.3
H(63E)-C(63C)-H(63F)107.9
N(3)-C(71)-C(72A) 115.0(5)
N(3)-C(71)-H(71A) 108.5
C(72A)-C(71)-H(71A) 108.5
N(3)-C(71)-H(71B) 108.5
C(72A)-C(71)-H(71B) 108.5
H(71A)-C(71)-H(71B) 107.5
C(73A)-C(72A)-C(71) 113.1(10)
C(73A)-C(72A)-H(72A)109.0
C(71)-C(72A)-H(72A) 109.0
C(73A)-C(72A)-H(72B)109.0
C(71)-C(72A)-H(72B) 109.0
H(72A)-C(72A)-H(72B)107.8
C(72A)-C(73A)-C(74A)109.5(15)
C(72A)-C(73A)-H(73A)109.8
C(74A)-C(73A)-H(73A)109.8

C(72A)-C(73A)-H(73B)109.8
C(74A)-C(73A)-H(73B)109.8
H(73A)-C(73A)-H(73B)108.2
C(74B)-C(73B)-H(73C)108.9
C(74B)-C(73B)-H(73D)108.9
H(73C)-C(73B)-H(73D)107.7
C(73B)-C(74B)-H(74D)109.5
C(73B)-C(74B)-H(74E)109.5
H(74D)-C(74B)-H(74E)109.5
C(73B)-C(74B)-H(74F)109.5
H(74D)-C(74B)-H(74F)109.5
H(74E)-C(74B)-H(74F)109.5
N(3)-C(81)-C(82) 114.1(5)
N(3)-C(81)-H(81A) 108.7
C(82)-C(81)-H(81A) 108.7
N(3)-C(81)-H(81B) 108.7
C(82)-C(81)-H(81B) 108.7
H(81A)-C(81)-H(81B) 107.6
C(81)-C(82)-C(83) 110.9(6)
C(81)-C(82)-H(82A) 109.5
C(83)-C(82)-H(82A) 109.5
C(81)-C(82)-H(82B) 109.5
C(83)-C(82)-H(82B) 109.5
H(82A)-C(82)-H(82B) 108.1
C(84)-C(83)-C(82) 113.4(6)
C(84)-C(83)-H(83A) 108.9
C(82)-C(83)-H(83A) 108.9
C(84)-C(83)-H(83B) 108.9
C(82)-C(83)-H(83B) 108.9
H(83A)-C(83)-H(83B) 107.7
C(83)-C(84)-H(84A) 109.5
C(83)-C(84)-H(84B) 109.5
H(84A)-C(84)-H(84B) 109.5
C(83)-C(84)-H(84C) 109.5
H(84A)-C(84)-H(84C) 109.5
H(84B)-C(84)-H(84C) 109.5

Symmetry transformations used to generate equivalent atoms:

Table 4. Anisotropic displacement parameters ($Å^2 x\ 10^3$) for Iodophenylimido Hexamolybdate.

The anisotropic displacement factor exponent takes the form: $-2\pi^2[\ h^2\ a^{*2}U^{11} + ...\ + 2\ h\ k\ a^*\ b^*\ U^{12}\ ]$

	U^{11}	U^{22}	U^{33}	U^{23}	U^{13}	U^{12}	
Mo(1)	16(1)	14(1)	13(1)	-4(1)	4(1)	-3(1)	
N(1)22(2)	18(2)	16(2)	-4(2)	1(2)	-2(2)		
C(1)29(3)	27(3)	19(3)	-5(2)	3(2)	2(2)		
C(2)45(4)	36(4)	38(4)	-12(3)	18(3)	-11(3)		
C(3)45(4)	42(4)	35(4)	-9(3)	22(3)	-9(3)		
C(4)35(3)	28(3)	26(3)	-4(2)	5(3)	3(3)		
I(1)50(1)	30(1)	25(1)	-8(1)	7(1)	6(1)		
C(5)31(3)	22(3)	31(3)	-7(2)	5(2)	-6(2)		
C(6)30(3)	33(3)	26(3)	-3(3)	10(2)	-3(3)		
Mo(2)	14(1)	22(1)	20(1)	-7(1)	7(1)	-1(1)	
O(2)18(2)	36(2)	26(2)	-6(2)	8(2)	1(2)		
Mo(3)	22(1)	17(1)	11(1)	-1(1)	1(1)	-2(1)	
O(3)28(2)	23(2)	16(2)	1(2)	1(2)	-1(2)		
Mo(4)	14(1)	17(1)	23(1)	-3(1)	8(1)	-2(1)	
O(4)18(2)	28(2)	32(2)	1(2)	12(2)	-1(2)		
Mo(5)	25(1)	18(1)	11(1)	0(1)	1(1)	0(1)	
O(5)38(2)	25(2)	14(2)	1(2)	4(2)	2(2)		
Mo(6)	17(1)	13(1)	16(1)	-4(1)	2(1)	-1(1)	
O(6)28(2)	16(2)	26(2)	-8(2)	3(2)	-3(2)		
O(7)13(2)	15(2)	11(2)	-4(1)	3(1)	0(1)		
O(12)18(2)	24(2)	16(2)	-6(2)	5(1)	-5(2)		
O(13)21(2)	16(2)	15(2)	2(1)	3(1)	-2(1)		
O(14)18(2)	19(2)	19(2)	-3(1)	8(1)	0(1)		
O(15)22(2)	19(2)	14(2)	-4(1)	3(1)	-3(2)		
O(26)18(2)	19(2)	18(2)	-7(1)	5(1)	2(2)		
O(36)20(2)	20(2)	12(2)	-4(1)	1(1)	-2(2)		
O(46)18(2)	18(2)	26(2)	-3(2)	5(2)	-5(2)		
O(56)25(2)	16(2)	16(2)	-2(1)	4(2)	1(2)		
O(23)20(2)	21(2)	12(2)	-2(1)	7(1)	-1(2)		
O(34)15(2)	19(2)	17(2)	0(1)	1(1)	0(1)		
O(45)21(2)	21(2)	14(2)	1(1)	6(1)	-1(2)		

O(52)15(2)	22(2)	17(2)	-2(2)	1(1)	1(2)	
N(2)15(2)	13(2)	12(2)	0(2)	2(2)	1(2)	
C(11)14(2)	20(3)	15(2)	-2(2)	4(2)	1(2)	
C(12)16(2)	22(3)	17(2)	-1(2)	3(2)	2(2)	
C(13)17(3)	35(3)	18(3)	-2(2)	3(2)	5(2)	
C(14)30(3)	40(4)	27(3)	-8(3)	14(3)	-1(3)	
C(21)16(2)	18(2)	14(2)	-1(2)	1(2)	6(2)	
C(22)24(3)	17(2)	16(2)	0(2)	6(2)	3(2)	
C(23)36(3)	17(3)	11(2)	1(2)	5(2)	9(2)	
C(24)52(4)	22(3)	27(3)	3(2)	17(3)	5(3)	
C(31)16(2)	17(2)	12(2)	-2(2)	2(2)	3(2)	
C(32)19(2)	19(2)	13(2)	-2(2)	6(2)	1(2)	
C(33)25(3)	23(3)	17(2)	-3(2)	7(2)	2(2)	
C(34)34(3)	35(3)	21(3)	2(2)	11(2)	6(3)	
C(41)15(2)	18(2)	16(2)	-2(2)	3(2)	1(2)	
C(42)19(2)	13(2)	21(2)	-1(2)	3(2)	1(2)	
C(43)26(3)	22(3)	24(3)	3(2)	9(2)	-1(2)	
C(44)45(4)	24(3)	21(3)	3(2)	8(3)	-4(3)	
N(3)30(3)	36(3)	25(3)	3(2)	9(2)	-16(2)	
C(51A)	26(4)	27(8)	20(9)	-2(6)	8(4)	-7(5)
C(52A)	24(4)	32(7)	44(7)	7(4)	9(5)	-10(5)
C(53A)	33(5)	46(7)	47(6)	8(5)	14(5)	3(5)
C(54A)	47(11)	24(10)	110(20)	0(11)	13(13)	4(9)
C(51B)	26(4)	27(8)	20(9)	-2(6)	8(4)	-7(5)
C(52B)	24(4)	32(7)	44(7)	7(4)	9(5)	-10(5)
C(53B)	33(5)	46(7)	47(6)	8(5)	14(5)	3(5)
C(54B)	30(7)	90(14)	45(9)	31(9)	9(6)	6(8)
C(61A)	23(8)	36(8)	24(4)	4(4)	10(5)	-9(5)
C(62A)	58(12)	36(8)	28(4)	4(5)	18(6)	-13(6)
C(63A)	36(7)	46(8)	25(7)	-3(5)	4(6)	-28(5)
C(64A)	55(6)	46(8)	41(9)	12(7)	28(11)	-5(7)
C(61B)	23(8)	36(8)	24(4)	4(4)	10(5)	-9(5)
C(62B)	58(12)	36(8)	28(4)	4(5)	18(6)	-13(6)
C(63B)	36(7)	46(8)	25(7)	-3(5)	4(6)	-28(5)
C(64B)	55(6)	46(8)	41(9)	12(7)	28(11)	-5(7)
C(61C)	23(8)	36(8)	24(4)	4(4)	10(5)	-9(5)

C(62C)	58(12)	36(8)	28(4)	4(5)	18(6)	-13(6)
C(63C)	36(7)	46(8)	25(7)	-3(5)	4(6)	-28(5)
C(64C)	55(6)	46(8)	41(9)	12(7)	28(11)	-5(7)
C(71)30(3)	21(3)	36(3)	-4(2)	20(3)	-6(2)	
C(72A)	58(5)	36(4)	62(5)	19(4)	41(4)	11(4)
C(73A)	55(5)	45(9)	55(12)	20(8)	52(7)	21(5)
C(74A)	67(9)	47(11)	59(11)	16(7)	48(8)	25(8)
C(72B)	58(5)	36(4)	62(5)	19(4)	41(4)	11(4)
C(73B)	55(5)	45(9)	55(12)	20(8)	52(7)	21(5)
C(74B)	67(9)	47(11)	59(11)	16(7)	48(8)	25(8)
C(81)32(3)	32(3)	25(3)	4(2)	13(2)	-9(3)	
C(82)46(4)	39(4)	35(4)	-9(3)	23(3)	-16(3)	
C(83)43(4)	50(4)	29(3)	2(3)	17(3)	-5(3)	
C(84)52(4)	28(3)	49(4)	4(3)	32(4)	3(3)	

Table 5. Hydrogen coordinates (x 10^4) and isotropic displacement parameters ($Å^2$x 10^3) for Iodophenylimido Hexamolybdate.

	x	y	z	U(eq)
H(2A)	5232	273	6134	46
H(3A)	5214	-741	5282	46
H(5A)	3395	-2023	5733	34
H(6A)	3422	-1052	6611	35
H(11A)	2208	5736	9183	20
H(11B)	2201	6720	8927	20
H(12A)	2907	7171	10023	22
H(12B)	2927	6180	10283	22
H(13A)	1476	7124	9737	28
H(13B)	1523	6159	10046	28
H(14A)	1311	7134	10856	46
H(14B)	2063	7707	10807	46
H(14C)	2189	6747	11128	46
H(21A)	4221	5259	9246	20
H(21B)	4030	5658	9906	20
H(22A)	3074	4334	9104	22
H(22B)	2971	4691	9813	22
H(23A)	4349	3765	9654	26
H(23B)	4268	4143	10362	26
H(24A)	3976	2648	10313	49
H(24B)	3303	2781	9622	49
H(24C)	3184	3177	10313	49
H(31A)	2518	6126	8070	18
H(31B)	2914	5193	8276	18
H(32A)	4117	5697	8061	20
H(32B)	3719	6637	7853	20
H(33A)	3236	5024	7142	26
H(33B)	2697	5884	6980	26
H(34A)	3500	5728	6209	44
H(34B)	4279	5789	6826	44

H(34C)	3706	6618	6628	44
H(41A)	4260	6817	8954	20
H(41B)	3960	7073	9603	20
H(42A)	3022	8004	9010	22
H(42B)	3016	7558	8300	22
H(43A)	4307	8588	9088	28
H(43B)	4323	8124	8391	28
H(44A)	3994	9624	8209	46
H(44B)	3231	9482	8494	46
H(44C)	3274	9031	7800	46
H(51A)	2023	6531	2775	29
H(51B)	2001	6822	3520	29
H(52A)	702	6369	3355	40
H(52B)	722	5832	2688	40
H(53A)	791	7158	2101	50
H(53B)	9	7147	2372	50
H(54A)	605	8087	3262	95
H(54B)	673	8524	2569	95
H(54C)	1427	8050	3052	95
H(51C)	2172	6868	3752	29
H(51D)	2056	6795	2956	29
H(52C)	841	6621	3650	40
H(52D)	692	6343	2874	40
H(53C)	255	7816	3048	50
H(53D)	1169	8077	3332	50
H(54D)	470	7524	1976	83
H(54E)	1388	7772	2259	83
H(54F)	720	8508	2198	83
H(61A)	2277	4328	2999	32
H(61B)	1396	4706	2750	32
H(62A)	1724	5583	1953	47
H(62B)	2656	5451	2279	47
H(63A)	1608	4110	1603	44
H(63B)	2533	3963	1941	44
H(64A)	1881	5013	782	66
H(64B)	2382	4133	797	66

H(64C)	2810	5000	1150	66
H(61C)	1124	5152	2775	32
H(61D)	1801	4419	2908	32
H(62C)	1427	5504	1836	47
H(62D)	2280	5827	2271	47
H(63C)	2014	4024	1912	44
H(63D)	2858	4494	2174	44
H(64D)	2654	5255	1139	66
H(64E)	1791	4829	878	66
H(64F)	2565	4228	990	66
H(61E)	1153	5088	2775	32
H(61F)	1928	4563	2737	32
H(62E)	1270	6056	1983	47
H(62F)	2218	5973	2162	47
H(63E)	1237	4534	1544	44
H(63F)	1464	5284	1082	44
H(64G)	2715	4825	1266	66
H(64H)	2332	3912	1397	66
H(64I)	2761	4517	2022	66
H(71A)	3225	6059	3950	32
H(71B)	3215	5776	3198	32
H(72A)	3457	4662	4348	56
H(72B)	3201	4251	3605	56
H(73A)	4621	5246	4103	54
H(73B)	4369	4788	3375	54
H(74A)	4714	3842	4635	62
H(74B)	5292	3875	4142	62
H(74C)	4456	3382	3909	62
H(72C)	3343	4283	3528	56
H(72D)	3323	4550	4282	56
H(73C)	4545	5061	3631	54
H(73D)	4499	5468	4339	54
H(74D)	5454	4349	4508	62
H(74E)	4786	3666	4142	62
H(74F)	4759	4086	4851	62
H(81A)	2044	4552	4072	35

H(81B)	1282	5174	3878	35
H(82A)	2031	6288	4606	45
H(82B)	2755	5614	4829	45
H(83A)	1872	4644	5237	47
H(83B)	2086	5525	5665	47
H(84A)	740	5270	5477	59
H(84B)	635	5205	4679	59
H(84C)	851	6122	5058	59

Table 6. Torsion angles [°] for Iodophenylimido Hexamolybdate.

O(12)-Mo(1)-N(1)-C(1)	135.7(10)
O(13)-Mo(1)-N(1)-C(1)	-126.8(10)
O(14)-Mo(1)-N(1)-C(1)	-37.5(11)
O(15)-Mo(1)-N(1)-C(1)	46.1(11)
O(7)-Mo(1)-N(1)-C(1)	2(2)
Mo(1)-N(1)-C(1)-C(6)	-162.1(8)
Mo(1)-N(1)-C(1)-C(2)	15.6(14)
C(6)-C(1)-C(2)-C(3)	0.5(11)
N(1)-C(1)-C(2)-C(3)	-177.3(7)
C(1)-C(2)-C(3)-C(4)	2.3(12)
C(2)-C(3)-C(4)-C(5)	-4.0(11)
C(2)-C(3)-C(4)-I(1)	174.3(6)
C(3)-C(4)-C(5)-C(6)	2.8(10)
I(1)-C(4)-C(5)-C(6)	-175.3(5)
C(4)-C(5)-C(6)-C(1)	-0.1(10)
C(2)-C(1)-C(6)-C(5)	-1.6(10)
N(1)-C(1)-C(6)-C(5)	176.2(6)
N(1)-Mo(1)-O(7)-Mo(4)	-42.2(14)
O(12)-Mo(1)-O(7)-Mo(4)	-177.28(16)
O(13)-Mo(1)-O(7)-Mo(4)	87.81(15)
O(14)-Mo(1)-O(7)-Mo(4)	-1.91(13)
O(15)-Mo(1)-O(7)-Mo(4)	-87.40(14)
N(1)-Mo(1)-O(7)-Mo(3)	-132.8(13)
O(12)-Mo(1)-O(7)-Mo(3)	92.14(15)
O(13)-Mo(1)-O(7)-Mo(3)	-2.77(14)
O(14)-Mo(1)-O(7)-Mo(3)	-92.48(14)
O(15)-Mo(1)-O(7)-Mo(3)	-177.98(15)
N(1)-Mo(1)-O(7)-Mo(2)	137.4(13)
O(12)-Mo(1)-O(7)-Mo(2)	2.31(14)
O(13)-Mo(1)-O(7)-Mo(2)	-92.60(15)
O(14)-Mo(1)-O(7)-Mo(2)	177.69(15)
O(15)-Mo(1)-O(7)-Mo(2)	92.19(14)
N(1)-Mo(1)-O(7)-Mo(5)	47.8(13)
O(12)-Mo(1)-O(7)-Mo(5)	-87.29(15)

O(13)-Mo(1)-O(7)-Mo(5)	177.79(15)
O(14)-Mo(1)-O(7)-Mo(5)	88.08(14)
O(15)-Mo(1)-O(7)-Mo(5)	2.58(13)
N(1)-Mo(1)-O(7)-Mo(6)	145(30)
O(12)-Mo(1)-O(7)-Mo(6)	10(31)
O(13)-Mo(1)-O(7)-Mo(6)	-85(31)
O(14)-Mo(1)-O(7)-Mo(6)	-175(100)
O(15)-Mo(1)-O(7)-Mo(6)	100(31)
O(4)-Mo(4)-O(7)-Mo(1)	-152(5)
O(14)-Mo(4)-O(7)-Mo(1)	2.06(14)
O(45)-Mo(4)-O(7)-Mo(1)	94.57(15)
O(34)-Mo(4)-O(7)-Mo(1)	-90.12(15)
O(46)-Mo(4)-O(7)-Mo(1)	-177.69(16)
O(4)-Mo(4)-O(7)-Mo(3)	-61(5)
O(14)-Mo(4)-O(7)-Mo(3)	92.49(15)
O(45)-Mo(4)-O(7)-Mo(3)	-175.00(16)
O(34)-Mo(4)-O(7)-Mo(3)	0.31(13)
O(46)-Mo(4)-O(7)-Mo(3)	-87.25(15)
O(4)-Mo(4)-O(7)-Mo(2)	39(8)
O(14)-Mo(4)-O(7)-Mo(2)	-167(5)
O(45)-Mo(4)-O(7)-Mo(2)	-74(5)
O(34)-Mo(4)-O(7)-Mo(2)	101(5)
O(46)-Mo(4)-O(7)-Mo(2)	13(4)
O(4)-Mo(4)-O(7)-Mo(5)	118(5)
O(14)-Mo(4)-O(7)-Mo(5)	-88.85(15)
O(45)-Mo(4)-O(7)-Mo(5)	3.66(13)
O(34)-Mo(4)-O(7)-Mo(5)	178.97(16)
O(46)-Mo(4)-O(7)-Mo(5)	91.40(15)
O(4)-Mo(4)-O(7)-Mo(6)	28(5)
O(14)-Mo(4)-O(7)-Mo(6)	-178.00(16)
O(45)-Mo(4)-O(7)-Mo(6)	-85.49(14)
O(34)-Mo(4)-O(7)-Mo(6)	89.83(14)
O(46)-Mo(4)-O(7)-Mo(6)	2.26(14)
O(3)-Mo(3)-O(7)-Mo(1)	43(10)
O(36)-Mo(3)-O(7)-Mo(1)	-177.18(16)
O(34)-Mo(3)-O(7)-Mo(1)	91.20(15)

O(23)-Mo(3)-O(7)-Mo(1)	-86.39(15)
O(13)-Mo(3)-O(7)-Mo(1)	2.73(13)
O(3)-Mo(3)-O(7)-Mo(4)	-49(10)
O(36)-Mo(3)-O(7)-Mo(4)	91.30(15)
O(34)-Mo(3)-O(7)-Mo(4)	-0.32(13)
O(23)-Mo(3)-O(7)-Mo(4)	-177.91(16)
O(13)-Mo(3)-O(7)-Mo(4)	-88.79(15)
O(3)-Mo(3)-O(7)-Mo(2)	133(10)
O(36)-Mo(3)-O(7)-Mo(2)	-86.60(15)
O(34)-Mo(3)-O(7)-Mo(2)	-178.22(16)
O(23)-Mo(3)-O(7)-Mo(2)	4.19(13)
O(13)-Mo(3)-O(7)-Mo(2)	93.31(15)
O(3)-Mo(3)-O(7)-Mo(5)	-160(9)
O(36)-Mo(3)-O(7)-Mo(5)	-20(7)
O(34)-Mo(3)-O(7)-Mo(5)	-112(7)
O(23)-Mo(3)-O(7)-Mo(5)	71(7)
O(13)-Mo(3)-O(7)-Mo(5)	160(7)
O(3)-Mo(3)-O(7)-Mo(6)	-138(10)
O(36)-Mo(3)-O(7)-Mo(6)	2.40(14)
O(34)-Mo(3)-O(7)-Mo(6)	-89.21(14)
O(23)-Mo(3)-O(7)-Mo(6)	93.19(14)
O(13)-Mo(3)-O(7)-Mo(6)	-177.69(15)
O(2)-Mo(2)-O(7)-Mo(1)	0(5)
O(26)-Mo(2)-O(7)-Mo(1)	178.44(16)
O(23)-Mo(2)-O(7)-Mo(1)	86.22(15)
O(52)-Mo(2)-O(7)-Mo(1)	-90.20(15)
O(12)-Mo(2)-O(7)-Mo(1)	-2.26(13)
O(2)-Mo(2)-O(7)-Mo(4)	169(5)
O(26)-Mo(2)-O(7)-Mo(4)	-13(4)
O(23)-Mo(2)-O(7)-Mo(4)	-105(5)
O(52)-Mo(2)-O(7)-Mo(4)	79(5)
O(12)-Mo(2)-O(7)-Mo(4)	167(5)
O(2)-Mo(2)-O(7)-Mo(3)	-91(5)
O(26)-Mo(2)-O(7)-Mo(3)	88.02(15)
O(23)-Mo(2)-O(7)-Mo(3)	-4.20(13)
O(52)-Mo(2)-O(7)-Mo(3)	179.38(16)

O(12)-Mo(2)-O(7)-Mo(3)	-92.68(15)
O(2)-Mo(2)-O(7)-Mo(5)	91(5)
O(26)-Mo(2)-O(7)-Mo(5)	-90.66(15)
O(23)-Mo(2)-O(7)-Mo(5)	177.12(16)
O(52)-Mo(2)-O(7)-Mo(5)	0.70(13)
O(12)-Mo(2)-O(7)-Mo(5)	88.65(14)
O(2)-Mo(2)-O(7)-Mo(6)	180(100)
O(26)-Mo(2)-O(7)-Mo(6)	-1.51(14)
O(23)-Mo(2)-O(7)-Mo(6)	-93.73(14)
O(52)-Mo(2)-O(7)-Mo(6)	89.85(15)
O(12)-Mo(2)-O(7)-Mo(6)	177.79(16)
O(5)-Mo(5)-O(7)-Mo(1)	-179(100)
O(15)-Mo(5)-O(7)-Mo(1)	-2.81(14)
O(52)-Mo(5)-O(7)-Mo(1)	89.87(15)
O(45)-Mo(5)-O(7)-Mo(1)	-95.15(15)
O(56)-Mo(5)-O(7)-Mo(1)	177.84(16)
O(5)-Mo(5)-O(7)-Mo(4)	-88(7)
O(15)-Mo(5)-O(7)-Mo(4)	88.71(15)
O(52)-Mo(5)-O(7)-Mo(4)	-178.62(16)
O(45)-Mo(5)-O(7)-Mo(4)	-3.64(13)
O(56)-Mo(5)-O(7)-Mo(4)	-90.65(15)
O(5)-Mo(5)-O(7)-Mo(3)	24(11)
O(15)-Mo(5)-O(7)-Mo(3)	-160(7)
O(52)-Mo(5)-O(7)-Mo(3)	-67(7)
O(45)-Mo(5)-O(7)-Mo(3)	108(7)
O(56)-Mo(5)-O(7)-Mo(3)	21(7)
O(5)-Mo(5)-O(7)-Mo(2)	90(7)
O(15)-Mo(5)-O(7)-Mo(2)	-93.38(15)
O(52)-Mo(5)-O(7)-Mo(2)	-0.70(13)
O(45)-Mo(5)-O(7)-Mo(2)	174.27(16)
O(56)-Mo(5)-O(7)-Mo(2)	87.26(15)
O(5)-Mo(5)-O(7)-Mo(6)	1(7)
O(15)-Mo(5)-O(7)-Mo(6)	177.61(16)
O(52)-Mo(5)-O(7)-Mo(6)	-89.71(14)
O(45)-Mo(5)-O(7)-Mo(6)	85.26(14)
O(56)-Mo(5)-O(7)-Mo(6)	-1.75(13)

O(6)-Mo(6)-O(7)-Mo(1)	29(32)
O(56)-Mo(6)-O(7)-Mo(1)	-95(31)
O(46)-Mo(6)-O(7)-Mo(1)	171(100)
O(36)-Mo(6)-O(7)-Mo(1)	80(31)
O(26)-Mo(6)-O(7)-Mo(1)	-6(31)
O(6)-Mo(6)-O(7)-Mo(4)	-144(3)
O(56)-Mo(6)-O(7)-Mo(4)	91.82(15)
O(46)-Mo(6)-O(7)-Mo(4)	-2.38(14)
O(36)-Mo(6)-O(7)-Mo(4)	-92.90(14)
O(26)-Mo(6)-O(7)-Mo(4)	-178.98(15)
O(6)-Mo(6)-O(7)-Mo(3)	-54(3)
O(56)-Mo(6)-O(7)-Mo(3)	-177.61(16)
O(46)-Mo(6)-O(7)-Mo(3)	88.19(15)
O(36)-Mo(6)-O(7)-Mo(3)	-2.33(13)
O(26)-Mo(6)-O(7)-Mo(3)	-88.40(14)
O(6)-Mo(6)-O(7)-Mo(2)	36(3)
O(56)-Mo(6)-O(7)-Mo(2)	-87.77(15)
O(46)-Mo(6)-O(7)-Mo(2)	178.03(16)
O(36)-Mo(6)-O(7)-Mo(2)	87.50(14)
O(26)-Mo(6)-O(7)-Mo(2)	1.43(13)
O(6)-Mo(6)-O(7)-Mo(5)	126(3)
O(56)-Mo(6)-O(7)-Mo(5)	1.84(14)
O(46)-Mo(6)-O(7)-Mo(5)	-92.36(15)
O(36)-Mo(6)-O(7)-Mo(5)	177.12(15)
O(26)-Mo(6)-O(7)-Mo(5)	91.04(14)
N(1)-Mo(1)-O(12)-Mo(2)	-177.3(2)
O(13)-Mo(1)-O(12)-Mo(2)	76.1(2)
O(14)-Mo(1)-O(12)-Mo(2)	-14.2(5)
O(15)-Mo(1)-O(12)-Mo(2)	-80.5(2)
O(7)-Mo(1)-O(12)-Mo(2)	-3.04(18)
O(2)-Mo(2)-O(12)-Mo(1)	-177.0(2)
O(26)-Mo(2)-O(12)-Mo(1)	4.4(5)
O(23)-Mo(2)-O(12)-Mo(1)	-74.0(2)
O(52)-Mo(2)-O(12)-Mo(1)	80.4(2)
O(7)-Mo(2)-O(12)-Mo(1)	2.92(17)
N(1)-Mo(1)-O(13)-Mo(3)	177.4(2)

O(12)-Mo(1)-O(13)-Mo(3)	-75.4(2)
O(14)-Mo(1)-O(13)-Mo(3)	80.7(2)
O(15)-Mo(1)-O(13)-Mo(3)	15.5(5)
O(7)-Mo(1)-O(13)-Mo(3)	3.60(18)
O(3)-Mo(3)-O(13)-Mo(1)	177.2(2)
O(36)-Mo(3)-O(13)-Mo(1)	-3.3(5)
O(34)-Mo(3)-O(13)-Mo(1)	-80.6(2)
O(23)-Mo(3)-O(13)-Mo(1)	73.6(2)
O(7)-Mo(3)-O(13)-Mo(1)	-3.48(17)
O(4)-Mo(4)-O(14)-Mo(1)	176.5(2)
O(45)-Mo(4)-O(14)-Mo(1)	-79.8(2)
O(34)-Mo(4)-O(14)-Mo(1)	73.6(2)
O(46)-Mo(4)-O(14)-Mo(1)	-1.9(5)
O(7)-Mo(4)-O(14)-Mo(1)	-2.49(17)
N(1)-Mo(1)-O(14)-Mo(4)	177.5(2)
O(12)-Mo(1)-O(14)-Mo(4)	13.9(5)
O(13)-Mo(1)-O(14)-Mo(4)	-77.6(2)
O(15)-Mo(1)-O(14)-Mo(4)	81.2(2)
O(7)-Mo(1)-O(14)-Mo(4)	2.61(18)
O(5)-Mo(5)-O(15)-Mo(1)	-176.7(2)
O(52)-Mo(5)-O(15)-Mo(1)	-72.8(2)
O(45)-Mo(5)-O(15)-Mo(1)	79.5(2)
O(56)-Mo(5)-O(15)-Mo(1)	4.7(5)
O(7)-Mo(5)-O(15)-Mo(1)	3.41(17)
N(1)-Mo(1)-O(15)-Mo(5)	-178.1(2)
O(12)-Mo(1)-O(15)-Mo(5)	76.4(2)
O(13)-Mo(1)-O(15)-Mo(5)	-15.6(5)
O(14)-Mo(1)-O(15)-Mo(5)	-81.7(2)
O(7)-Mo(1)-O(15)-Mo(5)	-3.61(18)
O(2)-Mo(2)-O(26)-Mo(6)	-178.0(2)
O(23)-Mo(2)-O(26)-Mo(6)	77.9(2)
O(52)-Mo(2)-O(26)-Mo(6)	-74.5(2)
O(12)-Mo(2)-O(26)-Mo(6)	0.5(5)
O(7)-Mo(2)-O(26)-Mo(6)	2.02(18)
O(6)-Mo(6)-O(26)-Mo(2)	179.8(2)
O(56)-Mo(6)-O(26)-Mo(2)	75.9(2)

O(46)-Mo(6)-O(26)-Mo(2)	-9.4(5)
O(36)-Mo(6)-O(26)-Mo(2)	-78.8(2)
O(7)-Mo(6)-O(26)-Mo(2)	-2.03(18)
O(3)-Mo(3)-O(36)-Mo(6)	176.1(2)
O(34)-Mo(3)-O(36)-Mo(6)	73.1(2)
O(23)-Mo(3)-O(36)-Mo(6)	-79.9(2)
O(13)-Mo(3)-O(36)-Mo(6)	-3.4(5)
O(7)-Mo(3)-O(36)-Mo(6)	-3.24(18)
O(6)-Mo(6)-O(36)-Mo(3)	-179.2(2)
O(56)-Mo(6)-O(36)-Mo(3)	13.2(5)
O(46)-Mo(6)-O(36)-Mo(3)	-74.9(2)
O(26)-Mo(6)-O(36)-Mo(3)	80.1(2)
O(7)-Mo(6)-O(36)-Mo(3)	3.23(18)
O(6)-Mo(6)-O(46)-Mo(4)	-178.9(2)
O(56)-Mo(6)-O(46)-Mo(4)	-73.7(2)
O(36)-Mo(6)-O(46)-Mo(4)	78.8(2)
O(26)-Mo(6)-O(46)-Mo(4)	10.4(5)
O(7)-Mo(6)-O(46)-Mo(4)	3.11(19)
O(4)-Mo(4)-O(46)-Mo(6)	177.8(2)
O(14)-Mo(4)-O(46)-Mo(6)	-3.7(5)
O(45)-Mo(4)-O(46)-Mo(6)	75.2(2)
O(34)-Mo(4)-O(46)-Mo(6)	-80.3(2)
O(7)-Mo(4)-O(46)-Mo(6)	-3.17(19)
O(6)-Mo(6)-O(56)-Mo(5)	-179.8(2)
O(46)-Mo(6)-O(56)-Mo(5)	74.8(2)
O(36)-Mo(6)-O(56)-Mo(5)	-12.4(5)
O(26)-Mo(6)-O(56)-Mo(5)	-78.5(2)
O(7)-Mo(6)-O(56)-Mo(5)	-2.47(19)
O(5)-Mo(5)-O(56)-Mo(6)	-177.4(2)
O(15)-Mo(5)-O(56)-Mo(6)	1.1(5)
O(52)-Mo(5)-O(56)-Mo(6)	79.9(2)
O(45)-Mo(5)-O(56)-Mo(6)	-74.9(2)
O(7)-Mo(5)-O(56)-Mo(6)	2.49(19)
O(2)-Mo(2)-O(23)-Mo(3)	-176.4(2)
O(26)-Mo(2)-O(23)-Mo(3)	-72.1(2)
O(52)-Mo(2)-O(23)-Mo(3)	13.2(5)

O(12)-Mo(2)-O(23)-Mo(3)	81.4(2)
O(7)-Mo(2)-O(23)-Mo(3)	5.69(18)
O(3)-Mo(3)-O(23)-Mo(2)	175.1(2)
O(36)-Mo(3)-O(23)-Mo(2)	72.0(2)
O(34)-Mo(3)-O(23)-Mo(2)	-10.8(5)
O(13)-Mo(3)-O(23)-Mo(2)	-82.2(2)
O(7)-Mo(3)-O(23)-Mo(2)	-5.73(18)
O(3)-Mo(3)-O(34)-Mo(4)	179.7(2)
O(36)-Mo(3)-O(34)-Mo(4)	-77.1(2)
O(23)-Mo(3)-O(34)-Mo(4)	5.5(5)
O(13)-Mo(3)-O(34)-Mo(4)	77.1(2)
O(7)-Mo(3)-O(34)-Mo(4)	0.42(18)
O(4)-Mo(4)-O(34)-Mo(3)	177.6(2)
O(14)-Mo(4)-O(34)-Mo(3)	-77.4(2)
O(45)-Mo(4)-O(34)-Mo(3)	9.8(5)
O(46)-Mo(4)-O(34)-Mo(3)	77.3(2)
O(7)-Mo(4)-O(34)-Mo(3)	-0.42(18)
O(4)-Mo(4)-O(45)-Mo(5)	177.1(2)
O(14)-Mo(4)-O(45)-Mo(5)	72.0(2)
O(34)-Mo(4)-O(45)-Mo(5)	-15.1(5)
O(46)-Mo(4)-O(45)-Mo(5)	-82.4(2)
O(7)-Mo(4)-O(45)-Mo(5)	-4.89(18)
O(5)-Mo(5)-O(45)-Mo(4)	-176.7(2)
O(15)-Mo(5)-O(45)-Mo(4)	-71.8(2)
O(52)-Mo(5)-O(45)-Mo(4)	15.4(5)
O(56)-Mo(5)-O(45)-Mo(4)	81.2(2)
O(7)-Mo(5)-O(45)-Mo(4)	4.84(18)
O(5)-Mo(5)-O(52)-Mo(2)	-177.5(2)
O(15)-Mo(5)-O(52)-Mo(2)	77.6(2)
O(45)-Mo(5)-O(52)-Mo(2)	-9.6(5)
O(56)-Mo(5)-O(52)-Mo(2)	-75.2(2)
O(7)-Mo(5)-O(52)-Mo(2)	0.96(18)
O(2)-Mo(2)-O(52)-Mo(5)	-178.9(2)
O(26)-Mo(2)-O(52)-Mo(5)	77.0(2)
O(23)-Mo(2)-O(52)-Mo(5)	-8.5(5)
O(12)-Mo(2)-O(52)-Mo(5)	-76.7(2)

O(7)-Mo(2)-O(52)-Mo(5)	-0.96(18)
C(41)-N(2)-C(11)-C(12)	-57.0(6)
C(21)-N(2)-C(11)-C(12)	61.3(6)
C(31)-N(2)-C(11)-C(12)	-178.2(4)
N(2)-C(11)-C(12)-C(13)	-179.2(5)
C(11)-C(12)-C(13)-C(14)	-176.1(5)
C(41)-N(2)-C(21)-C(22)	169.3(4)
C(11)-N(2)-C(21)-C(22)	48.9(6)
C(31)-N(2)-C(21)-C(22)	-69.5(5)
N(2)-C(21)-C(22)-C(23)	173.9(4)
C(21)-C(22)-C(23)-C(24)	178.1(5)
C(41)-N(2)-C(31)-C(32)	33.4(6)
C(11)-N(2)-C(31)-C(32)	153.6(4)
C(21)-N(2)-C(31)-C(32)	-84.7(5)
N(2)-C(31)-C(32)-C(33)	-180.0(4)
C(31)-C(32)-C(33)-C(34)	169.0(5)
C(11)-N(2)-C(41)-C(42)	-56.0(5)
C(21)-N(2)-C(41)-C(42)	-177.6(4)
C(31)-N(2)-C(41)-C(42)	62.1(5)
N(2)-C(41)-C(42)-C(43)	-158.7(4)
C(41)-C(42)-C(43)-C(44)	178.2(5)
C(61B)-N(3)-C(51A)-C(52A)	52(2)
C(61C)-N(3)-C(51A)-C(52A)	57(3)
C(71)-N(3)-C(51A)-C(52A)	178.0(12)
C(81)-N(3)-C(51A)-C(52A)	-54.9(16)
C(61A)-N(3)-C(51A)-C(52A)	66.1(17)
C(51B)-N(3)-C(51A)-C(52A)	-114(7)
N(3)-C(51A)-C(52A)-C(53A)	-165.3(14)
C(51A)-C(52A)-C(53A)-C(54A)	-60(2)
C(51A)-N(3)-C(51B)-C(52B)	70(5)
C(61B)-N(3)-C(51B)-C(52B)	55(2)
C(61C)-N(3)-C(51B)-C(52B)	61(3)
C(71)-N(3)-C(51B)-C(52B)	-174.0(11)
C(81)-N(3)-C(51B)-C(52B)	-56.3(14)
C(61A)-N(3)-C(51B)-C(52B)	69.9(18)
N(3)-C(51B)-C(52B)-C(53B)	-168.4(13)

C(51B)-C(52B)-C(53B)-C(54B)	71.4(17)
C(51A)-N(3)-C(61A)-C(62A)	48.0(15)
C(61B)-N(3)-C(61A)-C(62A)	92(6)
C(61C)-N(3)-C(61A)-C(62A)	71(7)
C(71)-N(3)-C(61A)-C(62A)	-68.5(11)
C(81)-N(3)-C(61A)-C(62A)	174.1(10)
C(51B)-N(3)-C(61A)-C(62A)	48.0(16)
N(3)-C(61A)-C(62A)-C(63A)	165.3(17)
C(61A)-C(62A)-C(63A)-C(64A)	-179(2)
C(51A)-N(3)-C(61B)-C(62B)	63(3)
C(61C)-N(3)-C(61B)-C(62B)	25(30)
C(71)-N(3)-C(61B)-C(62B)	-53(4)
C(81)-N(3)-C(61B)-C(62B)	-179(3)
C(61A)-N(3)-C(61B)-C(62B)	-75(5)
C(51B)-N(3)-C(61B)-C(62B)	67(3)
N(3)-C(61B)-C(62B)-C(63B)	115(5)
C(61B)-C(62B)-C(63B)-C(64B)	165(7)
C(51A)-N(3)-C(61C)-C(62C)	44(6)
C(61B)-N(3)-C(61C)-C(62C)	-174(38)
C(71)-N(3)-C(61C)-C(62C)	-67(6)
C(81)-N(3)-C(61C)-C(62C)	161(5)
C(61A)-N(3)-C(61C)-C(62C)	-114(11)
C(51B)-N(3)-C(61C)-C(62C)	47(6)
N(3)-C(61C)-C(62C)-C(63C)	150(5)
C(61C)-C(62C)-C(63C)-C(64C)	-78(6)
C(51A)-N(3)-C(71)-C(72A)	-178.8(10)
C(61B)-N(3)-C(71)-C(72A)	-71(2)
C(61C)-N(3)-C(71)-C(72A)	-80(3)
C(81)-N(3)-C(71)-C(72A)	51.5(7)
C(61A)-N(3)-C(71)-C(72A)	-63.2(8)
C(51B)-N(3)-C(71)-C(72A)	166.6(9)
N(3)-C(71)-C(72A)-C(73A)	162.8(14)
C(71)-C(72A)-C(73A)-C(74A)	177.2(15)
C(51A)-N(3)-C(81)-C(82)	-71.0(10)
C(61B)-N(3)-C(81)-C(82)	-172(2)
C(61C)-N(3)-C(81)-C(82)	-168(3)

C(71)-N(3)-C(81)-C(82)	55.6(8)
C(61A)-N(3)-C(81)-C(82)	167.5(8)
C(51B)-N(3)-C(81)-C(82)	-57.1(9)
N(3)-C(81)-C(82)-C(83)	175.5(6)
C(81)-C(82)-C(83)-C(84)	-70.7(9)

Symmetry transformations used to generate equivalent atoms:

4-Nitro-2,2'-Bipyridine

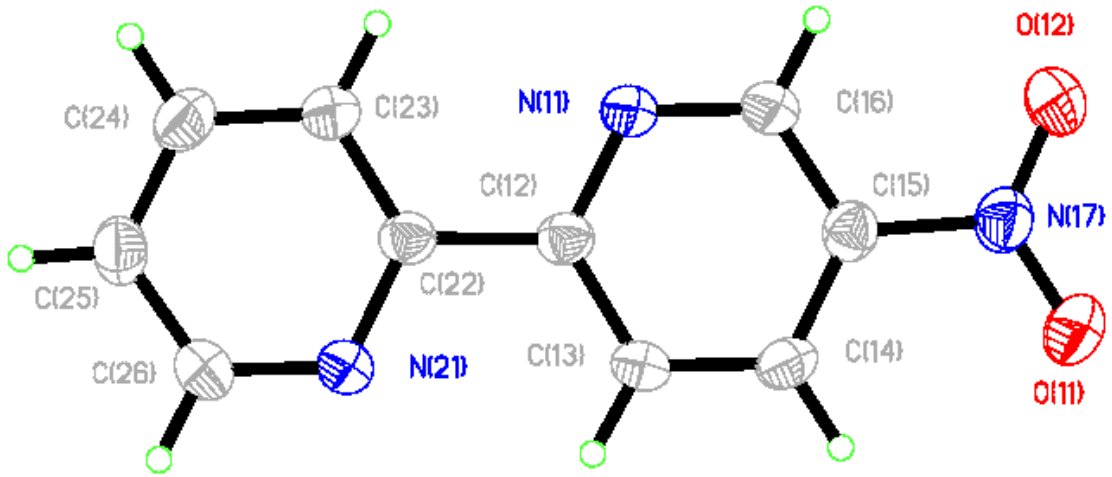

Figure B-3 ORTEP drawing of 4-nitro-2,2'-bipyridine

Table 1. Crystal data and structure refinement for 4-nitro-2,2'-bipyridine.

Identification code	jk0302m	
Empirical formula	C10 H7 N3 O2	
Formula weight	201.19	
Temperature	203(2) K	
Wavelength	0.71073 Å	
Crystal system	Monoclinic	
Space group	P2(1)/n	
Unit cell dimensions	a = 6.2532(8) Å	α= 90°.
	b = 12.1226(16) Å	β= 94.096(9)°.
	c = 11.6829(14) Å	γ = 90°.
Volume	883.36(19) $Å^3$	
Z	4	
Density (calculated)	1.513 g/cm^3	
Absorption coefficient	0.110 mm^{-1}	
F(000)	416	
Crystal size	0.45 x 0.30 x 0.25 mm^3	
Theta range for data collection	2.42 to 28.28°.	
Index ranges	-8<=h<=7, -14<=k<=15, -15<=l<=15	
Reflections collected	5782	
Independent reflections	2053 [R(int) = 0.0742]	
Completeness to theta = 28.28°	93.2 %	
Absorption correction	None	
Refinement method	Full-matrix least-squares on F^2	
Data / restraints / parameters	2053 / 0 / 136	
Goodness-of-fit on F^2	0.975	
Final R indices [I>2sigma(I)]	R1 = 0.0494, wR2 = 0.1104	
R indices (all data)	R1 = 0.0979, wR2 = 0.1359	
Largest diff. peak and hole	0.193 and -0.315 $e.Å^{-3}$	

Table 2. Atomic coordinates (x 10^4) and equivalent isotropic displacement parameters ($Å^2$x 10^3) for 4-nitro-2,2'-bipyridine. U(eq) is defined as one third of the trace of the orthogonalized U^{ij} tensor.

	x	y	z	U(eq)
N(11)	6963(2)	1048(1)	9343(1)	32(1)
C(12)	8195(3)	1754(2)	8807(2)	28(1)
C(13)	7804(3)	2880(2)	8777(2)	34(1)
C(14)	6111(3)	3300(2)	9314(2)	34(1)
C(15)	4859(3)	2564(2)	9852(2)	31(1)
C(16)	5314(3)	1453(2)	9855(2)	33(1)
N(17)	3014(3)	2948(1)	10424(1)	37(1)
O(11)	2657(3)	3935(1)	10433(1)	55(1)
O(12)	1907(2)	2266(1)	10866(1)	50(1)
N(21)	11224(2)	1991(1)	7700(1)	33(1)
C(22)	10006(3)	1271(1)	8232(2)	28(1)
C(23)	10403(3)	152(2)	8246(2)	35(1)
C(24)	12096(3)	-242(2)	7679(2)	41(1)
C(25)	13335(3)	482(2)	7121(2)	37(1)
C(26)	12847(3)	1581(2)	7161(2)	36(1)

Table 3. Bond lengths [Å] and angles [°] for 4-nitro-2,2'-bipyridine.

N(11)-C(16)	1.323(2)
N(11)-C(12)	1.337(2)
C(12)-C(13)	1.387(3)
C(12)-C(22)	1.478(2)
C(13)-C(14)	1.367(3)
C(13)-H(13A)	0.9400
C(14)-C(15)	1.370(3)
C(14)-H(14A)	0.9400
C(15)-C(16)	1.376(3)
C(15)-N(17)	1.450(2)
C(16)-H(16A)	0.9400
N(17)-O(11)	1.217(2)
N(17)-O(12)	1.218(2)
N(21)-C(26)	1.328(2)
N(21)-C(22)	1.340(2)
C(22)-C(23)	1.378(2)
C(23)-C(24)	1.374(3)
C(23)-H(23A)	0.9400
C(24)-C(25)	1.366(3)
C(24)-H(24A)	0.9400
C(25)-C(26)	1.369(3)
C(25)-H(25A)	0.9400
C(26)-H(26A)	0.9400
C(16)-N(11)-C(12)	117.89(16)
N(11)-C(12)-C(13)	122.37(16)
N(11)-C(12)-C(22)	116.43(16)
C(13)-C(12)-C(22)	121.20(16)
C(14)-C(13)-C(12)	119.75(17)
C(14)-C(13)-H(13A)	120.1
C(12)-C(13)-H(13A)	120.1
C(13)-C(14)-C(15)	117.05(17)
C(13)-C(14)-H(14A)	121.5
C(15)-C(14)-H(14A)	121.5

C(14)-C(15)-C(16)	120.92(17)
C(14)-C(15)-N(17)	120.09(17)
C(16)-C(15)-N(17)	119.00(16)
N(11)-C(16)-C(15)	122.01(16)
N(11)-C(16)-H(16A)	119.0
C(15)-C(16)-H(16A)	119.0
O(11)-N(17)-O(12)	123.62(16)
O(11)-N(17)-C(15)	118.23(16)
O(12)-N(17)-C(15)	118.15(17)
C(26)-N(21)-C(22)	117.02(16)
N(21)-C(22)-C(23)	122.59(16)
N(21)-C(22)-C(12)	115.58(15)
C(23)-C(22)-C(12)	121.83(16)
C(24)-C(23)-C(22)	118.73(17)
C(24)-C(23)-H(23A)	120.6
C(22)-C(23)-H(23A)	120.6
C(25)-C(24)-C(23)	119.33(18)
C(25)-C(24)-H(24A)	120.3
C(23)-C(24)-H(24A)	120.3
C(24)-C(25)-C(26)	118.20(17)
C(24)-C(25)-H(25A)	120.9
C(26)-C(25)-H(25A)	120.9
N(21)-C(26)-C(25)	124.12(18)
N(21)-C(26)-H(26A)	117.9
C(25)-C(26)-H(26A)	117.9

Symmetry transformations used to generate equivalent atoms:

Table 4. Anisotropic displacement parameters ($Å^2 x\ 10^3$) for 4-nitro-2,2'-bipyridine. The anisotropic displacement factor exponent takes the form: $-2\pi^2[\ h^2\ a^{*2}U^{11} + ...\ + 2\ h\ k\ a^*\ b^*\ U^{12}\ ]$

U^{11}	U^{22}	U^{33}	U^{23}	U^{13}	U^{12}
N(11)30(1)	26(1)	41(1)	4(1)	8(1)	-1(1)
C(12)27(1)	25(1)	32(1)	1(1)	0(1)	-2(1)
C(13)34(1)	26(1)	43(1)	3(1)	10(1)	-5(1)
C(14)36(1)	22(1)	45(1)	-1(1)	5(1)	0(1)
C(15)27(1)	31(1)	34(1)	-3(1)	2(1)	1(1)
C(16)30(1)	28(1)	40(1)	3(1)	8(1)	-3(1)
N(17)33(1)	36(1)	43(1)	-3(1)	6(1)	3(1)
O(11)52(1)	37(1)	78(1)	-3(1)	26(1)	11(1)
O(12)42(1)	45(1)	66(1)	0(1)	26(1)	-2(1)
N(21)29(1)	28(1)	44(1)	3(1)	8(1)	-1(1)
C(22)27(1)	26(1)	31(1)	1(1)	0(1)	-2(1)
C(23)35(1)	25(1)	47(1)	1(1)	8(1)	-1(1)
C(24)42(1)	29(1)	52(1)	-4(1)	6(1)	5(1)
C(25)31(1)	41(1)	41(1)	-5(1)	8(1)	3(1)
C(26)30(1)	37(1)	42(1)	1(1)	7(1)	-3(1)

Table 5. Hydrogen coordinates (x 10^4) and isotropic displacement parameters ($Å^2$x 10^3) for 4-nitro-2,2'-bipyridine.

	x	y	z	U(eq)
H(13A)	8701	3352	8390	41
H(14A)	5819	4061	9314	41
H(16A)	4427	967	10232	39
H(23A)	9533	-331	8636	42
H(24A)	12398	-1001	7675	49
H(25A)	14492	231	6720	45
H(26A)	13714	2077	6785	44

Table 6. Torsion angles [°] for 4-nitro-2,2'-bipyridine.

C(16)-N(11)-C(12)-C(13)	0.3(3)
C(16)-N(11)-C(12)-C(22)	-179.27(16)
N(11)-C(12)-C(13)-C(14)	0.2(3)
C(22)-C(12)-C(13)-C(14)	179.76(18)
C(12)-C(13)-C(14)-C(15)	-0.6(3)
C(13)-C(14)-C(15)-C(16)	0.6(3)
C(13)-C(14)-C(15)-N(17)	-179.04(18)
C(12)-N(11)-C(16)-C(15)	-0.4(3)
C(14)-C(15)-C(16)-N(11)	-0.1(3)
N(17)-C(15)-C(16)-N(11)	179.54(18)
C(14)-C(15)-N(17)-O(11)	-1.8(3)
C(16)-C(15)-N(17)-O(11)	178.58(19)
C(14)-C(15)-N(17)-O(12)	178.07(19)
C(16)-C(15)-N(17)-O(12)	-1.6(3)
C(26)-N(21)-C(22)-C(23)	0.9(3)
C(26)-N(21)-C(22)-C(12)	-179.08(17)
N(11)-C(12)-C(22)-N(21)	-179.96(17)
C(13)-C(12)-C(22)-N(21)	0.5(3)
N(11)-C(12)-C(22)-C(23)	0.1(3)
C(13)-C(12)-C(22)-C(23)	-179.5(2)
N(21)-C(22)-C(23)-C(24)	-0.9(3)
C(12)-C(22)-C(23)-C(24)	179.01(18)
C(22)-C(23)-C(24)-C(25)	0.1(3)
C(23)-C(24)-C(25)-C(26)	0.7(3)
C(22)-N(21)-C(26)-C(25)	0.0(3)
C(24)-C(25)-C(26)-N(21)	-0.8(3)

Symmetry transformations used to generate equivalent atoms:

4-Amino-2,2'-Bipyridine

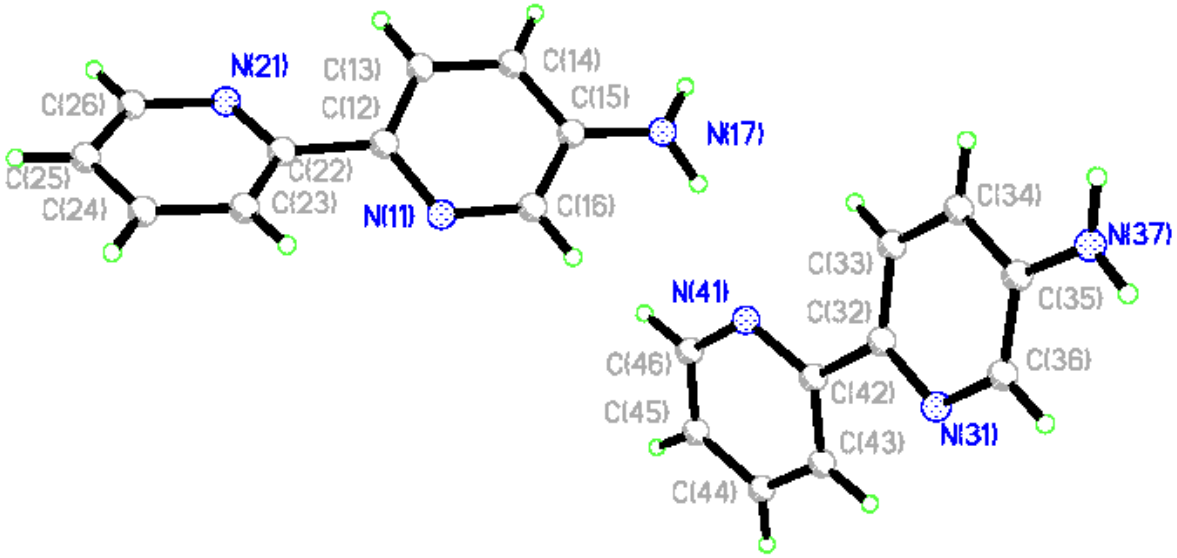

Figure B-4 ORTEP drawing 4-amino-2,2'-bipyridine

Table 1. Crystal data and structure refinement for 4-amino-2,2'-bipyridine.

Identification code	jk0301m	
Empirical formula	C10 H9 N3	
Formula weight	171.20	
Temperature	203(2) K	
Wavelength	0.71073 Å	
Crystal system	Orthorhombic	
Space group	P2(1)2(1)2(1)	
Unit cell dimensions	a = 11.062(3) Å	α= 90°.
	b = 11.212(3) Å	β= 90°.
	c = 13.886(4) Å	γ = 90°.
Volume	1722.2(9) $Å^3$	
Z	8	
Density (calculated)	1.321 g/cm^3	
Absorption coefficient	0.083 mm^{-1}	
F(000)	720	
Crystal size	0.30 x 0.20 x 0.10 mm^3	
Theta range for data collection	2.35 to 28.71°.	
Index ranges	-14<=h<=14, -14<=k<=14, -18<=l<=16	
Reflections collected	11932	
Independent reflections	4080 [R(int) = 0.0890]	
Completeness to theta = 28.71°	93.0 %	
Absorption correction	None	
Refinement method	Full-matrix least-squares on F^2	
Data / restraints / parameters	4080 / 0 / 248	
Goodness-of-fit on F^2	0.889	
Final R indices [I>2sigma(I)]	R1 = 0.0455, wR2 = 0.0791	
R indices (all data)	R1 = 0.1205, wR2 = 0.0993	
Absolute structure parameter	3(3)	
Extinction coefficient	0.034(2)	
Largest diff. peak and hole	0.207 and -0.216 e.$Å^{-3}$	

Table 2. Atomic coordinates (x 10^4) and equivalent isotropic displacement parameters ($Å^2$x 10^3) for 4-amino-2,2'-bipyridine. U(eq) is defined as one third of the trace of the orthogonalized U^{ij} tensor.

	x	y	z	U(eq)
N(11)	1108(2)	1525(2)	5539(1)	38(1)
C(12)	1715(2)	1375(2)	6367(2)	35(1)
C(13)	2816(2)	1930(2)	6516(2)	43(1)
C(14)	3294(2)	2646(2)	5820(2)	42(1)
C(15)	2678(2)	2829(2)	4971(2)	38(1)
C(16)	1591(2)	2225(2)	4874(2)	38(1)
N(17)	3116(2)	3524(2)	4252(2)	56(1)
N(21)	1542(2)	748(2)	8003(1)	45(1)
C(22)	1178(2)	590(2)	7093(2)	35(1)
C(23)	366(2)	-290(2)	6850(2)	45(1)
C(24)	-87(3)	-1018(3)	7559(2)	56(1)
C(25)	282(3)	-867(2)	8487(2)	56(1)
C(26)	1091(3)	11(2)	8670(2)	53(1)
N(31)	940(2)	3674(2)	522(1)	37(1)
C(32)	1481(2)	3962(2)	1351(2)	35(1)
C(33)	2669(2)	3662(2)	1514(2)	44(1)
C(34)	3306(2)	3041(2)	838(2)	44(1)
C(35)	2746(2)	2702(2)	-10(2)	35(1)
C(36)	1574(2)	3074(2)	-126(2)	37(1)
N(37)	3309(2)	2054(2)	-700(2)	51(1)
N(41)	1158(2)	4574(2)	2983(1)	47(1)
C(42)	747(2)	4603(2)	2071(2)	36(1)
C(43)	-289(2)	5198(2)	1825(2)	41(1)
C(44)	-929(2)	5796(2)	2520(2)	49(1)
C(45)	-517(3)	5770(2)	3450(2)	56(1)
C(46)	506(3)	5156(2)	3646(2)	55(1)

Table 3. Bond lengths [Å] and angles [°] for 4-amino-2,2'-bipyridine.

N(11)-C(16)	1.324(3)
N(11)-C(12)	1.343(3)
C(12)-C(13)	1.383(3)
C(12)-C(22)	1.464(3)
C(13)-C(14)	1.363(3)
C(14)-C(15)	1.377(3)
C(15)-N(17)	1.356(3)
C(15)-C(16)	1.387(3)
N(21)-C(26)	1.337(3)
N(21)-C(22)	1.339(3)
C(22)-C(23)	1.376(3)
C(23)-C(24)	1.373(3)
C(24)-C(25)	1.362(3)
C(25)-C(26)	1.355(4)
N(31)-C(36)	1.324(3)
N(31)-C(32)	1.337(3)
C(32)-C(33)	1.375(3)
C(32)-C(42)	1.474(3)
C(33)-C(34)	1.365(3)
C(34)-C(35)	1.383(3)
C(35)-N(37)	1.355(3)
C(35)-C(36)	1.371(3)
N(41)-C(46)	1.338(3)
N(41)-C(42)	1.346(3)
C(42)-C(43)	1.369(3)
C(43)-C(44)	1.372(3)
C(44)-C(45)	1.370(3)
C(45)-C(46)	1.353(4)

C(16)-N(11)-C(12)	118.0(2)
N(11)-C(12)-C(13)	120.8(2)
N(11)-C(12)-C(22)	117.5(2)
C(13)-C(12)-C(22)	121.7(2)
C(14)-C(13)-C(12)	120.0(2)

C(13)-C(14)-C(15)	120.2(2)
N(17)-C(15)-C(14)	122.7(2)
N(17)-C(15)-C(16)	121.2(2)
C(14)-C(15)-C(16)	116.1(2)
N(11)-C(16)-C(15)	124.8(2)
C(26)-N(21)-C(22)	117.4(2)
N(21)-C(22)-C(23)	121.5(2)
N(21)-C(22)-C(12)	116.6(2)
C(23)-C(22)-C(12)	121.8(2)
C(24)-C(23)-C(22)	119.2(2)
C(25)-C(24)-C(23)	119.8(3)
C(26)-C(25)-C(24)	117.7(3)
N(21)-C(26)-C(25)	124.5(2)
C(36)-N(31)-C(32)	118.1(2)
N(31)-C(32)-C(33)	120.6(2)
N(31)-C(32)-C(42)	117.1(2)
C(33)-C(32)-C(42)	122.3(2)
C(34)-C(33)-C(32)	120.4(2)
C(33)-C(34)-C(35)	119.6(2)
N(37)-C(35)-C(36)	121.0(2)
N(37)-C(35)-C(34)	122.9(2)
C(36)-C(35)-C(34)	116.1(2)
N(31)-C(36)-C(35)	125.1(2)
C(46)-N(41)-C(42)	116.9(2)
N(41)-C(42)-C(43)	121.9(2)
N(41)-C(42)-C(32)	116.1(2)
C(43)-C(42)-C(32)	121.9(2)
C(42)-C(43)-C(44)	119.7(2)
C(45)-C(44)-C(43)	118.8(3)
C(46)-C(45)-C(44)	118.6(3)
N(41)-C(46)-C(45)	124.1(3)

Symmetry transformations used to generate equivalent atoms:

Table 4. Anisotropic displacement parameters ($Å^2 x\ 10^3$) for 4-amino-2,2'-bipyridine. The anisotropic displacement factor exponent takes the form: $-2\pi^2[\ h^2\ a^{*2}U^{11} + ... + 2\ h\ k\ a^*\ b^*\ U^{12}\ ]$

U^{11}	U^{22}	U^{33}	U^{23}	U^{13}	U^{12}
N(11)39(1)	37(1)	37(1)	0(1)	-3(1)	-1(1)
C(12)36(2)	32(1)	38(1)	-3(1)	0(1)	-1(1)
C(13)42(2)	46(2)	40(1)	1(1)	-5(1)	-6(1)
C(14)31(2)	45(2)	49(1)	-2(1)	-3(1)	-9(1)
C(15)42(2)	35(2)	37(1)	0(1)	4(1)	-2(1)
C(16)37(2)	40(2)	38(1)	0(1)	-1(1)	-5(1)
N(17)48(2)	64(2)	55(1)	14(1)	1(1)	-17(1)
N(21)51(2)	47(1)	36(1)	-1(1)	0(1)	-5(1)
C(22)36(2)	31(1)	38(1)	-1(1)	0(1)	3(1)
C(23)52(2)	38(2)	45(1)	1(1)	-6(1)	-8(1)
C(24)68(2)	46(2)	54(2)	2(1)	-2(2)	-17(2)
C(25)73(2)	51(2)	46(2)	7(1)	5(2)	-7(2)
C(26)64(2)	60(2)	35(1)	1(1)	1(1)	1(2)
N(31)37(1)	40(1)	33(1)	0(1)	0(1)	2(1)
C(32)40(2)	32(1)	33(1)	1(1)	-1(1)	-1(1)
C(33)41(2)	52(2)	39(1)	-6(1)	-6(1)	-4(1)
C(34)30(2)	56(2)	46(1)	-8(1)	-3(1)	5(1)
C(35)29(2)	39(2)	36(1)	-2(1)	2(1)	1(1)
C(36)38(2)	42(1)	30(1)	-3(1)	-2(1)	-2(1)
N(37)37(2)	64(2)	53(1)	-18(1)	-1(1)	8(1)
N(41)61(2)	46(1)	34(1)	-4(1)	-2(1)	-3(1)
C(42)43(2)	28(1)	36(1)	0(1)	2(1)	-4(1)
C(43)45(2)	35(1)	42(1)	-2(1)	5(1)	-2(1)
C(44)53(2)	34(2)	59(2)	-2(1)	9(2)	-1(1)
C(45)75(2)	44(2)	49(2)	-12(1)	13(2)	-1(2)
C(46)77(2)	50(2)	40(1)	-8(1)	3(2)	-5(2)

Table 5. Hydrogen coordinates (x 10^4) and isotropic displacement parameters ($Å^2$x 10^3) for 4-amino-2,2'-bipyridine.

	x	y	z	U(eq)
H(13)	3234	1814	7098	51
H(14)	4046	3015	5920	50
H(16)	1165	2320	4293	46
H(17A)	2630(20)	3750(20)	3746(18)	67
H(17B)	3790(30)	3800(20)	4275(19)	67
H(23)	123	-391	6206	54
H(24)	-648	-1617	7405	67
H(25)	-15	-1356	8984	68
H(26)	1354	109	9309	64
H(33)	3044	3887	2094	53
H(34)	4120	2844	948	53
H(36)	1190	2887	-711	44
H(37A)	4050(30)	1730(20)	-608(17)	62
H(37B)	2890(20)	1790(20)	-1226(18)	62
H(43)	-560	5196	1184	49
H(44)	-1637	6216	2361	58
H(45)	-937	6170	3942	67
H(46)	777	5137	4287	66

Table 6. Torsion angles [°] for 4-amino-2,2'-bipyridine.

C(16)-N(11)-C(12)-C(13)	-0.4(3)
C(16)-N(11)-C(12)-C(22)	-179.4(2)
N(11)-C(12)-C(13)-C(14)	0.4(4)
C(22)-C(12)-C(13)-C(14)	179.3(2)
C(12)-C(13)-C(14)-C(15)	0.7(4)
C(13)-C(14)-C(15)-N(17)	-179.5(2)
C(13)-C(14)-C(15)-C(16)	-1.6(3)
C(12)-N(11)-C(16)-C(15)	-0.6(3)
N(17)-C(15)-C(16)-N(11)	179.5(2)
C(14)-C(15)-C(16)-N(11)	1.6(3)
C(26)-N(21)-C(22)-C(23)	0.4(4)
C(26)-N(21)-C(22)-C(12)	-177.7(2)
N(11)-C(12)-C(22)-N(21)	-158.2(2)
C(13)-C(12)-C(22)-N(21)	22.8(3)
N(11)-C(12)-C(22)-C(23)	23.6(3)
C(13)-C(12)-C(22)-C(23)	-155.3(2)
N(21)-C(22)-C(23)-C(24)	0.4(4)
C(12)-C(22)-C(23)-C(24)	178.5(2)
C(22)-C(23)-C(24)-C(25)	-0.6(4)
C(23)-C(24)-C(25)-C(26)	0.1(4)
C(22)-N(21)-C(26)-C(25)	-1.1(4)
C(24)-C(25)-C(26)-N(21)	0.8(4)
C(36)-N(31)-C(32)-C(33)	1.4(3)
C(36)-N(31)-C(32)-C(42)	-178.4(2)
N(31)-C(32)-C(33)-C(34)	-1.5(4)
C(42)-C(32)-C(33)-C(34)	178.3(2)
C(32)-C(33)-C(34)-C(35)	-0.7(4)
C(33)-C(34)-C(35)-N(37)	-178.0(3)
C(33)-C(34)-C(35)-C(36)	2.8(4)
C(32)-N(31)-C(36)-C(35)	1.0(3)
N(37)-C(35)-C(36)-N(31)	177.6(2)
C(34)-C(35)-C(36)-N(31)	-3.1(4)
C(46)-N(41)-C(42)-C(43)	0.0(3)
C(46)-N(41)-C(42)-C(32)	179.7(2)

N(31)-C(32)-C(42)-N(41)	160.8(2)
C(33)-C(32)-C(42)-N(41)	-19.0(3)
N(31)-C(32)-C(42)-C(43)	-19.4(3)
C(33)-C(32)-C(42)-C(43)	160.8(2)
N(41)-C(42)-C(43)-C(44)	0.7(4)
C(32)-C(42)-C(43)-C(44)	-179.0(2)
C(42)-C(43)-C(44)-C(45)	-0.8(4)
C(43)-C(44)-C(45)-C(46)	0.1(4)
C(42)-N(41)-C(46)-C(45)	-0.6(4)
C(44)-C(45)-C(46)-N(41)	0.6(4)

Symmetry transformations used to generate equivalent atoms:

Table 7. Hydrogen bonds for 4-amino-2,2'-bipyridine [Å and °].

D-H...A	d(D-H)	d(H...A)	d(D...A)	<(DHA)
N(17)-H(17A)...N(41)	0.92(2)	2.15(3)	3.030(3)	159(2)
N(37)-H(37A)...N(31)#1	0.90(3)	2.14(3)	3.033(3)	168(2)

Symmetry transformations used to generate equivalent atoms:

#1 x+1/2,-y+1/2,-z